From the Research Center Borstel

Center for Medicine and Biosciences

Managing Director: Prof. Dr. Stefan Ehlers

Division of Structural Biochemistry

Head: Prof. Dr. Otto Holst

Structural and biological profiling of cell envelope constituents from the allergy-protective bacterium *Lactococcus lactis* G121

Dissertation

for

Fulfillment of Requirements

for the Doctoral Degree

of the University of Lübeck

from the Department of Natural Sciences

Submitted by

Kathleen Fischer

from Hagenow, Germany

Lübeck 2012

First referee: Prof. Dr. Otto Holst

Second referee: Prof. Dr. Tamás Laskay

Date of oral examination: 14.01.2013

Approved for printing. Lübeck, 23.01.2013

Table of Contents

List of Figures

List of Tables

List of Abbreviations

1D	one-dimensional
2D	two-dimensional
ABC	ATP binding cassette(s)
AEX	anion-exchange chromatography
AHR	airway hyperresponsiveness
Ala	alanine
ALEX	allergy and endotoxin
APC	antigen-presenting cell
Asn	asparagine
Asp	aspartic acid
BAL	bronchoalveolar lavage
bp	base pairs
BSA	bovine serum albumin
CARD	caspase recruitment domain
CD	cluster of differentiation
cfu	colony forming units
CLA	conjugated linoleic acid(s)
COSY	correlation spectroscopy
CPS	capsular polysaccharide(s)
CTL	cytotoxic T-cell(s)
DAP	diaminopimelic acid
DC	dendritic cell(s)
DL	DNA library

DNA	deoxyribonucleic acid(s)
dNTP	deoxynucleoside triphosphate(s)
ds	double-stranded
e.g.	exempli gratia, for example
EC TA	extracellular teichoic acid(s)
ECP	eosinophil cationic protein
EDTA	ethylenediaminetetraacetic acid, 2-({2-[Bis(carboxymethyl) amino]ethyl}(carboxymethyl)amino)acetic acid
EI	electron impact
ELISA	enzyme-linked immunosorbent assay
EPS	exopolysaccharide(s)
ESI FT-ICR-MS	electrospray ionization Fourier-transformed ion cyclotron mass spectrometry
ESI-MS	in this thesis used to further abbreviate ESI FT-ICR-MS
et al.	et alii, and others
FA	fatty acid(s)
FAME	fatty acid methylester(s)
FcεRI	Fcε receptor I
FID	flame ionization detector
FPLC	fast-protein liquid chromatography
Gal*p*	galactopyranose
GINA	Global Initiative for Asthma
GLC	gas-liquid chromatograph(y)
Glc*p*	glucopyranose
Gln	glutamine

Glu	glutamic acid
GM-CSF	granulocyte-macrophage colony-stimulating factor
Gro	glycerol
GSP	gene-specific primer
HEK293	human embryonic kidney cells 293
HEPES	4-(2-hydroxyethyl)-1-piperazineethanesulfonic acid
Hex	hexose
HIC	hydrophobic interaction chromatography
HMBC	heteronuclear multiple bond correlation
hMNC	human mononuclear cell(s)
HMQC	heteronuclear multiple quantum correlation
HSQC	heteronuclear single quantum coherence
i	*iso*
iE-DAP	γ-D-glutamyl-*meso*-diaminopimelic acid
IFN	interferon
Ig	immunoglobulin
IL-	interleukin
IPTG	isopropyl β-D-1-thiogalactopyranoside
IRAK	IL-1R associated serine/threonine kinase
JNK	c-Jun N-terminal kinase
KOD	*Thermococcus kodakaraensis*
LA	linoleic acid
LAB	lactic acid bacterium (bacteria)
LMP	low melting point

LPS	lipopolysaccharide(s)
LRR	leucine-rich repeat(s)
LT	leukotriene(s)
LTA	lipoteichoic acid(s)
Lys	lysine
MALP	macrophage-activating lipopeptide
MBL	mannan-binding lectin
MBP	major basic protein
MDP	muramyl dipeptide (*N*-acetylmuramyl-L-alanyl-D-isoglutamine)
MHC	major histocompatibility
MMCO	molecular mass cut off
MSD	mass-selective detector
NAc	*N*-acetyl
NAG	*N*-acetyl-D-glucosamine
NALP	NACHT-, LRR- and pyrin domain-containing protein(s)
NAM	*N*-acetyl-D-muramic acid
n.d.	not determined
NF-κB	nuclear factor-κB
NGSP	nested gene-specific primer
NLR	NOD-like receptor(s)
NMR	nuclear magnetic resonance
NOD	nucleotide-binding oligomerization domain-containing protein(s)

NOE	nuclear Overhauser effect
OD	optical density
OVA	ovalbumin
P	phosphate
PAF	platelet-activating factor
Pam$_3$-CSK$_4$	*N*-Palmitoyl-*S*-[2,3-bis(palmitoyloxy)-(2*RS*)-propyl]-[*R*]-cysteinyl-[*S*]-seryl-[*S*]-lysyl-[*S*]-lysyl-[*S*]-lysyl-[*S*]-lysine
PAMP	pathogen-associated molecular pattern(s)
PARSIFAL	prevention of allergy, risk factors for sensitization related to farming and anthroposophic lifestyle
PASTURE	protection against allergy-study in rural environments
PAW	pyridinium acetate buffer
PBS	phosphate-buffered saline
PC	plasma cell(s)
PCR	polymerase chain reaction(s)
PG	prostaglandin(s)
PGN	peptidoglycan
PGRP	peptidoglycan recognition proteins
PRR	pattern recognition receptor(s)
PUFA	polyunsaturated fatty acid(s)
Rbo	ribitol
Rha*p*	rhamnopyranoside
RICK	serine/threonine kinase
RNA	ribonucleic acid
ROESY	rotating-frame Overhauser effect spectroscopy

RP HPLC	reverse-phase high-performance liquid chromatography
RSV	respiratory syncytial virus
SD	standard deviation
SDS	sodium dodecylsulfate
SEC	size-exclusion chromatography
SFA	saturated fatty acid(s)
SFB	Sonderforschungsbereich, special research area
sp.	species
ss	single-stranded
ssp.	subspecies
TCA	trichloroacetic acid
TCR	T-cell receptor
TFA	trifluoroacetic acid
TGF	transforming growth factor
T_H	T helper
TIR	Toll/interleukin-1 (IL-1) receptor
TLC	thin-layer chromatogram
TLR	Toll-like receptor(s)
TNF-α	tumor necrosis factor -α
TOCSY	total correlation spectroscopy
TRAF	TNF receptor-associated factor
T_{Reg}	T regulatory
Tris	tris(hydroxymethyl)aminomethane
TSB	tryptic soy broth

UFA	unsaturated fatty acid(s)
UV	ultraviolet
VIS	visible
vol	volume
WBA	washed biomass assay
WHO	World Health Organization
WPS	wall polysaccharide(s)
WTA	wall teichoic acid(s)
X-gal	5-bromo-4-chloro-indolyl-β-D-galactopyranoside
Xyl	xylose

1 Introduction

1.1 Medico-epidemiological background

1.1.1 Allergic asthma bronchiale is a chronic inflammatory disorder

In virtue of the World Health Organization (WHO) in 2011 roughly 235 million people all over the world were suffering from asthma bronchiale. It represents the most frequent chronic disease during infancy (1). As late as in 2002 the WHO estimated 150 million asthmatics worldwide, so in narrow one decade the number of affected individuals increased by more than half. This means an enormous economic debit, because allergic asthma is beyond remedy and needs to be controlled by a lifelong medication.

By definition of the Global Initiative for Asthma (GINA): "Asthma is a chronic inflammatory disorder of the airways in which many cells and cellular elements play a role. The chronic inflammation causes an associated increase in airway hyperresponsiveness (AHR) that leads to recurrent episodes of wheezing, breathlessness, chest tightness, and coughing, particularly at night or in the early morning. These episodes are usually associated with widespread but variable airflow obstruction that is often reversible either spontaneously or with treatment." Asthma attacks leading to daytime fatigue, abjection and even school absenteeism entail a severe degradation of life quality (2).

Allergic asthma is the clinical outcome of hypersensitivity towards usually harmless environmental agents, the so called allergens. These can be for instance birch pollen, house dust mite scat, cat hair or mildew spores which are inhaled and react with the sub mucosa of the lower airways. The risk to become allergic involves about 50% of environmental influences and 50% of genetic conditions of a person (3). The genetic variability of several gen loci on different chromosomes has been found to contribute to hypersensitivity. So far 43 candidate genes have been linked to allergies. A polymorphism in the gene encoding the interleukin (IL)-4 receptor α-subunit represents one of them (4–6). Generally, higher immunoglobulin E (IgE) levels and eosinophil granulocytes (eosinophils) in the blood are symptomatic for atopic patients. Therefore, atopy is a familial tendency to produce IgE against ordinary substances (7).

According to the underlying induction mechanism allergies are classified into different types of hypersensitivity. The IgE-mediated mast cell activation leading to asthma belongs to the type I hypersensitivity. Type II reactions are characterized by high IgG levels directed against cell surfaces and matrix antigens involving the complement (e.g., penicillin allergy). Immune complexes of antibody and soluble antigens are the trigger for type III hypersensitivities resulting in tissue destruction (e.g., serum sickness). In contrast, T-cells [T_H1, T_H2 and cytotoxic T-cells (CTL)] are the cause of type IV reactions effecting inflammatory cytokines or cytotoxic mechanisms (e.g., autoimmunity, chronic asthma) (3).

Allergens often have enzymatic function for hydrolyzation of tight junctions between epithelial cells whereby the entering of the mucosa is enabled. This is the case for Der p 1, an allergen from mite excretion (8,9). An important precondition is the sensitization, a first time contact at which the allergen is taken up by dendritic cells (DC) and presented by these via the adaptor molecule major histocompatibility complex class II (MHC class II) in the lymph nodes. Naïve T-lymphocytes interact via their T-cell receptor (TCR) and cluster of differentiation 4 (CD4) co-receptor on their surface with the MHC class II-allergen complex on the DC leading to an activated allergen specific T helper cell population of the subtype 2 (T_H2). T_H2 cells release IL-4 and IL-13 which differentiate B-lymphocytes to allergen specific IgE producing plasma cells (10,11). IgE subsequently binds to the high-affine Fcε-receptor I (FcεRI) on the surface of mast cells and basophil granulocytes (12). A second contact between the allergen and IgE-coated mast cells activates these commencing an allergic response. In the case of asthma the response can be divided in the "early and late phase reaction" (13).

In the early phase of allergic asthma the allergen crosslinks receptor-bound IgE resulting in degranulation of the mast cells. Histamine as one main granula component contracts the smooth muscle cells and raises the permeability of vessels. Enzymes as chymase or tryptase digest the local tissue. Activated mast cells further release and synthesize important mediators such as the eosinophils activating cytokines IL-3 and IL-5. In addition IL-4- and IL-13-stimulated T_H2 lymphocytes realize the isotype switch in naïve B-cells to allergen specific IgE and tumor necrosis factor (TNF-α) activates the endothelium for a boosted influx of inflammatory lymphocytes and other leukocytes. The T_H2 cell-, eosinophil- and basophil-attracting lipid mediators leukotriene B_4 (LTB_4) and prostaglandin D_2 (PGD_2) are produced by activated mast cells similarly as the platelet-activating factor

(PAF) which recruits neutrophils as the hallmark of acute inflammation (14,15). Their significance for the pathogenesis of asthma is still discussed oppositional (16–18).

The late phase reaction, which is depicted in **Figure 1.1**, is marked by the influx of inflammatory cells such as eosinophils, basophils, T_H2 and B-cells, taking place ca. 4–6 hours post allergen contact (19). Eosinophils secrete amongst others the major basic protein (MBP) and eosinophil cationic protein (ECP) which in turn leads to degranulation of mast cells and basophils as well as tissue damage. IL-3 and IL-5 being released by eosinophils further corroborate the T_H2 skewed immune response and ensure eosinophil survival ending up in a permanent loop of proliferation, activation and degranulation (20). Especially LTB_4 and PGD_2 contribute to the maintenance of the inflammatory reaction. Once the CD4+ T_H2 lymphocyte subset is switched on it promotes its own profile and with it a constant infiltration of immune cells while suppressing the T_H1 path (21,22). Characteristic is the metaplasia of epithelial cells towards goblet cells induced by the T_H2 cytokines IL-9 and IL-13 accompanied by an increase in mucus production (23,24). The toxic substances of eosinophils and basophils lead to a considerable damage of the tissue. The sum of the mentioned triggers causes a common accession in sensitivity named airway hyperactivity (AHR). A repeated exposure to the allergen will lead to a chronification of the inflammation. Thickening of the airways and mucus overproduction are leading to bronchoobstruction. During airway remodeling areas of the lung get irreversibly destroyed and replaced by connective tissue (fibrosis) resulting in loss of function (25). This means a life-long disturbance of respiration which left untreated will lead to death of a patient.

Current medications are based on immunosuppressant for instance corticosteroids or antihistamine which can only abate the symptoms. A successful approach works by blocking FcεRI with a monoclonal antibody (Omalizumab) (26). Since the discovery of a new population of lymphocytes in 2001, namely T regulatory cells (T_{Reg}), which have shown to be able to control allergic disorders new pharmaceuticals tend to target this regulation. T_{Reg} can suppress T_H1 and T_H2 cells as well as mast cells, basophils and eosinophils reversing a mislead immune system and this is thought to be inducible by vaccines (27–30).
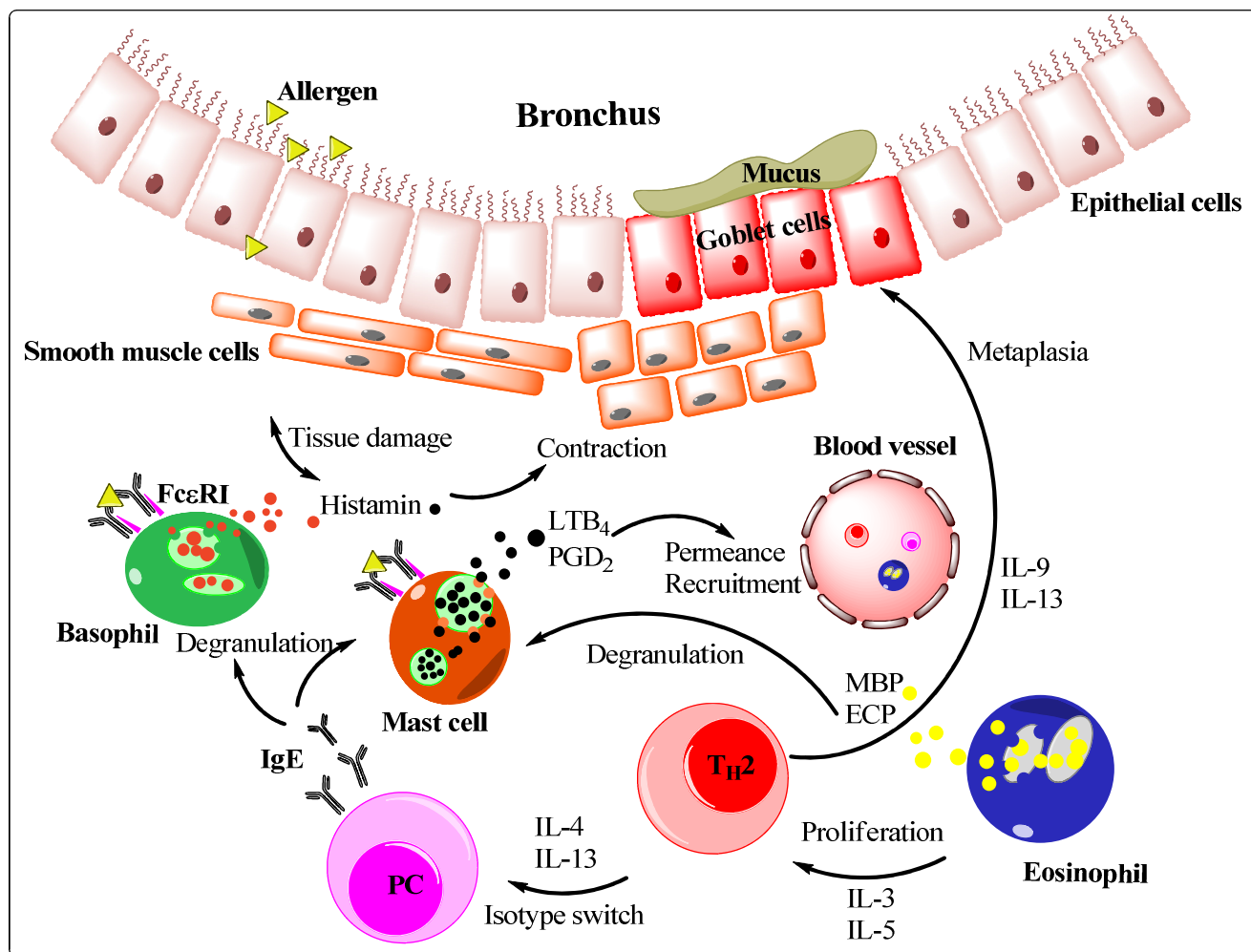
Figure 1.1 The pathophysiology of the late phase of asthma bronchiale. Degranulation of mast cells is triggered by the allergen crosslinked IgE bound at FcεRI on their surface. Released lipid mediators LTB_4 and PGD_2 elevate the permeability of vessels attracting further T_H2 cells, eosinophils and basophils. IL-3 and IL-5 produced by eosinophils keep up their own population as well as the T_H2 phenotype. T_H2 cells, in turn, promote the allergen specific IgE production of plasma cells (PC) through release of IL-4 and IL-13. The IgE molecules in turn associate with the FcεRI on mast cells and basophils setting free tissue damaging and muscle cell constructing histamine and further lipid mediators. Moreover, the conversion of epithelial cells to mucus overproducing goblet cells is switched by T_H2 cells. A permanent contact to the allergen leads to a chronification characterized by narrowed, obstructed bronchi, irreversibly damaged lung tissue and AHR.

1.1.2   The hygiene hypothesis 2012

The farming way of life unambiguously features a lower risk to come down with allergic sensitizations such as rhinitis (hay fever), dermatitis (neurodermitis), conjunctivitis (pink eye) or asthma bronchiale (atopic as well as non-atopic type). A multitude of cross-sectional epidemiological studies in Europe, Australasia and North America authenticated and fathomed more detailed what Strachan noted in 1989 (31–36). In his comment: "Hay fever, hygiene, and household size" he described the inverse correlation between the prevalence of hay fever and number of siblings in a cohort of 17,414 British children. This was the foundation of the hygiene hypothesis (37). Ten years later he stated that a reduced family size is merely one of a bunch of risk factors contributing to the increase in asthma and hay fever since industrial revolution (38). A recent population study hauntingly certified the allergy-protective effect of a constant contact to animals, stables and drinking of raw milk in Swiss farm families compared to Swiss nonfarm families. Most striking was the even lower prevalence for allergic sensitization in an Amish cohort (7.2%) compared to the Swiss farm cohort (25.2%) at which the family size was the nearest obvious difference (39).

One of the substantial tasks for scientists was and still is to pin-point the numerous epidemiological observations to the responsible agent(s) and mechanism(s). With the allergy and endotoxin study (ALEX, conducted in 1999 on Bavarian, Swiss and Austrian alpine farms) the first concrete compounds inversely associated with the development of atopic diseases could be identified as bacterial endotoxins (lipopolysaccharide, LPS) (40). However, LPS maybe a toxin and its character in allergy prevention has been regarded argumentative (41,42). Besides, extracts from dust probes taken on alpine farms revealed high potential to prevent mice from getting allergic and effected human dendritic cells in IL-10, IL12p70 and TNF-α production *in vitro* (43,44). One of the active molecules of these extracts was found out to be arabinogalactan from *Alopecurus pratensis* (field meadow foxtail) (45). Furthermore, *L. lactis* G121 and *Acinetobacter lwoffii* F78 isolated from dust samples out of the ALEX study showed anti-asthmatic properties in a mouse model and thus were clearly relatable to the rural-effect (explained in detail in chapter 1.1.3) (46,47).

Accordingly, an early and consistent exposure to farm stimuli like animals (mainly cattle, pigs and poultry) (48), fodder (e.g., hay, straw, silage) (35,49,50), a diversity of microorganisms (bacteria and fungi) (17–19), and raw milk consumption (31,53,54) appeared to be important triggers for a non-allergic development of the human immune system.

Other studies indicated the influences of non-farming effectors. For instance, the intestinal microbiome has a huge impact on the establishment of a well-functioning immune system. This was described for gnotobiotic mice showing histological abnormalities in the colon compared to colonized mice (55). Other reports showed the importance of gut microbiota for the suppression of pulmonary allergic responses (56,57). Whether parasitic infections display an advantage or a risk for hypersensitivity probably depends on the species. *Ascaris lumbricoides* infections were found out to be irrelevant for allergy (58), whereas the egg antigen of *Schistosoma japonicum* inhibited asthma in a mouse model (59) and *S. mansoni* antigen activated T_{Reg} (60). Apparently, some helminths have evolved mechanisms to suppress the hosts T_H2 response prolonging their own survival going along with allergy blanking (61).

The current knowledge about the adaptive cellular machinery as well as epigenetics behind the farm effect is explained more detailed in chapter 1.2.2.

Apart from all the reports concerning protection, some bacterial and viral infections [e.g., *Mycoplasma pneumonia*, respiratory syncytial virus (RSV) or rhinovirus] have been connected to an exacerbation of asthma (62–64). Nevertheless, Fishbein and Fuleihan reviewed the influence of infection on an asthmatic outcome controversially (65). Tuberculosis in infancy for instance has been discussed to preclude (66) as well as to non-affect atopy (67). *Varicella zoster* infections have been considered to prevent eczema, whereas vaccination was related to a higher chance of having dermatitis (68). At moment the underlying mechanisms are poorly understood and it seems unlikely that one specific infection can be directly associated with asthma or other allergies.

Obviously the farm effect cannot be explained by single factors. A rather new perspective tries to correlate all the findings by putting the hygiene hypothesis in context to human evolution during past 10,000 years. Briefly, the so called Darwinian medicine understands the rise in allergic disorders as a result of a missing immunological evolution. Mankind has developed quite rapidly in social and technical ways particularly since the last 300

years. The central question of Darwinian medicine is: "Does the clean westernized world offer enough input for the correct formation of the human immune system?" (69).

1.1.3 *L. lactis* G121 and *A. lwoffii* F78 prevented from ovalbumin-induced allergy *in vivo*

The farming milieu houses a myriad of different bacteria. In the European ALEX study more than 900 farm and non-farm children in Austria, Switzerland and Germany were examined for their prevalence for allergies. In addition, dust and bacteria samples were taken from traditionally run barnyards in Bavaria, and three bacterial species were selected for detailed analyses. These were the Gram-negative *A. lwoffii* F78 as well as the Gram-positive *L. lactis* G121 (**Figure 1.2**) and *Bacillus licheniformis* 467. Characterisation was performed by means of 16S ribosomal deoxyribonucleic acid (rDNA) sequencing and alignment (46,70). Due to their relative abundance and the fact that antibodies against them were detected in the sera of the farm children, it seemed very likely that these organisms occur permanently in the cowshed microflora. *B. licheniformis* 467 spores elevated the IL-12 and interferon (IFN)-γ levels in DC. Contrary incubation of DC with vegetative cells led to higher amounts of T_H2 shifting IL-5 and IL-13 (70).
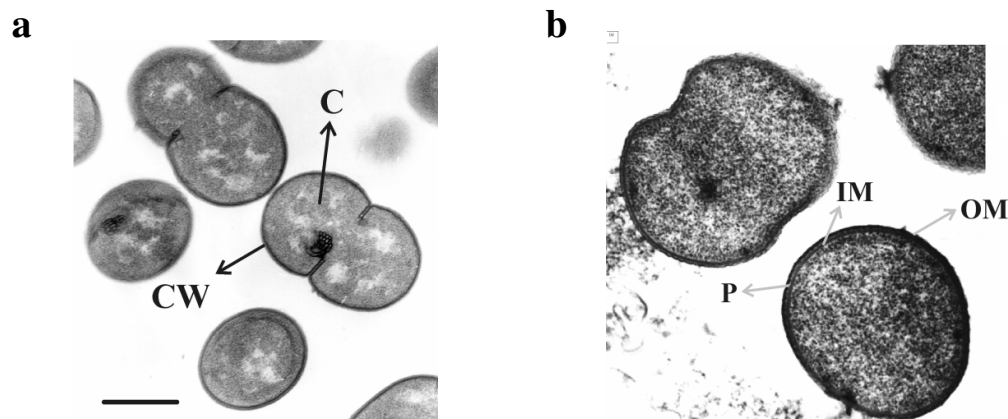
Figure 1.2 Ultrathin sections of a) *L. lactis* G121 and b) *A. lwoffii* F78. Cells were recorded by transmission electron microscopy. The bar corresponds to 0.5 μm. C, cell; CW, cell wall; IM, inner membrane; P, periplasm; OM, outer membrane. With permission of Dr. A. Hanuszkiewicz.

Mutual *in vitro* and *in vivo* studies by Debarry et al. documented the asthma protective features of *A. lwoffii* F78 and *L. lactis* G121. In order to identify innate immune receptors to which the bacteria could bind, transfected human embryonic kidney (HEK)293 cell

assays where performed. *L. lactis* G121 showed signaling via TLR2 and NOD2, whereas *A. lwoffii* F78 activated via TLR2 and TLR4 as well as NOD1 and NOD2.

Further *in vitro* experiments were conducted to define the impact of the bacteria on T_H lymphocyte polarization. Upon treatment of DC total ribonucleic acid (RNA) was extracted after 3, 6 and 12 hours, reverse transcribed into cDNA and transcripts were determined by real-time quantitative PCR. The IL-12 subunit p40 mRNA concentrations were lifted about 200-fold and accordingly the amount of the cytokine IL-12p70 in the DC supernatant after 24 hours was raised. Since IL-12 is an important T_H1 polarizing cytokine, these results indicated that *A. lwoffii* F78 and *L. lactis* G121 conveyed a non-allergic human immune response.

In addition to that, the bacteria were tested in an ovalbumin (OVA)-induced mouse-model of asthma. Therefore 10^8 colony forming units (cfu) of lyophilized bacteria or phosphate-buffered saline (PBS) were applied intranasally every second day beginning 10 days before the first sensitization over the whole sensitization and challenge period. The mice were sensitized to OVA by 3 intraperitoneal injections on days 0, 7, and 14 and on days 19, 20, and 21 OVA was applied per inhalation for allergy provocation. The negative control group received PBS instead of OVA during sensitization and challenge and for treatment.

Cell counts in the bronchoalveolar lavage (BAL) showed only low numbers of neutrophils and lymphocytes notwithstanding the intranasal application every second day and also macrophages were only slightly influenced. Most striking was a significant decrease of eosinophils in the BAL of the bacteria treated mice, proving the suppression of an airway inflammation by *A. lwoffii* F78 and *L. lactis* G121. This suppression was reflected in the lung histology of the mice which had received the bacteria, characterized by minor appearance of eosinophils and mucus-producing goblet cells. The positive control group showed goblet cell hyperplasia and eosinophilia as characteristics for asthmatic bronchi.

Debarry et al. could attribute the allergy-protective properties of *A. lwoffii* F78 to its LPS (47) and Conrad et al. specified the protection happening already *in utero* being transferred from the mother to the fetus via TLR (71).

In order to understand the underlying mechanisms of the asthma protection mediated by *L. lactis* G121 including host immune receptor(s) and signaling route(s), its cell envelope compounds needed to be structurally and functionally defined.

1.2 Processing of bacteria by the human immunity

1.2.1   Pathogen-associated molecular patterns and pattern recognition receptors

As the first line of defense acting 0–4 hours post infection the innate immunity works in an immediate but unspecific way. Certain conserved surface structures from microorganisms such as LPS, PGN or lipoproteins as well as double-stranded (ds)DNA or single-stranded (ss)RNA display common patterns, so called pathogen-associated molecular patterns (PAMP). These are detected by innate pattern recognition receptors (PRR). PAMP do not exist on human cells allowing for clear self-nonself discrimination. PRR are expressed on the surface or in the cytoplasm of macrophages, DC, neutrophils and mast cells. Moreover, PRR occur free in the blood or tissue fluids (72). The expression of innate receptors does not need a rearrangement of gene segments, the distribution is non-clonal and each cell hast the same receptor set enabling an undelayed response (73). If the infection is not cleared, the maintained PRR activation will lead to a release of specific effector molecules which induce adaptive responses.

The activation of PRR initiates 3 different mechanisms depending on the nature of the PRR: phagocytosis, complement activation or killing by anti-microbial peptides. The mannan-binding lectin (MBL), for example, a secreted PRR specifically binds to surface mannose residues abundant on many microorganisms by which the lectin pathway of the complement is initiated and the invader finally will be opsonized (74). Anti-microbial peptides lyse bacteria and they are produced by other bacteria (*E. coli* in the gut, colicins) but mainly by neutrophils (defensins and cathelicidins) (73,75). Direct phagocytosis will be executed upon binding of a PAMP to a surface PRR of macrophages, neutrophils or monocytes. The evolutionary most ancient PRR belong to the family of the Toll-like receptors (TLR). Other PRR such as NOD-like receptors (NLR) and also members of the TLR family are located intracellularly and they signal bacterial fragments or intracellular pathogens like viruses.

1.2.1.1 TLR

The TLR of mammals are homologues to the Toll receptors first discovered in the fruit fly *Drosophila melanogaster*. *Toll* mutants showed high susceptibility to fungal infections indicating an important role for the immunity of the fly (76). To date, thirteen different TLR are described for mammals of which ten (TLR1–10) are expressed in humans (77). The membrane-spanning proteins have different specificities leading to different effects. Thus, the detection of a broad spectrum of the most common microbial patterns is ensured. For activation of TLR dimerization is prerequisite.

Ligands for heterodimers of TLR2/TLR1 are triacylated lipoproteins like, for instance, Lip-OspA from *Borrelia burgdorferi*. In contrast, TLR2/TLR6 heterodimers signal diacylated lipoproteins such as the *Mycoplasma* sp. derived macrophage-activating lipopeptide (MALP-2) (78–80). Previous reports indicated that LTA and PGN are agonists of TLR2 as well, but recent studies with synthetic LTA and pure PGN recalled this assumptions (81–83). The detection of LPS from Gram-negative bacteria by TLR4 homodimers involves two further accessory molecules, namely CD14 and lymphocyte antigen 96 (MD-2) (84). TLR 5 recognizes the highly conserved regions of monomeric flagellin (85). The intracellular TLR3, TLR7, TLR8 and TLR9 are located at the membranes of endosomes or lysosomes and they signal dsDNA, ssRNA, G-rich oligonucleotides and unmethylated CpG DNA, respectively (77). However, the ligand of TLR10 still has to be identified.

All TLR exhibit a leucine-rich repeat (LRR) in their ectodomain which is important for dimerization and ligand binding. Despite the wide range of triggers the activated signal cascade is almost identical for different TLR to our current knowledge. The cytoplasmic residue of each TLR is displayed by the Toll/interleukin-1 (IL-1) receptor (TIR) domain. The TIR domain is involved in forwarding the signal downstream by interaction with the TIR-domain of the adaptor MyD88. The latter recruits the IL-1R associated serine/threonine kinase (IRAK) by interaction of their death domains. Autophosphorylation of IRAK and association of TNF-α receptor-associated factor (TRAF) 6 leads to activation of mitogen-activated protein (MAP) kinases TAK1 and MKK6 which, in turn, execute nuclear factor (NF)-κB, c-Jun N-terminal kinase (JNK) and p38 activation (86,87).

Subsequently, the latter three can translocate into the nucleus and activate the transcription of genes encoding for cell proliferation or inflammatory cytokines (TNF-α, IL-

12p70, and IL-10). Recent studies clearly indicated that TLR work in a synergistic manner (88).

Ultimately, activated TLR will lead to the maturation of DC. By the presentation of antigens on their surfaces DC can prime naïve T-cells and thus initiate adaptive responses (89). T-cell polarization is discussed in chapter 1.2.2.

1.2.1.2 NLR

Microorganisms which could evade recognition by surface receptors will face a second important group of PRR, the NLR, localized in the inside of innate immune cells. So far, 22 NLR proteins could be defined in humans, of which the two main groups are the nucleotide-binding oligomerization domain (NOD1–5) and NACHT-, LRR- and pyrin domain-containing proteins (NALP1–14) receptors, respectively (90). All of them have the conserved central NOD domain (also called NACHT) in common. NLR activate a variety of signaling pathways involved in apoptosis and host defense (91). The topology of NLR was found to be homologous to plant disease resistance proteins illustrating how primordial these receptors are. NLR can be divided in three domains. The C-terminal domain of LRR which is in charge of microbial pattern recognition. The activation signal leads to a self-oligomerization of the central NOD domain enabling the contact of the N-terminal protein-protein interaction effector module to signal downstream. For NOD1 and NOD2 this effector module is the caspase recruitment domain (CARD).

Activated CARD can interact with the serine/threonine kinase RICK which, in turn, activates NF-κB and MAP kinase resulting in transcription of pro-inflammatory cytokines (IL-1, TNF-α) or apoptotic factors (A1, c-IAPs) (92,93). To date, functions of NOD1 and NOD2 are the best explored. Both are PRR for PAMP derived from bacterial PGN. The minimal active motif for NOD1 is γ-D-glutamyl-*meso*-diaminopimelic acid (iE-DAP) which is a dipeptide originating from the DAP-type PGN found in most Gram-negative bacteria and Gram-positive *Bacillus* sp. (94). Opposite to that, is muramyl dipeptide (MDP, *N*-acetylmuramyl-L-alanyl-D-isoglutamine) the minimum necessary structure for activation of NOD2 (95). MDP occurs in DAP-type as well as Lys-type PGN. The latter one is found in most Gram-positive species. MDP and iE-DAP are illustrated in **Figure 1.3**. Besides the role of a first line innate PRR it has been described that NOD1 and NOD2 triggering contributes to adaptive immunity (96). Genetic variations of NOD1 are associated with atopic eczema or asthma whereas NOD2 polymorphisms are considered

as the cause of Crohn's disease (97). Nonetheless, ligands and functions of several NLR remain elusive (90).
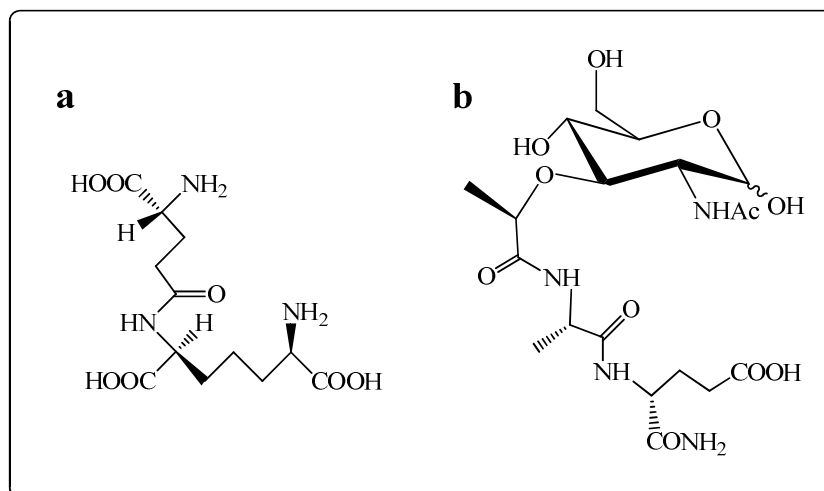
Figure 1.3 Chemical structure of a) iE-DAP, the minimal motif necessary for NOD1 activation and b) MDP, the minimal active structure for NOD2. iE-DAP originates from the DAP-type PGN, mainly found in Gram-negative species and Gram-positive bacilli. MDP is a part-structure of DAP-type as well as Lys-type PGN. The latter one occurs in most Gram-positive bacteria.

1.2.2 T-cell polarization in general, for allergy and for the farm effect

Environmental signals be it pathogens or allergens which are not cleared by the innate immune answer will be recognized by the acquired system. This is realized by antigen-presenting cells (APC) of the innate immune system. Macrophages and DC which have taken up and processed microorganisms display peptides of these on their surface to T-lymphocytes and thereby initiate an adaptive response. With the MHC class I adaptor mostly fragments from viruses are presented and recognized solely by naïve T cells carrying the CD8 adaptor. However, MHC class II molecules are in charge of displaying signals from intra and extracellular microbes as well as eukaryotic parasites. A mature naïve T cell (T_H0) wandering between blood and peripheral lymph tissue will differentiate only per contact to an APC in the lymph nodes (98). The signaling between TCR and MHC molecule just as the signaling between co-receptors (e.g., B7 and CD28) of the APC and the T-cell is necessary for activation and survival, respectively. The third indispensable trigger is the cytokine profile expressed by the APC and in correspondence to the nature of antigen a new subpopulation of effector T cells will be promoted (99). In case of a vi-

rus infection CD8+ cytotoxic T cells will proliferate and kill infected cells (100). CD4+ T cells can divide into 4 different effector types, namely T_H1, T_H2, T_H17 or T_{Reg} cells (101).
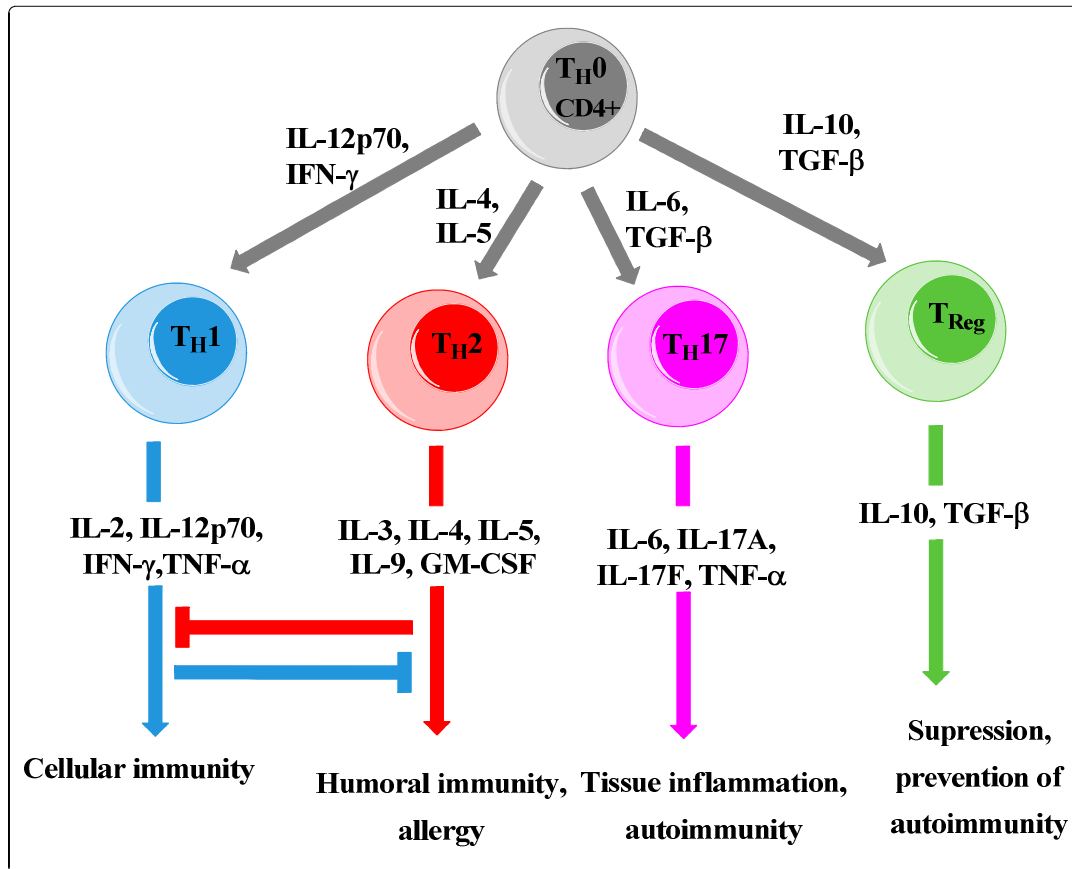
Figure 1.4 Scheme of the T_H lymphocyte polarization. Depending on the antigen being presented and the local cytokine milieu established by macrophages or DC naïve CD4+ T_H0 cells differentiate towards T_H1, T_H2, T_H17 or T_{Reg} effector cells. Each subpopulation of effector cells expresses a specific cytokine pattern which promotes their survival and leads to the different indicated adaptive immune responses. Moreover, the cytokine profiles of the T_H1 and T_H2 population act antagonistically.

As illustrated in **Figure 1.4** each primed subset maintains its own survival and affects other immune cells by specific cytokines. In detail, the T_H1 population secretes IL-2, IL-12p70, IFN-γ and TNF-α essential for proliferation and activation of bacteria loaded macrophages. This effect is denoted as cell-mediated immunity (102–105). The production of the cytokines IL-3, IL-4, IL-5, IL-9, IL-13 and granulocyte-macrophage colony-stimulating factor (GM-CSF) by the T_H2 lineage leads to B-lymphocyte differentiation (isotype switch) and is called humoral immune response. Furthermore, haematopoiesis of macrophages and DC during parasitosis are influenced by these effector cells (98,106,107). Eosinophils, basophils and mast cells also contribute to the T_H2 answer with IL-3, IL-4 and IL-5 (15,108,109). The T_H1 and T_H2 profiles are antagonistic (21,22).

T_H17 cells which defend the host against extracellular invaders attract neutrophils and are promoted by IL-6, IL-17A, IL-17F and TNF-α. Additionally, T_H17 cells are involved in autoimmune reactions (110,111). Only one group of the CD4+ effector subtype has suppressive functions on all other CD4+ populations and these are the T_{Reg} cells. IL-10 and transforming growth factor (TGF)-β are the main cytokines expressed by T_{Reg} contributing to self-tolerance and prevention of autoimmunity just as adaptive immune responses (112,113).

As already mentioned in detail in chapter 1.1.1 in asthma bronchiale the T_H2 phenotype is expressed in an exaggerated manner upon a normally harmless compound. During pregnancy the fetus is in the T_H2 immunological condition contrary to the mothers T_H1 state. This is of tremendous importance for harmless coexistence of both individuals. Discrepancies of this T_H1/T_H2 balance betwixt mother and child are associated with preterm labor and preeclampsia (114). In the first two years of life the effector subtype is then normally shifted towards the healthy non-inflammatory T_H1/T_H2 equilibrium in case of a proper contact to environmental immune stimuli (115,116).

To understand which steps on the cellular level are pivotal for a correct immune deviation many previous, mainly epidemiological, studies were very helpful. Several studies proved an involvement of T_H1 favoring triggers (31,44,46,117,118). *L. lactis* G121 and *A. lwoffii* F78, for instance, induced IL-12p70 in DC *in vitro* (46).

In the birth cohort protection against allergy-study in rural environments (PASTURE) it was shown that the T_H1 promoting IFN-γ in the cord blood from children whose mothers did not farm during pregnancy were significantly reduced. Interestingly the consumption of raw milk products by the mother could be inversely correlated with this finding (119,120). Presenting that a sustained histone acetylation at the *IFNG* promoter in murine offspring was influenced by contact to *A. lwoffii* F78 (121) Brand et al. again pointed out the impact of IFN-γ. This gave completely new insights into an microbacterial-epigenetical mode of action for asthma protection. The relevance of epigenetics has been recently emphasized to link early environmental conditions to the development of chronic inflammatory diseases later in life (122).

Other studies revealed the involvement of innate immune receptors. The prevention of allergy, risk factors for sensitization related to farming and anthroposophic lifestyle (PARSIFAL) study revealed that maternal farming during pregnancy resulted in enhanced

CD14, TLR2 and TLR4 mRNA levels in school-age children. The contact of the mother to a variety of animal species had an impact, in this case, on PRR expression (123). Furthermore genetic variation in TLR2 was concluded to contribute to asthma (124).

Nevertheless, the rather new subgroup of acquired effector cells, the T_{Reg}, were found to be another important or even the most important gateway of keeping the T_H1/T_H2 balance in infants. Schaub et al. demonstrated that the quantity of animals a mother had faced during pregnancy elevated T_{Reg} cells and with it dampened T_H2 cytokine secretion in the cord blood of their neonates (125,126). A high bacterial exposure was proposed to be mediated by DC producing TNF-α which activates T_{Reg}. The model is considered as a natural immunotherapy transmitted from the mother to the child in which IFN-γ is considered as "key mediator of the farm effect" (127).

Additionally the PASTURE project detected a significant rise in allergen specific IgE in the cord blood from children whose mothers did not farm during pregnancy (128). This was a clear proof for the participation of the humoral immunity. Even in school aged farm children the protection from IgE overproduction was demonstrated (129).

An early and frequent contact to the farming environment primes innate immunity mediating a non-allergic T_H1/T_H2 balance maintained by adaptive teammates. It is maternally transmissible and can last life-long (127,130).

1.3 The Gram-positive cell envelope

The PGN of Gram-positive bacteria is, compared to Gram-negative and mycobacterial cell walls, much thicker. But this is not the only difference. The Gram-positive envelope lacks the typical Gram-negative LPS-based outer membrane and harbors instead other cell wall glycopolymers like LTA, WTA or wall polysaccharides (WPS) (131).

Due to its complexity, the PGN (also called murein) sacculus provides an impressive stability (20 atm) and protects the cell from osmotic and mechanical stress (132). The murein backbone is a polymer consisting of *N*-acetyl-β-D-glucosamine (NAG)-(1→4)-*N*-acetyl-β-D-muramic acid (NAM) as indicated in (**Figure 1.5**). The stem peptide attached to the lactyl group of NAM has a primary structure of L-Ala-D-Glu-X-D-Ala. According to the third amino acid (X) in the stem peptide two different PGN types are characterized. The DAP-type PGN carries the *meso*-diaminopimelic (DAP) acid in the third position

whereas the Lys-type PGN harbors L-Lys in that position. Crosslinking between the parallel peptide chains occurs in DAP-type PGN directly between DAP and the terminal D-Ala of the adjacent stem peptide. In contrast many different so called interpeptide bridges facilitate crosslinking in the Lys-type PGN. In *Staphylococcus aureus*, for instance, it is a pentaglycine bridge. Gram-positive species were found to contain DAP-type (*Bacillus* sp.) but mainly Lys-type PGN (132,133).

Fragments of murein display important PAMP for host defense since they are universal in bacteria. The detection by the innate immune receptors NOD1 and NOD2 is described in detail in chapter 1.2.1.2. The intracellular PGN recognition leads to NF-κB activation and release of pro-inflammatory cytokines such as CXCL-8 or TNF-α (95,134,135). Recently, the isolation of NOD1 stimulating DAP-type structures from the supernatant of *Escherichia coli* cultures approved the incidence of immuno-modulative bacterial structures in the environment (136,137). In addition to that, in insects and mammals PGN fragments can be recognized by other soluble peptidoglycan recognition proteins (PGRP). MBL, for instance, detect the NAG moiety and initiate opsonization (138). On the other hand, PGRP-S, -Iα and -Iβ expressed by granulocytes or sweat glands function directly bactericidal (133).

The *O*-6 position of NAM in the backbone serves as connection of the WTA to the PGN via phosphodiesters (139,140). WTA as well as LTA are poly(alditol phosphates). Together with PGN they account for a major part of the cells biomass. A variety of different TA structures have been found since their discovery in 1958 by Baddiley and coworkers (141). Mainly, the backbones of TA consist of either 1,5-poly[D-ribitol phosphate (RboP)] or 1,3-poly[glycerol phosphate (GroP)]. Rather unusual main chains were found for the WTA of *Agromyces cerinus* (arabitol phosphate) and *Glycomyces tenius* (erythritol phosphate) Popular decorations of these polyols are D-alanylation (e.g., *S. aureus* LTA and WTA) and glycosylation by α- or β-D-Glc*p*NAc (e.g., *S. aureus* WTA), α-D-Glc*p* (e.g., *B. substilis* WTA) or α-D-Gal*p* (e.g., *B. megaterium* LTA) (140,142). The backbone of LTA is connected to the *O*-6 of the non-reducing sugar of the lipid anchor via a phosphodiester. Examples of such glycolipid anchors are α-D-Glc*p*-(1→2)-α-D-Glc*p*-(1→3)-diacylglycerol found in *Enterococcus faecalis* and *Streptococcus* species or β-D- Glc*p*-(1→6)-β-D-Glc*p*-(1→3)-diacylglycerol known from staphylococci, bacilli and
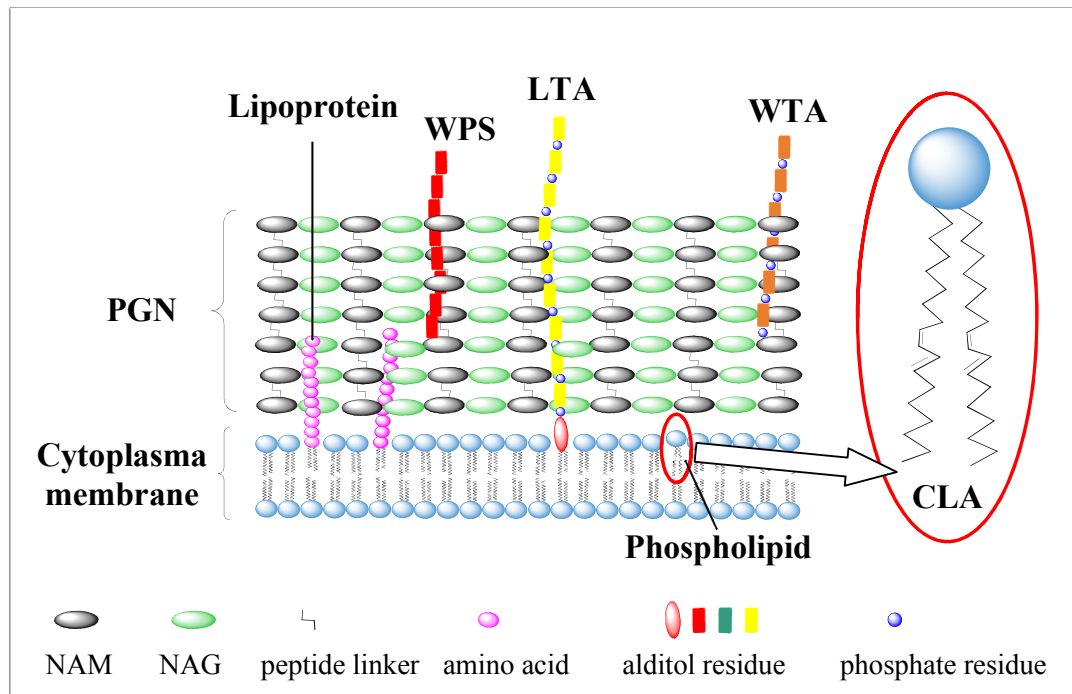
Figure 1.5 The topology of the Gram-positive cell envelope. The lipid bilayer hosts lipoproteins and LTA via their diacylglycerol anchor. The LTA protrudes beyond the PGN sacculus. WTA is covalently linked to the NAM residues of the PGN whereas WPS may be bound to the same residue or occur loosely associated. Additionally, the location of *cis*-9, *trans*-11 CLA as acyl chains of membrane phospholipids is indicated. Further envelope components such as capsular polysaccharides, extracellular polysaccharides or proteins are not illustrated.

other streptococci (142,143). As already mentioned, WTA have no lipid anchor contrary to LTA (**Figure 1.5**) but they are covalently linked to the PGN. A species may have different types of WTA (*B. subtilis*) but only one type of LTA (144). The pivotal role of TA is apparent since they occur in almost every Gram-positive bacterium (e.g., *B. circulans* has no TA). Only recently WTA and LTA deficient mutants have become available (145–147) and we began to understand the full spectrum of functions. The phosphate residues create a negative charge of the main chain and in case of D-Ala substitution TA are negatively as well as positively charged. These zwitterionic and polyanionic wall polymers are involved in pivotal cell processes such as growth, cell division, autolysis, protein secretion, scavenging of Mg^{2+} and electrostatic interactions as well as resistance against antibiotics and lysozyme (147–152).

Several studies indicated that WTA are essential virulence factors for pathogenic species in order to adhere to host tissues and artificial surfaces. Especially in nosocomial infections, for example, with *S. aureus* or *E. faecum* the WTA enabled colonization of im-

plants or the endothelium (147,150,153). It was further shown that the biofilm produced by *S. aureus* contains WTA and is pivotal for invasion (154–156). Up to now, an involvement of WTA structures in signaling through innate immune receptors or activation of immune cells was not reported. Nonetheless, WTA seem to display structures which can be processed by the human immunity since antibodies towards WTA occur in human sera (157,158).

In contrast LTA were described to trigger the production of divers cytokines and chemokines such as IL-1β, CXCL-8, IL-10, IL-23, TNF-α or GM-CSF mainly of hMNC and macrophages (159–163). Furthermore, they possess antigenic function (158,164,165). Initial data presenting TLR2 as well as TLR4 as possible PRR could be attributed to lipoprotein and LPS contaminations, respectively (166–170). Studies with synthetic LTA and H_2O_2 treated preparations enormously contributed to these findings (171–173). The H_2O_2 treatment leads to an inactivation of bacterial lipoproteins by oxidation of the thioether group to the sulfoxide in the invariant *N*-terminal cysteine (78,80). However, the identification of PRR and pathway(s) involved in cytokine release as well as the role of LTA as a PAMP is still challenging.

Another distinct group of amphiphils in the Gram-positive cell wall are lipoproteins. Embedded to the lipid bilayer via their lipid anchor (**Figure 1.5**), just as LTA, lipoproteins probably display the most heterogeneous compound group among bacteria since more than 130 isolates were identified (174). They are involved in membrane phospholipid turnover, protein folding and scavenging of nutrients. Due to their function as substrate-binding protein for ATP binding cassettes (ABC)-transporters they are considered as analogues of the periplasmic proteins in Gram-negative bacteria (175–179). Braun and coworkers identified the first bacterial lipoprotein, from *Escherichia coli* with 58 amino acids and three acyl chains (180,181).

The lipidation of lipoproteins requires 2 steps in Gram-positive bacteria. First, transfer of a diacylglycerol residue to the sulfhydryl group of the invariant *N*-terminal cysteine of the peptide precursor by the lipoprotein diacylglycerol transferase (Lgt). Second, the cleavage of the signal peptide by the enzyme lipoprotein signal peptidase (Lsp). The signal peptide is the *N*-terminal sequence bound to the cysteine and carries the so called lipobox motif (typically $L_{-3}–(A/S/T)_{-2}–(G/A)_{-1}–C_{+1}$), a recognition sequence characteristic for all prelipoproteins (182). The cleavage of the signal peptide from the amino function of the

cysteine leaves the diacylated lipoprotein in the outer face of the membrane. In addition to that, a third enzyme, the lipoprotein *N*-acyl transferase (Lnt), may in Gram-negative bacteria add a third acyl chain to the amino function of the cysteine (177,179). *Lgt, lsp* and *lnt* are indispensable for viability and especially outer membrane construction in Gram-negative species (183). However, during the last decade several Δ*lgt* mutants from Gram-positive species such as *S. pneumoniae, B. subtilis and S. aureus* could be generated indicating that the Lgt protein is remissible for those bacteria at least for viability. Thus, the *lgt* knockout displays a promising tool for the investigation of structure-function relations of lipoproteins from any desired Gram-positive bacterium (184–186).

Lipoproteins containing three fatty acids (FA) (e.g., Lip-OspA from *B. burgdorferi*) are known ligands of TLR2/TLR1 heterodimers whereas lipoproteins furnished with two FA (e.g., MALP-2 from *Mycoplasma* sp.) have shown to activate TLR2/TLR6 heterodimers (78–80). The signal cascade of TLR activation is explained in detail in chapter 1.2.1.1. Picomolar quantities of MALP-2 were described to be able to activate macrophages (78,187).

Besides the diacylglycerol anchors of LTA and lipoproteins the lipid bilayer is mainly composed of phospholipids (**Figure 1.5**). The glycerol attached acyl chains of the hydrophobic part vary from 14 to 20 carbons and *cis* double bonds as well as *iso* and *antheiso* methyl branches are common. To maintain membrane fluidity bacteria are able to regulate the *de novo* biosynthesis. The so called homoviscous adaption enables the response to changes in temperature, osmolarity and pH (188). A second mechanism leads to the alteration of already existing FA which is important to react to rapid environmental changes especially in periods of limited nutrition. Free living bacteria often face such situations. *B. subtilis*, an ubiquitous soil bacterium, is able to introduce a *cis* double bond into saturated FA (SFA) with a desaturase (189). Unsaturated FA (UFA) as well as poly UFA (PUFA) lead to an increase in the membrane fluidity due to the kink caused by the double bond (175). An important group of PUFA are the isomers (mainly *cis*- and *trans*-9,11- and -10,12) of the conjugated linoleic acid (CLA, 18:2, **Figure 1.5**). They can be isomerized by bacteria from other PUFA [e.g., linoleic acid (LA)] during starvation as well as by ruminal bacteria during digestion processes. The natural CLA enrichment of dairy products was clearly related to PUFA rich fodder. Since CLA are discussed as allergy suppressive and anti cancerogenic agents a possible enrichment of food with the help of bacteria is examined by the dairy industry (119,190–195).

The makeup of the Gram-positive cell envelope gains further complexity by WPS which are located within the PGN layer and may be covalently linked to it. From that capsular polysaccharides (CPS) are distinguished by their outermost and coating position and may be as well covalently linked or loosely associated to the PGN. Additionally, extracellular polysaccharides (EPS), which have no connection to the wall at all but are released to the environment, can occur. However, differentiation between these three is often difficult (132).

2 Aims of the Study

The significant lower incidence of atopic sensitizations such as asthma bronchiale, hay fever or dermatitis in children from the traditional farming environment compared to non-farming children has been proven in a multitude of epidemiological studies. In line with the ALEX study, dust samples were collected from animal sheds and farm children's mattresses. Besides plant derived compounds, fungi (*Mucor* ssp.), the Gram-negative *A. lwoffii* F78 as well as *L. lactis* G121 and the spore forming *B. licheniformes* 467 (both Gram-positive) were selected to be studied in detail with regard to their anti-allergic properties.

Mouse experiments demonstrated that the mentioned microorganisms and a 0.9% saline extract of the dust samples prevented the mice from OVA induced allergy. After profound investigations during the last years we know now that arabinogalactan was one of the anti-asthmatic components from dust extract, that vegetative cells of *B. licheniformes* evoked T_H2 responses and that the allergy protection of *A. lwoffii* F78 was conveyed by its LPS. So far, the results observed *in vivo* for *L. lactis* G121 were very promising but were not yet related to a defined cell component. Since the cell envelope as the outer border of a bacterium displays the first surface of contact the focus was on wall polymers.

The main question of this thesis was: "can the protective property be attributed to one or more specific bacterial structure(s)?" LTA, WTA and PGN have been described in literature to evoke innate or even adaptive responses of the human immunity. Therefore, this study intended their isolation and structural as well as immunological characterization. Bacterial lipoproteins are known TLR2 ligands but pure isolation is difficult to achieve. Hence, another aim of this study was the generation of a Δ*lgt L. lactis* G121 mutant deficient in lipidation of prelipoproteins. Such a mutant was thought to be useful to investigate the role of lipoproteins for the allergy-protection. Furthermore, the ability of *L. lactis* G121 to accumulate CLA was tested because this was shown for another lactic acid bacterium (LAB) and because CLA were reported to possibly contribute to the attenuation of airway inflammation.

This thesis in particular aimed to contribute to the:

1. Evaluation of existing methods for isolation of cell wall compounds.

2. Pure isolation of cell wall structures from *L. lactis* G121.

3. Structural analysis of obtained compounds by means of chemical composition analysis, high-resolution electrospray ionization Fourier-transformed ion cyclotron mass spectrometry (ESI FT-ICR-MS) and high-resolution nuclear magnetic resonance (NMR) spectroscopy.

4. Investigation of the biological relevance of pure wall compounds *in vitro* by transiently transfected HEK293 assays or stimulation of hMNC.

5. Correlation of the T_H1 promoting effect of *L. lactis* G121 to one or more defined cell wall structures.

3 Materials and Methods

3.1 Reagents, nutrients and kits

Table 3.1 Chemicals, reagents, growth media and kits used in this work.

Item	Manufacturer
(R)-and *(RS)*-butan-2-ol	Sigma-Aldrich
Acetic acid	Merck
Acetic anhydride (Ac$_2$O)	Sigma-Aldrich
Acetone	Merck
Acetonitrile ROTISOLV® (CH$_3$CN)	Roth
Agarose	Beckton Dickinson
Alkaline phosphatase from bovine intestinal mucosa	
≥ 4,000 DEA units/mg protein	Sigma-Aldrich
Ammonium acetate (NH$_4$Ac)	Merck
Ammonium bicarbonate (NH$_4$HCO$_3$)	Merck
Ammonium heptamolybdate [(NH$_4$)$_6$Mo$_7$O$_{24}$ × 4 H$_2$O]	Merck
Ampicillin (Amp)	USB Products
Aqua bidest. pyrogen free	Millipore
Ascorbic acid	Merck
Bacto tryptone	Beckton Dickinson
*Bam*HI 20 kU/ml	New England Biolabs
Bio-Gel P-2, P-10 and P-60 all fine	Bio-Rad
Boric acid	Roth
Bromophenol blue	Merck
BSA 100 ×	New England Biolabs

Table 3.1 continued

Calcium chloride dihydrate (CaCl$_2$ × 2H$_2$O)	Merck
Ceric sulfate tetrahydrate [Ce(SO$_4$) × 4 H$_2$O]	Merck
Chloramphenicol (Cm)	Roth
Chloroform LiChrosolv® (CHCl$_3$)	Merck
Citric acid monohydrate	Merck
CLA-ME standard mixture of *cis*- and *trans*-9,11- and -10,12-octadecadienoic acid methyl esters	Sigma-Aldrich
D,L threonine	Serva Feinbiochemica
Deoxynucleotides (dATP, dTTP, dGTP, dCTP)	Invitrogen
Deuterium oxide 99.9% and 99.98% (D$_2$O)	Deutero
Diethyl ether	Merck
Dimethyl sulfoxide (DMSO)	Merck
Dimethylformamid (DMF)	Merck
Dipotassium phosphate (K$_2$HPO$_4$)	Merck
Disodium phosphate (Na$_2$HPO$_4$)	Merck
DNA Clean & Concentrator™-5	Zymo Research
DNase I from bovine pancreas	
≥ 400 Kunitz units/mg protein	Sigma-Aldrich
*Dpn*I 20 kU/ml	New England Biolabs
ELISA for IL-6 and CXCL-8 detection	Invitrogen
Erythromycin (Ery)	Sigma-Aldrich
Ethanol (EtOH)	Merck
Ethidium bromide (EtBr)	Sigma-Aldrich
FD buffer 10 ×	Fermentas
Gene Ruler™ 1 kbp Plus DNA ladder	Fermentas

Table 3.1 continued

Genome Walker Universal Kit™	Clontech
Glucose	Roth
Glycerol	Merck
Glycine	ICN Biomedicals
4-(2-hydroxyethyl)-1-piperazineethanesulfonic acid (HEPES)	Sigma-Aldrich
Heptadecanoic acid (17:0)	Sigma-Aldrich
High Pure PCR Product Purification Kit	Roche
HiPrep Octyl FF 16/10 column	GE Healthcare
HiTrap Q-Sepharose® Fast Flow column	GE Healthcare
Hydrazine (N_2H_4)	Eastman Kodak Company
Hydrochloric acid (HCl)	Merck
Hydrofluoric acid (HF)	Merck
Hydrogen peroxide (H_2O_2)	Merck
IPTG	MP Biomedicals
Jupiter Proteo RP-12 250 × 4.6 mm column	Phenomenex
Kanamycin (Kana)	Roth
KOD polymerase	Novagen
KOD polymerase buffer 10 ×	Novagen
Lab Pack Sephacryl S-200	
High resolution in 20% ethanol	GE Healthcare
Lactose	Merck
LA	Sigma-Aldrich
Lithium chloride (LiCl)	Merck
Lysozyme from chicken egg white 49.7 kU/mg	Sigma-Aldrich

Table 3.1 continued

M17 broth	Beckton Dickinson
Magnesium chloride (MgCl$_2$)	Merck
Magnesium sulfate heptahydrate (MgSO$_4$ × 7 H$_2$O)	Sigma-Aldrich
Methanol LiChrosolv® (MeOH)	Merck
Mutanolysin from *Streptomyces globisporus*	
ATCC 21553 ≥ 4,000 units/mg protein	Sigma-Aldrich
n-Butanol (BuOH) LiChrosolv®	Merck
NEB 1 buffer 10 ×	New England Biolabs
NEB 2 buffer 10 ×	New England Biolabs
NEB buffer *Bam*HI 10 ×	New England Biolabs
NEB buffer T4 ligase 10 ×	New England Biolabs
*Nhe*I not determined (n.d.) U/ml	Fermentas
n-Hexane	Merck
Nitrogen (N$_2$)	Linde
n-Propanol CHROMASOLV®	Sigma-Aldrich
Nuclease free water	Gibco
Pam$_3$C-SK$_4$	EMC Microcollections
Penicillin	Biochrom
Phenol	Merck
Phenol solution - equilibrated with 10 mM tris(hydroxymethyl)aminomethane (Tris)-HCl, pH 8.0, 1 mM ethylenediaminetetraacetic acid (EDTA)	Sigma-Aldrich
Phenyl isothiocyanate	Waters
Pico·Tag diluent	Waters
Pico·Tag HPLC column	Waters

Table 3.1 continued

Platinum dioxide hydrate (PtO_2)	Ventron
Potassium chloride (KCl)	Merck
Potassium dihydrogen phosphate (KH_2PO_4)	Merck
Potassium hydroxide (KOH)	Merck
Proteinase K	Roche
Pyridine	FLUKA
QIAGEN PCR Cloning Kit	Qiagen
Recovery medium	Lucigen
RNase A from bovine pancreas	
50-100 Kunitz units/mg protein	Sigma-Aldrich
*Sac*I 20 kU/ml	New England Biolabs
Sephadex G10	Pharmacia
Sodium acetate (NaAc)	Merck
Sodium azide (NaN_3)	FLUKA
Sodium borohydride ($NaBH_4$)	Merck
Sodium borodeuteride ($NaBD_4$)	Sigma-Aldrich
Sodium chloride (NaCl)	Merck
Sodium citrate	Merck
Sodium dodecylsulfate (SDS)	Bio-Rad
Sodium hydroxide (NaOH)	Merck
*Sph*I 10 kU/ml	New England Biolabs
Streptomycin	Biochrom
Sucrose	ICN Biomedicals
Sulfuric acid (H_2SO_4)	Merck

Table 3.1 continued

T4 DNA ligase 2 MU/ml	New England Biolabs
TA Cloning® Kit	Invitrogen
Taq polymerase 10 U/µl	Fermentas
Taq polymerase buffer 10 ×	Fermentas
Titriplex III® EDTA	Merck
Toyopearl HW-40S	Sigma-Aldrich
Trichloroacetic acid (TCA)	Roth
Triethylamine	Sigma-Aldrich
Trifluoroacetic acid (TFA)	Merck
Tris	ICN Biomedicals
Trisodium citrate dihydrate	Merck
Triton® X-100	Sigma-Aldrich
Trypsin from bovine pancreas	
10–15 kBAEE units/mg protein	Sigma-Aldrich
Tryptic soy broth (TSB)	Beckton Dickinson
Tryptone-peptone	Beckton Dickinson
Tween® 80	Sigma-Aldrich
UltraPure™ agarose	Invitrogen
UltraPure™ low melting point agarose	Invitrogen
Wizard® *Plus* SV Minipreps DNA Purification System	Promega
X-Gal	Appligene
*Xma*I 10 kU/ml	New England Biolabs
Yeast extract	Beckton Dickinson
α-Amylase	Sigma-Aldrich

3.2   Laboratory devices and consumables

Table 3.2 Instruments, devices and disposables used in this study.

Item	Manufacturer
0.1- and 0.2-cm gap electroporation cuvettes	Bio-Rad
Acrodisc® syringe filter with GHP membrane 0.45 µm for HPLC samples	Pall Corporation
Analytical balance	Kern
Autoclave V 150	Systec
Cell disintegrator	B. Braun
Centrifuge Avanti J-26xP	Beckman Coulter
Centrifuge Rotanta 460 RC	Hettich
Centrifuge tubes 250 and 1000 ml	Beckmann-Coulter
Filter for organic and watery solutions 0.45 µm	Dionex
Flow box Hera Safe	Heraeus Instruments
FPLC Äkta P-950	Amersham Pharmacia Biotech
Fraction collector FC 203B	Gilson
Gel documentation	Biometra TI 3
Gene Pulser®	Bio-Rad
GeneAmp PCR system 9700	PE Applied Biosystems
Glass beads 0.1 mm	Roth
HPLC 15X UV/VIS detector	Gilson
HPLC 506C system interface	Gilson
HPLC GX direct injection module	Gilson
HPLC pump 305/306	Gilson
Mars 1200 biohazard safety cabinet	Scanlaf

Table 3.2 continued

Membrane pump	Vacuubrand
Membrane tubing 3.5 or 16 ku	Spectra/Por
Microcentrifuge Rotina 380 R	Hettich
NMR sample tubes 3 and 5 mm diameter	Norell
Power PAC™ 300 power supply	Bio-Rad
RI detector K2301	Knauer
SEC pump Minipuls S3	Gilson
Silica gel 60 WF254S TLC aluminum plates	Merck
Sterile filter membranes	
for syringes 0.22 and 0.45 µm	Sarstedt
Steritop™ Filter Units 0.22 µm	Millipore
Ultracentrifuge TLA-100.3	Beckmann
UV spectrometer MBA 2000	Perkin Elmer
UV/VIS spectrometer Helios ε	Thermo Spectronic
Vibrogen cell mill	Edmund Bühler

3.3   General methods

3.3.1   General recommendations

For all buffers and solutions prepared for structural analyses, pyrogen-free deionized water of bidest. quality was used produced with a Milli-Q device. Furthermore, all glassware underwent special heating of 4 hours at 240°C to inactivate endotoxin. This handling was an important prerequisite to prevent any interference of biological data caused by LPS contaminations. All buffers were sterilized by filtration through a 0.22-µm membrane, and media were autoclaved (15 minutes, 121°C, 200 kPa).

3.3.2   Growth and harvest of *L. lactis* G121

L. lactis G121 was isolated from a traditionally run farm in Bavaria/Germany and identified by means of 16S rDNA sequence analyses as described elsewhere (46). Growth conditions were adopted from previous studies performed by Dr. A. Hanuszkiewicz (196). Accordingly, *L. lactis* G121 was cultivated either on TSB (Tryptic Soy Broth; supplemented with 0.3% yeast extract) agar (1.5%) plates or as TSB liquid cultures at 30°C and 170 rpm. A single colony from an agar plate was used to inoculate the pre-culture, which was further used to inoculate the main batch. The biomass was harvested by centrifugation at 4°C and 3,000 g for 15 minutes and washed twice with PBS.

PBS	Solution 1:	$Na_2HPO_4 \times 2\ H_2O$	13.35 g
		NaCl	12.9 g
		H_2O	1500 ml
	Solution 2:	KH_2PO_4	3.40 g
		NaCl	4.0 g
		H_2O	500 ml

Solution 1 and 2 were combined and gave pH 7.2

3.3.3   Size-exclusion chromatography

For size-exclusion chromatography (SEC), Bio-Gel (P-2, P-10, P-60), Sephadex (G10) and Toyopearl (HW-40S) matrices were utilized in glass columns. A peristaltic pump was used to assure a constant flow rate, whereas P-2 separations were run without the pump. Fractions containing the separated samples were identified with a refractive index (RI) detector, collected with an automated fraction collector, and chromatograms were recorded with the software Clarity (Data Apex). The corresponding peak fractions were pooled, evaporated and lyophilized. The following buffer was used:

Pyridinium acetate buffer (PAW)	Pyridine	50 mM
	Acetic acid	160 mM
	In H_2O, pH 4.7	

3.3.4   Agarose gel electrophoresis

Genomic DNA, plasmids and DNA fragments were subjected to electrophoresis using 0.8% agarose gels in 1 × TBE buffer. Mixtures of 1 µl sample, 4 µl TE buffer and 1 µl 6 × loading buffer were prepared and analyzed alongside with the Gene Ruler™ 1 kbp Plus DNA ladder (0.5 µl of a 0.5 µg/µl stock). The electrophoresis was run at 80 V in 1 × TBE buffer, followed by staining of the DNA in EtBr solution (1 mg/l) for 10 minutes. After an additional incubation time for 15 minutes in H_2O to allow for de-staining of the background of the gel, the DNA samples were visualized by UV light at 312 nm.

5 × TBE buffer	Tris	54.5 g/l
	Boric acid	28 g/l
	EDTA	10 mM
	pH 8.2	

TE buffer	Tris	10 mM
	EDTA	1 mM
	pH 8.0	

| 6 × Loading buffer | Glycerol | 50 ml |
| | Bromophenol blue | 0.372 g |

3.3.5   Purification of plasmids and DNA samples

Plasmids were isolated and purified with the Wizard® *Plus* Minipreps DNA Purification System. The kit is based on the alkaline SDS method for isolation of plasmid DNA as

originally described by Birnboim & Doly (197). Briefly, the cells of a 5-ml 12-hours culture grown at 37°C in lysogeny broth (LB) containing 100 µg/ml ampicillin were harvested and subsequently treated with a solution containing SDS and NaOH. As a result, the cells were disintegrated, leading to release of denatured genomic and plasmid DNA under the alkaline conditions. While neutralization of the sample by addition of an acidic KAc solution resulted in renaturation of the plasmid DNA, the genomic DNA remained denatured and precipitated together with denatured proteins. A centrifugation step yielded the plasmid DNA in the supernatant, which was then loaded onto a SiO_2 matrix miniprep column. Repeated centrifugation steps with wash buffer containing EtOH separated contaminating cell material. Finally, the plasmid DNA was eluted with nuclease-free water and analyzed by 0.8% agarose gel electrophoresis. PCR products and DNA inserts digested with restriction endonucleases were purified in exactly the same way using the High Pure PCR Product Purification Kit. Recombinant DNA of ligation mixtures was purified with the DNA Clean & Concentrator™-5 Kit prior to transformation by electroporation.

LB (Lennox)		
	Tryptone	10 g/l
	Yeast extract	5 g/l
	NaCl	5 g/l
	Agar	15 g/l

3.4   Washed biomass assay for determination of CLA (190)

According to Macouzet et al. a 12-hours culture of *L. lactis* G121 served for inoculation of 1.5 l TSB (1% by vol), which were cultivated and harvested after 24 hours under indicated conditions. The cell pellet was washed 2 times with PBS, dissolved in 180 ml of PBS and aliquots underwent two different preparations. Treatment A was the washed biomass assay (WBA)-control with a final concentration of 0.2% Tween®80 as the emulsifier of treatment B, which was the WBA-sample with a final concentration of 1.4 mᴍ linoleic acid (LA). Treatment A and B were incubated at 20–22°C with slight mixing (50 rpm). After 24, 48 and 72 hours, the samples were centrifuged and biomass and supernatant were lyophilized and subjected to conjugated linoleic acids (CLA).

Cfu of treatment A and B after 24 hours were determined for *in vivo* analysis of the biomass. These are performed by Hani Harb (University of Marburg) from the SFB TR22 platform Z02.

3.5   Combined method for isolation of LTA, WTA and PGN

In order to obtain LTA, WTA and PGN from one batch of growth a method was developed based on the work of de Jonge et al., Morath et al. and Sánchez-Carballo et al.(198–200). Therefore, *L. lactis* G121 was harvested after 12 hours and cells were kept on ice to minimize autolysis of PGN. The cell pellet was dissolved in ice-cold citric buffer and transferred drop-wise to a boiling SDS solution reaching 4% final concentration continuing boiling for 30 minutes. This step is supposed to inactivate PGN degrading autolysins. Disruption of the bacterial cells succeeded with the Vibrogen cell mill. A maximum of 40 g wet biomass/100 ml citric buffer was added to an equal volume of glass beads (0.1 mm) and disrupted for 3 minutes. The mixture was centrifuged (2,000 *g*, 10 minutes, 4°C) to separate the beads from the debris and the beads were washed two more times with citric buffer.

The combined supernatants were boiled once more in a final content of 4% SDS in order to bind the LTA to it. Centrifugation (30,000 *g*, 15 minutes, 4°C) for isolation of the SDS-LTA was conducted and the PGN and TA containing pellet was washed 6 times with citric buffer. Spots of 2 µl of the citric buffer re-suspended pellet on a silica gel plate were compared to a 2 µl spot of 1% SDS checking if the pellet was SDS free. The thin-layer chromatogram (TLC) was developed in MeOH/CHCl$_3$/AcOH (60:40:1.5 by vol) and stained with Mo-stain. The SDS-LTA containing supernatants were consecutively lyophilized and then washed 10-fold with EtOH for removal of SDS. Thereafter, the pellet of crude LTA was subjected to *n*-butanol extraction and hydrophobic interaction chromatography (HIC) as specified in chapter 3.6.

The PGN and WTA comprising pellet (after six-fold citric buffer washing) was washed with 5% trichloroacetic acid (TCA, 5,000 *g*, 20 minutes, 4°C) and incubated in 5% TCA for 24 hours at 4°C for cleavage of the WTA from the PGN sacculus. Subsequently the mixture was centrifuged (5,000 *g*, 20 minutes, 4°C) to obtain the TA in the supernatant. The extraction was repeated twice. As a last step the three combined TCA isolates were dialyzed against 50 mM NH$_4$Ac [4-5 days, 3.5 ku molecular mass cut off (MMCO)] with

one water change per day. The lyophilized retentat was then further purified by HIC and anion-exchange chromatography (AEX) as described in chapter 3.8.

The remaining pellet after three-fold 5% TCA hydrolysis was treated with a number of enzymes to dissect the insoluble PGN scaffold from other undesired macromolecules. Therefore, the pellet was dissolved in 100 mM Tris-HCl (pH 7.5) and digested with α-amylase (100 µg/ml) for 2 hours at 37°C. DNase (10 µg/ml), RNase (50 µg/ml) and MgSO$_4$ (20 mM) were added and incubation proceeded for further 2 hours. Afterwards the mixture was adjusted to 10 mM CaCl$_2$ and the digest with trypsin (100 µg/ml) was performed for 16 hours at 37°C. Boiling for 15 minutes in 1% SDS inactivated all enzymes. SDS, digestion fragments and enzyme residues were removed by the following washing steps: six-fold washing with H$_2$O (30,000 g, 10 minutes, 4°C), once with LiCl (8 M), once with EDTA (100 mM), twice with H$_2$O and twice with acetone. The resulting pellet was lyophilized and phosphate bound components were cleaved by 48% HF for 48 hours at 4°C. Neutralization of the reaction mixture was achieved with 4 M KOH. Then centrifugation (30,000 g, 1.5 hours, 20–22°C) and washing (15 minutes) twice with H$_2$O, once with Tris-HCl (100 mM, pH 7.5) and four-fold with H$_2$O was carried out.

Finally, the freeze dried insoluble PGN isolate (1 mg/ml) was digested with mutanolysin (5 µg/ml) in 12.5 mM phosphate buffer (pH 5.5) and 0.02% NaN$_3$ at 37°C for 16 hours. Mutanolysin is a muramidase which hydrolyzes the β-glycosidic (1→4) bond between NAM and NAG within the murein. The solubilized PGN sample was boiled for 5 minutes, cooled to 20–22°C and centrifuged (45,000 g, 10 minutes, 20–22°C). The remaining pellet underwent again mutanolysin cleavage. Reduction of the muramyl residues was not performed, thus leaving the structures as natural as possible. In chapter 3.7 the purification of the PGN fragments by Toyopearl HW-40S SEC and C-12 reverse-phase high-performance liquid chromatography (RP-12 HPLC) is explained. **Figure 3.1** gives an overview on the combinatory method developed for isolation of LTA, WTA and PGN from one batch.

Citric buffer   Solution 1:   0.1 M citric acid monohydrate   21 g/l

                             Solution 2:   0.1 M trisodium citrate dihydrate   29 g/l

                             400 ml of solution 1 and 600 ml of solution 2 were combined
                             and resulted in pH 4.7

Mo-stain H_2O 471 ml

                             H_2SO_4 29 ml

                             $Ce(SO_4) \times 4\ H_2O$ 0.5 g

                             $(NH_4)_6Mo_7O_{24} \times 4\ H_2O$ 25 g

                             Development at 150°C until spots appear blue

Phosphate buffer (12.5 mM)   PBS ($\triangleq$ 50 mM) 1:4 diluted, pH 5.5
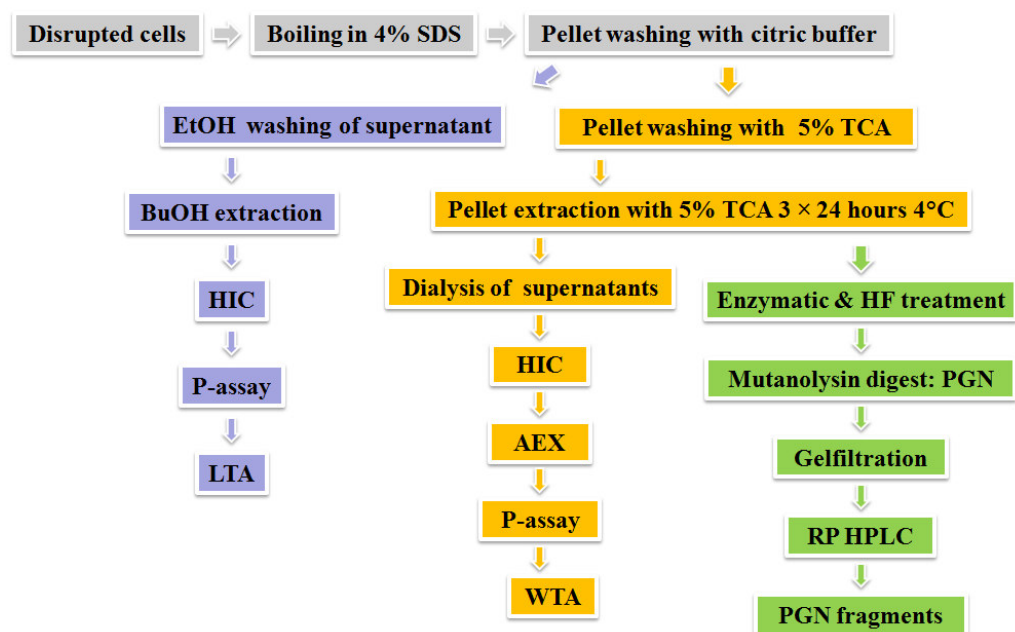
Figure 3.1 Scheme of the main steps during simultaneous isolation of LTA, WTA and PGN. The method was developed by connection of three published methods from Morath et al., Sánchez Carballo et al. and de Jonge et al. in order to obtain these cell envelope constituents from a single culture.

3.6   Purification of LTA

3.6.1   Butanol extraction of LTA (199)

The butanol extraction as well as the HIC purification of LTA have been conducted according to Morath et al. Therefore the crude LTA pellet after EtOH washing was re-suspended in citric buffer, an equal volume of *n*-butanol was added and the suspension was stirred for 30 minutes at 20–22°C. Centrifugation (13,000 *g*, 20 minutes, 20°C) was applied separating the watery from the butanol phase. After this dialysis of the LTA-comprising watery phase against 50 mM NH_4Ac (4-5 days, 3.5 ku MMCO) was performed with one water change per day followed by lyophilization and subjection to HIC.

3.6.2   HIC of LTA

The crude LTA obtained from *n*-butanol isolation was purified by a method actually originating from fast protein liquid chromatography (FPLC). The reversible interaction between the lipids of the LTA and the hydrophobic column material was utilized to separate it from nucleic acids or proteins. The sample was re-suspended in buffer A (0.1 M NH_4Ac in 15% *n*-propanol, max. 15 mg/ml), insoluble material was separated (45,000 *g*, 3 minutes, 20–22°C) and the supernatant was filtrated (0.45 µm). One ml per HIC run was injected on the HiPrep column (100 × 16 mm, bed volume 20 ml) of octyl sepharose and a flow of 2 ml/minute was applied. High salt concentrations in the start buffer A retained the sample to the column and a linear decreasing salt gradient over 60 minutes to 100% buffer B (0.1 M NH_4Ac in 60% *n*-propanol) eluted the LTA in the middle of the gradient. A photometric phosphate assay (chapter 3.10.2) served for identification of LTA. Phosphorus-containing fractions were pooled and washed four-fold with H_2O by lyophilization for removal of the volatile NH_4Ac buffer from the pure LTA.

3.6.3   LTA treatment with H_2O_2 (80)

Following Zähringer et al. LTA samples investigated biologically were pre-treated with 1% H_2O_2 at 37°C for 24 hours. Lyophilization of the sample evaporized the H_2O_2 afterwards. This procedure inactivated any possible contaminating lipoproteins which have shown to be co-isolated with LTA. Thus, the thioether moiety on the N-terminal cysteine of each lipopeptide- and protein was oxidized to a sulfoxide leading to a loss of TLR2

ligand function (78). This step was important for a doubtless attribution of a possible activation for example of HEK293 cells via TLR2 to LTA solely.

3.7   Separation of PGN fragments

3.7.1   SEC on Toyopearl HW-40S

The digest of the PGN sacculus with mutanolysin resulted in a myriad of different undefined PGN fragments. In a first attempt the sample was subjected to gel filtration giving a rather rough pre-separation depending on the size of the substances. This separation was not supposed to yield molecules varying in one amino acid but grouping them into mono-, di-, tri-, and tetramers. For this purpose a glass column of 120 cm length and 2.5 cm diameter was packed with Toyopearl HW-40S hydroxylated methacrylic polymer that offered an exclusion limit of about 10 ku. The PGN samples were eluted with PAW buffer at a flow of 0.4 ml/minute.

3.7.2   HPLC with Jupiter Proteo RP-12 (201)

In order to obtain defined PGN fragments in mg scale for testing their biological activity an HPLC method had to be established. Therefore, experiments were carried out on an analytical column (150 × 0.5 mm) of silica gel modified with C-12 alkyl chains with a particle size of 90 Å (Jupiter Proteo), which was recommended by the supplier to separate peptides differing in one amino acid. The sample was dissolved in H_2O and first a 100 µg sample per 100 µl injection was tested. A gradient system of buffer A (0.1% TFA in H_2O) and buffer B (0.1% TFA in CH_3CN) was checked for reproducible dissociation of PGN fragments. The program started from 2% buffer A for 10 minutes, and variations of buffer B (100%–10%) as well as gradient length were checked. Detection of the substances was achieved by UV light monitoring at 206 nm at a flow rate of 1 ml/minute. ESI-MS spectrometry was used to analyze eluted substances.

3.8   Purification of WTA

3.8.1   HIC of WTA

With the intention to rule out any possible lipophilic contaminants from the WTA extract and to assure that the glycerol phosphate repeats do not originate from LTA, samples were subjected to HIC (156). The method used was identical to LTA purification with the difference that WTA did not retain to the octyl-sepharose material and thus, eluted in the void volume. Detailed HPLC conditions are given at chapter 3.6.2 and the WTA was detected with the phosphate assay described in chapter 3.10.2.

3.8.2   AEX

After HIC the TA sample underwent a second chromatographic separation step. The AEX on HiTrap Q-Sepharose was described to be useful to separate neutral polysaccharides (155,156). The TA probe ($\leq$ 50 mg) was injected dissolved in 2 ml H_2O. With a flow of 3 ml/minutes H_2O was run during the first 10 minutes adsorbing the negatively charged TA to the quaternary amine (NR_4^+) groups. Then the gradient was changed to 1 M NaCl within one hour eluting the TA around 0.2 M NaCl. For 10 minutes 1 M NaCl was kept and finally the gradient went to 2 M NaCl for 10 minutes. Fractions were detected at UV light of 220 nm and additionally the phosphate assay explained in chapter 3.10.2 was performed to identify the TA. For desalting of the fractions SEC on Sephadex G10 material was an appropriate method using PAW buffer with a flow of 0.5 ml/minute.

3.9   Isolation and purification of CPS

The components of the CPS could be elucidated in parts by Dr. A. Hanuszkiewicz (196). For the completion of the structure the lyophilized biomass of a 10 l 24-hours culture of *L. lactis* G121 was dissolved in 900 ml of sterile 0.9% NaCl solution and extracted for 6 hours at 20–22°C at 170 rpm. The NaCl extract after centrifugation (10,000 *g*, 45 minutes, 4°C) was then dialyzed (3–4 days, 3 water changes per day, 16 ku MMCO) against 0.02% NaN_3 and lyophilized. Immediately after centrifugation the residual pellet was put to 1% phenol extraction for 48 hours at 4°C and gentle stirring. Likewise the phenol extract was centrifuged, dialyzed and lyophilized (Ph extract). In the next step SEC of both extracts was conducted, separately. Therefore, these were first applied to a

column (80 × 2.5 cm) of Bio-Gel P-60 and nucleic acid free fractions were further puri-fied on a column of Bio-Gel P-10 (80 × 1.5 cm). The samples were eluted with PAW without using a pump. The nucleic acid content of fractions (0.5 mg/ml and 0.1 mg/ml dilutions) was measured at 260 nm with an UV/VIS light spectrometer. Last, the P-10 fractions of both NaCl and Ph extract were ultracentrifuged (≤ 10 mg/ml, 500,000 g, 16 hours, 4°C). The supernatant comprising the CPS was lyophilized.

3.10   Chemical composition analysis

3.10.1 Gas-liquid chromatography

3.10.1.1 CLA analysis

Lipid extraction and fatty acid methyl ester (FAME) derivatization have been performed in line with the protocol of Dionisi et al.(202). The internal standard (100 µg 17:0) and 2 ml n-hexane were added to the freeze dried samples of treatment A and B prior to extrac-tion by mixing the samples for 30 minutes at 150 rpm at 20–22°C. Methanolysis by methanolic hydrochloric acid (HCl/MeOH, 0.5 M) for 30 minutes at 60°C was conducted. After chilling to 20–22°C the mixture was washed with 2 ml of NaCl (5 M) for 2 minutes and the organic phase was transferred to a new vial. The extraction was repeated and the combined organic phases were dried with Na_2SO_4, evaporated with N_2 and redissolved in 300 µl $CHCl_3$. One µl was injected to a gas-liquid chromatograph (GLC) coupled with a mass selective detector (MSD) for identification of the CLA and to a GLC coupled with a flame ionization detector (FID) for quantification. A 18:2 CLA-ME (mixture of *cis*- and *trans*-9,11- and -10,12-octadecadienoic acid methyl esters) standard was used for assign-ment of CLA in the samples.

GLC-FID was carried out with an Agilent Technologies 6890N device utilizing a HP-5ms (5% diphenyl-95% dimethyl polysiloxane) capillary column (30 m × 250 µm, 0.25 µm film thickness) with H_2 as mobile phase (70 kPa). A temperature program of 120°C/3 minutes/ 5°C minute $^{-1}$/ 10 minutes/320°C was applied. Data were analyzed with the ChemStation software (Agilent Technologies). Mass selective detection was per-formed with a Hewlett Packard GLC 5890 equipped with an Ultra 1 (100% dimethyl polysiloxane) column and MSD 5970 with electron impact (EI) in autotune at 70 eV.

3.10.1.2 Methanolysis

Samples of 100 µg were methanolyzed with HCl/MeOH in two different manners. During weak methanolysis 200 µl of 0.5 M HCl/MeOH was added to the sample in a glass vial and incubated for 45 minutes at 85°C. In contrast to that, strong methanolysis was applied with 2 M HCl/MeOH for 16 hours at 85°C. After chilling to 20–22°C, the HCl/MeOH solution was evaporated under a stream of N_2 and the probe was washed 3 times with 300 µl MeOH. Peracetylation was achieved by adding 150 µl of pyridine/Ac_2O (1:1 by vol) and incubation at 85°C for 7 minutes. The mixture was dried under N_2 and the sample was transferred to a new vial with $CHCl_3$ and 1/100 µl was injected to the GLC.

A Hewlett-Packard 5880 GLC provided with a SPB-5 (5% diphenyl-95% dimethyl siloxane) capillary column (30 m × 250 µm, 0.25 µm film thickness) was used for GLC-FID running a temperature program of 150°C/3 minutes/ 3°C minute $^{-1}$/ 10 minutes/260°C with H_2 as carrier gas. Furthermore, samples were injected to a Hewlett-Packard 5989A system equipped with a HP-5ms column for GLC-MSD utilizing He as carrier gas (70 kPa) and EI at 70 eV.

3.10.1.3 Neutral sugar analysis

For neutral sugar determination samples of 100 µg were hydrolyzed with 250 µl 0.1 M HCl at 100°C for 48 hours. The HCl was evaporated under N_2 and 3 µg of xylose (Xyl) were added as internal standard. Fatty acids were removed by 3 times purging of the vial with 300 µl 10% ether/hexane and the sample was dried. To reduce the aldehyde function 150 µl of H_2O were added, the pH was adjusted to 8 dropping stepwise 5 µl of 1 M NaOH to the probe and a tip of a spatula of $NaBH_4$ was added. Reduction was conducted for 16 hours at 20–22°C in the dark allowing for air exchange from the vial. The reaction was stopped with 2 M HCl and the dried sample was flushed 3 times with 300 µl 5% AcOH/MeOH and further 3 times with MeOH. Subsequently, peracetylation proceeded and 1/100 µl $CHCl_3$ were analyzed by GLC as described under chapter 3.10.1.2. Alditol acetates were detected by comparison to a defined standard of different monosaccharides derivatized likewise (203). Quantification was achieved by relating the area under curve values of the sample to that of the Xyl.

3.10.1.4 Amino sugar analysis

Samples of 100 µg were hydrolyzed by incubation at 100°C for 16 hours with 300 µl of 4 M HCl. The acid was evaporated under N_2 and the sample was washed with 2×300 µl H_2O. After three-fold washing with 300 µl methanol the protocol progressed with peracetylation, reduction and again acetylation as explained in chapter 3.10.1.3. One of 100 µl CHCl$_3$ was injected to the GLC applying the same temperature program as for neutral sugars. Amino sugars were not quantified but identified in analogy to a known mixture of *C*-2 aminated hexoses.

3.10.1.5 Determination of the absolute configuration (156,204)

To investigate whether sugars and alanine were D or L configured samples of 200 µg were hydrolyzed by weak methanolysis, peracetylated and washed three-fold with MeOH. Subsequently, 200 µg were butanolyzed with 150 µl 2 M HCl/*(RS)*-butan-2-ol and another 200 µg with 2 M HCl/*(S)*-butan-2-ol at 85°C for 4 hours. The mixture was dried, peracetylated and 1/100 µl CHCl$_3$ was analyzed in the GLC-FID system as described for methanolysis with a temperature program of 150°C/3 minutes/ 3°C minute^{-1}/ 10 minutes/260°C in comparison to authentic D or L standards.

3.10.1.6 Fatty acid analysis

To determine fatty acids (FA) qualitatively and quantitatively the total FA and the ester FA protocol were performed. During the total FA analysis samples of 200 µg were combined with 10 µg of C17:0 ME used as internal standard. The probe was dried under N_2 and 1 ml of 4 M HCl was added for hydrolysis at 100°C for 4 hours. In the next step 1 ml of 5 M NaOH was transferred to the reaction mix and incubated for 30 minutes at 100°C. After dilution with 3 ml of H_2O and adjustment of pH 3 with 300 µl of 4 M HCl free lipids were extracted three-fold in CHCl$_3$/H_2O (1:3 by vol) by intense shaking of the glass vial and centrifugation (200 *g*, 2 minutes, 20–22°C) for phase separation. The combined organic phases were evaporated under a stream of N_2 and methylation followed. Therefore, 100 µl CH$_2$N$_2$ were added to the sample for 3 minutes at 20–22°C, the step was repeated and CH$_2$N$_2$ was evaporated with N_2 indicated by the fading yellow color of CH$_2$N$_2$. One of 100 µl CHCl$_3$ was injected to GLC-FID temperature program as in 3.10.1.1 indentifying FA in comparison to a known standard mix of FAMEs. The internal standard served for quantification by comparing the area under curve values of the lipids.

Ester FA were extracted by addition of 1 ml 0.5 M NaOH in 50% aqueous MeOH to the material together with the standard and incubation at 85°C for 2 hours. Then extraction with $CHCl_3$ and methylation with CH_2N_2 progressed.

3.10.1.7 Hydrogenation of FA

In order to differentiate between unsaturated FA and their cyclic form 50 µg of the derivatized FA sample were dissolved in 400 µl $CHCl_3$/MeOH (9:1 by vol). A catalytic amount of PtO_2 was added to the probe and H_2 was introduced for 5 minutes at 20–22°C. After the Pt metal was formed (clumping of the Pt powder) H_2 was introduced for additional 2 minutes. The whole mixture was filtered through glass wool into a new vial and the old vial was rinsed 3 times with $CHCl_3$/MeOH (9:1 by vol) passing the wool as well. The solution was then subjected to a second filter step over a 0.45 µm organic filter. For GLC-MSD 1/50 µl $CHCl_3$ was injected running the temperature program presented in chapter 3.10.1.1.

3.10.1.8 Linkage analysis of the LTA linker (205)

For definition of the linkages within the LTA linker analysis by GLC-MS the following methylation procedure was performed. The lyophilized deacylated linker (600 µg) was resuspended in 1 ml of dry DMSO and 300 µg of powdered NaOH were added. After 500 µl of CH_3I were filled carefully to the reaction mix permethylation succeeded in the closed vial at 20–22°C for 1 hours. Repeated extraction with $CHCl_3$/H_2O (2:7 by vol) and washing of the combined organic phases with H_2O yielded the methylated product which was dried under N_2. During the next step hydrolysis with 100 µl 4 M TFA at 100°C for 4 hours was executed. The solution was evaporated with 3 × 100 µl H_2O under N_2. To reduce the monosaccharides the probe was dissolved in 200 µl H_2O/MeOH (1:1 by vol), a tip of a spatula of powdered $NaBD_4$ was added and the mixture was incubated at 50°C for 2 hours. The reaction was terminated with 3 drops of 2 M HCl and the sample was evaporated under N_2 with 6 × 200 µl of 5% AcOH/MeOH as well as 6 × 300 µl of MeOH. Finally peracetylation was conducted and 1/50 µl $CHCl_3$ was analyzed in the GLC-MS applying the temperature program as explained for methanolysis.

3.10.2 Phosphate determination (206)

For simple detection of phosphate after AEX and HIC 100 µl of each fraction, 10 µl of the standard (Na_2HPO_4) as positive control and 100 µl of H_2O as a blank were pipetted into heat stable glass tubes and the samples were evaporated *in vacuo*. For hydrolysis 100 µl of cold releasing reagent were incubated together with the sample for 1 hour at 100°C and followed of 2 hours incubation at 165°C. After cooling on ice 1 ml of freshly prepared color reagent was added (still on ice) and the reaction proceeded for 90 minutes in a water bath of 37°C. Subsequently, extinction at 820 nm was measured with an UV/VIS light spectrometer.

Determining the inorganic phosphate concentration pairs of 25, 50 and 75 µg of the sample as well as pairs of 10, 20, 30, 40 and 50 mM of the standard were transferred into glass tubes. After addition of 100 µl H_2O and 900 µl of the color reagent to all tubes, the blank and the standards incubation at 37°C for 30 minutes was conducted. Afterwards, detection at 820 nm was performed.

Furthermore, duplicates of 10, 20 and 40 µg of sample and 10, 20, 30, 40 and 50 mM of the standard were pipetted to the glass tubes for quantification of the total phosphate content. To each sample, standard and the blank 50 µl of H_2O were added and drying of all tubes *in vacuo* was performed. Thereafter, all probes were incubated with the releasing reagent and the color reagent as stated earlier in this chapter.

<u>Standard</u>	5 mM Na_2HPO_4
<u>Color reagent</u>	1 ml 1 M NaAc
Freshly mixed prior to use	1 ml 2.5% $[(NH_4)_6Mo_7O_{24} \times 4\ H_2O]$
on ice	7 ml H_2O
	1 ml 10% ascorbic acid (freshly prepared)
<u>Releasing reagent</u>	62.7 ml H_2O
	30.6 ml H_2SO_4
	6.7 ml 70% $HClO_4$

3.10.3 Automated amino acid analyses

Samples of 100 µg were investigated for their amino acid content by the Waters Pico·Tag method performed by Volker Grote from the Division of Structural Biochemistry, Research Center Borstel (RCB) (207). In brief, probes were depolymerized by incubation with 150 µl of 4 M HCl at 120°C for 16 hours. Subsequently, amino acids were treated with phenyl isothiocyanate (PITC) at pH 9-10 yielding phenyl thiocarbamyl amino acid derivatives (PTC-AA). These were then dissolved in Pico·Tag diluent and applied on the Pico·Tag C-18 RP-HPLC column. A gradient of 100% buffer A (0.14 M NaAc in 0.05% triethylamine, pH 5.3) to 40% buffer B (60% CH_3CN) from 0 to 10 minutes at a flow of 1 ml/minute separated the amino acids detected by UV light at 254 nm. Comparison of the retention time as well as area under curve values of authentic external standards identified amino acids and their concentration in the sample.

3.10.4 HF treatment

In order to cleave phosphodiester bonds 5 mg of sample were incubated with 100 µl of 48% aqueous HF at 4°C for 48 hours. The reaction mixture needed to be in a plastic tube, since HF dissolves glass, which was in turn placed in second plastic tube. In case of the LTA backbone cleavage from the lipid anchor three-fold extraction with H_2O/$CHCl_3$/MeOH (3:3:1 by vol) and centrifugation (800 g, 2 minutes, 20–22°C) for phase separation revealed the anchor in the organic phase. Then the lyophilized anchor underwent hydrazine treatment for *O*-deacylation. HF depolymerized EC TA was applied to Bio-Gel P-2 SEC (120 × 1.5 cm) with PAW buffer for separation of monomers.

3.10.5 Hydrazine treatment (208)

Prior to ester cleavage by N_2H_2 all used glass material was dried thoroughly *in vacuo* due to the high reactivity of N_2H_2 with H_2O. To the completely dry sample 1 ml N_2H_4/20 mg was pipetted and incubated at 37°C for 1 hour vortexing the vial each 15 minutes for 1 minute. Afterwards the sample was put for 15 minutes to an ice bath, cold acetone was added (1:10 by vol) and evaporation under N_2 was conducted. The acetone washing was repeated 3 more times with 500 µl for total removal of N_2H_2 and the obtained *O*-deacylated LTA linker was lyophilized.

3.11   ESI-MS analysis

Purified cell wall components were investigated by high-resolution electrospray ioniza-tion Fourier-transformed ion cyclotron mass spectrometry (ESI FT-ICR-MS) in coopera-tion with Dr. Buko Lindner under technical assistance of Brigitte Kunz both from the Division of Immunochemistry at RCB. Samples of 10 ng were redissolved in an ESI spray solution containing propan-2-ol, water and triethylamine (50:50:0.001 by vol). In-jection was conducted at a flow rate of 2 µl/minute. The APEX Qe-Instrument (Bruker Daltonics, Billerica, MA, USA) was equipped with a 7 Tesla magnet and a dual Apollo ion source. Drying gas temperature was adjusted to 150°C and capillary entrance voltage to 3.8 kV. Spectra were recorded under standard instrumental parameters in the negative ion mode and charge deconvolution was carried out for 5 V spectra. The displayed mass peaks refer to the monoisotopic peaks.

3.12   NMR spectroscopic analysis

Recording of NMR spectra was carried out by Heiko Käßner and Dr. Nicolas Gisch of the Division of Immunochemistry at RCB. Probes were measured in D_2O at 700 and 360 MHz at 27°C. The Bruker DRX Avance III 700 MHz spectrometer was used at operating frequencies of 700.75 MHz for ^{1}H, 176.20 MHz for ^{13}C, and 283.67 for ^{31}P NMR spec-troscopy. The Bruker Avance II 360 MHz spectrometer was used at operating frequencies of 360.13 MHz for ^{1}H and 90.55 MHz for ^{13}C NMR spectroscopy. To record and interpret one-dimensional (1D) and two-dimensional (2D) homonuclear ^{1}H,^{1}H correlation spec-troscopy (COSY), total correlation spectroscopy (TOCSY) and rotating-frame Overhauser effect sprectroscopy (ROESY) as well as ^{1}H,^{13}C heteronuclear single quan-tum coherence (HSQC), heteronuclear multiple bond correlation (HMBC) and ^{1}H,^{31}P heteronuclear multiple quantum correlation (HMQC) experiments, standard Bruker soft-ware was applied. Calibration was accomplished relative to external acetone (δ_H 2.225, δ_C 31.50) and external phosphoric acid (δP 0.0) (200). The structural analysis of the EC TA structure was performed together with Dr. Evgueny Vinogradov from the National Re-search Council (NRC) in Ottawa/Canada. He used a Varian INOVA 600 MHz (^{1}H) spec-trometer with 3 mm gradient probe at 25°C in D_2O, with acetone as internal reference (δ_H 2.225 and δ_C 31.45).

3.13 Transient transfections and cytokine assays (209)

Design and performance of *in vitro* experiments was done in cooperation with Dr. Holger Heine and Karina Stein under technical assistance of Ina Goroncy from the Division of Innate Immunity at RCB. Briefly, HEK293 cells were transiently transfected with the plasmids coding for the respective innate immune receptor as denoted for 24 hours. Afterwards cells were washed and incubation with the respective *L. lactis* G121 cell wall component as indicated in various concentrations. Furthermore, positive controls were used, namely the synthetic lipopeptide *N*-Palmitoyl-*S*-[2,3-bis(palmitoyloxy)-(2*RS*)-propyl]-[*R*]-cysteinyl-[*S*]-seryl-[*S*]-lysyl-[*S*]-lysyl-[*S*]-lysyl-[*S*]-lysine (Pam$_3$C-SK$_4$) for TLR2, LPS from *S. enterica* sv. Friedenau (kind gift of Prof. Helmut Brade, RCB) for TLR4, iE-DAP (courtesy of Prof. Koichi Fukase, Osaka, Japan) for NOD1 and MDP (provided by Prof. Shoichi Kusomoto, Osaka, Japan) for NOD2. The CXCL-8 content of collected supernatants was quantified after 18 hours of stimulation by a commercial ELISA.

Utilizing the Ficoll-Isopaque density gradient centrifugation human mononuclear cells (hMNC) were separated from sodium citrate blood of healthy adult donors (210). After PBS washing hMNC were cultivated in RPMI 1640 medium supplemented with 10% autologous human serum, 100 U/ml penicillin and 100 µg/ml streptomycin. Stimulation of hMNC (1×10^6/ml) was performed in duplicates of different concentrations of the indicated cell wall component from *L. lactis* G121, synthetic lipopeptide Pam$_3$C-SK$_4$ or LPS. The IL-6 concentration of collected supernatants after 20 hours of stimulation was quantified by ELISA as well.

3.14 Identification of the *lgt* gene in the *L. lactis* G121 genome

3.14.1 Isolation of genomic DNA (211)

For isolation of the genomic DNA from *L. lactis* G121, the protocol of Marmur *et al*. was used with minor modifications. Briefly, the cells of an 12-hours culture grown in 50 ml TSB and 0.3% yeast extract were harvested by centrifugation and resuspended in 1 ml pre-lysis buffer, followed by addition of 20 mg lysozyme and incubation of the mixture in a water bath at 37°C for 30 minutes. This step was required to disintegrate the thick PGN layer. Afterwards, 1 ml of the 0.5% SDS solution and 1 mg of proteinase K were added to

the mixture and incubated in a water bath at 50°C for 60 minutes. The solution was then extracted with 6 ml of Tris-equilibrated phenol by gentle mixing for 10 minutes. Following centrifugation (10,000 g, 15 minutes, 20°C) to separate the organic and water phases, the top water phase was carefully transferred to a new centrifuge tube, avoiding any contamination with material of the interface. Extraction of the water phase with Tris-equilibrated phenol was repeated once as described above. For precipitation of the DNA, 0.1 volumes of 3 M NaAc, pH 4.8, (mix gently) and 2 volumes of 95% EtOH (mix by inverting) were added to the water phase. The DNA was spooled out onto a rod, transferred to 5 ml of an RNase solution and stored with permanent rocking at 4°C for three days to dissolve the DNA. Thereafter, the solution was extracted with an equal volume of CHCl$_3$ and centrifuged (10,000 g, 5 minutes, 4°C). The DNA was then precipitated from the upper water phase with 0.1 volumes of 3 M NaAc, pH 4.8, and 2 volumes of 95% EtOH, spooled out as outlined above and dissolved in 2 ml of TE buffer. The purity and integrity of the isolated genomic DNA was analyzed by agarose gel electrophoresis, and photometric measurements at 260 nm were carried out to determine the concentration of the double-stranded (ds) DNA.

Pre-lysis buffer	Tris-HCl	20 mM, pH 8.0
	EDTA	2 mM
	Triton® X-100	1.2%

SDS solution	SDS	0.5%
	Tris-HCl	50 mM, pH 7.5
	EDTA	0.4 M

RNase solution	RNase	200 µg/ml
	Tris-HCl	50 mM, pH 7.5
	EDTA	1 mM

<u>TE buffer</u>	Tris-HCl	50 mM, pH 7.5
	EDTA	1 mM

3.14.2 Construction of Genome Walker™ libraries

To identify and determine the DNA sequence of the *lgt* region of *L. lactis* G121, the Genome Walker™ Universal Kit was applied according to the recommendations of the manufacturer. For generation of DNA libraries (DL) as a first step of the methodology, the genomic DNA was digested with four different blunt-end restriction enzymes (RE), namely *Dra*I (DL-*Dra*I), *Eco*RV (DL-*Eco*RV), *Pvu*II (DL- *Pvu*II) and *Stu*I (DL- *Stu*I). A *Pvu*II digest of human genomic DNA provided with the kit (pctrl) served as a positive control. For each library, the reaction mixes were prepared in a 1.5-ml tube as shown in **Table 3.3**.

Table 3.3 Reaction mixture for the DNA libraries.

Component	Volume
Genomic DNA (0.1 µg/µl)	25 µl
Restriction enzyme (10 U/µl)	8 µl
Restriction enzyme buffer (10×)	10 µl
Deionized H_2O	57 µl
Total volume	100 µl

The reaction mixes were incubated at 37°C for 2 hours, vortexed at slow speed for 5–10 seconds and incubated at 37°C for additional 16–18 hours. After vortexing of the tubes, 5 µl of each reaction was subjected to 0.8% agarose gel electrophoresis.

For purification of the libraries, an equal volume (95 µl) of Tris-equilibrated phenol was added and vortexed at slow speed for 5–10 seconds. The upper aqueous phase was transferred to a new tube after phase separation in a microfuge, and an equal volume (95 µl) of $CHCl_3$: isoamyl alcohol (24:1, v/v) was added. After vortexing at slow speed for 5–10 seconds and phase separation, the upper aqueous phase was transferred to a fresh tube, and 2 volumes (190 µl) of ice cold 95% EtOH, 1/10 volume (9.5 µl) of 3 M NaAc (pH 4.5), and 20 µg of glycogen were added. This mixture was then vortexed at slow speed

for 5–10 seconds and centrifuged (21,000 g, 15 minutes, 4°C). The supernatant was de-canted and the pellet washed with 100 µl of ice cold 80% EtOH. After centrifugation (21,000 g, 10 minutes, 4°C), the supernatant was decanted and the air-dried pellet re-dissolved in 20 µl of TE buffer (10/0.1 mM, pH 8.0) by vortexing at slow speed for 5–10 seconds. Finally, the libraries were ligated to the GenomeWalker™ Adaptor as shown in **Table 3.4**. A total of 4 µl of each DNA library of *L. lactis* G121 and the positive control were incubated at 16°C for 12 hours.

Table 3.4 Mixture for ligation with the GenomeWalker™ Adaptor.

Component	Volume
DL-*Dra*I, DL-*Eco*RV	
DL-*Pvu*II, DL-*Stu*I or pctrl	4.0 µl
GenomeWalker Adaptor (25 µM)	1.9 µl
Ligation buffer 10 ×	1.6 µl
T4 DNA ligase (6 U/µl)	0.5 µl
Total volume	8.0 µl

Incubation at 70°C for 5 minutes stopped the reactions, and to every vial 72 µl of TE (10/0.1 mM, pH 8.0) was added and mixed.
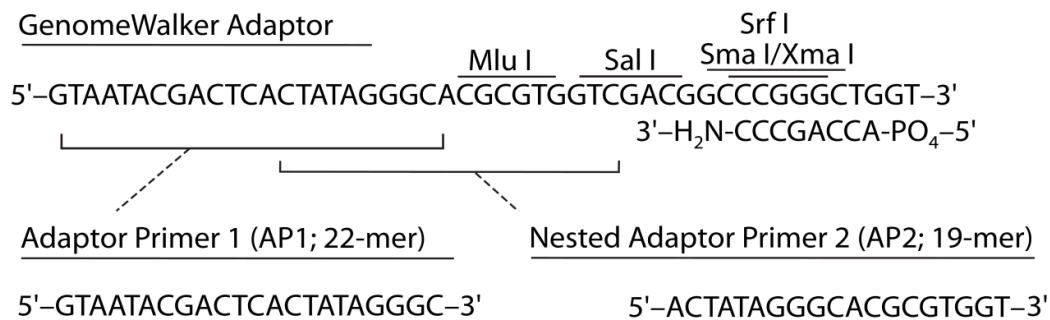
Figure 3.2 DNA sequences of the GenomeWalker Adaptor, Adaptor Primer 1 (AP1) and Nested Primer 2 (AP2). The adaptor carried two important features. First, the adaptor lacks an AP1 binding site, so this site was generated only after initial PCR cycles with gene specific primer 1 (GSP1). The extension of the 3'-end was protected with an amine group. With permission of Clontech.

3.14.3 Amplification of *lgt* sequences

The adaptor-ligated DNA libraries (DL-*Dra*I, DL-*Eco*RV, DL-*Pvu*II and DL-*Stu*I) served as templates for amplification of putative *lgt* fragments. Adaptor primers 1 and 2 (AP1, AP2) were delivered with the kit, whereas gene-specific primers 1 and 2 (GSP1, GSP2) for primary PCRs (1° PCR) and gene-specific primers 1 and 2 (NGSP1, NGSP2) for secondary nested PCR (2° PCR) were designed based on conserved *lgt* sequences of *L. lactis* subspecies (ssp.) KF147, IL1403, cremoris MG1363 and cremoris NZ9000. GSP1 and NGSP1 were generated to amplify partial sequences upstream of *lgt*, whereas GSP2 and NGSP2 were expected to bind downstream. The primers were designed as degenerated oligonucleotides, meaning that they would bind to the target sequences even if they were not 100% complementary. For the pctrl reaction (*Pvu*II-digested human genomic DNA), the provided gene-specific primers PCP1 and PCP2 were applied. The primers used for amplification of *lgt* fragments from the DNA libraries are shown in **Table 3.5**

Table 3.5 Primers for amplification of *lgt* sequences from DNA libraries of *L. lactis* G121.

Primer	DNA sequence 5'→3'
AP1	GTAATACGACTCACTATAGGGC
AP2	ACTATAGGGCACGCGTGGT
GSP1	GAARGTRGGCATTCGATAATGACCMTCRATAAACATTTGAT TTCTAATA
GSP2	AGCCARTCTAAATTTGAAACAATTTTWCCRTARGCYTCTTG
NGSP1	TATTAGAAATCAAATGTTTATYGAKGGTCATTATCGAATGCC YACYTTC
NGSP2	TAAGYGGWTTTATTCTGGTYATGGTYTTTAGACATCG

A: adenine, T: thymine, G: guanine, C: cytosine, R: G or A, Y: C or T, M: C or A, W: A or T, K: G or T

Non-kit primers were designed by Dr. Uwe Mamat and synthesized by Eurofins MWG Operon.

While 1 µl of each library and pctrl was used in 1° PCRs, 1 µl of a 50× dilution of each 1° PCR product served as a template for the 2° PCR. The Advantage 2 polymerase mix containing the TaqStart Antibody for hot start PCR was used for all PCRs of the GenomeWalker™ method. DNA amplifications were performed according to the scheme provided in **Table 3.6**.

Table 3.6 Scheme for amplification of *lgt* sequences in 1° and 2° PCR.

DL	Tube label	1° PCR primer	Tube label	2° PCR primer
*Dra*I	*Dra*I-GSP1	AP1 and GSP1	*Dra*I-NGSP1	AP2 and NGSP1
*Dra*I	*Dra*I-GSP2	AP1 and GSP2	*Dra*I-NGSP2	AP2 and NGSP2
*Eco*RV	*Eco*RV-GSP1	AP1 and GSP1	*Eco*RV-NGSP1	AP2 and NGSP1
*Eco*RV	*Eco*RV-GSP2	AP1 and GSP2	*Eco*RV-NGSP2	AP2 and NGSP2
*Pvu*II	*Pvu*II-GSP1	AP1 and GSP1	*Pvu*II-NGSP1	AP2 and NGSP1
*Pvu*II	*Pvu*II-GSP2	AP1 and GSP2	*Pvu*II-NGSP2	AP2 and NGSP2
*Stu*I	*Stu*I-GSP1	AP1 and GSP1	*Stu*I-NGSP1	AP2 and NGSP1
*Stu*I	*Stu*I-GSP2	AP1 and GSP2	*Stu*I-NGSP2	AP2 and NGSP2
pctrl	pctrl-PCP1	AP1 and PCP1	pctrl-PCP2	AP2 and PCP2

To keep variations of the 1° PCR mixes to a minimum, a master mix sufficient for nine reactions was prepared. For 1° PCRs and according to the experimental set-ups shown in **Table 3.6**, 1 µl of the corresponding DNA library and either 1 µl of GSP1 or 1 µl of GSP2 were added to 48 µl of the reaction as shown in **Table 3.7**. For the pctrl reaction, 1 µl of the PCP1 primer was added.

Table 3.7 Mix for one reaction of the 1° PCR.

Component	Volume
dNTP (10 mM each)	1 µl
AP1 (10 μM)	1 µl
Deionized H$_2$O	40 µl
Advantage 2 PCR buffer 10 ×	5 µl
Advantage 2 polymerase mix 50 ×	1 µl
Total volume	48 µl

The cycling parameters were as follows:

- 7 cycles:

  94°C 25 seconds

  72°C 3 minutes

- 32 cycles:

  94°C 25 seconds

  67°C 3 minutes

- 67°C for an additional 7 minutes after the final cycle

Following PCR amplification, 5 µl of each reaction (plus 1 µl loading dye) was analyzed by 0.8% agarose gel electrophoresis.

In the 2° nested PCR, 1 µl of a 1:50 dilution of each 1° PCR product was used as a template in the reaction shown in **Table 3.8**.

Table 3.8 Mix for one 2° PCR reaction.

Component	Volume
dNTP (10 mM each)	1 µl
AP2 (10 µM)	1 µl
Deionized H_2O	40 µl
Advantage 2 PCR buffer 10 ×	5 µl
Advantage 2 polymerase mix 50 ×	1 µl
Total volume	48 µl

Finally, 1 µl of NGSP1, NGSP2 or PCP2 were transferred to the corresponding reaction mix, referring to the scheme shown in **Table 3.6**. The following thermal cycling parameters were applied:

- 5 cycles:

  94°C 25 seconds

  72°C 3 minutes

- 20 cycles:

  94°C 25 seconds

67°C 3 minutes

- 67°C for an additional 7 minutes after the final cycle

The resulting 2° PCR products (5 µl each plus 1 µl loading dye) were analyzed by 0.8% agarose gel electrophoresis.

After the upstream (C1) and downstream (D1) *lgt* part sequences were identified the fragment of 500 bp between these regions (*lgt'*) was amplified from the genome for completion of *lgt* with the primers listed in **Table 3.9** according to the reaction mix as shown in Table 3.10.

Table 3.9 Primer pair used for amplification of *lgt'* between C1 and D1 from genomic DNA.

Primer	DNA sequence 5'→ 3'
LLAlgtAmplPri4	CCAATGGTCTTACTATAGTCAACATCCTTC
LLAlgtAmplPri5	CTGAAAGCCATTGTGACACACGAG

A: adenine, T: thymine, G: guanine, C: cytosine, primers were designed by Dr. Uwe Mamat and synthesized by Eurofins MWG Operon.

Table 3.10 Reagents for the PCR of *lgt'* between C1 and D1.

Component	Volume (concentration)
$MgSO_4$	1.0 µl (0.5 mM)
Advantage 2 PCR buffer 10 ×	5.0 µl
Nuclease free water	33.0 µl
dNTP	each 1.0 µl (0.2 mM each)
LLAlgtAmplPri 4	2.5 µl (0.5 µM)
LLAlgtAmplPri 5	2.5 µl (0.5 µM)
Genomic DNA	1.0 µl (100 ng)
Advantage 2 polymerase mix 50 ×	1.0 µl
Total volume	50 µl

PCR-conditions:

Primers: LLAlgtAmplPri 4 and LLAlgtAmplPri 5

- 40 cycles:

    95°C   30 seconds

    60°C   30 seconds

    68°C   1 minute

- 68°C   30 minutes
- 4°C   ∞

From the amplification product 1 µl was analyzed by 0.8% agarose gel electrophoresis. To remove the template DNA, 1 µl of *Dpn*I was added to each PCR mix and incubated at 37°C for at least 3 hours prior to T/A cloning.

3.14.4 Cloning of PCR products

3.14.4.1 Low melting point agarose gel electrophoresis

PCR products C1 and D1 were purified by a low melting-point (LMP) agarose gel electrophoresis following the method described in chapter 3.3.4. In brief, 1 g LMP agarose was dissolved in 100 ml 1 × TAE buffer (1%), poured into a gel tray, left in place until jellied and kept at +4° for at least 2 hours. Twenty µl of each PCR product, C1 and D1, and 4 µl of the dye were loaded onto the gel and separated at 60 V for 2 hours. The DNA bands were then excised with a blade under UV light of 312 nm and purified in accordance with the instructions for purification of DNA fragments from agarose gels of the High Pure PCR Product Purification Kit. To assess the success of the DNA extractions from the gel, a standard 0.8% agarose gel electrophoresis was performed as a control.

5 × TAE buffer	Tris	24.2 g/l
	acetic acid	5.7 ml/l
	0.5 M EDTA	20 ml/l
	pH 8.0	

3.14.4.2 Production of competent *E. coli* XL1-Blue cells

Electrocompetent *E. coli* cells were generated by the following method. Pre-cultures of 12 hours in LB medium were inoculated 1:50 into 50 ml of fresh LB medium and grown at 37°C and 220 rpm to an OD_{600} between 0.6 and 0.8. Following incubation of the suspension on ice for 20 minutes, the cells were sedimented by centrifugation (3,800 *g*, 10 minutes, 4°C) and resuspended in 50 ml ice-cold sterile H_2O. Centrifugation was repeated four more times (5,500 *g*, 15 minutes, 4°C) to remove any salt from the suspension and gradually increase the number of bacterial cells per volume unit. Accordingly, the cell pellet was resuspended in 25 ml and 10 ml ice-cold sterile H_2O, and in 5 ml and 1 ml ice-cold sterile 10% glycerol, respectively. The pellet of the final centrifugation step (21,000 *g*, 1 minute, 4°C) was resuspended in 150 µl ice-cold sterile 10% glycerol, and aliquots of 50 µl were stored at −80°C.

3.14.4.3 T/A cloning

Prior to ligation, DNA inserts were generally subjected to 3' A-tailing. The reaction mixes as shown in **Table 3.11** were incubated at 72°C for 30 minutes, followed by purification of the inserts using the High Pure PCR Product Purification Kit.

Table 3.11 Composition of a reaction mix for 3' A-tailing.

Component	Volume
Taq polymerase 10 U/µl	0.5 µl
Purified insert	43.5 µl
Nuclease free water	----
Taq polymerase buffer 10 ×	5.0 µl
dATP 10 mM	1.0 µl
Total volume	50.0 µl

The Invitrogen TA Cloning® Kit with the vector pCR®2.1 of 3.9 kbp (**Figure 3.3**) encoding resistances (^{R}) to ampicillin (Amp) and kanamycin (Kana) was utilized for cloning of the C1, D1 and *lgt*' PCR products. Selection for transformants was performed on LB

agar plates containing Amp (100 µg/ml) and/or Kana (30 µg/ml). The ligation mixture was prepared as follows:

Table 3.12 Ligation mix according to the recommendations of the TA Cloning® Kit.

Component	Volume
Purified PCR product* (C1, D1 or *lgt'*)	1.25 µl
10 × ligation buffer	1.0 µl
pCR2.1 vector (25 ng/µl)	2.0 µl
nuclease free water	4.75 µl
T4 DNA ligase (4.0 Weiss units)	1.0 µl
Total volume	10.0 µl

* The amount of the PCR products (C1, D1 or *lgt'*) was estimated from the gel by visual inspection of the brightness of the bands, compared to 40 ng of the 1500-bp band of the Fermentas 1kb plus DNA ladder. As recommended, the ratio of the vector to the insert was adjusted to 1:1 (by mass).

The ligation reactions were incubated at 14°C for at least 2 hours or max. 12 hours and purified with the DNA Clean & Concentrator™-5 Kit.
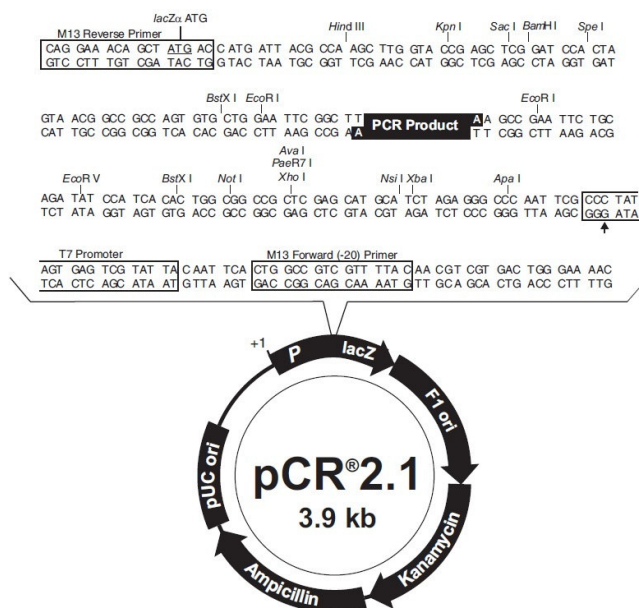
Figure 3.3 Plasmid map of pCR®2.1. This plasmid was used for cloning of partial *lgt* fragments. With permission of Life Technologies.

3.14.4.4 Electroporation of *E. coli* cells

For cloning of the partial *lgt* sequences of *L. lactis* G121, electrocompetent *E. coli* XL1-Blue were used. The frozen cells were thawed on ice for 10 minutes, and 1 µl of the purified ligation mix was added to the cells. After an incubation period of 1 minute on ice, the mixture was transferred to a pre-chilled 0.2-cm gap electroporation cuvette, followed by transformation of the cells using the following settings on the Bio-Rad Gene Pulser: 2.5 kV, 200 ohms and 25 µFd. Immediately after the pulse, 1 ml of either SOC or Recovery Medium (pre-warmed to 37°C) was added. The transformed cells were then transferred to a 15-ml culture tube and incubated at 37°C and 220 rpm for 1 hour (212).

Furthermore, 25 µl aliquots of commercially available electrocompetent *E. cloni*® 10G (Lucigen) cells were transformed by using 0.1-cm gap cuvettes and settings of the Gene Pulser of 1.7 kV, 200 Ohms and 25 µF. In this case, 925 µl of Recovery Medium was used to recover the cells following transformation.

SOC medium	SOB medium	100 ml
	1 M glucose	2 ml
SOB medium	Tryptone-peptone	2 g
	Yeast extract	0.5 g
	5 M NaCl	0.2 ml
	1 M KCl	0.25 ml
	H_2O	ad. 100 ml
	pH 7.0, added after autoclaving:	
	1 M $MgCl_2$	1 ml
	1 M $MgSO_4 \times 7\ H_2O$	1 ml

3.14.4.5 Blue-white screening of transformants

The use of cloning vectors encoding the *lacZα* gene for the α-subunit of the β-galactosidase together with *E. coli* strains carrying the *lacZΔM15* deletion mutation allowed performing blue-white screening of the transformants, a method based on disruption of the α-complementation process by insertional inactivation of the *lacZα* gene of the cloning vector. Following transformations, serial dilutions of *E. coli* cells were spread onto LB agar plates containing 100 µg/ml Amp, which were coated in advance with 50 µl of 0.1 M IPTG and 50 µl of 40 mg/ml X-Gal in DMF.

While the development of blue-colored colonies as a result of isopropyl β-D-1-thiogalactopyranoside (IPTG)-induced *lac* expression and hydrolysis of the colorless analog of lactose, 5-bromo-4-chloro-indolyl-β-D-galactopyranoside (X-gal), suggested a functional β-galactosidase was operative, the appearance of white colonies indicated a loss of function of the α-subunit of the β-galactosidase by insertion of a DNA fragment into the *lacZα* gene. Therefore, white colonies were picked and grown for 12 hours at 37°C and 220 rpm in 5 ml LB medium with 100 µg/ml Amp and 30 µg/ml Kana for plasmid preparation as described in chapter 3.3.5.

3.14.5 DNA sequencing

Recombinant plasmids carrying DNA inserts of expected size were sent to LGC Standards for determination of their sequence by the fluorescence dye termination dideoxyNTP method according to Sanger et al. (213). Sequencing primers used were M13 forward, M13 reverse as well as internal gene-specific primers LLAlgtSeqPri1 and LLAlgtSeqPri2 to cover the entire length of the C1 fragment of about 1.3 kbp (**Table 3.13**). DNA sequence alignments were performed with the BioEdit Sequence Alignment Editor software by Dr. Uwe Mamat.

Table 3.13 Primers used for sequencing of *lgt* fragments.

Primer	DNA sequence 5'→ 3'
M13-29R	CAGGAAACAGCTATGACC
M13-21F	TGTAAAACGACGGCCAGT
LLAlgtSeqPri1	TATTTCACACCCGAACGAATTCAAC
LLAlgtSeqPri2	AGCTTCAACAATTACTGACACATTCC

A: adenine, T: thymine, G: guanine, C: cytosine, primers were designed by
Dr. Uwe Mamat and synthesized by Eurofins MWG Operon.

3.15 Construction of an *lgt* knockout plasmid

In order to carry out an insertional inactivation of the *lgt* gene in the *L. lactis* G121 ge-
nome by the chloramphenicol acetyltransferase (*cat*) gene, a pUC18-based knockout con-
struct was assembled. The plasmid map is shown in **Figure 3.4**. As the pBR322-derived
replication origin of pUC18 is known to be non-functional in bacteria of the genus
Lactococcus, the pUC18 cloning vector could be used as a suicide plasmid in *L. lactis*
G121 to deliver a chloramphenicol resistance (Cm^R) cassette and inactivate the *lgt* gene
by homologous recombination. Thus, to achieve the exchange of the DNA sequences by
recombination events, the Cm^R cassette was supposed to contain the *cat* gene flanked by
upstream (C1') and downstream (D1') regions of *lgt*. These three DNA molecules were
amplified separately with the primers listed in **Table 3.16**, introducing the indicated
recognition sites for restriction endonucleases to facilitate ligation.
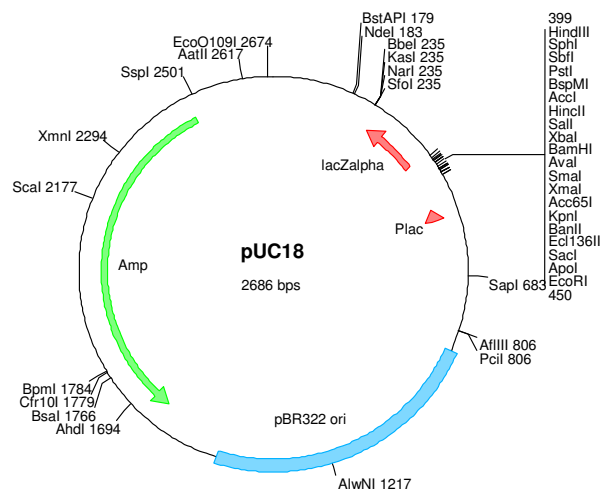
Figure 3.4 Map of the pUC18
cloning vector. This vector was
used for the transformation of *L.
lactis* G121 with the *lgt* knock-
out construct.

3.15.1 Amplification of *cat*, C1' and D1'

Amplification of *cat* from pKD3

Table 3.14 Components for *cat* amplification.

Component	Volume (concentration)
MgSO$_4$	3 µl (1.5 mM)
KOD polymerase buffer 10 ×	5 µl
Nuclease free water	33 µl
dNTP mix	5 µl (0.2 mM each)
pKD3NheICm1	1 µl (0.2 µM)
pKD3XmaICm2	1 µl (0.2 µM)
pKD3	2 µl (100 ng)
KOD polymerase	1 µl (0.02 U)
Total volume	50 µl

PCR-conditions:

- 95°C   2 minutes
- 4 cycles:

  95°C   20 seconds

  60°C   10 seconds

  70°C   20 seconds

- 35 cycles:

  95°C   20 seconds

  68°C   10 seconds

  70°C   20 seconds

- 70°C   7 minutes
- 4°C   ∞

Amplification of C1' and D1' from *L. lactis* G121 genomic DNA

Table 3.15 Reaction mix for C1' and D1' amplification.

Component	Volume (concentration)
MgSO$_4$	3 µl (1.5 mM)
KOD polymerase buffer 10 ×	5 µl
Nuclease free water	33 µl
dNTP mix	5 µl (0.2 mM each)
5' primer	1 µl (0.2 µM)
3' primer	1 µl (0.2 µM)
Genomic DNA	1 µl (100 ng)
KOD polymerase	1 µl (0.02 U)
Total volume	50 µl

Primers for C1': 5SphILLAlgt and 3BamHINheIC1, primers for D1':
5BamHIXmaID1 and 3SacILLAlgt, sequences are given in **Table 3.16**.

PCR-conditions:

- 95°C   2 minutes
- 4 cycles:

   95°C   20 seconds

   58°C   10 seconds

   70°C   20 seconds

- 36 cycles:

   95°C   20 seconds

   65°C   10 seconds

   70°C   20 seconds

- 70°C   5 minutes
- 4°C   ∞

The PCR products (1 µl) were analyzed by 0.8% agarose gel electrophoresis, the template DNA was digested with *Dpn*I (1 µl, 37°C, 3 hours), and purification of the PCR products was performed using the High Pure PCR Product Purification Kit as described in chapter 3.3.5.

Table 3.16 Primers utilized for amplification of *cat*, C1' and D1'.

Primer	DNA sequence 5'→ 3'
pKD3NheICm1	ATAT**GCTAGC**GTGTAGGCTGGAGCTGCTTC
pKD3XmaICm2	ATAT**CCCGGG**ATGGGAATTAGCCATGGTCCATATG
5SphILLAlgt	ATAT**GCATGC**CTGGTCCTTCCTATCTGCTTCGTG
3BamHINheIC1	ATAT**GGATCC****GCTAGC**CGGCCCTAATTGGAGTGCAATC
5BamHIXmaID1	ATAT**GGATCC****CGGGG**CAGTTTTATTAGTAATTGTAGGACTT GTTCTC
3SacILLAlgt	ATAT**GAGCTC**AAATCATCATAAATTTTTCCAGCCCCTTC

A: adenine, T: thymine, G: guanine, C: cytosine, primers were designed by Dr. Uwe Mamat and synthesized by Eurofins MWG Operon, recognition sites for restriction endonucleases are color-coded.

3.15.2 Cloning of *cat*, C1' and D1'

The vector pUC18 was isolated from *E. coli* XL1-Blue with the plasmid preparation kit as outlined in chapter 3.3.5. As a first step, the pUC18, C1' and D1' DNA were digested with *Bam*HI at 37°C for 3 hours as shown in **Table 3.17**. The control for linearization of pUC18 was performed by standard 0.8% agarose gel electrophoresis. After digestion, the DNA were purified with the High Pure PCR Product Purification Kit.

Table 3.17 Reaction mix for *Bam*HI digestion of pU18, C1' and D1'.

Component	pUC18 aliquot Volume	C1'or D1' aliquot Volume
pUC18	15.0 µl	----
C1' or D1'	----	25.0 µl
Nuclease free water	27.5 µl	17.5 µl
NEB buffer BamHI 10 ×	5.0 µl	5.0 µl
*Bam*HI 20 kU/ml	2.0 µl	2.0 µl
BSA 100 ×	0.5 µl	0.5 µl
Total volume	50.0 µl	50.0 µl

In the next step, the DNA were digested for 12 hours at 37°C with *Sph*I (C1', pUC18) and *Sac*I (D1') (**Table 3.18** and **Table 3.19**).

Table 3.18 Mixtures for *Sph*I digests of pUC18 and C1´.

Component	pUC18 aliquot Volume	C1' aliquot Volume
pUC18 *Bam*HI digested	42 µl	----
C1' *Bam*HI digested	----	42 µl
NEB 2 buffer 10 ×	5 µl	5 µl
*Sph*I 10 kU/ml	3 µl	3 µl
Total volume	50 µl	50 µl

Table 3.19 Mixture for *Sac*I digests of D1´.

Component	Volume
pUC18 *Bam*HI digested	----
D1' *Bam*HI digested	42.5 µl
NEB 1 buffer 10 ×	5.0 µl
*Sac*I 20 U/ml	2.0 µl
BSA 100 ×	0.5 µl
Total volume	50.0 µl

The mixtures for the ligation reactions of pUC18 and C1' (*Bam*HI and *Sph*I digested) were prepared as shown in **Table 3.20** and incubated at 16°C for 12 hours.

Table 3.20 Reaction mixes for ligation of pUC18 with C1'.

Component	Volume
pUC18 digested	1.0 µl
C1' digested	1.0 µl
Nuclease free water	6.5 µl
NEB buffer T4 ligase 10 ×	1.0 µl
T4 DNA ligase 2 MU/ml	0.5 µl
Total volume	10.0 µl

The ligation mixtures were purified with the DNA Clean & Concentrator™-5 Kit and subjected to electroporation of *E. cloni*® 10G as described in chapter 3.14.4.4, and the blue-white screening of the transformants was carried out as specified above in chapter 3.14.4.5.

Recombinant pUC18 plasmids carrying C1´ were subsequently linearized with *Bam*HI at 37°C for 3 hours (**Table 3.21**) and purified with the High Pure PCR Product Purification Kit, followed by another digestion with *Sac*I at 37°C for 3 hours (**Table 3.22**). The linear-

ized plasmid as analyzed by 0.8% agarose gel electrophoresis was ligated with digested D1' (**Table 3.23**) to yield plasmid pUC18C1'D1'.

Table 3.21 *Bam*HI digestion mixes for pUC18C1'.

Component	Volume
Plasmid pUC18C1'	15.0 µl
Nuclease free water	27.5 µl
NEB 2 buffer 10 ×	5.0 µl
*Bam*HI 20 kU/ml	2.0 µl
BSA, 100 ×	0.5 µl
Total volume	50.0 µl

Table 3.22 Reaction mix for *Sac*I digestion of *Bam*HI-linearized pUC18C1'.

Component	Volume
pUC18C1'	42.5 µl
NEB 1 buffer 10 ×	5.0 µl
*Sac*I 20 kU/ml	2.0 µl
BSA 100 ×	0.5 µl
Total volume	50.0 µl

The ligation reactions were incubated for 12 hours at 16°C, and the mixes were purified using the DNA Clean & Concentrator™-5 Kit prior to electroporation of *E. coli* XL1-Blue cells as explained in chapter 3.14.4.4. Recombinant plasmids were prepared from randomly selected transformants and analyzed as in chapter 3.3.5.

The pUC18C1'D1' plasmid and the *cat* amplification product were subjected each to digestions with *Nhe*I and *Xma*I at 37°C for 2 hours (**Table 3.24** and **Table 3.25**). Linearization of pUC18C1'D1' was validated as described above.

Table 3.23 Reaction mixtures for ligation of digested pUC18C1' with D1'.

Component	Volume
pUC18C1' digested	1.0 µl
D1' digested	1.0 µl
Nuclease free water	6.5 µl
NEB buffer T4 ligase 10 ×	1.0 µl
T4 DNA ligase 2 MU/ml	0.5 µl
Total volume	10.0 µl

Table 3.24 *Nhe*I reaction mix for digestion of pUC18C1'D1' and *cat*.

Component	pUC18C1'D1' aliquot Volume	*cat* aliquot Volume
pUC18C1'D1'	15 µl	----
cat	----	25 µl
Nuclease free water	29 µl	19 µl
FD buffer 10 ×	5 µl	5 µl
*Nhe*I, n.d. U/ml	1 µl	1 µl
Total volume	50 µl	50 µl

In the last step, *Nhe*I/*Xma*I-digested pUC18C1'D1' and *cat* DNA were ligated at 16°C for 12 hours in a reaction mix shown in **Table 3.26**, in order to obtain plasmid pUC18C1'*cat*D1', carrying the Cm^R cassette for insertional inactivation of *lgt*.

The purified ligation reaction (1 µl) was used to transform *E. coli* XL1-Blue cells by electroporation as described in chapter 3.14.4.4, followed by isolation and analysis of the plasmids (chapter 3.3.5).

Table 3.25 *Xma*I reaction mix for digestion of pUC18C1'D1' and *cat*.

Component	pUC18C1'D1' aliquot Volume	*cat* aliquot Volume
*Nhe*I-linearized pUC18C1'D1'	41.5 µl	----
*Nhe*I-digested *cat*	----	41.5 µl
FD buffer 10 ×	5.0 µl	5.0 µl
*Xma*I 10 kU/ml	3.0 µl	3.0 µl
BSA 100 ×	0.5 µl	0.5 µl
Total volume	50.0 µl	50.0 µl

Table 3.26 Reaction mix for ligation of pUC18C1'D1' with *cat*.

Component	Volume
*Nhe*I and *Xma*I digested pUC18C1'D1'	1.0 µl
*Nhe*I and *Xma*I digested *cat*	1.0 µl
Nuclease free water	6.5 µl
NEB buffer T4 ligase 10 ×	1.0 µl
T4 DNA ligase 2 MU/ml	0.5 µl
Total volume	10.0 µl

3.16 Electroporation of *L. lactis* G121

3.16.1 Protocol according to Gerber et al. (214)

For preparation of electrocompetent *L. lactis* G121 cells, a main batch of 450 ml of SGM17GM medium was inoculated (1:10, v/v) with 50 ml of a 24-hours bacterial culture and incubated at 30°C. The growth of the culture was monitored by measurements of the optical density of the cell suspension at 546 nm and was stopped by centrifugation (8,000 g, 10 minutes, 4°C) when the cells reached an OD_{546} of about 0.4. The cell pellet was resuspended in 400 ml of ice-cold, EDTA-free electroporation buffer and centrifuged as before. The cells were then resuspended in 200 ml of ice-cold electroporation buffer with EDTA, incubated at 4°C for 15 minutes and sedimented as described above. The bacteria were washed with another 400 ml of ice-cold, EDTA-free electroporation buffer, resuspended in 2 ml of electroporation buffer at 4°C and flash-frozen in liquid nitrogen. Aliquots of 50 µl were stored at −80°C.

The electrocompetent cells were thawed on ice, proceeding the following steps as quick as possible. The pUC18C1'*cat*D1' plasmid DNA was added to the thawed cells at a concentration of 2.3 µg and mixed carefully. After transfer of the cells to a pre-chilled 0.2-cm gap cuvette, electroporation was performed with 2.5 kV, 200 Ω and 25 µFd. Immediately after the pulse, the cells were resuspended with 900 µl of ice-cold SM17MC medium, transferred to a new culture tube and placed on ice for 5 minutes. The cells were then recovered at 30°C for 90 minutes, plated on M17 agar plates containing 15 µg/ml of chloramphenicol and incubated at 30°C.

SGM17GM	M17 broth	
	$MgSO_4$	1 mM
	Sucrose	0.5 M
	Glycine	2%
	Glucose	1.5%

Electroporation buffer with EDTA

Sucrose	0.5 M
Glycerol	10%
EDTA	50 mM
pH 7.0	

Electroporation buffer without EDTA

Sucrose	0.5 M
Glycerol	10%
pH 7.0	

SM17MC	M17 broth	
	Sucrose	0.5 M
	MgCl$_2$	10 mM
	CaCl$_2$	2 mM

3.16.2 Protocol according to Powell et al. (215)

A 10-ml culture of *L. lactis* G121 grown for 12 hours in GM17 medium at 30°C without shaking was used to inoculate (1:10, by vol) 100 ml of fresh GM17 medium. Incubation of the main culture at 30°C was terminated at an OD$_{600}$ between 0.3 and 0.7. The cells were sedimented by centrifugation (7,000 *g*, 10 minutes, 4°C), resuspended in ice-cold electroporation buffer and centrifuged as before. The cells were then resuspended in 0.1 culture volumes of ice-cold electroporation buffer, heated to 37°C, and egg white lyso-zyme was added to 2 kU/ml. This mixture was incubated at 37°C for 20 minutes. Subse-quently, the cells were centrifuged (3,000 *g*, 15 minutes, 4°C), washed with ice-cold elec-troporation buffer and ultimately diluted in 0.05 culture volumes of electroporation buffer and kept on ice.

For transformation, 3.4 µg of plasmid DNA were carefully mixed with 50 µl of competent cells in a pre-chilled 0.2-cm gap cuvette. After electroporation at 2.5 kV, 200 Ω and 25 µF, the suspension was placed on ice for an additional time of 25 minutes. Afterwards, 0.5 ml of 5 × SGM17 medium was added, and the mixture was incubated at 30°C for 1 hour. Transformants were selected at 30°C on plates containing 1 × SGM17 agar with 15 µg/ml Cm.

GM17   M17 broth

                              Glucose   0.5%

Electroporation buffer

                              Sucrose   0.5 M

                              $MgCl_2$ 1 mM

                              K_2HPO_4-KH_2PO_4 7 mM

                              pH 7.4

5 × SGM17   M17 broth

                              Glucose   2.5%

                              Sucrose   2.5 M

3.16.3 Protocol of the MolGen group of Rijksuniversiteit Groningen (RUG) (216)

In order to obtain electrocompetent *L. lactis* G121 cells according to the protocol of the MolGen group of Rijksuniversiteit Groningen, the bacteria of a 10-ml culture grown at 30°C for 12 hours in SGM17G were diluted in 100 ml (1:10 by vol) of fresh SGM17G medium. The cells were grown at 30°C to an OD_{600} of 0.2–0.7 and harvested by centrifu-

gation (3,000 g, 15 minutes, 4°C). After three washing steps of the cells with 50 ml of ice-cold wash buffer, the sedimented cells were resuspended in 100 µl of wash buffer and directly transformed by electroporation.

For electroporation, 3.4 µg of pUC18C1'*cat*D1' plasmid DNA were mixed thoroughly with 50 µl of competent cells in an ice-cold 0.2-cm gap cuvette, followed by transformation at 2.5 kV, 200 Ω and 25 µF. Immediately after the pulse, the suspension was transferred from the cuvette to a 15-ml culture tube, and 4 ml of SGM17MC medium were added to recover the cells at 30°C for 2 hours, Finally, the cells were concentrated by centrifugation to a volume of 0.5 ml (3,000 g, 15 minutes, 4°C) and spread onto SGM17 agar plates containing 15 µg/ml Cm.

SGM17G	M17 broth	
	Sucrose	0.5 M
	Glycine	1%
	Glucose	0.5%

Wash buffer	Sucrose	0.5 M
	Glycerol	10%

SGM17MC	M17 broth	
	Sucrose	0.5 M
	Glucose	0.5%
	$MgCl_2$	20 mM
	$CaCl_2$	2 mM

3.16.4 Protocol according to Brückner et al. (217)

For preparation of electrocompetent *L. lactis* G121 cells as described by Brückner *et al.*, the cultures were grown as described in chapter 3.17.2 and harvested by centrifugation

(5,000 *g*, 10 minutes, 4°C) at an OD_{578} of 0.5–0.6. Washing of the bacteria with electroporation buffer was performed three times in volumes of 30 ml, 10 ml and 2.5 ml, respectively. The cell pellet was resuspended in 130 µl of electroporation buffer, and aliquots of 50 µl were kept on ice for transformation.

For electroporation, 2 µg of plasmid DNA were incubated with 50 µl of competent cells at 20–22°C for 30 minutes. Electroporation was performed in a pre-chilled 0.2-cm cuvette at 2 kV, 100 Ω, 25 µF. The transformed cells were resuspended with 1 ml of SGM17MC medium, incubated at 30°C for 90 minutes with moderate shaking (50 rpm) and plated onto SGM17 agar plates containing 15 µg/ml Cm.

Electroporation buffer   Glycine   10%

3.16.5 Protocol according to Wells et al. (218)

A 3-ml *L. lactis* G121 culture grown in GM17 medium for 12 hours was used to inoculate 30 ml of fresh SGM17G medium. The culture was grown at 30°C to an OD_{600} of about 0.35, supplemented with traces of DL-threonine and then allowed to continue the growth to an OD_{600} of about 0.6. The bacteria were harvested by centrifugation (3,100 *g*, 10 minutes, 4°C) and washed three times with 10 ml of ice-cold SMEB buffer. The final sediment was resuspended in 500 µl SMEB, and the competent cells were either directly subjected to electroporation or stored as 50 µl aliquots at −80°C.

The transformation was performed by incubating 1 µg of plasmid DNA with 50 µl of competent cells in a 0.2-cm gap cuvette on ice for 10 minutes, followed by electroporation at 1.8 kV, 200 Ω and 25 µF and immediate addition of 900 µl of pre-chilled SGM17MC medium. After an incubation on ice for 15 minutes, the cells were transferred to another tube and recovered at 30°C for 2 hours. Transformants were selected at 30°C on GM17 agar plates with 25 µg/ml Cm. The *E. coli-L. lactis* shuttle-expression vector pORI23 (kind gift of Dr. G. Burchhardt, University of Greifswald) was used as a transformation control. It coded for an *ermAM* macrolide-lincosamide-streptogramin resistance gene conferring an erythromycin resistance (Ery^R) (219). In this case, the transformants were selected on GM17 agar plates containing 100 µg/ml Ery.

SMEB   HEPES   1 mM

                        Sucrose   300 mM

                        MgCl$_2$ 1 mM

4 Results

4.1 Production of CLA by *L. lactis* G121

The determination and quantification of CLA in the biomass of *L. lactis* G121 was achieved by GLC. After 24, 48 and 72 hours aliquots were taken and the lyophilized biomass was subjected to FAME extraction. **Figure 4.1** shows a paradigm of a chromatogram obtained after injection of FAME extracts of the WBA-control after 24 hours. Next to 18:0, cyclo-19:0 and hydroxyl-18:0 a portion of conjugated 18:2 (CLA) could be detected. The internal standard was 17:0. The used CLA standard was described by the provider as a mix of *cis*- and *trans*-9,11- and -10,12 18:2.
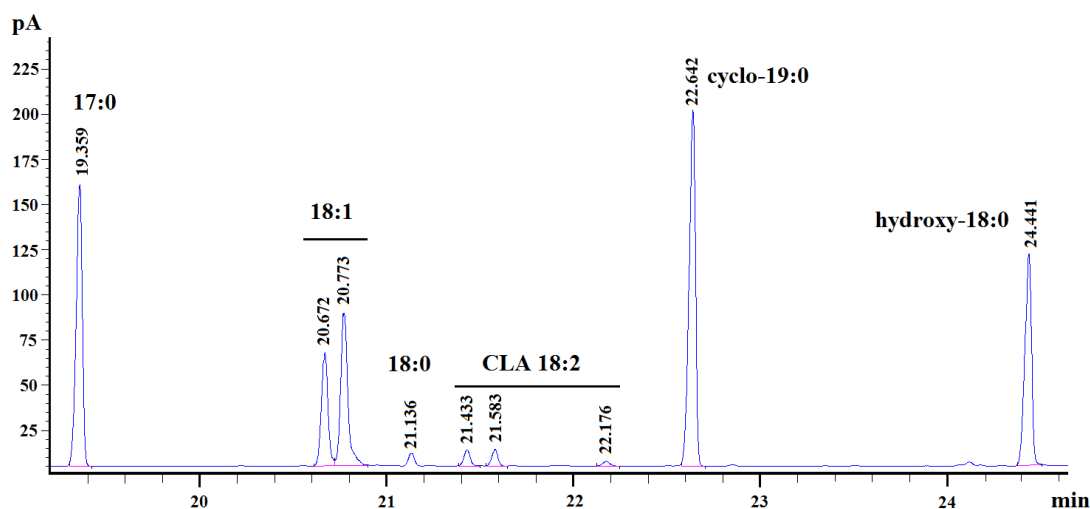
Figure 4.1 The GLC chromatogram of a WBA-control FAME extract. Displayed is an example obtained from the 24 hours extract. One representative result from 3 independent WBA is shown.

Three isomers could be verified by GLC-MSD in the standard of which the retention times (21.43, 21.56 and 22.16 minutes) were congruent with those of the CLA isomers detected in the WBA-control and sample, respectively. Nevertheless, the isomers could not be distinguished among one another by GLC-MSD and therefore values given are the sum of the three isomers.

An exemplary chromatogram of the WBA-sample after 24 hours, which was supplemented with LA during incubation of the bacteria, is demonstrated in **Figure 4.2**. In compari-

son to the WBA-control LA was identified as well as a slightly gain of the CLA areas. **Figure 4.3** depicts the calculated differences in the CLA concentration between control and sample from 24 to 72 hours.
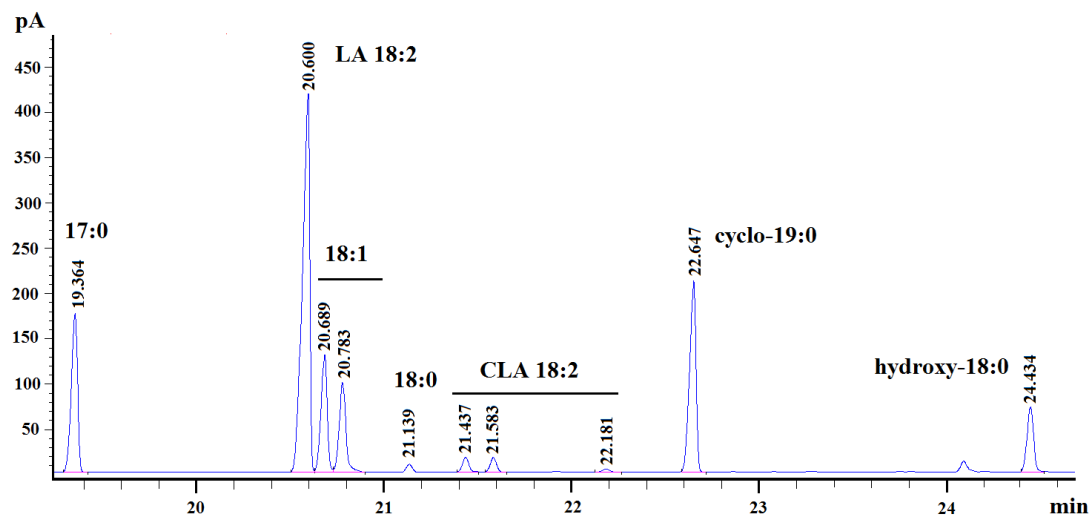
Figure 4.2 Chromatogram of FAME extract from WBA-sample. Illustrated is an example obtained from the 24 hours extract. One representative result from 3 independent WBA is shown.
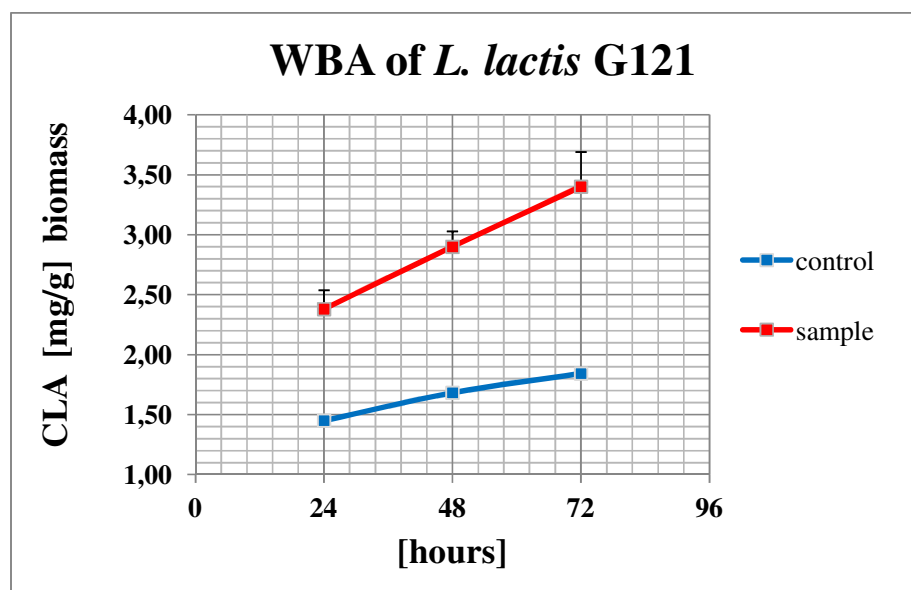
Figure 4.3 Concentrations of CLA determined from FAME extracts. The *L. lactis* G121 biomass was incubated in PBS with either 0.2% Tween®80 (control) or 1.4 mM LA in 0.2% Tween®80 (sample). The measurements were conducted from 24 to 72 hours and one example from two independent repeats is depicted. Values are expressed as the mean ± standard deviation (SD) from duplicates.

Accordingly, the biomass of LA supplemented *L. lactis* G121 accumulated about 1.7 times more CLA compared the non-supplemented biomass. Furthermore only a minor increase of the CLA concentration from 24 to 72 hours could be observed. Hence, the WBA-control and -sample biomasses from 24 hours were chosen for further studies. Currently the material is investigated by H. Harb (University of Marburg) in an *in vivo* mouse model with regard to asthma protective properties.

4.2 PGN of *L. lactis* G121

4.2.1 Isolation, chemical composition and SEC of PGN

From 51.3 g wet mass of bacteria 70 mg of insoluble PGN were obtained (0.14%). In weak methanolysis NAG and NAM (not quantified) were the main components detected. Automated amino acid analysis revealed aspartic acid (Asp, 575.06 pmol/µg), glutamic acid (Glu, 584.14 pmol/µg), Ala (996.15 pmol/µg) and Lys (478.28 pmol/µg). Conditional on the derivatization the method could not differentiate between Asp or asparagines (Asn) and Glu or glutamine (Gln). Subsequently, 40 mg of the PGN sacculus were subjected to mutanolysin degradation in 12.5 mM phosphate buffer and applied to a Toyopearl (formerly TSK) HW-40S SEC for purification as well as pre-separation. **Figure 4.4** depicts the chromatogram of half of the digested 40 mg sample. It was applied in two steps aiming to avoid column overload. The size exclusion resulted in one major peak which eluted first and several smaller peaks which were split into 5 further pools. These six TSK pools (I–VI) were then used in ESI-MS and *in vitro* analysis as well as further separation by RP-12 HPLC.
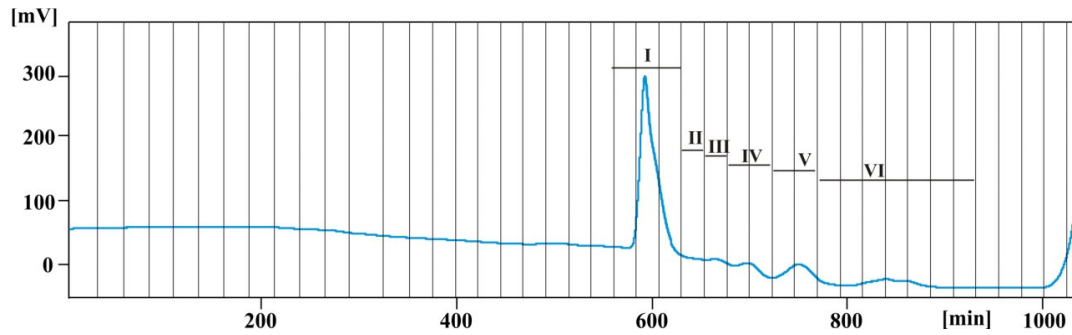
Figure 4.4 Chromatogram of ca. 20 mg solubilized PGN subjected to SEC on Toyopearl HW-40S. The digest of 40 mg PGN was purified and pre-separated by two runs with PAW buffer, yielding in total 12.03 mg of I (30%), 0.93 mg of II (2.3%), 1.82 mg of III (4.5%), 3.13 mg of IV (7.8%), 2.6 mg of V (6.5%) and 3.71 mg of VI (9.3%).

4.2.2 Biological activity of PGN

To receive an initial insight into the immunomodulatory competence of the PGN from *L. lactis* G121 TSK fractions I–VI were subjected to HEK293 cell assays. These were transfected with TLR2, TLR4, NOD1 or NOD2 and stimulated with 0.1, 1 or 10 µg/ml of each fraction as demonstrated in **Figure 4.5** and **Figure 4.6**. The activation was measured as CXCL-8 concentration in the supernatant of the cultures. **Figure 4.5** shows that neither TLR2 nor TLR4 transfected HEK cells could be activated by any of the TSK fractions. Furthermore, the upper panel of **Figure 4.6** illustrates that HEK293 cells expressing NOD1 were not affected by the PGN fragments. However, HEK293 cells expressing NOD2 clearly showed CXCL-8 release upon stimulation with all six TSK fractions. Cultures incubated with TSK IV–VI revealed the highest CXCL-8 concentrations compared to un-stimulated cells (ctrl).
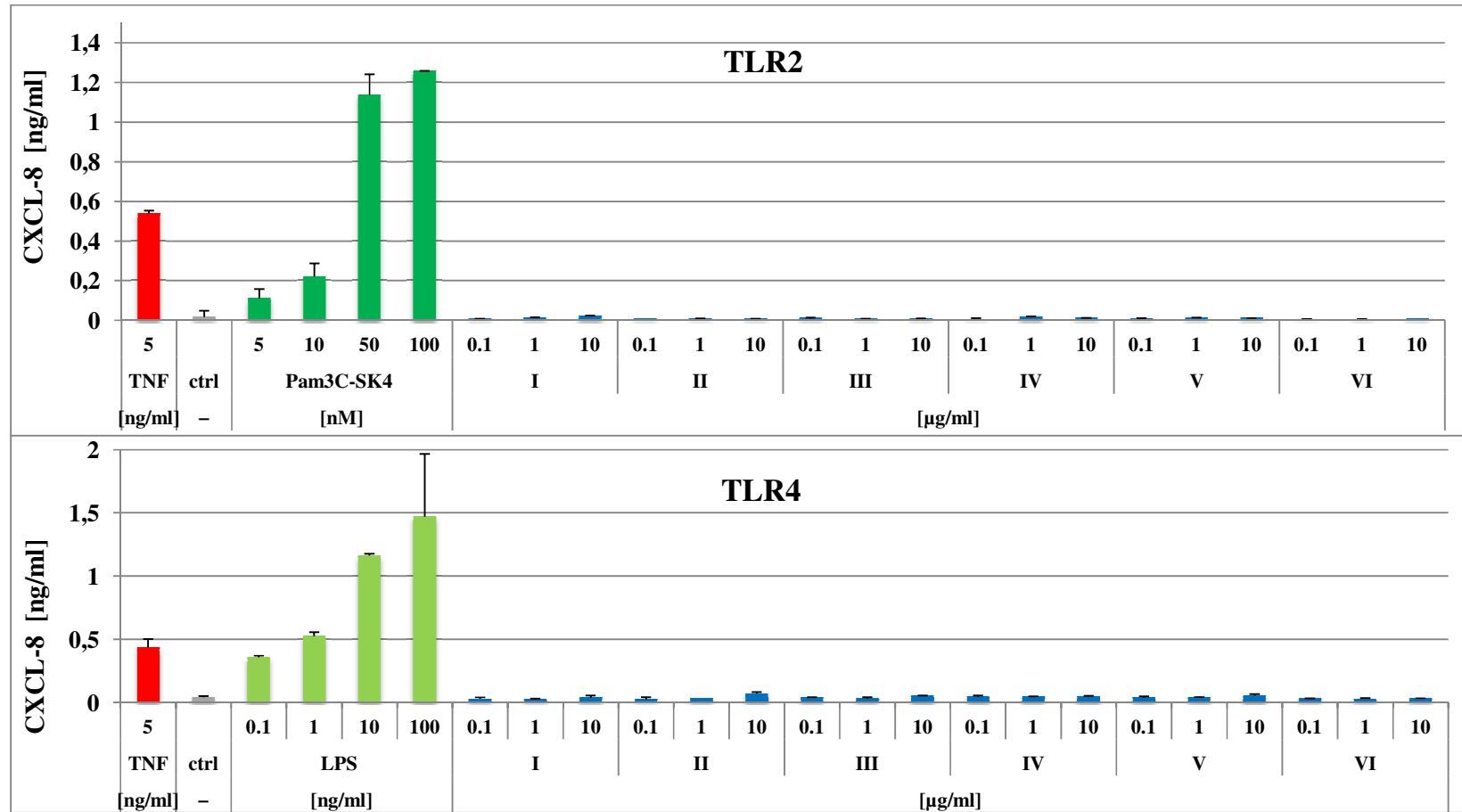
Figure 4.5 *In vitro* assay of HEK293 cultures incubated with increasing concentrations of PGN TSK fractions I–VI (0.1, 1 and 10 µg/ml) after transfections with either TLR2 or TLR4. TNF-α and Pam₃C-SK₄ or LPS were used as positive controls and the negative control were un-stimulated cells. Concentrations of CXCL-8 in the supernatant after 18 hours given in pg/ml were unimpaired by the PGN samples in both assays. Results are expressed as the mean ± SD. One representative from two independent experiments is presented.
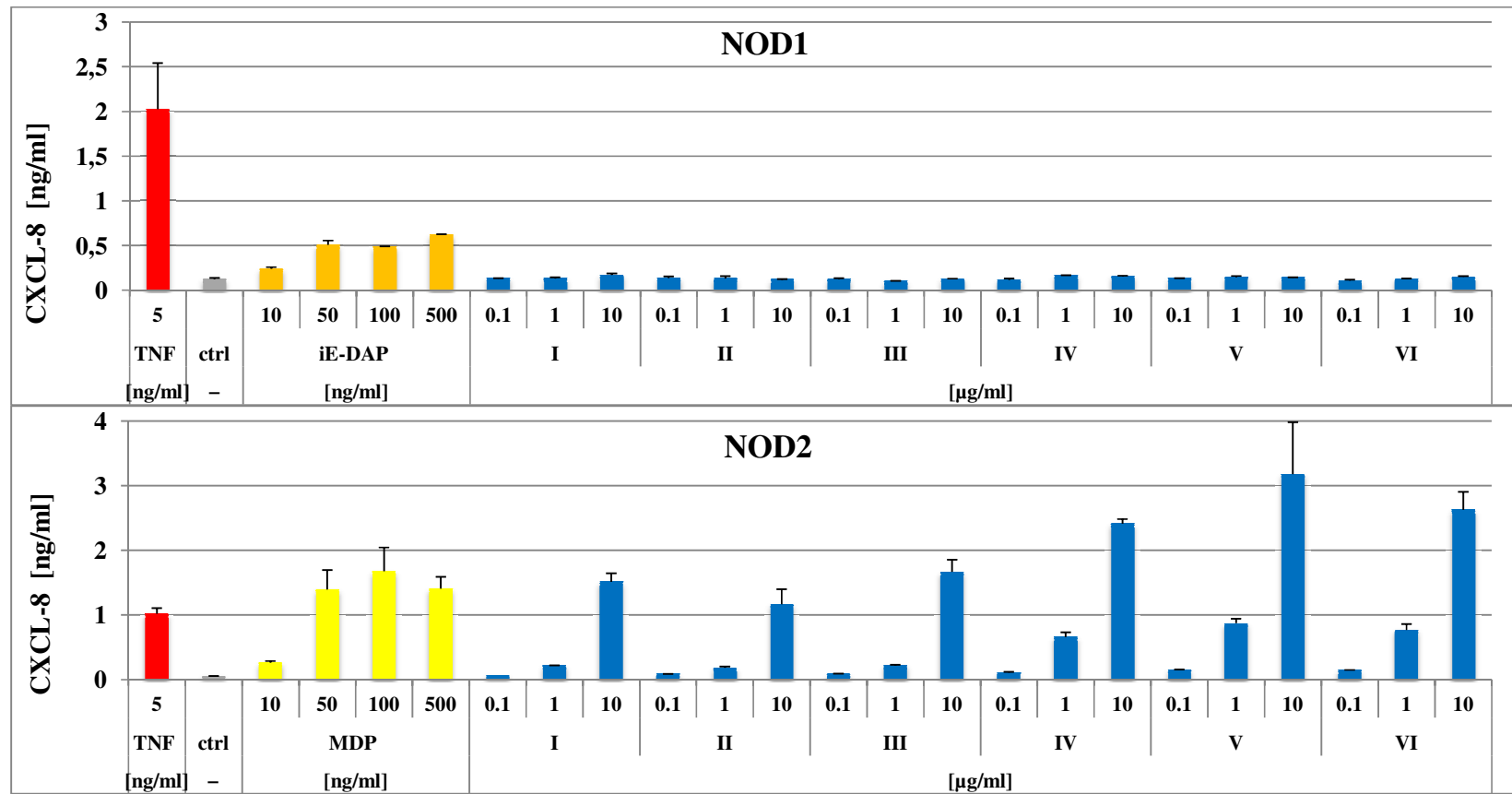
Figure 4.6 HEK293 *in vitro* tests on the influence of PGN TSK fractions I–VI (0.1, 1 and 10 µg/ml) on intracellularly NOD1 or NOD2 mediated CXCL-8 release. Incubation with TNF-α and the known ligands iE-DAP or MDP served as positive controls and un-stimulated cells as the negative control. Each of the 6 fractions showed ability to induce CXCL-8 production in NOD2 but not NOD1 expressing cells, in a dose dependant mode. Given is the mean ± SD and one representative out of two independent experiments is depicted.

4.2.3 Separation of PGN fragments by RP HPLC

The TSK I–VI fractions underwent further purification by analytical RP-12 HPLC. Therefore, a widely used buffer system was applied (220). A gradient of 2–100% aqueous CH_3CN in TFA (0.1%) over 60 minutes was utilized in first experiments to learn about the elution profile of each TSK fraction. First, 100 µg per run were applied. The material from fraction I–V eluted mainly in the void volume. Additionally, a minor sample cluster was detected from minute 17–23 for TSK I-IV. The HPLC of 100 µg from TSK VI yielded a similar cluster of higher intensity, but the detected sample peaks were poorly separated (**Figure 9.1**, shown in the appendix). This initial test indicated that variation of the buffer gradient was necessary to enhance the separation of the PGN fragments from each TSK fraction. Furthermore, it was found out that for the work with aqueous CH_3CN an inline degasser was pivotal. During the first HPLC performances problems with unequal tube volumes came up. Several changes in the compressibility and refill adjustments, pump exchange or long (1 hour) degassing of the buffers with He did not improve the situation until finally the use of an inline degasser resulted in constant flow rates.

Despite the marginal separation of the PGN components of TSK I–VI after the first HPLC test with 2–100% aqueous CH_3CN in TFA (0.1%) the pools were analyzed by ESI-MS to get a first idea of the nature and size of the PGN fragments that were generated by mutanolysin digest. ESI-MS results concerning the PGN of *L. lactis* G121 are presented in the next chapter.

In the following separation trials TSK V and VI were used. The main goal of the PGN studies was to purify monomeric (1 NAM and 1 NAG in the backbone) and dimeric PGN structures in a preparative scale for *in vitro* and *in vivo* investigations. These structures were found by ESI-MS in TSK V and VI. Randomly, the optimization of the gradient was tested with 200 µg of TSK V per injection. Hence, the percentage of buffer B (CH_3CN in 0.1% TFA) was decreased from 60–10% stepwise, as shown in the overlay of the chromatograms in **Figure 4.7**. The best resolution of the cluster gave a gradient of 2–15% buffer B (**Figure 4.8**).
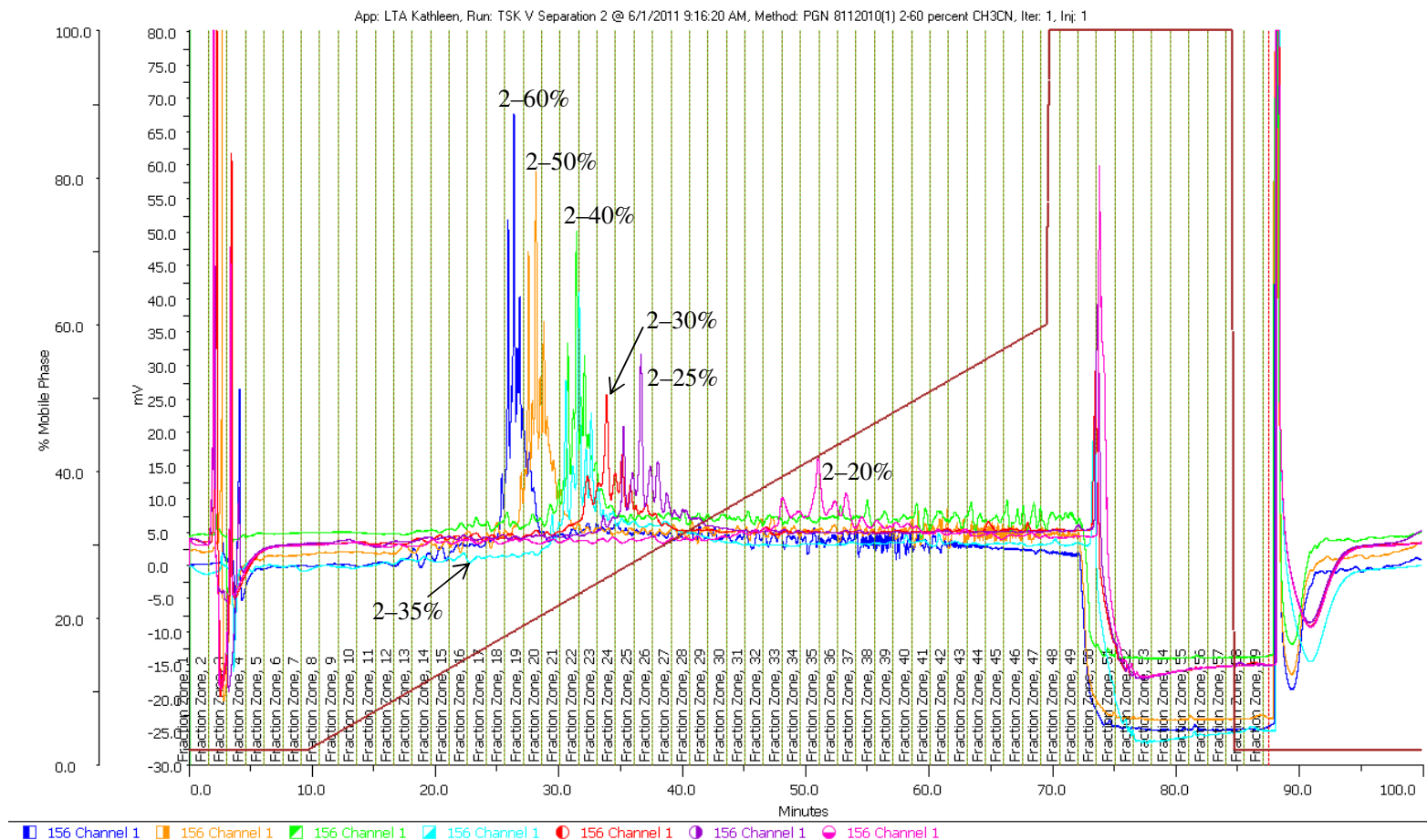
Figure 4.7 Overlay of seven RP-12 HPLC runs, performed in an analytical scale for evaluation of the gradient suitable for purification of multiple PGN fragments. The buffers used were 0.1% TFA in H_2O (A) and 0.1% TFA in CH_3CN (B). For each run 200 µg of PGN TSK fraction V were injected at 1 ml/ minute. Changing the gradient from 60% to 20% B influenced the elution profile and provided a sharper separation of the substance fragments.
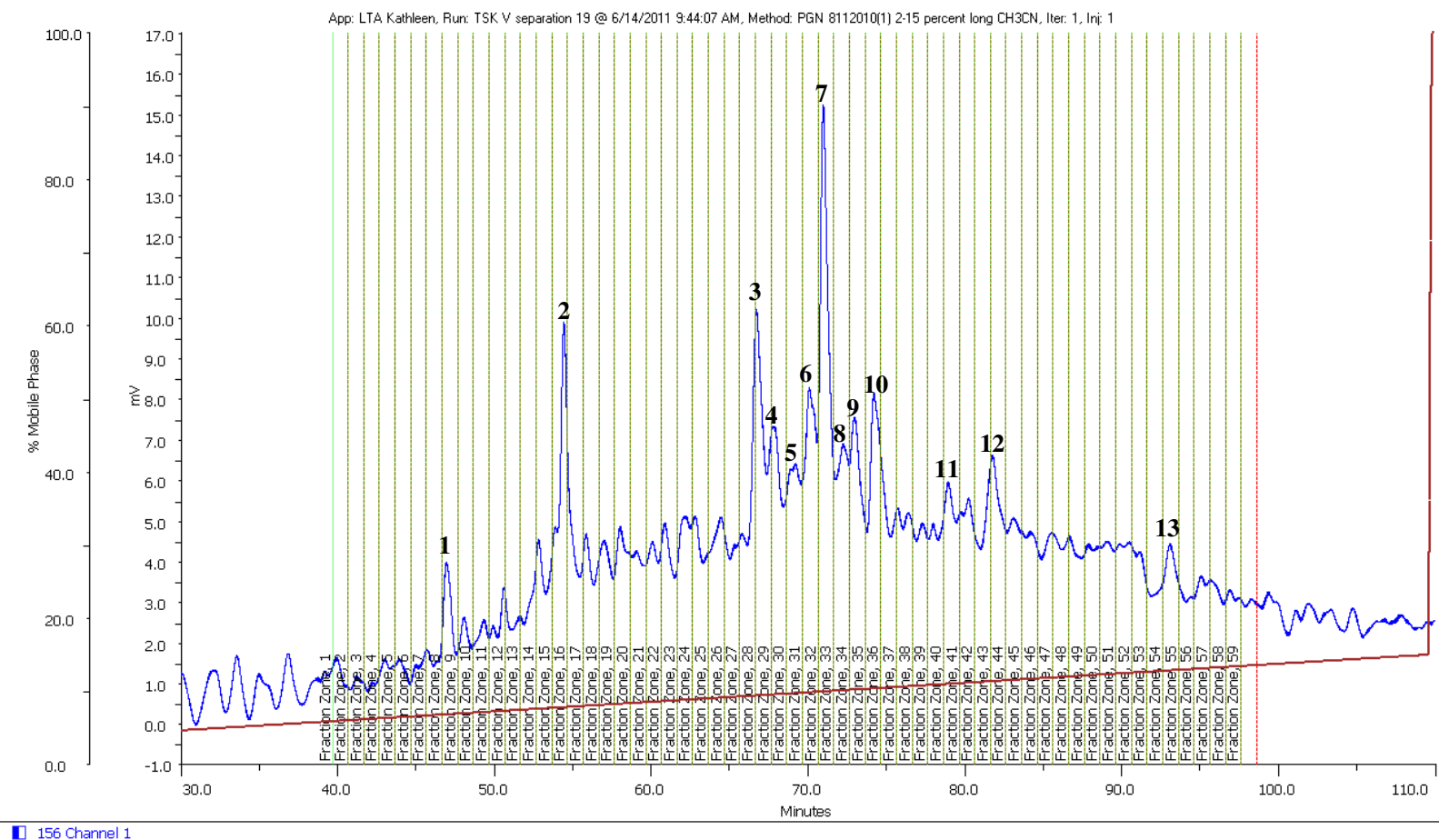
Figure 4.8 RP-12 HPLC chromatogram recorded from separation of 200 µg of PGN TSK fraction V with a gradient of 2–15% buffer B at a flow rate of 1 ml/minute on a RP-12 column. This gradient gave the best separation judged on the chromatogram. A gradient from 2–10% buffer B (**Figure 9.2**, shown in the appendix) did not retain the sample to the column anymore. Thirteen pools were picked for ESI-MS analysis.

Additionally the prolongation of the gradient to 110 minutes improved the peak separation. Ten percent of buffer B (**Figure 9.2**, shown in the appendix) led to elution of the entire sample in the void volume.

Pools 1–13 indicated in **Figure 4.8** were chosen for ESI-MS analysis. The identified major mass peaks from pool 1 and 3 were mono- and dimeric PGN structures, respectively, which could be obtained quite pure but not 100% free of other structures (**Figure 4.10**). For this reason, the next step was accumulation of material of pool 1 and 3 by several HPLC runs for a final purification by re-chromatography of these isolates. Re-chromatography was thought to give a pure separation of the structures of interest (938.408 u, 1080.482 u, 1521.721 u and 1927.865 u), either by the same or changed buffers and gradient system. From 8 runs of 200 µg with a gradient of 2–15% buffer B from minute 10–110, 230 µg of pool 1 and 150 µg of pool 3 were yielded. This was not enough for several re-chromatography runs. Future continuation of these experiments in the future would consequentially consist of piling more material of TSK V HPLC pool 1 and 3 and conduction of further HPLC separations.

4.2.4   ESI-MS analysis of PGN RP-HPLC fractions

The ESI mass spectra of TSK I–VI after HPLC (2–100% buffer B) revealed the presence of a myriad of PGN fragments. **Figure 4.9** displays the spectrum of TSK VI and points out the heterogeneity of the obtained mutanolysin digest. Several monomeric fragments could be identified from three to five amino acids in the stem peptide. The sum of the defined structures of TSK I–VI is presented in **Table 4.1** and termination of the fragments was in agreement with data of Courtin et al. (221). In general, the findings of these ESI-MS experiments corroborated those of the compositional analysis. Thus, the PGN of *L. lactis* G121 was approved to be of the Lys-type. Moreover, variations of *iso*-(i)Glu and iGln in the peptide chain were found just as Asp and/or Asn types of compounds. In TSK I and II only one mass peak was assigned, namely that of the dimer Penta-N-Penta-N (1184.690 u). TSK III and IV consisted mainly of tetramers and trimers with 2513.154 u and 2919.308 u as the most abundant masses. PGN dimers were the majority of the structures of TSK pool V. Strikingly, acylated as well as deacylated fragments within TSK III-VI were detected.
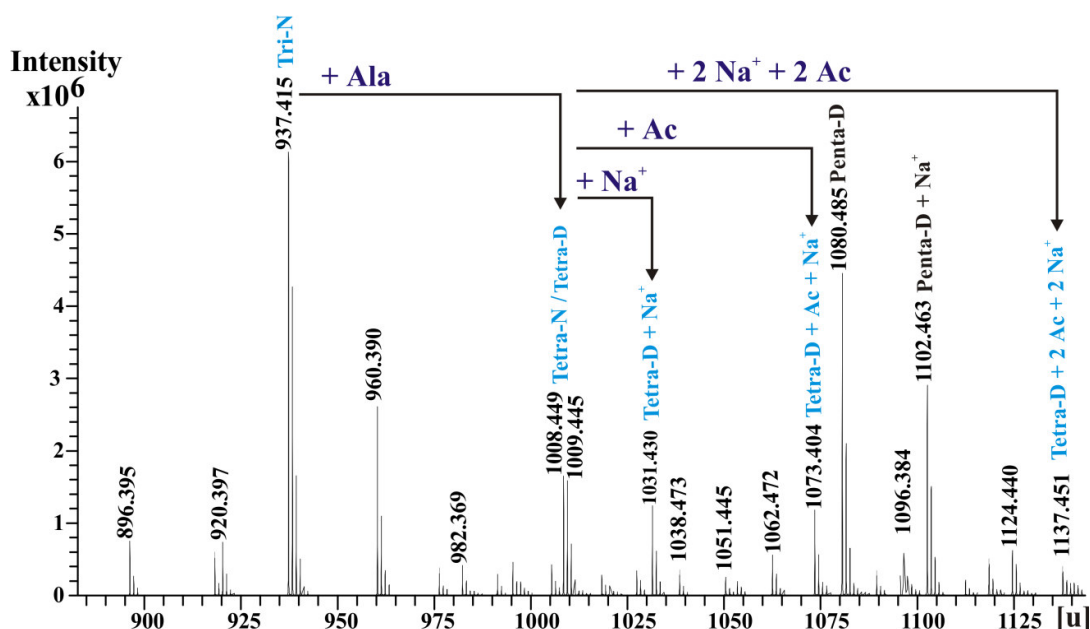
Figure 4.9 Detail of the ESI-MS spectrum of PGN TSK fraction VI illustrating a high level of heterogeneity. The mass of 937.415 u named Tri-N (Tri: disaccharide tripeptide (Ala-iGln-Lys), N: Asn) is described and the corresponding compound Tetra-N or -D (D: Asp) with one Ala substitution. Na$^+$ adducts as well as de- and acetylated fragments were identified. **Table 4.1** lists all mass peaks found in TSK I–VI.

Table 4.1 Summary of identified mass peaks from ESI-MS of PGN TSK fraction I-VI. Average mass units of 203.079 for NAG, 275.10 for NAM, 71.037 for Ala, 128.058 for iGln, 129.042 for iGlu, 128.098 for Lys, 115.026 for Asp, 114.042 for Asn, 21.982 for Na$^+$ and 42.010 for Ac were used for calculations. Denotations are explained at the end of the table.

TSK pool	Detected u	Composition	Calculated u
I	1184.690	Penta-N-Penta-N	1184.626
II	1184.687	Penta-N-Penta-N	1184.626
III	1184.689	Penta-N-Penta-N	1184.626
	2128.004	Penta-N-Penta-N + Ala – 2 Ac	2128.023
	2513.154	Tri-N-Tetra-N-Tetra-D – 2 NAG	2513.150
	2716.218	Tri-N-Tetra-N-Tetra-D – NAG	2716.229
	2859.290	Penta-N-Tetra-D-Tetra-D – NAG	2859.288
	2919.308	Tri-N-Tetra-N-Tetra-D	2919.309
	2935.263	Tri*-N-Tri*-N-Tetra*-D + 2 Ac	2935.224

Table 4.1 continued

	2990.331	Tetra-N-Tetra-N-Tetra-D	2990.346
	3060.363	Penta-N-Tetra-N-Tetra-N	3060.399
	3061.369	Penta-N-Tetra-N-Tetra-D	3061.383
IV	1543.686	Tri-N-Tetra-N – 2 NAG + Na$^+$	1543.698
	1544.687	Tri-N-Tetra-D – 2 NAG + Na$^+$	1544.682
	1928.854	Tri-N-Tetra-D	1928.856
	1999.898	Tetra-N-Tetra-D	1999.895
	2070.920	Penta-N-Tetra-D	2070.932
	2513.162	Tri-N-Tetra-N-Tetra-D – 2 NAG	2513.150
	2716.224	Tri-N-Tetra-N-Tetra-D – NAG	2716.229
	2919.310	Tri-N-Tetra-N-Tetra-D	2919.309
V	1137.534	Tri-D + Ala + Lys	1137.540
	1479.703	Tri-N-Tetra-N – 2 NAG – Ac	1479.715
	1521.723	Tri-N-Tetra-N – 2 NAG	1521.715
	1592.743	Tetra-N-Tetra-N – 2 NAG	1592.753
	1724.795	Tri-N-Tetra-N – NAG	1724.795
	1928.858	Tri-N-Tetra-D	1928.856
VI	896.395	Tri-D – Ac	896.408
	920.397	Di-NAG + Na$^+$	920.347
	937.415	Tri-N	937.424
	960.390	Tri-D + Na$^+$	960.390
	982.369	Tri-D + 2 Na$^+$	982.372
	1008.450	Tetra-N	1008.461

Table 4.1 continued

1009.445	Tetra-D	1009.445
1031.430	Tetra-D + Na$^+$	1031.427
1038.473	Penta-D − Ac	1038.482
1051.445	Tetra-D + Ac	1051.445
1062.472	Tetra-D-D − 2 Ac + Na$^+$	1062.454
1073.404	Tetra-D + Ac + Na$^+$	1073.427
1080.485	Penta-D	1080.482
1096.384	Tetra*-D + Ac + 2 Na$^+$	1096.393
1102.463	Penta-D + Na$^+$	1102.464
1122.530	Tetra-N-N	1122.504
1124.440	Tetra-D-D	1124.472
1137.451	Tetra-D + 2 Ac + 2 Na$^+$	1137.409

Di: disaccharide dipeptide (Ala-iGln), **Tri**: disaccharide tripeptide (Ala-iGln-Lys), **Tri***: disaccharide tripeptide (Ala-iGlu-Lys), **Tetra:** disaccharide tetrapeptide (Ala-iGln-Lys-Ala), **Penta:** disaccharide pentapeptide (Ala-iGln-Lys-Ala-Ala), **D:** Asp, **N:** Asn, **disaccharide:** NAG-NAM, **Ac:** acetyl

After improvement of the HPLC method to a gradient of 2–15% buffer B over 100 minutes, 13 pools of separated TSK V material (**Figure 4.8**) were subjected to ESI-MS analysis. Pool 1 contained two major fragments which were Tri-D and Penta-D each with its Na$^+$ adduct. Penta-D (1080.482 u) and Penta-D-D + Ac (1238.441 u) could be identified from pool 2. The dimer Tri-N-Tetra-N (1927.864 u) and a fragment of it – 2 NAG (1521.720 u) were found in pool 3. The latter was the major component of pool 4 and Tri-N-Tetra-D – 2 NAG + Na$^+$ (1544.683 u) of pool 5. Pool 6–11 and 13 revealed multiple mass peaks of low intensity and poor separation. Additionally, the trimer Tri-N-Tetra-N-Tetra-D (2919.303 u) could be assigned as main component in good purity of pool 12. Since the focus was put on mono- and dimeric structures for purification and later biological tests pool 1 and 3, whose ESI-MS spectra are depicted in **Figure 4.10**, were chosen for further experiments. Repeated HPLC runs were performed to amass material of these two pools and use them for final separation by re-chromatography (chapter 4.2.3).
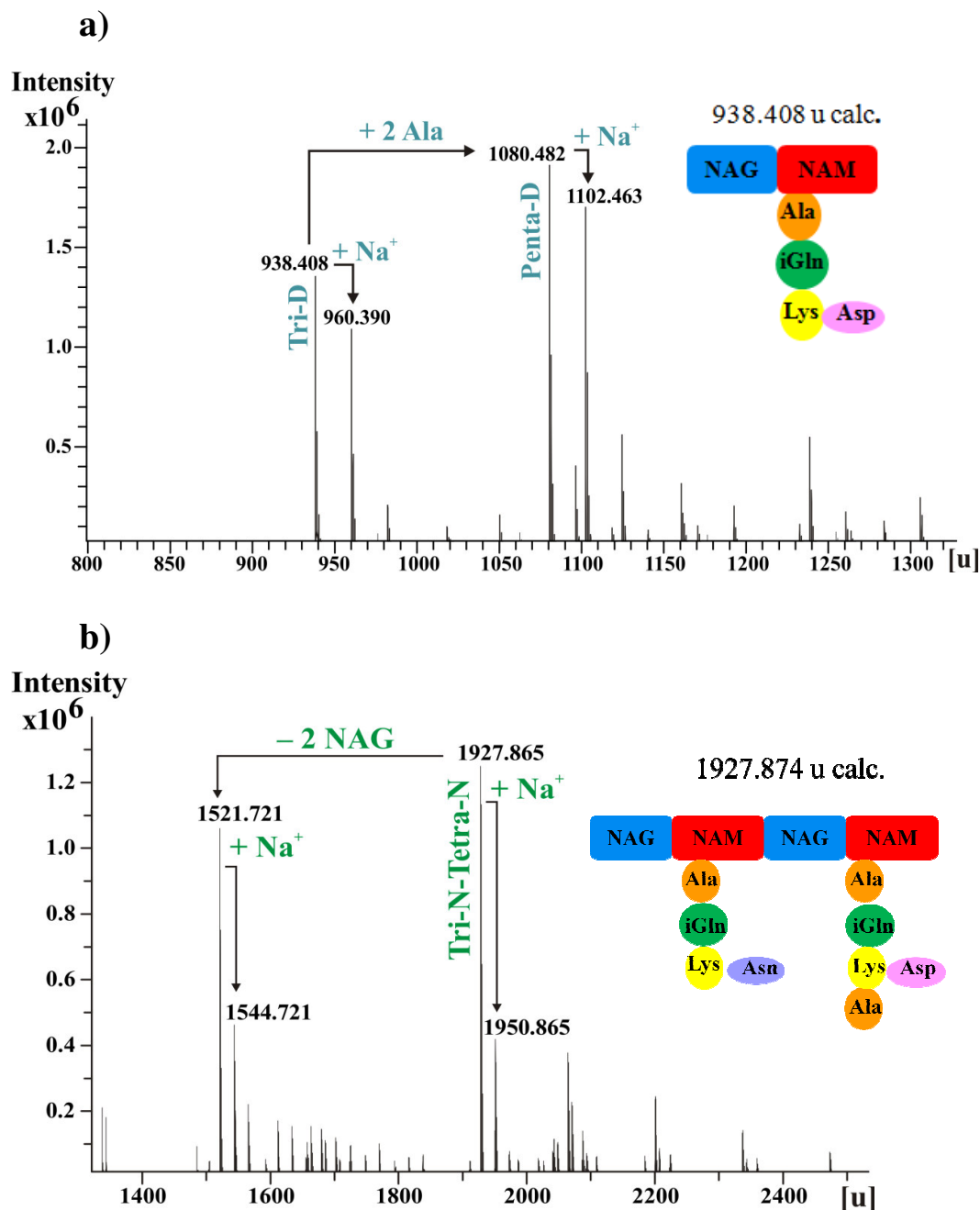
Figure 4.10 ESI-MS analysis of a) PGN TSK V HPLC pool 1 and b) pool 3. From spectrum a) two major monomeric structures, namely Tri-D and Penta-D as well as the Na$^+$ adducts of both were identified. A sketch illustrates the constitution of the components of Tri-D (938.408 u). In the lower panel b) the spectrum of pool 3 is presented. Pool 3 was also chosen for further analysis since it contained the two monomers Tri-N-Tetra-N and Tri-N-Tetra-N − 2 NAG (1521.721 u) with only little impurities. One possible arrangement of the constituents of Tri-N-Tetra-N is displayed in the cartoon. Unlabeled peaks refer to further PGN fragments as well as their Na$^+$ adducts of these.

4.3   CPS of *L. lactis* G121

4.3.1.1 CPS extraction and purification

To obtain CPS from *L. lactis* G121 5.3 g dry biomass was extracted with sterile 0.9% aqueous NaCl (77 mg, 1.45%) and the pellet thereof was further extracted with 1% phenol (102 mg, 1.92%). Due to previous results of Dr. A. Hanuszkiewicz (196)the first two fractions from P-60 filtration of each extract (Na1, Na2, Ph1 and Ph2) contained the CPS and were therefore further purified by P-10 SEC. After ultracentrifugation each fraction was proven to be free of nucleic acids (measured at 260 nm) and 5.2 mg of Na1 (0.1%), 21.4 mg of Na2 (0.4%), 4.8 mg of Ph1 (0.09%) and 23 mg of Ph2 (0.43%) were yielded. These samples were provided to Dr. E. Vinogradov from the NRC in Ottawa/Canada for detailed NMR spectroscopic investigations.

It revealed that none of the 4 fractions contained the original CPS. For instance Glc, Gal, GlcN, GalN, ManN and NAM were detected as CPS constituents. In contrast, the new extract contained Rha, Glc, GlcNAc and GalNAc as well as Gro and P. By full assignment of 2D NMR spectra a TA structure with contaminating Rha oligomers could be identified. This sample was completely identical to the TA structure isolated with 5% TCA as it is described in the next chapter. Thus, the TA of *L. lactis* G121 was denoted as extracellular (EC) TA since it was obtained by watery 0.9% NaCl and 1% phenol extraction besides mild TCA hydrolysis. The CPS protocol was performed twice but no such structure could be found

4.4   EC TA of *L. lactis* G121

4.4.1   Isolation and chemical composition of the EC TA

From the TCA extraction of 24 g bacterial wet mass 290 mg (1.21%) crude TA was obtained. The phosphate-containing fraction after HIC (38 mg, 0.16 %) was applied to AEX for separation of possible contaminating neutral polysaccharides. As shown in **Figure 4.11** the AEX yielded two phosphate containing pools (Q2 and Q3) which eluted quite close between minute 16 and 44 whereas Q3 exhibited a 4.5-fold higher extinction at 820 nm in the phosphate assay. SEC on Sephadex G10 yielded the desalted samples Q2 (2.8 mg, 0.012%) and Q3 (8.6 mg, 0.036%).
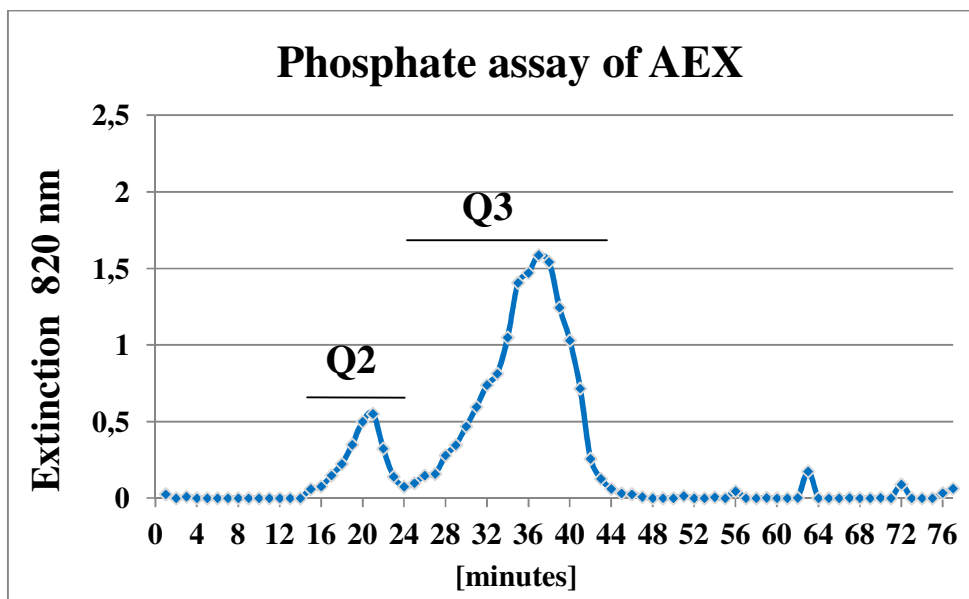
Figure 4.11 For detection of the TA after AEX a phosphate assay was performed. After hydrolysis and reaction of the sample with a color reagent the extinction was measured at 820 nm. The AEX of TA from *L. lactis* G121 revealed two phosphate-containing pools named Q2 and Q3, respectively. One example from three independent repeats is shown.

Components of Q2 were found out to be L-Rha (525.8 nmol/mg) D-GalN (not quantified), D-GlcN (not quantified), D-Glc (329.4 nmol/mg), P (1 µmol/mg) and Gro (not quantified). D-Gal (465.1 nmol/mg), D-Glc (142.9 nmol/mg), P (3.7 µmol/mg) and Gro (not quantified) were identified as constituents of the Q3. GLC FA analysis showed that both samples were free of lipids.

To verify if *L. lactis* G121 possessed two types of TA or if Q3 originated from LTA 2 mg of LTA were incubated with 5% TCA for 24 hours at 4°C. The ^{1}H NMR spectrum (**Figure 9.3**, shown in the appendix) clarified that TCA treatment did not deacylate the LTA molecule. In addition to that, 3 mg of Q3 were applied on Bio-Gel P-2 in PAW buffer without pump to check if the D-Glc was a part of the molecule or an impurity. One fraction was obtained, NMR spectroscopy of which still identified two anomeric Glc signals which were identical to those from the LTA linker (chapter 4.5.5). This indicated that Q3 was deacylated LTA (deacLTA) which was isolated together with the EC TA. ESI-MS data (presented in chapter 4.5.4) and assignments of 1D as well as 2D NMR spectra of the deacLTA corroborated this finding. Hence, solely Q2 was considered as EC TA of *L. lactis* G121.

4.4.2   ESI-MS analysis of the EC TA

Figure 4.12 shows the charge-deconvoluted ESI-MS spectrum recorded in the negative ion mode under soft-ionization conditions. Referring to the number of repeating units 8 different EC TA species were identified. One repeat was calculated to contain 1 P, 1 hexose (Hex), 3 *N*-acetyl hexosamines (HexNAc) and 1 Gro with an average mass of 925.294 u (H_2O subtracted). The complete assignments of the EC TA are summarized in **Table 4.2**. Multiplicity of mass peaks was correlated to Na^+ and/or K^+ adducts and fragments of the EC TA.

4.4.3   Depolymerization of EC TA

To analyze EC TA monomers, 3.2 mg of the probe were subjected to 48% HF treatment. Afterwards SEC on Bio-Gel P-2 was conducted for isolation of monomers. Two major fractions could be obtained. The first fraction yielded 390 µg (12.2 % of EC TA) and the second fraction 210 µg (6.6 % of EC TA). Both fractions underwent detailed NMR spectroscopic studies.

Table 4.2 Assigned mass peaks of EC TA from *L. lactis* G121. Average mass units of 74.04 for Gro, 79.97 for P, 162.05 for Hex, 203.04 for HexNAc and 21.982 for Na^+ were used for calculations.

Detected u	Composition	Calculated u	Repeats
1868.606	2 P, 2 Hex, 6 HexNAc, 2 Gro	1868.598	2
2793.883	3 P, 3 Hex, 9 HexNAc, 3 Gro	2793.892	3
3741.172	4 P, 4 Hex, 12 HexNAc, 4 Gro + Na^+	3741.169	4
4644.473	5 P, 5 Hex, 15 HexNAc, 5 Gro	4644.480	5
5569.811	6 P, 6 Hex, 18 HexNAc, 6 Gro	5569.774	6
6495.081	7 P, 7 Hex, 21HexNAc, 7 Gro	6495.068	7
7420.370	8 P, 8 Hex, 24 HexNAc, 8 Gro	7420.636	8
7442.429	8 P, 8 Hex, 24 HexNAc, 8 Gro + Na^+	7442.345	8
8367.629	9 P, 9 Hex, 27 HexNAc, 9 Gro + Na^+	8367.639	9
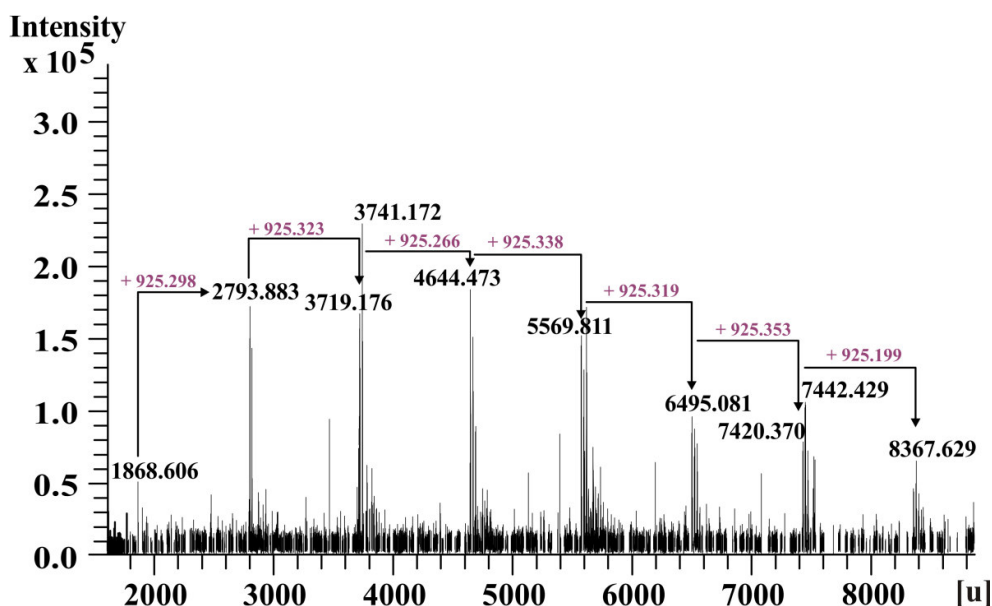
Figure 4.12 The ESI-MS spectrum of the EC TA from *L. lactis* G121. One EC TA repeat contained 1 P, 1 Hex, 3 HexNAc and 1 Gro with an average mass of 925.294 u (H$_2$O subtracted). In total 8 species from 2 (1868.606 u) to 9 repeats (8367.6294 u) could be distinguished. Furthermore, Na$^+$ and/or K$^+$ adducts of the EC TA as well as fragments of it were detected and refer to unlabeled signals. The identified mass peaks are summarized in **Table 4.2**.

4.4.4   NMR spectroscopy of the EC TA

Three major anomeric signals could be detected from the ^{1}H NMR spectrum of the EC TA (**Figure 4.13**). A fourth spin system was assigned with the help of 2D homonuclear and heteronuclear correlation experiments. The H-1 of this system was saturated with the HOD signal. The anomeric protons could be identified as H-1 of α-D-Gal*p*NAc [residue A, δ_H 5.60, $^3J_{1,2}$ 3.85 Hz, H-1/H-2 coupling in the ROESY spectrum (**Figure 4.14**) at δ_H 5.60/4.49], H-1 of α-D-Glc*p*NAc (residue B, δ_H 5.03, cross peak of H-1/H-2 in the ROESY spectrum at δ_H 5.03/3.93), H-1 of β-D-Glc*p* (residue C, δ_H 4.44, $^3J_{1,2}$ 7.96 Hz) and H-1 of β-D-Glc*p*NAc (residue D, δ_H 4.74, $^3J_{1,2}$ 8.22 Hz).

Inter-molecular linkages were indicated in the HMBC spectrum (**Figure 9.4**, shown in the appendix) were cross peaks between proton/carbon resonances C1/A3 (δ_H 4.44/δ_C 77.20), B1/A4 (δ_H 5.03/δ_C 75.70) and A1/D3 (δ_H 5.60/δ_C 78.20) were recorded. A ROESY experiment (**Figure 4.14**) confirmed these linkages proving *inter*-residual connectivities between C1/A3 (δ_H 4.44/3.87), B1/A4 (δ_H 5.03/4.34) and A1/D3 (δ_H 5.60/3.81). The connec-

tion to Gro (residue E) was affirmed by nuclear Overhauser effect (NOE) cross peak of proton signals D1 and E2 (δ_H 4.74/3.97).
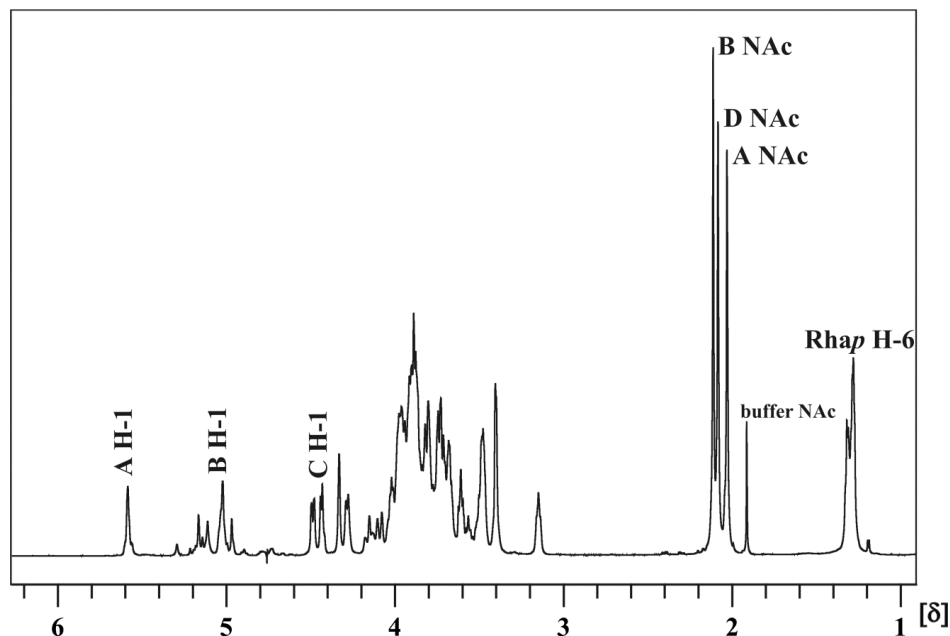
Figure 4.13 ^{1}H NMR spectrum of EC TA from *L. lactis* G121. Three major anomeric protons could be identified and a fourth was saturated with the HOD signal. Besides three NAc CH_3 shifts the characteristic 6-deoxy-Hex CH_3 of Rha*p* was found. Capital letters are denoted in **Table 4.3** and corresponding structures in **Figure 4.15**. Recordings were performed in D$_2$O at 700 MHz and 27°C.

Additionally these substitutions were corroborated by strong downfield resonances of carbons A3, A4, D3, and E2 (**Table 4.3**). In the high field region of the ^{1}H spectrum (**Figure 4.13**) three *N*-acetyl-CH_3 shifts were indicated. Correlations observed in the HMBC spectrum between the ring H-2 and carbonyl carbons assigned each CH_3 group to their respective moiety. **Figure 4.15** represents the complete structure of the EC TA polymer of *L. lactis* G121 concluded from compositional analysis, ESI-MS and NMR spectroscopy data.

As shown in **Figure 4.13**, the presence of L-Rha*p* was confirmed by its characteristic H-6 high field shift of the 6-deoxy group (δ_H 1.29 and δ_H 1.33) and ring protons as well as anomeric resonances of lower intensity. After detailed NMR spectroscopic studies no connectivities between L-Rha*p* and the EC TA were identified, either from the HMBC or NOE experiments. This together with the ESI MS results suggested the Rha to be a contamination.
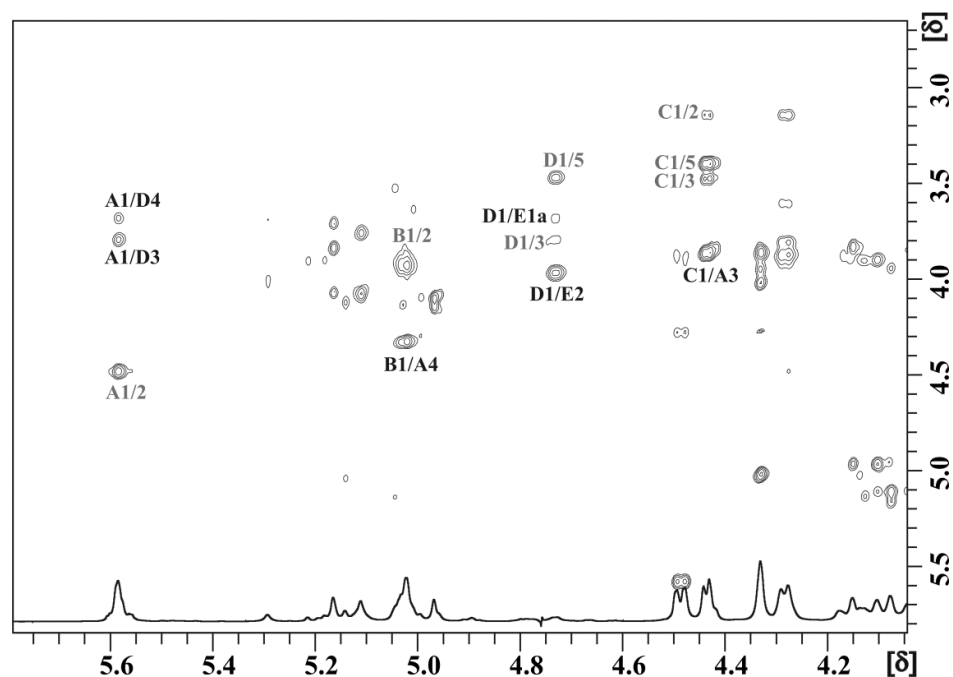
Figure 4.14 Anomeric region of the ^{1}H and ^{1}H,^{1}H ROESY NMR spectra of the EC TA. Cross resonances recorded with the ROESY spectrum proved the *inter*-molecular connectivities (displayed by black labels) within the EC TA as depicted in **Figure 4.15**. Arabic numerals refer to the respective proton and capital letters are explained in **Table 4.3** as well as **Figure 4.15**. Minor couplings could be referred to contaminating L-rhamnan signals and were left unlabeled. Measurements were conducted in D$_2$O at 700 MHz and 27°C.
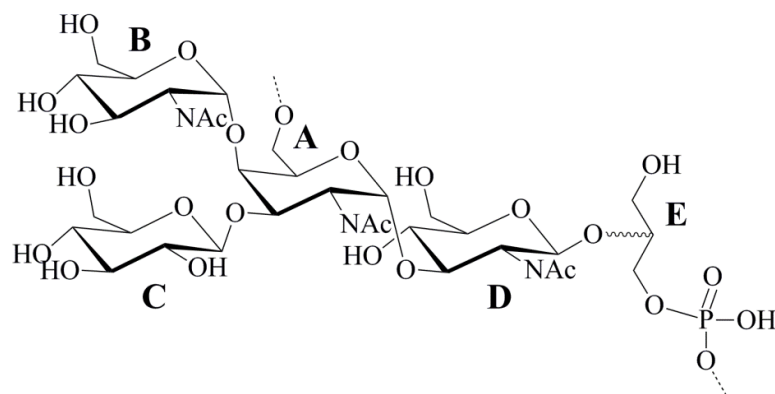
Figure 4.15 The structure of the EC TA isolated from *L. lactis* G121. NMR spectroscopy data are summarized in **Table 4.3**.

Table 4.3 NMR spectroscopy shifts of the intact EC TA polymer of *L. lactis* G121 obtained from recordings at 600 MHz. The data of the EC TA monomer yielded from 48% HF cleavage were measured at 700 MHz and are presented in brackets. The ^{1}H/^{1}H,^{13}C HSQC-DEPT overlay of the EC TA monomer is displayed in **Figure 4.16** and depicts the assigned proton/carbon cross peaks. Linked positions are emphasized.

Residue		Chemical shifts of protons and carbons (δ)						
		1 a/b	2	3 a/b	4	5	6 a/b	CH$_3$ NAc
α-D-GalpNAc A	^{1}H	5.60 (5.48)	4.49 (4.48)	3.87 (3.91)	4.34 (4.29)	4.03 (3.94)	3.96 (3.67)	2.03 (2.02)
	^{13}C	97.90 (98.38)	49.80 (49.96)	<u>77.20</u> (<u>77.09</u>)	<u>75.70</u> (<u>75.60</u>)	72.0 (72.93)	<u>64.60</u> (60.68)	23.10 (23.05)
α-D-GlcpNAc B	^{1}H	5.03 (4.99)	3.93 (3.89)	3.88 (3.89)	3.61 (3.60)	4.28 (4.29)	3.83/3.88 (3.80/3.87)	2.08 (2.07)
	^{13}C	98.30 (98.21)	55.10 (55.08)	71.60 (71.44)	70.60 (70.54)	72.90 (72.62)	61.10 (61.01)	22.80 (23.15)
β-D-Glcp C	^{1}H	4.44 (4.44)	3.16 (3.14)	3.48 (3.45)	3.41 (3.38)	3.41 (3.38)	3.74/3.90 (3.73/3.90)	
	^{13}C	106.0 (105.97)	74.20 (74.08)	76.80 (76.76)	70.90 (70.88)	77.0 (76.95)	61.80 (61.71)	
β-D-GlcpNAc D	^{1}H	4.74 (4.71)	3.81 (3.80)	3.81 (3.75)	3.69 (3.70)	3.48 (3.45)	3.74/ 3.90 (3.73/3.90)	2.06 (2.05)
	^{13}C	102.10 (101.89)	55.50 (55.50)	<u>78.20</u> (<u>78.96</u>)	72.50 (72.13)	76.80 (76.76)	61.80 (61.71)	23.50 (23.51)
Gro E	^{1}H	3.68/3.73 (3.62/3.65)	3.97 (3.85)	3.99 (3.66/3.71)				
	^{13}C	61.90 (62.03)	<u>81.0</u> (<u>82.37</u>)	<u>65.80</u> (62.37)				

The depolymerization of the EC TA was conducted to further approve the Rha contamination. Two fractions after Bio-Gel P-2 separation were analyzed. From the ^{1}H spectrum of the first fraction (390 µg) EC TA and Rha signals could be verified. Couplings ob-

served in the ^{1}H,^{31}P HMQC spectrum (**Figure 9.5**, shown in the appendix) for two phosphodiester signals at (δ_P 0.76) and (δ_P 0.82) and protons E3 (δ_H 3.99) as well as A5 (δ_H 4.03) and A6 (δ_H 3.96) corroborated the connection between the TA repeating units. Additionally, it indicated that HF cleavage of the sample was incomplete. In comparison to that, the ^{1}H spectrum of the second fraction (210 µg) gave shifts of solely the EC TA monomer. Full assignment of the 1D and 2D NMR spectra of both fractions finally ascertained that the Rha was not a part of the EC TA structure. The ^{1}H,^{13}C HSQC-DEPT spectrum of the EC TA monomer is depicted in **Figure 4.16** and **Table 4.3** summarizes all NMR spectroscopy data of the EC TA poly- and monomer.
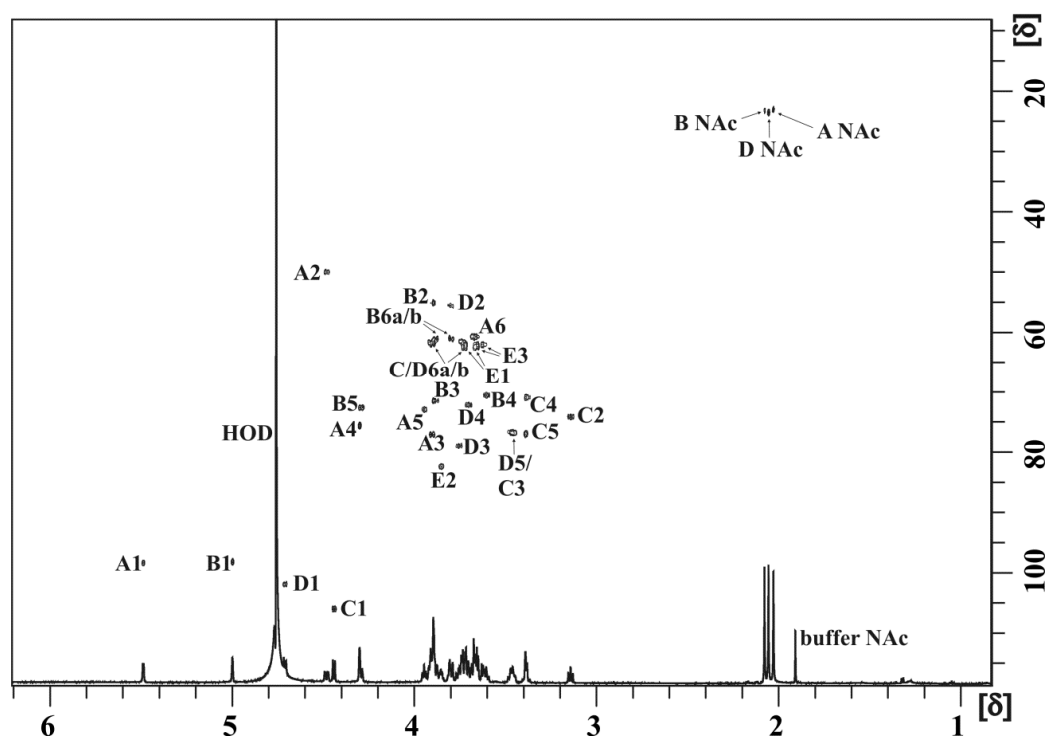
Figure 4.16 Overlay of the ^{1}H and ^{1}H,^{13}C HSQC-DEPT NMR spectra of the EC TA monomer yielded from 48% HF treatment. No Rha resonances were present. Arabic numerals refer to the respective proton/carbon atom and capital letters are explained in **Table 4.3** as well as **Figure 4.15**. Recordings were carried out in D$_2$O at 700 MHz and 27°C.

4.4.5   HEK293 assay of EC TA

To investigate the biological activity of the EC TA it was applied in HEK293 transfection assays. Increasing concentrations of the sample (0.1, 1 and 10 µg/ml) were used for stimulation of transiently transfected HEK293 cells. **Figure 4.17** shows that neither TLR2 nor TLR4 expressing cells produced CXCL-8 upon EC TA treatment. Furthermore the same EC TA concentrations were tested with HEK293 cells which were transfected with the

intracellular receptors NOD1 or NOD2. Again, the CXCL-8 levels were similar to that of
the untreated control as depicted in **Figure 4.18**.
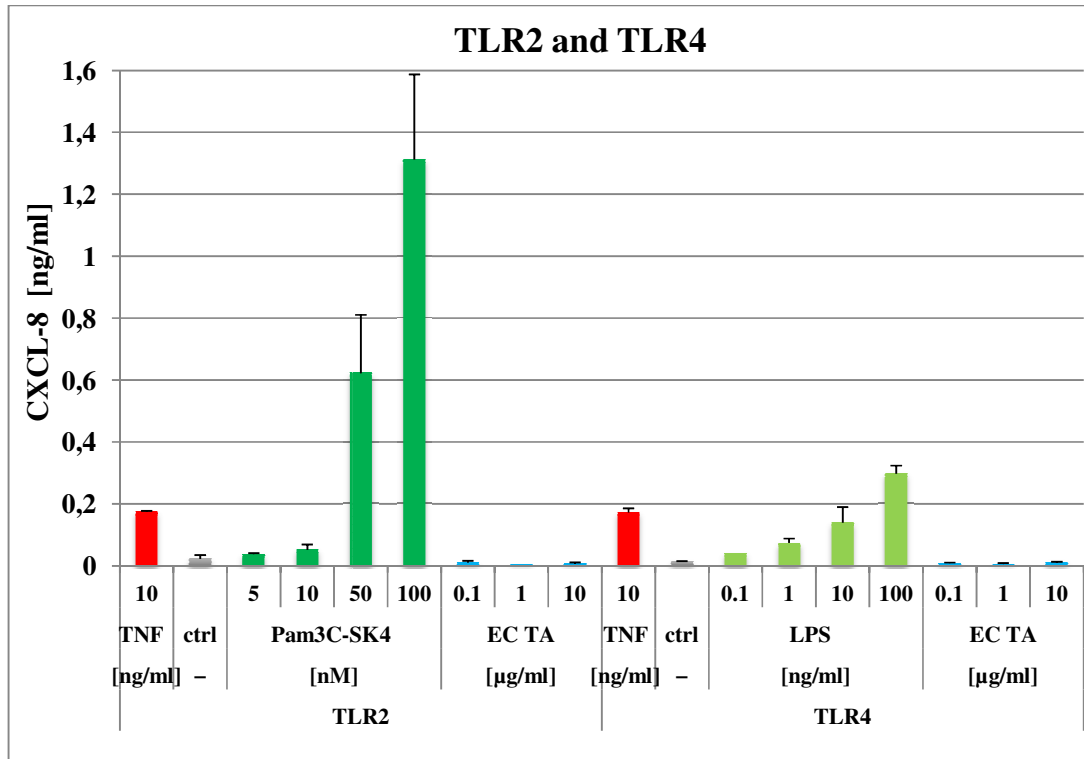
Figure 4.17 The stimulation of HEK293 cells which were either TLR2 or TLR4 transfected with EC TA
(0.1, 1 and 10 µg/ml) did not induce a CXCL-8 release. TNF-α and Pam$_3$C-SK$_4$ or LPS were used as posi-
tive controls. Untreated cells served as negative control. Results are given as mean ± SD. One representa-
tive out of two is shown.
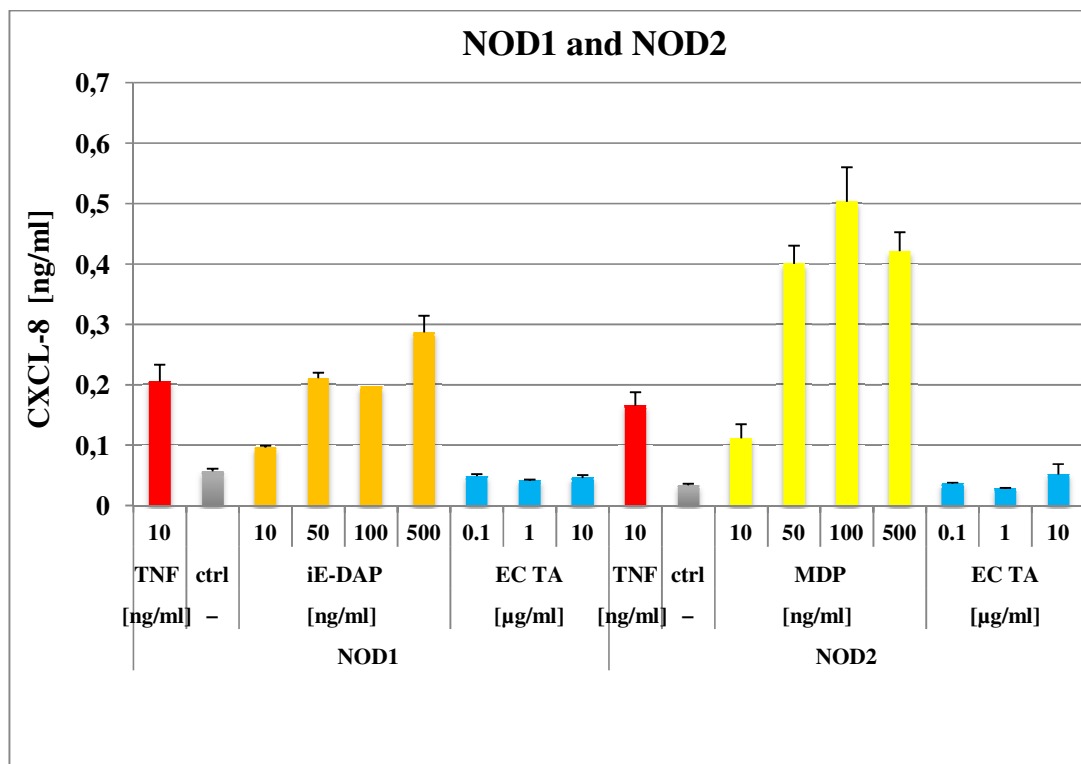
Figure 4.18 The CXCL-8 release of either NOD1 or NOD2 transfected HEK293 cells was not induced by increasing concentrations (0.1, 1 and 10 µg/ml) of EC TA. As positive stimulant TNF-α and iE-DAP or MDP were used. The negative control was an aliquot of un-stimulated cells. Results are expressed as mean ± SD. One representative experiment from two is shown.

4.5   LTA of *L. lactis* G121

4.5.1   Isolation and composition of the LTA

From 51.3 g wet mass of *L. lactis* G121 6.98 g of the EtOH washed supernatant were obtained and subjected to *n*-butanol extraction. The crude LTA preparation obtained from the water phase yielded 735 mg (1.4%) after dialysis and before HIC, respectively. Purification by HIC and several freeze-drying steps with H_2O for removal of residual buffer yielded 40.8 mg (0.08%) of LTA.

Neutral sugar analysis and determination of the absolute configuration revealed D-Gal (322.5 nmol/mg) and D-Glc (201.5 nmol/mg). Additionally P (4.2 µmol/mg), Gro (not quantified) and D-Ala (412.0 nmol/mg) were found out to be elements of the LTA isolated from *L. lactis* G121. Besides minor portions of 12:0 (4.0 nmol/mg), 15:0 (4.7 nmol/mg) and 18:0 (4.8 nmol/mg), 14:0 (112.1 nmol/mg), 16:0 (305.4 nmol/mg), 16:1 (23.0 nmol/mg), 18:1 (200.0 nmol/mg), and Δ-19:0 (105.4 nmol/mg) could be detected

during FA analysis. Hydrogenation of the FAME sample was utilized to distinguish be-
tween a Δ-19:0 or a 19:1 in case of the detected peak at 24.67 minutes with a mass of
296.72 u. Since the mass was not modified after hydrogenation Δ-19:0 was identified.
The FA 12:0, 15:0 and 18:0 were excluded from LTA considerations due to their low
abundance.

4.5.2 Preparation of the LTA linker and its methylation

An aliquot of LTA (12 mg) was subjected to treatment with 48% HF to cleave the GroP
backbone. Extraction with H_2O/CHCl$_3$/MeOH obtained 9.9 mg (82.4%) of the lipid an-
chor in the organic phase. To eliminate the FA a mild hydrazine treatment was conducted.
The *O*-deacylation yielded the LTA linking backbone (4.9 mg, 49.5%) which was further
investigated by NMR spectroscopy and methylation analysis. With the latter method
equal analytical amounts of 1,5-*O*-acetyl-2,3,4-*O*-methylglucitol and 1,2,5-*O*-acetyl-3,4-
O-methylglucitol could be identified.

4.5.3 ESI-MS analysis of the LTA

The ESI-MS analysis of the LTA from *L. lactis* G121 displayed a complex mixture of
different species. Not only the number of GroP repeating units and the degree of D-
alanylation of these but also different types of FA accounted for the heterogeneous com-
position. **Figure 4.19** shows the example of one LTA lipid anchor species with 932.642 u
made up of two FA (16:0 and Δ-19:0), 1 Gro, and 2 Hex. Based on this anchor 8 further
species could be detected differing in the number of GroP repeats and D-Ala substituents.

For the lipid part of the LTA diverse combinations of FA were proven. The most abun-
dant molecular species of 3 Gro, 2 P and 2 Hex is presented in a section of the ESI-mass
spectrum (**Figure 4.20**). Five different acylation patterns of the Gro residue in the linker
were defined (14:0 and 16:0, 14:0 and Δ-19:0, 14:0 and 18:1, 16:0 and 16:1, 16:0 and
18:1 or 16:0 and Δ19:0). This is indicated by the difference in one CH$_2$-group (14.015 u).
Two FA combinations could not be discriminated by MS means due to the same average
mass (14:0 and 18:1 or 16:0 and 16:1). A sixth combination with 14:0 and 16:0
(1172.581 u), which is not depicted lacked any double bonds. In **Table 4.4** the summary
of all assigned mass peaks is given. The data obtained from ESI-MS experiments were
consistent with the compositional analysis, but Gal (Hex) substitutions could not be de-
tected.
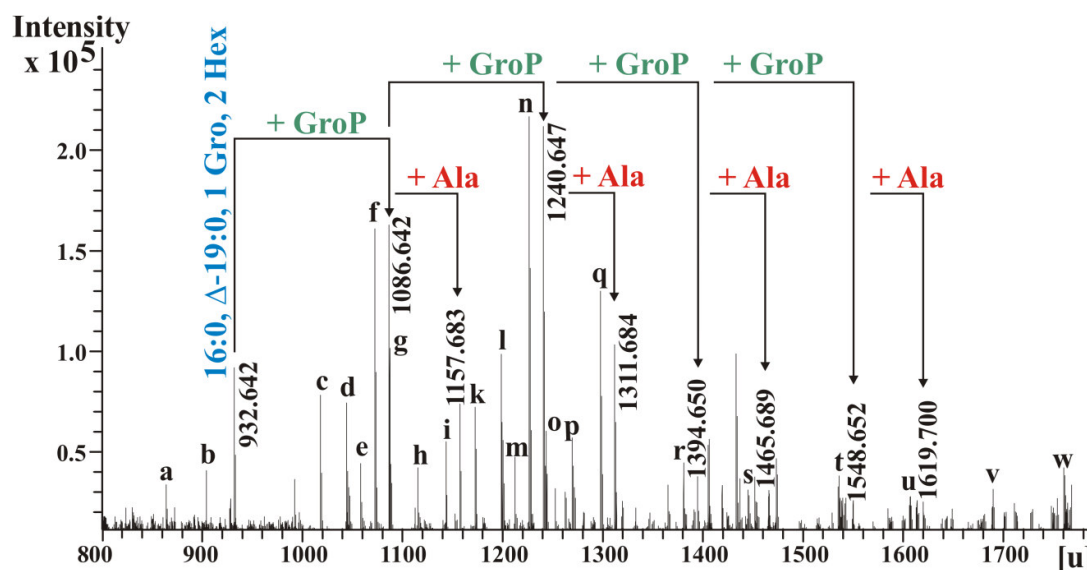
Figure 4.19 Overview on the ESI-mass spectrum of LTA from *L. lactis* G121. As a paradigm the species with the lipid anchor of 932.642 u (16:0, Δ-19:0, 1 Gro and 2 Hex) is described with its GroP and Ala decorations. The spectrum shows a huge heterogeneity within the sample. **Table 4.4** summarizes all identified LTA species. Up to 5 GroP repeats were defined with the help of this experiment.
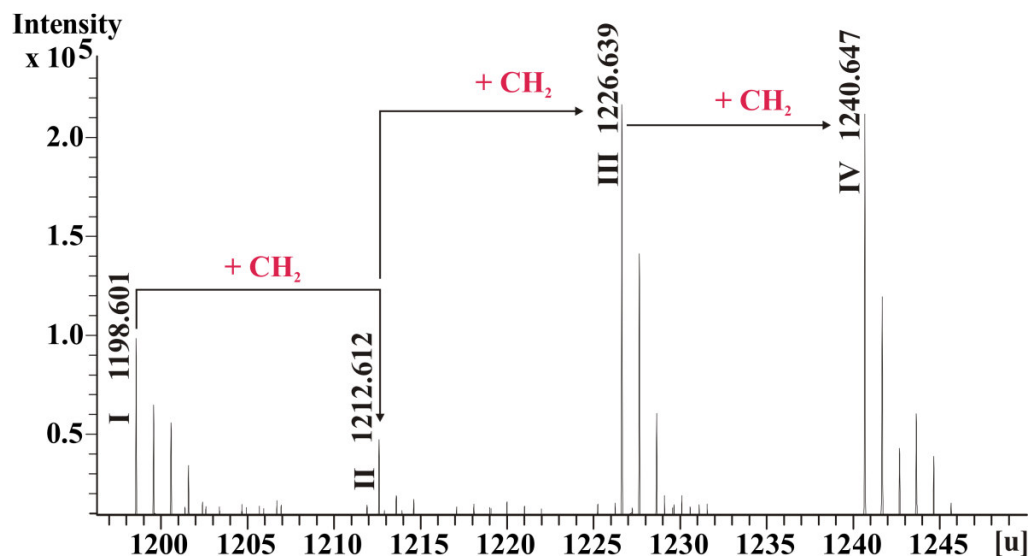
Figure 4.20 Section of the ESI-mass spectrum of the LTA. Using the example of the most prevalent species consisting of 3 Gro, 2 P and 2 Hex the high degree of heterogeneity due to FA variations is demonstrated. This LTA type could be identified with 6 different acylation patterns (shown are 5). I, 14:0 and 18:1 or 16:0 and 16:1; II, 14:0 and Δ-19:0; III, 16:0 and 18:1; IV, 16:0 and Δ-19:0.

Table 4.4 Summary of the assigned LTA mass peaks. For calculations average mass units of 79.966 for P, 74.036 for Gro, 71.037 for Ala, 162.052 for Hex, 210.198 for 14:0, 238.229 for 16:0, 236.214 for 16:1, 264.245 for 18:1 and 278.261 were used. Small letters are indicated in **Figure 4.19**.

Detected u	Components	Calculated u
a) 864.580	14:0, 16:0, 1 Gro, 2 Hex	864.581
b) 904.611	14:0, Δ-19:0, 1 Gro, 2 Hex	904.612
932.642	16:0, Δ-19:0, 1 Gro, 2 Hex	932.643
c) 1018.582	14:0, 16:0, 2 Gro, 2 Hex, 1 P	1018.584
d) 1044.605	14:0, 18:1, 2 Gro, 2 Hex, 1 P 16:0, 16:1, 2 Gro, 2 Hex, 1 P	1044.599
e) 1058.606	14:0, Δ-19:0, 2 Gro, 2 Hex, 1 P	1058.615
f) 1072.631	16:0, 18:1, 2 Gro, 2Hex, 1P	1072.634
1086.642	16:0, Δ-19:0, 2 Gro, 2 Hex, 1 P	1086.646
g) 1089.617	14:0, 16:0, 2 Gro, 2 Hex, 1 P, 1 Ala	1089.621
h) 1115.637	14:0, 18:1, 2 Gro, 2 Hex, 1 P, 1 Ala 16:0, 16:1, 2 Gro, 2 Hex, 1 P, 1 Ala	1115.636
i) 1143.665	16:0, 18:1, 2 Gro, 2 Hex, 1 P, 1 Ala	1143.668
1157.683	16:0, Δ-19:0, 2 Gro, 2 Hex, 1 P, 1 Ala	1157.683
k) 1172.581	14:0, 16:0, 3Gro, 2Hex, 2P	1172.587
l) 1198.601	14:0, 18:1, 3 Gro, 2 Hex, 2 P 16:0,16:1, 3 Gro, 2 Hex, 2 P	1198.602
m) 1212.612	14:0, Δ-19:0, 3 Gro, 2 Hex, 2 P	1212.618
n) 1226.629	16:0, 18:1, 3 Gro, 2 Hex, 2 P	1226.634
1240.647	16:0, Δ-19:0, 3 Gro, 2 Hex, 2 P	1240.649
o) 1243.621	14:0, 16:0, 3 Gro, 2 Hex, 2 P, 1 Ala	1243.624
p) 1269.634	14:0, 18:1, 3 Gro, 2 Hex, 2 P, 1 Ala 16:0,16:1, 3 Gro, 2 Hex, 2 P, 1 Ala	1269.640
q) 1297.666	16:0, 18:1, 3 Gro, 2 Hex, 2 P, 1 Ala	1297.671

Table 4.4 continued

1311.684	16:0, Δ-19:0, 3 Gro, 2 Hex, 2 P, 1 Ala	1311.687
r) 1380.634	16:0, 18:1, 4 Gro, 2 Hex, 3 P	1380.637
1394.650	16:0, Δ-19:0, 4 Gro, 2 Hex, 3 P	1394.653
s) 1451.669	16:0, 18:1, 4 Gro, 2 Hex, 3 P, 1 Ala	1451.674
1465.689	16:0, Δ-19:0, 4 Gro, 2 Hex, 3 P, 1 Ala	1465.690
t) 1534.633	16:0, 18:1, 5 Gro, 2 Hex, 4 P	1534.640
1548.652	16:0, Δ-19:0, 5 Gro, 2 Hex, 4 P	1548.656
u) 1605.673	16:0, 18:1, 5 Gro, 2Hex, 4P, 1Ala	1605.677
1619.700	16:0, Δ-19:0, 5 Gro, 2 Hex, 4 P, 1 Ala	1619.693
v) 1688.386	16:0, 18:1, 6 Gro, 2 Hex, 5 P	1605.677
w) 1759.674	16:0, 18:1, 6 Gro, 2 Hex, 5 P, 1 Ala	1759.680

4.5.4   ESI-MS analysis of deacLTA

The extraction of the EC TA additionally yielded *O*-deacylated LTA. ESI MS investigations of this sample (named deacLTA) revealed that this structure consisted of GroP repeating units decorated with hexoses. In the 5 V spectrum (**Figure 9.6**, shown in the appendix) recorded in the negative ion mode the longest chain was identified to comprise 19 GroP, 1 Gro and 5 Hex (3850.383 u, + Na^+). Furthermore, the highest degree of Hex substitution could be found for the deacLTA species of 18 GroP, 1 Gro and 7 Hex (4020.516 u, + Na^+). **Figure 4.21** depicts the fragmented ion spectrum of deacLTA obtained at high orifice voltage (30 V). It confirmed the findings from the 5 V spectrum and showed that the ion of 3 GroP, 1 P and 2 Hex (877.158 *m/z*) was a result of P and Gro eliminations. **Table 4.5** summarizes all identified ions of the 30 V spectrum, whereas **Table 9.1** (shown in the appendix) summarizes all assigned mass peaks of the 5 V spectrum of the deacLTA.
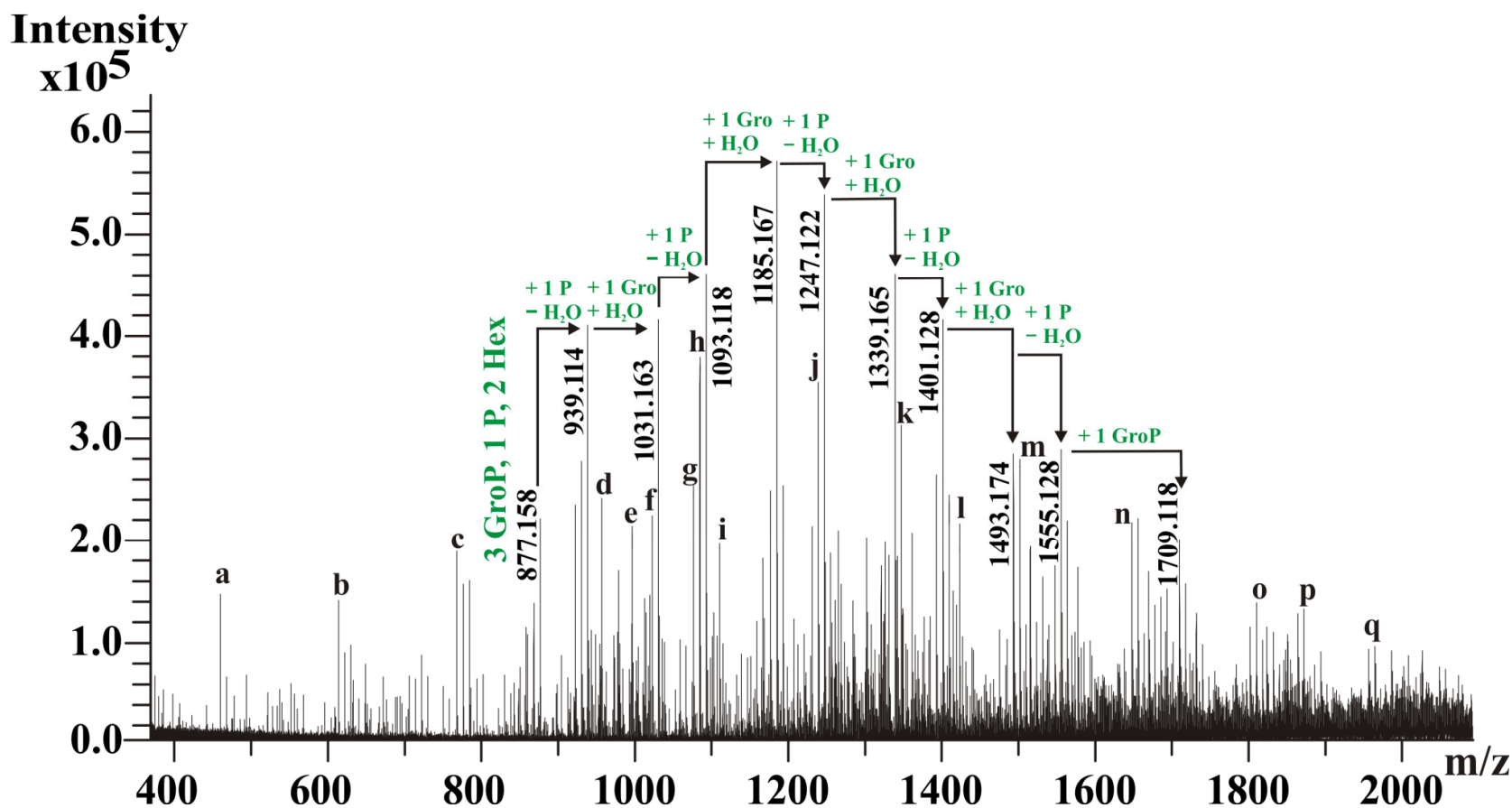
Figure 4.21 Fragmentation pattern of deacLTA obtained from ESI-mass spectrometry at 30 V in the negative ion mode. One chain unit could be defined of 1 GroP with or without 1 Hex. The ion of 3 GroP, 1 P and 2 Hex substitutions (877.1589 *m/z*) is shown with its corresponding fractions due to P and Gro defragmentation. Non-labeled peaks are attributed to other LTA fragments and Na$^+$ and/or K$^+$ ions. Detected ions were not charge deconvoluted. All assignments are listed in **Table 4.5**.

Table 4.5 Assessed ions from ESI-MS measurements at high orifice voltage (30 V) of the deacLTA of *L. lactis* G121. Average mass units of 74.04 for Gro, 79.97 for P, 162.05 for Hex, 203.04 for HexNAc, 21.982 for Na^+ and 18.010 for H_2O were used for calculations. Detected ions were not charge deconvoluted.

Detected ions *m/z*	Composition
a) 461.018	3 GroP – H_2O
b) 615.015	4 GroP – H_2O
c) 769.015	5 GroP – H_2O
877.158	4 Gro, 3 P, 2 Hex
939.114	4 GroP, 2 Hex – H_2O
d) 957.124	4 GroP, 2 Hex
e) 997.129	7 Gro,6 P – H_2O
f) 1023.113	6 Gro, 5 P, 1 Hex
1031.162	5 Gro, 4 P, 2 Hex
g) 1077.016	7 GroP – H_2O
h) 1085.065	6 GroP, 1 Hex – H_2O
1093.118	5 GroP, 2 Hex – H_2O
i) 1111.128	5 GroP, 2 Hex
1185.167	6 Gro, 5 P, 2 Hex
j) 1239.071	7 GroP, 1 Hex – H_2O
1247.122	6 GroP, 2 Hex – H_2O
1339.165	7 Gro,6 P, 2 Hex
k) 1347.213	6 Gro, 5 P, 3 Hex
1401.128	7 GroP, 2 Hex – H_2O
l) 1423.099	7 GroP, 2 Hex – H_2O + Na^+
1493.174	8 Gro, 7 P, 2 Hex
m) 1501.223	7 Gro, 6 P, 3 Hex
1555.128	8 GroP, 2 Hex – H_2O
n) 1655.222	8 Gro, 7 P, 3 Hex
1709.118	9 GroP, 2 Hex – H_2O
o) 1809.232	9 Gro, 8 P, 3 Hex
p) 1871.188	9 GroP, 3 Hex – H_2O
q) 1963.240	10 Gro, 9 P, 3 Hex

4.5.5   NMR spectroscopy of LTA

The ^{1}H NMR spectrum of the LTA (**Figure 4.22**, graph a) revealed two signals in the anomeric region. One resonance could be identified as H-1 of a D-Gal*p* residue (δ_H 5.21) whose vicinal coupling constant of ${}^3J_{1,2}$ 3.96 Hz indicated the α-configuration. The second anomeric resonance was H-2 of one Gro species from the backbone (termed Gro B, δ_H 5.40). The D-alanylation of *O*-2 in this species led to the strong downfield shift of H-2. A further distinct resonance was assigned for H-2 of D-Ala at δ_H 4.30. In the region δ_H 4.20–3.70 was a cluster of shifts originating from other Gro proton signals and the ring protons of D-Gal*p*. Fatty acid proton signals and D-Ala H-3 (bound and free) were additionally detected in the region δ_H 2.42–0.9.

The ROESY spectrum showed *inter*-residual connectivities of Gro B H-1/Ala H-3, Gro B H-3/Ala H-3, Gal*p* H-1/Gro C H-1, Gal*p*H-1/Gro C H-2, and Gal*p* H-1/Gro C H-3. Thus, structures Gro B and C were corroborated. The third type, Gro A, was not substituted at *O*-2.
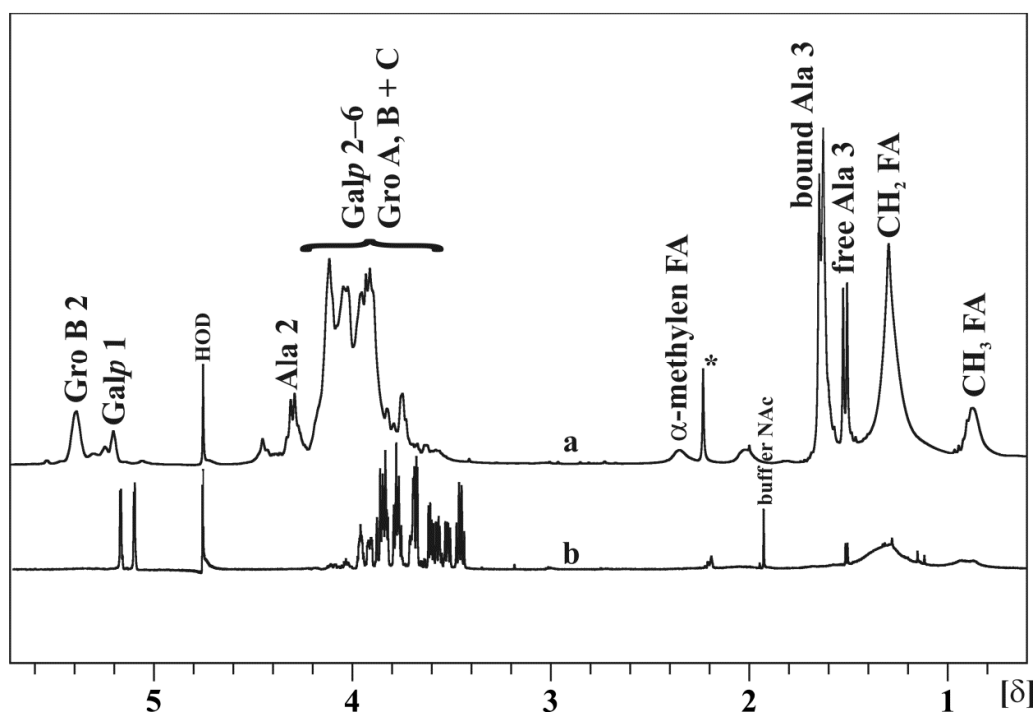
Figure 4.22 Comparison between the ^{1}H NMR spectrum of a) the intact LTA and b) the LTA linker yielded from HF and N_2H_4 treatment. Missing signals for FA, Gro A–C, Ala and Gal in spectrum b) corroborated the hydrolysis of GroP repeats and the *O*-deacylation as well. Residues Gro A–C are detailed in **Figure 4.25**. Measurements were conducted in D_2O at 700 MHz and 27°C. * no component of the LTA.

The ^{1}H spectrum (**Figure 4.22**, graph a) was used to determine the average number of the backbone units and the ratio of Ala to Gal*p* (199). An average chain length of 14–16 GroP repeats was defined from the integral ratio of the FA α-methylen group at δ_H 2.42–2.26 to glycerol at δ_H 3.84–4.16 [from which the integrals of the three subjacent Gal resonances at δ_H 3.90 (H-3), 4.02 (H-4) and 4.13 (H-5) were subtracted and the integral of Gro B H-2 at δ_H 5.40 was added]. In addition to that, the degree of substitution of Gro with Ala and/or Gal was determined likewise. The integral ratio of the α-methylen protons to Gro B H-2 (δ_H 5.40) and to D-Gal H-1 (δ_H 5.21) gave approximately 3 Ala and/or 3 Gal decorations. Since the resonance of Gro C H-2 (δ_H 4.13) was covered by ring protons and Gro protons it could not be used for integration (**Figure 4.22**, graph a).

The carbon shifts of the LTA backbone were assigned from the ^{1}H,^{13}C HSQC spectrum (**Figure 9.7**, shown in the appendix) and the summarized data are given in **Table 4.6**. The 1,3-connection of the poly(GroP) chain was defined by an ^{1}H,^{31}P HMQC experiment. Three phosphate shifts could be detected at δ_P 0.74, δ_P1.09 and δ_P1.40. The first signal correlated with Gro B H-1 and H-3, the second with Gro A H-3, Gro C H-1 and H-3, and the third with Gro A H-1.
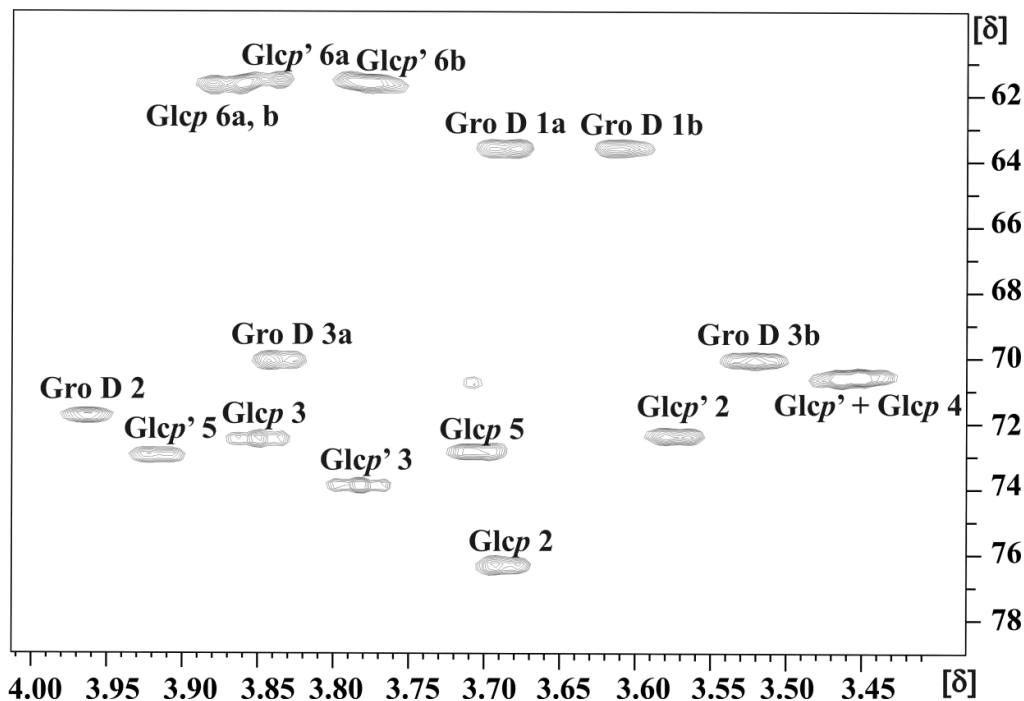
Figure 4.23 Detail of the ^{1}H,^{13}C HSQC spectrum of the LTA linker. The identified C-H cross peaks of each spin system are depicted. The protons/carbon atoms of the residues are designated by Arabic numerals. Glc' and Glc label the terminal and reducing sugar, respectively, depicted in **Figure 4.25**. Spectra were recorded in D$_2$O at 700 MHz and 27°C.

Table 4.6 ^{1}H and ^{13}C chemical shifts of the LTA backbone and corresponding substituents as well as the LTA linker. The respective residues are indicated in **Figure 4.25**. Spectra were recorded in D_2O at 700 MHz and 27°C. Substituted positions are emphasized.

Residue		1a	1b	2	3a	3b	4	5	6a	6b
					Chemical shifts of protons and carbons (δ)					
α-D-Gal*p*	[1]H	5.21		3.81	3.90		4.02	4.13	3.62	3.68
	[13]C	99.25		69.63	70.65		70.57	75.92	63.42	
D-Ala	[1]H			4.30	1.63					
	[13]C	171.30		50.27	16.68					
Gro A	[1]H	3.89	3.96	4.05	4.00	4.05				
	[13]C	67.55		70.82	65.82					
Gro B	[1]H	4.11	4.11	5.40	4.11	4.11				
	[13]C	65.01		<u>75.50</u>	65.01					
Gro C	[1]H	4.03	4.03	4.13	4.03	4.03				
	[13]C	66.61		<u>76.50</u>	66.61					
α-D-Glc*p*	[1]H	5.17		3.68	3.85		3.47	3.70	3.88	3.86
	[13]C	96.97		<u>76.37</u>	72.52		70.63	72.88	61.64	
α-D-Glc*p'*	[1]H	5.10		3.57	3.78		3.45	3.91	3.83	3.79
	[13]C	97.03		72.39	73.89		70.59	72.97	61.52	
Gro D	[1]H	3.68	3.62	3.96	3.83	3.52				
	[13]C	63.55		71.76	<u>70.19</u>					

After HF and N_2H_4 treatment of the LTA the resulting linker could be recorded with good resolution as shown in the ^{1}H NMR spectrum (**Figure 4.22** graph b). The cleavage of the GroP main chain was proven by missing chemical shifts of Gro B H-2 (δ_H 5.40), D-Gal H-1 (δ_H 5.21), Ala H-2 (δ_H 4.30) and Ala H-3 (δ_H 1.63), compared to the intact LTA in graph a.

From the ^{1}H,^{1}H COSY and TOCSY spectra of the linker two Hex and one Gro (Gro D) could be identified. With the help of *intra*-residual NOE coupling signals between H-1/H-2 and H-2/H-4 of the hexoses (ROESY) they were corroborated as *gluco*-configured. This result was in accordance with methylation analysis and therefore the reducing and the

terminal residue were named Glc*p* and Glc*p*', respectively. Furthermore, the α-configuration was determined with $^3J_{1,2}$ 3.52 Hz for Glc*p* and $^3J_{1,2}$ 3.96 Hz for Glc*p*'. The ^{1}H,^{13}C HSQC spectrum (**Figure 4.23**) was used to assigned the corresponding carbon shifts. All chemical shifts of the linker are summarized in **Table 4.6**.
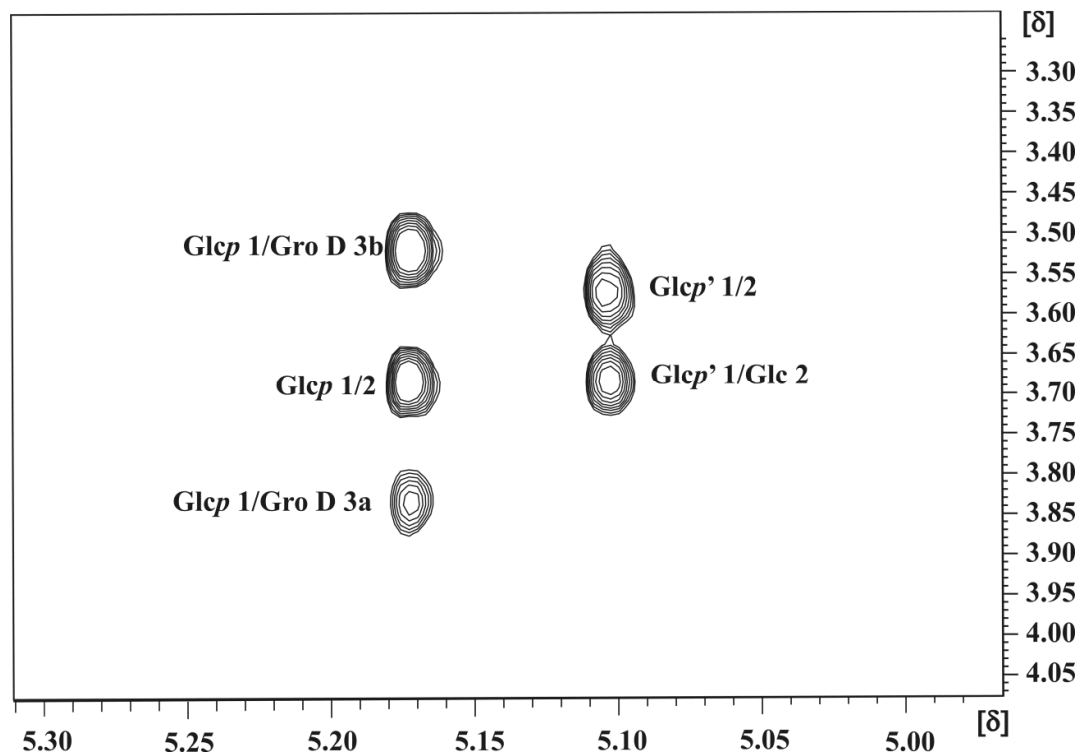
Figure 4.24 ^{1}H,^{1}H ROESY experiment which identified the linkages within the LTA linker. The section depicts *inter*-residual connectivities between Glc' H-1/Glc H-2, Glc H-1/ Gro D H-3a and Glc H-1/ Gro D H-3b leading to a final structure of α-D-Glc*p*-(1→2)-α-D-Glc*p*-(1→3)-glycerol for the linker in good agreement with the methylation analysis. Recordings were carried out in D$_2$O at 700 MHz and 27°C.

Figure 4.24 shows a detail of the ROESY spectrum of the LTA linker. Depicted are cross peaks between Glc' H-1/Glc H-2 and Glc H-1/Gro D H-3a,b which identified the *inter*-molecular linkages. Hence, the structure of the LTA linker was α-D-Glc*p*-(1→2)-α-D-Glc*p*-(1→3)-Gro. The ^{13}C resonances of Gro D C-2 (δ_C 71.76) and C-1 (δ_C 63.55) confirmed the *O*-deacylation. From the ^{1}H,^{31}P HMQC experiment the connection between the lipid anchor and the backbone was indicated by coupling signals for a phosphodiester at δ_P −1.29 and Glc*p*' H-5 (δ_H 3.91) and Glc*p*' H-6a (δ_H3.83), respectively. **Figure 4.25** displays the complete structure of the LTA from *L. lactis* G121.

R=   H ~ 60%, Gro A
     D-Ala ~ 20%, Gro B
     α-D-Gal*p* ~ 20%, Gro C
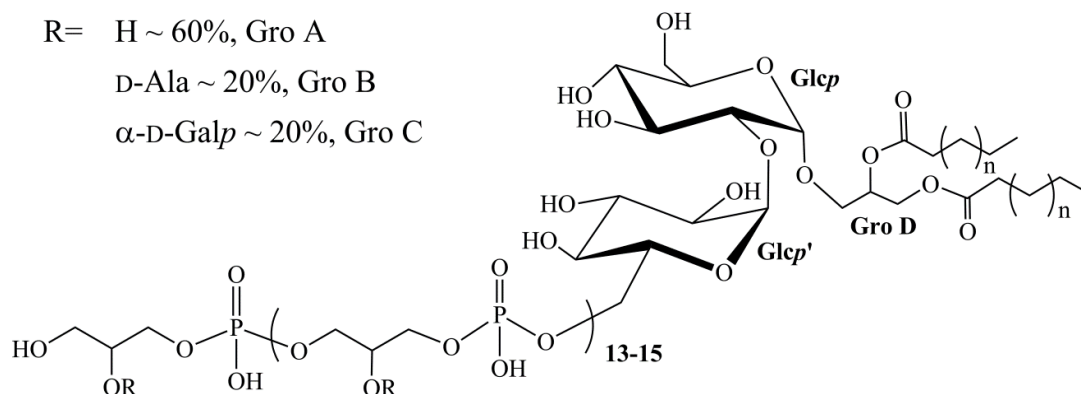
Figure 4.25 Structure of the LTA from *L. lactis* G121. The backbone was based on a poly(glycerol phos-phate) chain randomly substituted at *O*-2 of glycerol by D-Ala and/or α-D-Gal*p*. Six different variations of the FA 14:0, 16:0, 16:1, 18:1 and Δ-19:0 could be defined. The backbone of the LTA linker was determined as α-D-Glc*p*-(1→2)-α-D-Glc*p*-(1→3)-1,2-diacylglycerol.

Full assignment of 1D and 2D NMR spectra of the deacLTA obtained from TA extraction confirmed the LTA backbone and linker structure with the exception, that the deacLTA sample did not contain any Ala signals.

4.5.6   Biological activity of the LTA

To analyze the biological properties of the LTA it was added to hMNC. After 20 hours of stimulation the IL-6 concentration was determined from the cell supernatants. **Figure 4.26** demonstrates that LTA induced the IL-6 release from hMNC. Nevertheless, higher concentrations of the LTA isolate (at least 1 µg/ml) were necessary compared to other bacterial cell wall components like the synthetic lipopeptide Pam$_3$C-SK$_4$ or LPS.

In addition, the LTA preparation was investigated in a HEK293 transfection system. In the past LTA has been discussed quite controversially to be a ligand for TLR2 or TLR4. To check if the LTA obtained from *L. lactis* G121 signals through one of these innate receptors concentrations up to 30 µg/ml were tested. HEK293 cells transfected with either TLR2 or TLR4 were not activated by the purified LTA as presented in **Figure 4.27**.
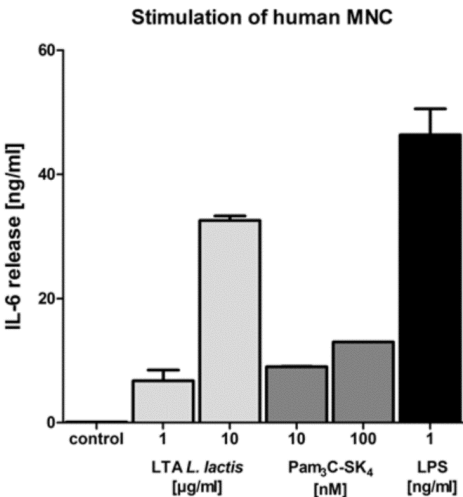
Figure 4.26 IL-6 release in hMNC was induced by LTA. hMNC were left untreated or underwent stimulation with LTA, the synthetic lipopeptide Pam$_3$C-SK$_4$, or LPS for 20 hours. Afterwards, the IL-6 level of culture supernatants was measured by ELISA. Results are given as mean ± SD. One representative experiment out of three is shown.
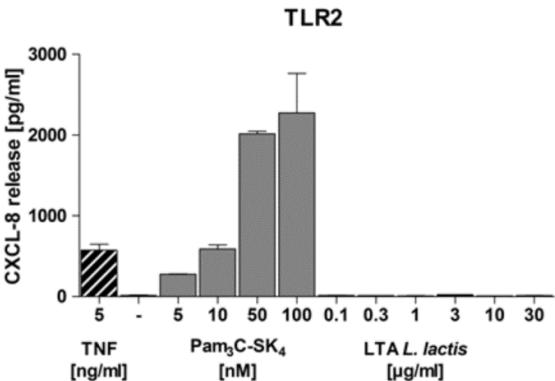
Figure 4.27 Influence of LTA on the CXCL-8 release from transfected HEK293 cells. These were either transfected with TLR2 or TLR4. TNF and Pam$_3$C-SK$_4$ were used as positive control in case of TLR2 transfections. TNF and LPS were used to stimulated TLR4 transfected cells. Untreated cells were utilized as negative control. H$_2$O-treated LTA was applied in 6 dilutions. After 18 hours of stimulation CXCL-8 concentrations were measured in the supernatants by ELISA. Results are expressed as mean ± SD. One representative experiment out of three is shown. The LTA did not elicit CXCL-8 production, neither of TLR2 nor of TLR4 expressing HEK293 cells.
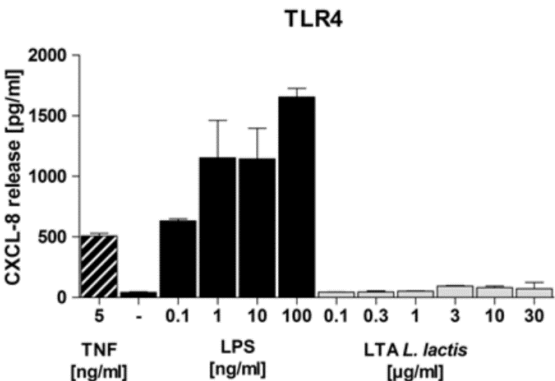
4.6   *L. lactis* G121 *lgt* knockout mutant

4.6.1   Sequence of *lgt* from *L. lactis* G121

To identify the *lgt* gene of *L. lactis* G121 and determine its DNA sequence, the genomic DNA of the bacterium was isolated essentially as described previously by Marmur et al. However, in contrast to the Marmur protocol, the bacterial cells were resuspended in pre-lysis buffer but not in the original Tris-buffer containing EDTA. Treatment of the cells with pre-lysis buffer proved to play a critical role in efficient lysis of the Gram-positive cells and release of the genomic DNA, most likely due to the presence of the non-ionic detergent Triton® X-100 to facilitate disintegration of the thick PGN layer. DNA isolations using a buffer lacking Triton® X-100 turned out to be ineffective. As a result, genomic DNA of *L. lactis* G121 of high quality could be isolated (**Figure 4.28**). The DNA was stored at 4°C to prevent the DNA of high average molecular mass from fragmentation by repeated freezing and thawing cycles.
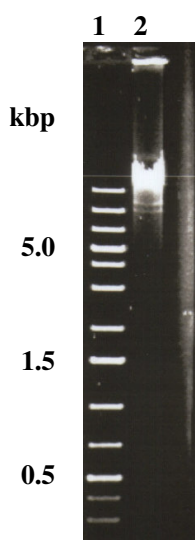
Figure 4.28 Agarose gel electrophoresis of genomic DNA isolated from *L. lactis* G121 (lane 2). In the marker lane 1, the 1 kbp Plus DNA ladder was separated.

For identification of the unknown *lgt* gene of *L. lactis* G121, the GenomeWalker™ technology has been chosen. The method is based on amplification of unknown DNA sequences adjacent to a region of known DNA sequence using pools ("libraries") of adaptor-ligated fragments of genomic DNA as templates. As a result, the sequences of the

known gene-specific part and the adaptor ligated to blunt-ended fragments of the genomic DNA may serve as primer binding sites for PCR amplification of unknown regions located between them. The sequence of the gene-specific part was deduced from alignments of highly conserved DNA sequences within known *lgt* genes of different *L. lactis* ssp. For the genomic DNA of *L. lactis* G121, a total of four libraries of blunt-ended DNA fragments were generated by digestion of the DNA with the restriction endonucleases *DraI* (DL-*DraI*), *EcoRV* (DL-*EcoRV*), *PvuII* (DL-*PvuII*) and *StuI* (DL-*StuI*). As a positive control (pctrl) a *PvuII* digest of human genomic DNA was applied (pctrl-*PvuII*). As expected and shown in **Figure 4.29**, digestion of the genomic DNA with the four different endonucleases yielded blunt-ended DNA fragments of required different size distribution. Following ligation of the differently blunt-ended DNA fragments with the GenomeWalker Adaptor, all four libraries were used as templates for 1° PCRs either with primer pair AP1/GSP1 or AP1/GSP2 to amplify unknown sequences downstream and upstream of the conserved *lgt* sequence, respectively. The primary PCR products as analyzed by agarose gel electrophoresis are shown in **Figure 4.30**.
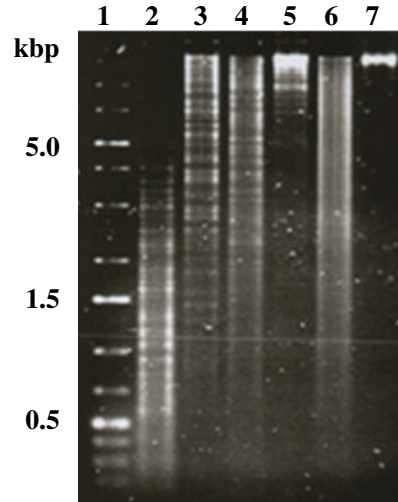
Figure 4.29 Agarose gel electrophoresis of GenomeWalker™ DNA libraries from *L. lactis* G121 genomic DNA. Lanes: 1, 1 kbp Plus ladder; 2, DL-*DraI*; 3, DL-*EcoRV*; 4, DL-*PvuII*; 5, DL-*StuI*; 6, pctrl-*PvuII*; 7, undigested genomic DNA.

To further increase specificity and eliminate unwanted amplification products, diluted primary PCR mixtures were used as templates for a second-round, so-called "nested" PCR (2° PCR) either with primers AP2/NGSP1 or AP2/NGSP2, respectively. Except for

DL-*Stu*I, the secondary PCR yielded major amplification products from all other libraries (**Figure 4.31**). Several attempts to reduce the significant background in the DL-*Stu*I reactions by using 1:50, 1:100 and 1:200 dilutions of the 1° PCR products as templates for the 2° PCRs have not been successful.
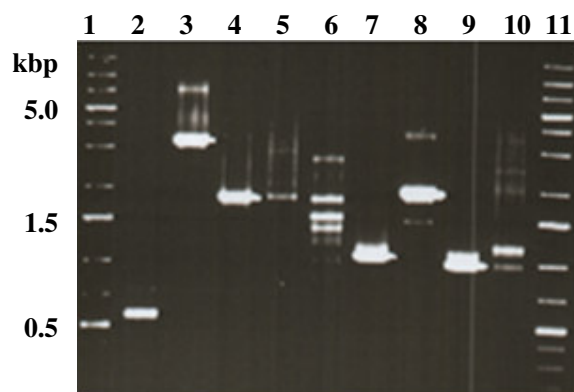
Figure 4.30 Agarose gel electrophoresis of the 1° PCR products from DNA libraries of *L. lactis* G121 genomic DNA. Lanes: 1, 1 kbp ladder; 2, *Dra*I-GSP1; 3, *Eco*RV-GSP1; 4, *Pvu*II-GSP1; 5, *Stu*I-GSP1; 6, pctrl-PCP1; 7, *Dra*I-GSP2; 8, *Eco*RV-GSP2; 9, *Pvu*II-GSP2; 10, *Stu*I-GSP2; 11, 1 kbp Plus ladder.
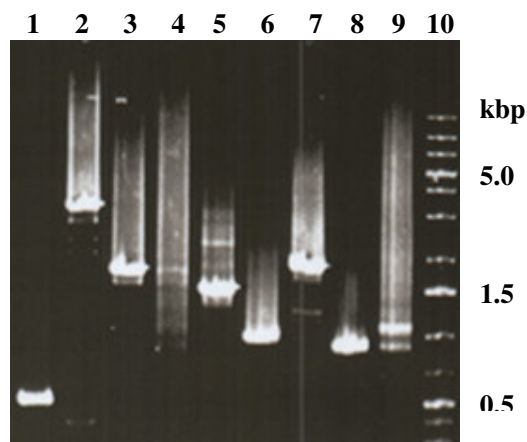
Figure 4.31 Agarose gel electrophoresis of products from nested 2° PCR. Lanes: 1, *Dra*I-NGSP1; 2, *Eco*RV-NGSP1; 3, *Pvu*II-NGSP1; 4, *Stu*I-NGSP1; 5, pctrl-PCP2; 6, *Dra*I-NGSP2; 7, *Eco*RV-NGSP2; 8, *Pvu*II-NGSP2; 9, *Stu*I-NGSP2; 10, 1 kbp ladder.

The single major product of 1.5 kbp obtained from the secondary control PCR was in good agreement with the specification of the manufacturer and suggested a correct implementation of the GenomeWalker™ technology (**Figure 4.31**, lane 5, pctrl-PCP2). For

cloning and determination of the DNA sequence, the 2° PCR products of the *Pvu*II and *Dra*I libraries comprising unknown DNA sequences up- and downstream of *lgt*, respectively, were chosen. From here on, the DNA fragments of the DL-*PvuII* and DL-*DraI* are referred to for convenience as C1 and D1, respectively. To purify C1 and D1, they were subjected to an LMP agarose gel electrophoresis (**Figure 4.32**), excised and extracted. The up- and downstream sequences of *lgt* were ligated into the U/A-cloning vector pDrive.
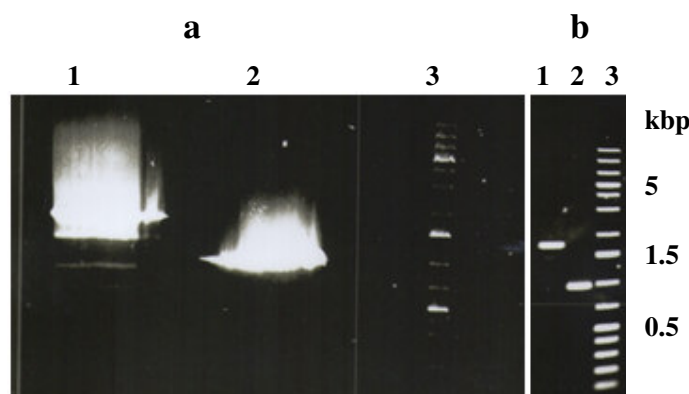
Figure 4.32 Preparative LMP agarose gel electrophoresis of C1 and D1. These unknown DNA fragments up- and downstream of *lgt*, respectively, were generated with the GenomeWalker™ technology (panel a). Agarose gel electrophoresis of C1 and D1 after purification (panel b). Lanes: a) 1, C1; 2, D1; 3, 1 kbp Plus ladder; b) 1, C1 purified; 2, D1 purified; 3, 1 kbp Plus ladder.
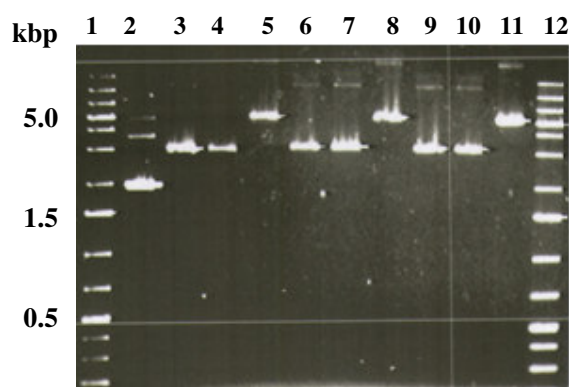
Figure 4.33 Agarose gel electrophoresis of isolated pCR2.1 plasmids which were ligated with C1 and transformed into *E. coli* XL1-Blue. Lanes: 1 and 12, 1 kbp Plus ladder; 2, LGC standard; 3, pCR2.1 control; 4–11, plasmids pCR2.1C1-17–24.

Following transformation of *E. coli* XL1-Blue cells with the purified ligation mixture by electroporation, the plasmids of 24 transformants of the pCR2.1C1 series showing white-colored colonies on X-Gal/IPTG plates were isolated. A total of four plasmids, namely

pCR2.1C1-11, -18, -21 and 24, as analyzed by agarose gel electrophoresis and shown for pCR2.1C1-18, -21 and 24 in **Figure 4.33** displayed a relative mobility of the expected size of about 5 kbp, which suggested the successful ligation of C1 of 1.6 kbp into the vector pCR2.1 of 3.9 kbp. All four plasmids were therefore sent out for sequencing of the cloned DNA inserts, providing in addition the internal primers LLAlgtSeqPri1 and LLAlgtSeqPri2 to generate overlapping sequence reads of the 1.6-kbp inserts.

Likewise, three plasmids isolated from eight transformants of the pCR2.1D1 series with white-colored colonies on X-Gal/IPTG plates (pCR2.1D1-1–8) were found to be of the expected size of about 5 kbp (**Figure 4.34**). Thus, the DNA sequences of the cloned inserts of plasmids pCR2.1D1-1, -2 and -5 were determined.
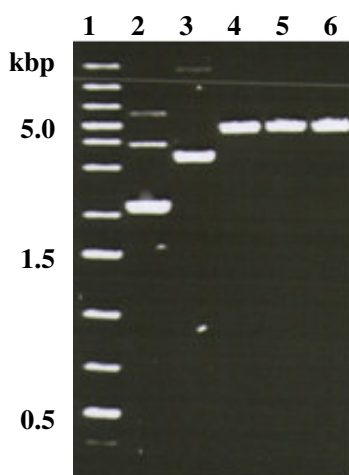
Figure 4.34 Agarose gel electrophoresis of isolated pCR2.1 plasmids which were ligated with D1 and transformed into *E. coli* XL1-Blue. Lanes: 1, 1 kbp Plus ladder; 2, LGC standard; 3, pCR2.1 control; 4–6, plasmids pCR2.1D1-1, -2 and -5.

Analysis of the DNA sequences using the Blast search tool of the Genbank (http://www.ncbi.nlm.nih.gov/blast/Blast.cgi) revealed that C1 of 1.687 kbp length contained partial sequences of the *ygaF* gene (*ygaF'*) for a hypothetical protein of unknown function, *ptsK* for the HPr kinase/phosphorylase and partial sequences of *lgt* (*lgt'*) upstream of the *lgt* gene. D1 of 0.920 kbp length carried partial sequences of *lgt* (*lgt'*), the entire *ygaI* gene for a putative methyl-accepting chemotaxis-like protein and partial sequences of *ygaJ* (*ygaJ'*) for a conserved hypothetical protein of unknown function downstream of *lgt* (**Figure 4.35**).
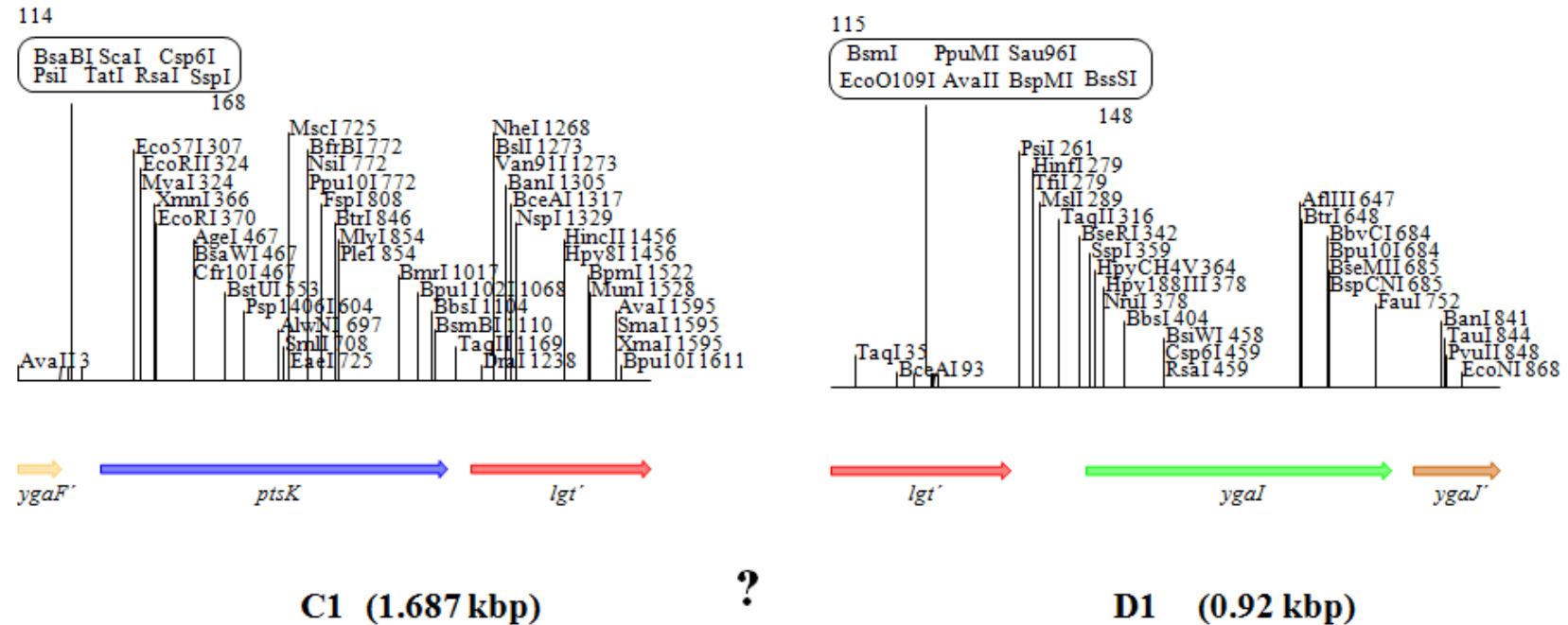
Figure 4.35 Restriction maps of C1 and D1. C1, the PCR product of DL-*PvuII* with AP2/NGSP1, was cloned with pDrive2.1 and sequencing revealed this DNA fragment of 1.687 kbp to code for *ygaF'*, *ptsK* and an upstream part sequence of *lgt'*. D1, the PCR product of DL-*DraI* with AP2/NGSP2, was likewise cloned and sent for sequencing. The sequence could be determined to consist of 0.92 kbp coding for a downstream part sequence of *lgt'* as well as *ygaI* and *ygaJ'*. The questionmark indicates the, until such time, unknown sequence between C1 and D1 of approximately 150 bp.

To close the gap between C1 and D1, a DNA fragment of *lgt* of 500 bp (named *lgt'*) containing the missing segment with a predicted size of about 150 bp was amplified with primer pair LLAlgtAmplPri 4 and LLAlgtAmplPri 5, and ligated into the T/A cloning vector pCR2.1, followed by transformation of *E. cloni* 10G cells with the purified ligation mixture using electroporation. As shown in **Figure 4.36**, the plasmids isolated from 16 transformants and analyzed by agarose gel electrophoresis (pCR2.1*lgt'*-1–16) were of the expected size of about 4.4 kbp.
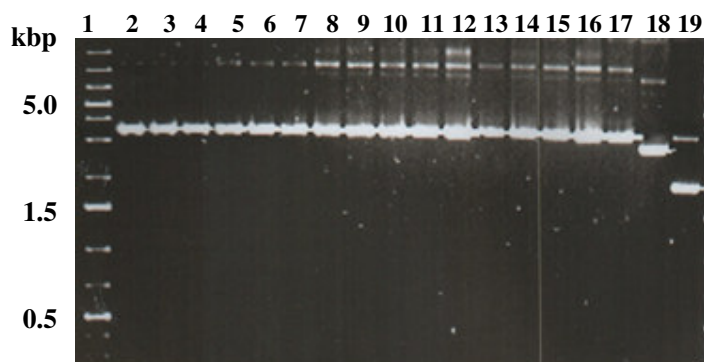
Figure 4.36 Agarose gel electrophoresis of isolated pCR2.1 plasmids which were ligated with *lgt'* (500 bp between C1 and D1) and transformed into *E. cloni* 10G. Sequencing of which completed the *lgt* sequence from the *L. lactis* G121 genome. Lanes: 1, 1 kbp Plus ladder; 2–17, plasmids pCR2.1*lgt'*-1–16; 18, pCR2.1 control; 19, LGC standard.

Determination of the DNA sequence of the 500-bp fragment of plasmids pCR2.1*lgt'*-1–3 closed the gap between C1 and D1, thus ultimately yielding the DNA sequence of the entire *lgt* region of *L. lactis* G121 (**Figure 4.37**). Multiple sequence alignments of the *lgt* region of *L. lactis* G121 with the corresponding regions of different *L. lactis* ssp. using the ClustalW algorithm indicated that both the *lgt* gene and the up- and downstream sequences of *lgt* are highly conserved in *L. lactis*.

Figure 4.37 Complete sequence of the *lgt* region from the genome of *L. lactis* G121 with a size of 2.687 kbp. Positions of applied primers are indicated.

Figure 4.37 continued

1 10 20 30 40 50 60 70 80
1,791 1,800 1,810 1,820 1,830 1,840 1,850 1,860 1,870
GTCTTTAGGCATCGAATTAAAGGATTAAAACGTGGGGATATTTTTAGTTTCTACCTCGTCTGGTATGGAGCCGTTCGTTTTA

lgt

90 100 110 120 130 140 150 160
1,880 1,890 1,900 1,910 1,920 1,930 1,940 1,950
TTGTTGAGGGAATGCGAACAGATAGCCTAATGTTAGGACCTGCTCGTGTGTCACAATGGCTTTCAGTTTTATTAGTAATTGT
5BamHIXmaID1
LLAlgtAmplPri5
lgt

170 180 190 200 210 220 230 240
1,960 1,970 1,980 1,990 2,000 2,010 2,020 2,030
AGGACTTGTTCTCTTTATTTATCGCAGAATGAAAAAAAATGTAAGTTATATTAGAAAATAGCGAAACAATTTGTTATAATTA
5BamHIXmaID1
lgt

250 260 270 280 290 300 310 320
2,040 2,050 2,060 2,070 2,080 2,090 2,100 2,110
AGTCAAATAGAATCGCTTTCATCAAAATGAAAGAAGATTGAAAAAATGGGTGCTGATTTATACCCGAATAAAGAGGAGGAAA

330 340 350 360 370 380 390 400 410
2,120 2,130 2,140 2,150 2,160 2,170 2,180 2,190 2,200
CGTGGGAAATATTGCATTATTGATTATCGCGATAGCATTTGCTGTATTGGTGGTCTTCTTAGTTATTGTATTACATAAAGTT

ygaI

420 430 440 450 460 470 480 490
2,210 2,220 2,230 2,240 2,250 2,260 2,270 2,280
TCTAAGGTTGTTGAAGAAGCCAACCGTACGGTTAAATTAGTTTCTAGCGATGTAGATGTCTTACTTCATCAAGCTGATGGCA

ygaI

500 510 520 530 540 550 560 570
2,290 2,300 2,310 2,320 2,330 2,340 2,350 2,360
TAATGACTAAAGCCAATACCTTGCTTGATGATGTTAATGGGAAAGTCGCCACGATTGACCCTTTGTTTACAGCGGTTGCTGA

ygaI

580 590 600 610 620 630 640 650
2,370 2,380 2,390 2,400 2,410 2,420 2,430 2,440
CTTGTCTGAAAGTGTTTCAGACATCAATGCTTCAAGTCGTAAACTTGTGACACGTCTTAATAGAGGTTCAACAAAACGAAAA

ygaI

660 670 680 690 700 710 720 730
2,450 2,460 2,470 2,480 2,490 2,500 2,510 2,520
ACAACCTCAGCTTCAGCAGTAGTTTTGGCAAAAACAGCCAAAAAATTCTTTGTTAAAAAAGATAAAACTGAAGCGGGTGTAA

ygaI

740 750 760 770 780 790 800 810 820
2,530 2,540 2,550 2,560 2,570 2,580 2,590 2,600 2,610
AAGTAAATTAAACTTGCTTACGAAAGAAAGGACTTAACCGATGTCAAAAAAAACAGGATTTCTAGTTGGTGCTTTAGTTGGT

ygaI ygaJ'

830 840 850 860 870 880 890 897
2,620 2,630 2,640 2,650 2,660 2,670 2,680 2,687
GCCGCAGCTGCTCTATTTTTAGCTCCTAAAAAAGGAAGCGAACTCCGCGAAGGGGCTGGAAAAATTTATGATGATTT
3SacILLAlgt
ygaJ'

Figure 4.37 continued

4.6.2   Construction of an *lgt* knockout plasmid

In order to knockout the *lgt* gene of *L. lactis* G121, a chloramphenicol resistance targeting cassette consisting of the *cat* gene flanked by up- and downstream sequences of *lgt* for homologous recombination was constructed. As plasmids carrying the pBR322 replication origin do not replicate in *L. lactis*, the cloning vector pUC18 has been chosen as a carrier of the targeting cassette for the technique of suicide plasmid directed mutagenesis. The strategy described below was used for stepwise assembly of the chloramphenicol resistance cassette targeting the *lgt* gene. Using the primer pairs 5SphILLAlgt/3BamINheIC1 and 5BamHIXmaID1/3SacILLAlgt, the flanking DNA regions C1´ and D1´ located up- and downstream of *lgt* were first amplified, followed by digestions of C1' with *Sph*I and *Bam*HI, and D1' with *Bam*HI and *Sac*I, respectively. The digested PCR product C1' was then ligated into the *Sph*I/*Bam*HI sites of pUC18, followed by transformation of electrocompetent *E. cloni* G10 cells with the ligation mixtures to yield the intermediate plasmid pUC18C1' (**Figure 4.38**).
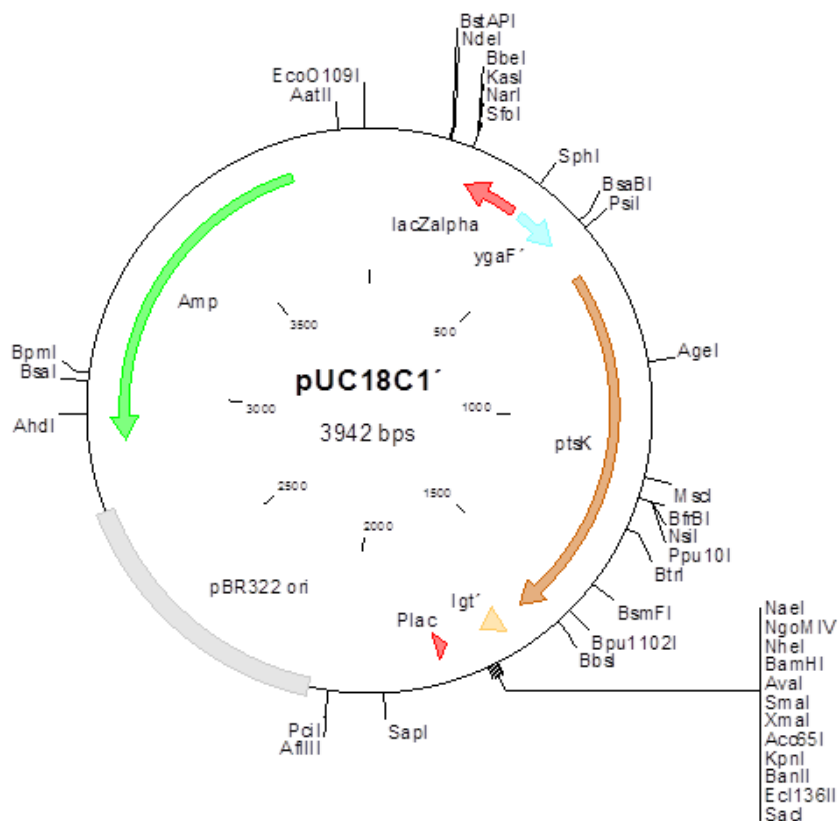
Figure 4.38 Plasmid map of pUC18C1'. All maps were generated with the Geneious software (Biomatters Ltd.).

Figure 4.39 Agarose gel electrophoresis of isolated pUC18 plasmids which were ligated with C1' and transformed into *E. cloni* G10. Ligation was facilitated after digest with *BamH*I and *Sph*I restriction endonucleases of C1' and pUC18. Lanes: 1, 1 kbp Plus ladder; 2–9, plasmids pUC18C1'-1–8; 10, pUC18 control.

The pUC18C1' plasmids of eight transformants each were isolated and subjected to agarose gel electrophoresis (**Figure 4.39**). The relative mobility of the plasmids showed that pUC18C1'-1–3 and -5–8 carried each an insert of the expected size of about 1.3 kbp.

In the next step, another intermediate plasmid, designated pUC18C1'D1', was constructed with the aim of joining the flanking C1´ and D1´ regions on one and the same recombinant plasmid. Therefore, pUC18C1' was prepared with *BamH*I/*Sac*I and ligated with the *BamH*I/*Sac*I digested D1'. **Figure 4.40** displays 18 plasmids isolated after cloning with *E. coli* XL-1 Blue.
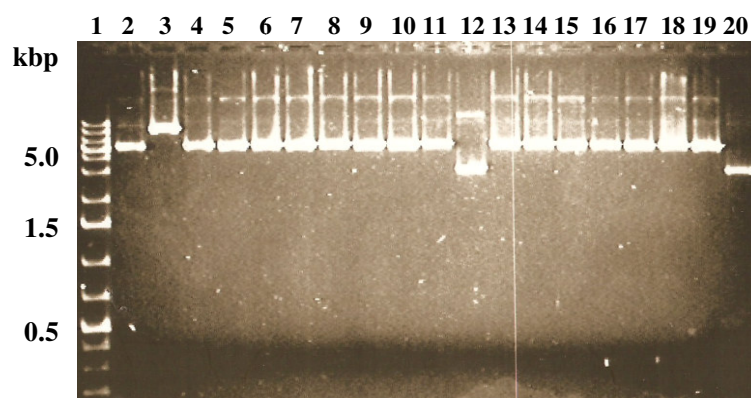
Figure 4.40 Agarose gel electrophoresis of isolated pUC18C1' plasmids which were ligated with D1' and transformed into *E. coli* XL-1 Blue. Ligation was enabled by generation of *BamH*I and *Sac*I sites in D1' and pUC18C1'. Lanes: 1, 1 kbp Plus ladder; 2–19, plasmids pUC18C1'D1'-19–36; 20, pUC18C1' control. Plasmids 20 and 29 did not contain the correct inserts.

The plasmids were isolated from a total of 36 transformants (pUC18C1'D1'-1–36) and analyzed by agarose gel electrophoresis. As shown exemplarily in **Figure 4.16**, the majority of recombinant pUC18C1'D1' plasmids of about 4.7 kbp carried an insert of the expected size of 2 kbp, suggesting the presence of C1´ joined to the D1´ fragment as demonstrated in **Figure 4.41**.
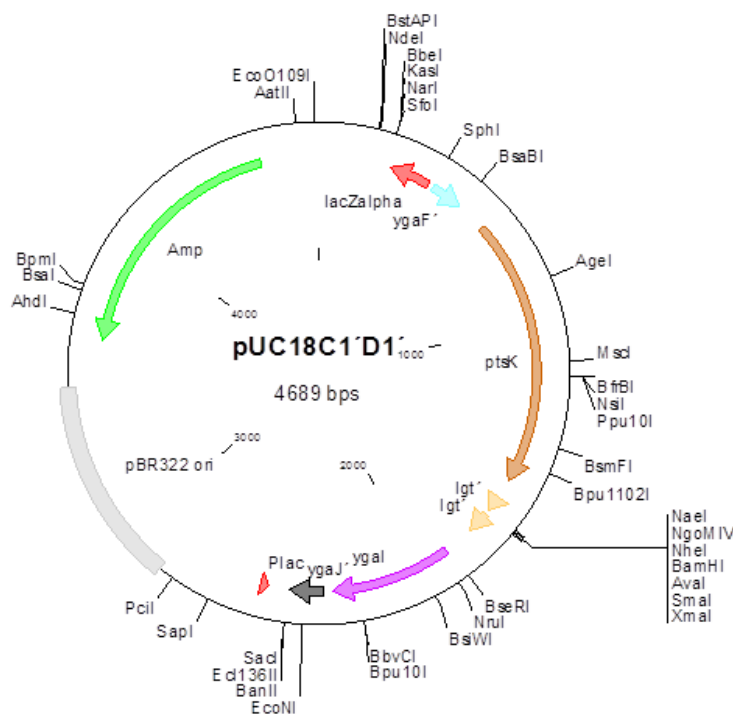
Figure 4.41 Plasmid map of pUC18C1´D1´ carrying the up- and downstream regions of the *lgt* gene.

Finally, the *cat* gene coding for chloramphenicol resistance was inserted between the flanking C1´/D1´ regions of pUC18C1'D1' by amplification of *cat* from pKD3 with primers pKD3NheICm1/pKD3XmaICm2, digestion of the resulting PCR product with *Nhe*I and *Xma*I and ligation into the *Nhe*I/*Xma*I sites of pUC18C1'D1' to yield plasmid pUC18C1'*cat*D1' (222). Transformation of *E. coli* XL-1 Blue cells with the purified ligation mixture was performed by electroporation, followed by positive selection for transformants on LB agar plates containing Amp (100 µg/ml) and Cm (15 µg/ml). A total of 11 plasmids as analyzed by agarose gel electrophoresis showed the expected size of about 5.7 kbp (**Figure 4.42**). The map of the final knockout plasmid pUC18C1'*cat*D1' carrying the chloramphenicol resistance targeting cassette of 3 kbp is shown **Figure 4.43**.
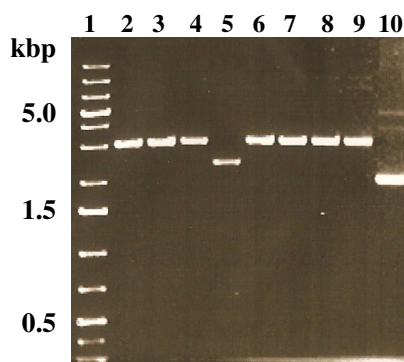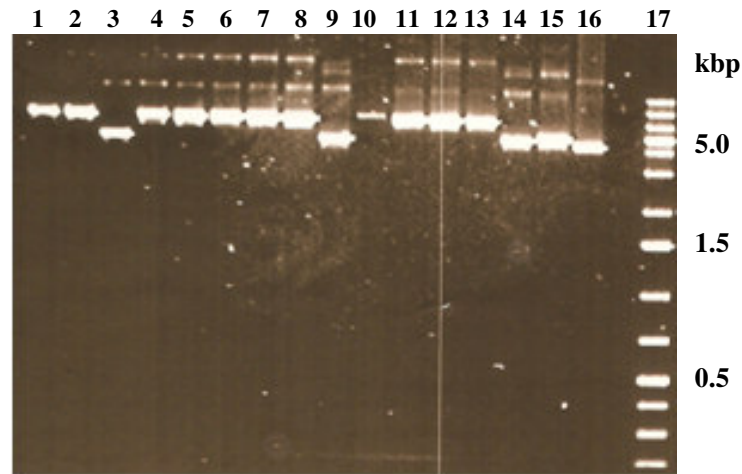
Figure 4.42 Agarose gel electrophoresis of isolated pUC18C1'D1'plasmids which were ligated with *cat* and transformed into *E. coli* XL-1 Blue. Ligation was facilitated after digest with *Nhe*I and *Xma*I of *cat* as well as pUC18C1'D1'. Lanes: 1–16, plasmids pUC18C1'*cat*D1'-1–16; 17, 1 kbp Plus ladder. Plasmids 3, 9 and 14–16 did not comprise *cat* since the plasmids were too small (~5 kbp).
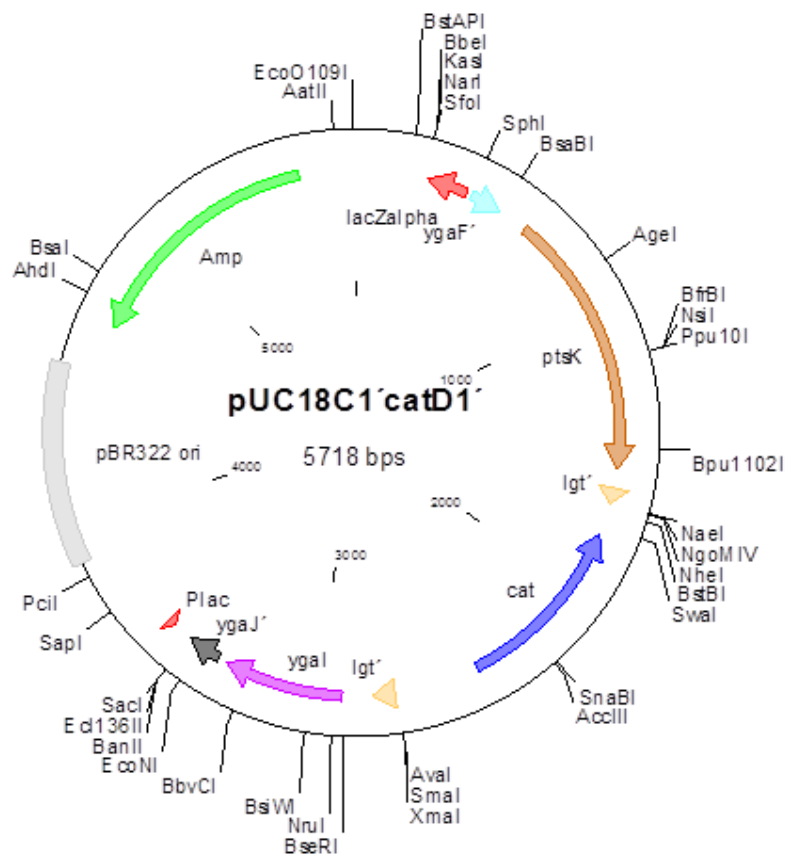
Figure 4.43 Plasmid map of pUC18C1'*cat*D1' with the chloramphenicol resistance cassette targeting the *lgt* gene of *L. lactis* G121.

4.6.3   Transformation of *L. lactis* G 121

The construction of pUC18C1'*cat*D1' was aimed to knockout the *lgt* gene of *L. lactis* G121 by homologous recombination using the method of suicide plasmid directed muta- genesis, which requires highly competent cells of the host for efficient transformation with the knockout construct. Despite the fact that five different methods for preparation of electrocompetent *L. lactis* G121 cells were used, each experiment performed at least in triplicate, no transformants resistant to Cm were obtained. Also, further modifications of the electroporation protocol such as the use of varying DNA amounts (1–4 µg) for trans- formation or extended cell recovery periods after electroporation of up to 4 h have not been successful in yielding potential *L. lactis* G121 *lgt* knockout mutants. In line with the protocol of Wells et al. the shuttle vector pORI23 was used as a positive control. After electroporation of *L. lactis* G121 with this plasmid transformants on Ery containing GM17 agar could be obtained easily.

5   Discussion

Being raised on a traditional farm reduces the prevalence for atopic diseases in children. In line with high impact epidemiological studies plant-based, fungal and microbial derivatives could be related to the immunomodulatory effect. *L. lactis* G121 was identified from stable dust collected on alpine farms in Germany. From *in vitro* experiments it was shown that *L. lactis* G121 polarizes the immune response in mammalian cells towards the non-allergic T_H1 subtype. These findings were supported by *in vivo* studies. BALB/c mice which received lyophilized *L. lactis* G121 intranasally were protected against an OVA-induced asthma phenotype. The work presented here investigated cell envelope molecules of the *L. lactis* G121 with respect to their structure and biological relevance.

Since it was known from studies with other bacteria that LTA, TA and PGN possessed biological activity these major envelope polymers were purified by known methods. After the compounds were structurally characterized by chemical composition analysis, ESI-MS spectrometry and NMR spectroscopy they served for immunological characterization by standardized HEK293 transfection assays. The ability of *L. lactis* G121 to accumulate CLA was tested, because these PUFA are discussed to dampen airway inflammation. In addition to that, molecular biological work was carried out to generate an *L. lactis* G121 Δ*lgt* mutant. Such mutants are deficient in acylation of protein precursors and represent an efficient tool to investigate the biological function of lipoproteins *L. lactis* G121.

5.1   CLA enriched *L. lactis* G121

The content of CLA in the biomass of PBS washed *L. lactis* G121 was monitored from 24–72 hours by GLC. Two preparations were investigated in the context of the WBA. The WBA-sample group was supplemented with LA (1.4 mм LA in 0.2% Tween®80) and the WBA-control group was incubated in 0.2% Tween®80.

After 24 hours the concentration of CLA in the sample was raised to the 1.7-fold amount of the control. Prolonging the incubation up to 72 hours did not further increase the CLA ratio of control to sample. Nonetheless, isomerization of LA to CLA by nongrowing *L. lactis* G121 was proven. This study was performed in dependence on data published by Macouzet et al. for *L. acidophilus* La-5. In case of this probiotic strain its ability to enrich

CLA was investigated with regard to its use in the fermentation of dairy products. *L. acidophilus* La-5 showed elevated CLA levels in the washed biomass (400 µg/g biomass of the 72 hours sample) but to a less extend compared to *L. lactis* G121 (3.4 mg/g biomass of the 72 hours sample). The GLC elution profile of a mix with three different CLA isomers was very similar to that of the *L. lactis* G121 probes.

In the rumen of cattle CLA are natural intermediates from hydrogenation of PUFA to SFA catalyzed by microbes such as *Butyrivibrio fibrisolvens* (192)*.* A constant consumption of milk fat was correlated to a lower prevalence for atopic diseases in children (223,224). Especially in the alpine regions were the fodder is predominantly PUFA-rich grass, the traditionally fermented milk, yoghurt or butter contain high amounts of CLA (225). Several publications indicated that CLA play an important role for a proper immune deviation, for instance by regulation of TNF-α (193–195). The PASTURE study related the increased IFN-γ and TNF-α levels in the cord blood of newborns to the constant consumption of CLA rich dairy products by pregnant farm mothers (119).

As it was described for *Pseudomonas putida* P8 the isomerisation of FA is a pivotal mechanism to sustain membrane fluidity in times of growth stagnation, because in that stage *de novo* synthesis of lipids is blocked (226). It is known that bacteria react to environmental changes with a set of enzymes to introduce double bonds into FA which loosen the bilayer (175). As a cowshed dust bacterium *L. lactis* G121 is exposed to nutrient-poor and frequently changing environmental conditions. Thus, the isomerization of existing FA is an important mechanism which enables the homoviscous adaption of *L. lactis* G121. Most certainly it is inhaled and contacts the epithelium of the upper respiratory tract. The uptake of *L. lactis* G121 by DC and acidification was observed to be essential for the protective effect (findings from PD Dr. H. Heine and K. Stein). The procession of the bacterium could release the CLA and thereby contribute to the non-allergic priming of an individual. Whether CLA enriched *L. lactis* G121 do have an impact on allergy prevention is currently under examination in *in vivo* mouse studies.

5.2   PGN fragments from *L. lactis* G121 signal via NOD2

For separation according to size the mutanolysin generated PGN fragments were applied to SEC on Toyopearl HW-40S material, from which six fractions were obtained. To check for biological activity TLR2-, TLR4-, NOD1- or NOD2-transfected HEK293 cells were stimulated with the obtained fractions (TSK I–VI). Only in NOD2 expressing cells CXCL-8 release was induced by all fractions, of which 10 µg/ml of TSK I-III induced the lowest CXCL-8 levels (~ 1.5 ng/ml) and TSK IV-VI the highest levels (IV: 2.4 ng/ml, V: 3.2 ng/ml and VI: 2.6 ng/ml). The minimal PGN motif which activates the intracellular NOD1 is iE-DAP, a fragment from the DAP-type PGN occurring in Gram-negative and Gram-positive bacilli (93,94). However, the minimal structure necessary for NOD2 activation was identified as MDP, a PGN fragment of both DAP- and Lys-type PGN (95,135). Since the PGN fragments from *L. lactis* G121 did not signal via NOD1 the Lys-type structure was verified. In addition to that, contaminations with endotoxin could be excluded because the preparation did not activate TLR4 expressing HEK293 cells.

The ESI-MS analyses of the TSK fractions corroborated chemical composition analyses which identified, Ala, iGlu, iGln, Lys, Asp and Asn in the PGN isolate from *L. lactis* G121. NAG-β-(1→4)-NAM polymers are the typical PGN backbone of all Bacteria. Opposite to that, is the backbone of the pseudomurein in Archaea composed of NAG-β-(1→3)-*N*‑acetyltalosaminuronic acid (227). Furthermore, these findings confirmed previous reports from other *L. lactis* ssp. such as MG1363 or cremoris, which described the primary PGN structure as NAG-NAM-L-Ala-γ-D-Glu (or iGlu)-L-Lys-D-Ala-D-Ala, with D-Asn (or D-Asp) in the cross-bridge linked to L-Ala of the neighbor stem peptide (221,228–230). In contrast to the backbone the interpeptide bridge in the Lys-type PGN varies within species. D-Asp is often found in LAB, whereas pentaglycine molecules connect the stem peptides of *S. aureus*. Another widespread crosslinker consists of different numbers of L-Ala [e.g., *S. thermophilus* and *M. roseus* (→L-Ala$_3$→), or *M*. sp. 7425 (→L-Ala$_5$→)] (132,230).

The ESI-mass spectra of the TSK fractions were characterized by a huge heterogeneity except for TSK I and II. Both of them contained only one main fragment namely the dimer Penta-N-Penta-N with the calculated mass of 1184.626 u. TSK I was the major peak in the SEC chromatogram. Probably the PGN fragments in this fraction and also fraction

II were too large for detection by ESI-MS. A mixture of PGN trimers was detected in TSK III and IV. The latter one also contained dimeric structures.

The focus was on the purification of PGN mono-and dimers and as TSK V contained such structures (as well as TSK VI) it was chosen for further separation studies by RP-HPLC. Additionally, it has to be mentioned that covalent modifications of *N*-deacetylation and *O*-acetylation of the PGN structures were present. The *N*-deacetylation of PGN fragments has been reported already in the 1970ies in, for instance, *B. cereus* and *L. fermentum* PGN and recently such structural alteration was published for PGN of *L. lactis* MG1363 (221,229,231–233). The acetyl groups can be removed from NAM and NAG by *N*-deacetylases and lead to a diminished recognition by autolysins. Secondly, the *O*-acetylation of the 6-position in NAM residues causes resistance to exogenous muramidase digest with the exception of mutanolysin (234,235). This latter bacterial regulation mechanism was found for several Gram-negative (e.g., *Proteus mirabilis*, *Pseudomonas alcaligenes*, and *Neisseria gonorrhoeae*) as well as Gram-positive (e.g., *S. aureus*, *E. faecalis* and *L. acidophilus*) genera and is considered as a structural modification of mainly pathogenic strains enabling persistence in the host (236,237).

Establishing the analytical RP-12 HPLC condition to 2–15% aqueous CH_3CN in 0.1% TFA for 100 minutes yielded a myriad of substances for TSK V in good separation. Mutanolysin degradation produces PGN fragments with α/β-NAM anomers. The reduction of the NAM residues with $NaBH_4$ would diminish the heterogeneity and surely relieve structural analysis as it was shown for *L. lactis* strain MG1363 and *S. aureus* (198,221). However, the PGN fragments obtained from *L. lactis* G121 were ought to be tested in *in vitro* assays and thus, reduction was omitted to keep the structures original.

Thirteen pools were yielded from the analytical RP12-HPLC separation of TSK V and were investigated by ESI-MS. Pool 1 and 3 were the most promising ones because two monomeric structures (pool 1, 938.408 u and 1080.482 u) and two dimeric structures (pool 2, 1521.721 u and 1927.865 u) were yielded with only minor contaminations of other PGN fragments. For the final purification of these four structures rechromatography was thought to be a proper way. Several RP-HPLC runs were performed to accumulate pool 1 and 3 but did so far not result in enough material for re-chromatography. Subsequent investigations can yield sufficient amounts of pool 1 and 3

and give the purified PGN structures of these by re-chromatography which can, in turn, serve for *in vitro* and *in vivo* studies.

5.3   The EC TA of *L. lactis* G121 consists of poly(glycosylglycerol phosphate) units

WTA are, besides LTA, the second major poly(alditol phosphate) wall polymer of Gram-positive bacteria (142,152). On the one hand it was stated that the WTA of the model organism *S. aureus* SA113 did activate neither hMNC nor mouse macrophages which is why they are not considered as a typical PAMP (238,239). On the other hand it was shown that antibodies against WTA structures can be found in human sera indicating that this molecule is somehow recognized by the immune system (157,158).

Extraction from PGN with 5% TCA was conducted threefold. After AEX of the extract two P-containing pools were detected (Q2 and Q3) leading to the initial conclusion that *L. lactis* G121 possessed two different types of TA. The results from the structural analysis of Q3 compared with the LTA backbone and linker were virtually identical except that Q3 did not contain D-Ala. Hence, further experiments were needed to confirm this finding or proof the contrary.

Incubation of LTA with 5% TCA did not cleave the FA. The signals of α-D-Glc$p$(1→2)-α-D-Glc$p$-(1→3)-glycerol observed by NMR spectroscopy in Q3 was the strongest indicator for an LTA origin of this second AEX pool. To prove this Q3 was subjected to SEC on Bio-Gel P-2 material. The obtained substance still revealed the same shifts affirming Q3 to be deacLTA of *L. lactis* G121. The loss of D-Ala could be explained by the WTA work-up conditions which were not acidic enough to prevent ester hydrolysis. The final question was how could this deacLTA occur? Delcour et al. answered this with the following lines: "Although LTA are born anchored to the cytoplasmic membrane and may remain attached when completed, a fraction of the chains may be released through deacylation, while others still holding their glyceroglycolipid anchor may become loose, possibly through dragging by the inside-to-outside PG expansion mechanism" (132).

Thus, Q2 was considered as the only TA of *L. lactis* G121. No TA structure for *L. lactis* has been described earlier. By chemical composition analysis, ESI-MS spectrometry and NMR spectroscopy one repeat of the EC TA was defined as -6)-[β-D-Glc$p$-(1→3)-][α-D-

Glc$p$NAc-(1→4)-]α-D-Gal$p$NAc-(1→3)-β-D-Glc$p$NAc-(1→2)-glycerol-(1-P-. According to the number of repeats eight different species (2–9 repeats) were detected by ESI-MS analysis. This kind of a poly(glycosylglycerol phosphate) TA is rather seldom. Currently, a similar structure was found for the WTA of *E. faecium* U0317 with -6)-α-D-Gal$p$NAc-(1→3)-β-D-Gal$p$NAc-(1→ in the glycosyl residue (153). The most common TA structures consist of 1,3-poly(GroP) and 1,5-poly(RboP) with D-alanylations as well as glycosylations (e.g., α- or β-D-Glc$p$NAc and α-D-Glc$p$) of the Gro moieties and were found in many bacilli (e.g., *B. megaterium* and *B. subtilis*) and staphylococci (e.g., *S. aureus* and *S. epidermidis*) (140,141,155,156,240). No such decorations were present in the EC TA of *L. lactis* G121.

Results from compositional analysis and NMR spectroscopy showed that small amounts of L-Rha were in the TA preparation as well. NMR spectroscopy could not identify a covalent connection between the L-Rha and the EC TA. To verify this, depolymerization with 48% HF of the EC TA was conducted. SEC of the obtained monomers yielded two fractions of which the first eluted contained EC TA and Rha signals and whereas the second showed only EC TA shifts. Fully assigned 2D NMR spectra further consolidated the hypothesis that the L-Rha was no EC TA component. Most probably the first fraction of SEC contained EC TA and rhamnan structures due to similar sizes. The EC TA fragments detected in this first fraction were of oligomeric nature assuming that HF cleavage was incomplete. The 6-deoxyhexose is often found in the WPS or EPS of lactobacilli and lactococci (139,241–243). It may therefore be permitted that the L-Rha contamination in the EC TA sample was a component of a WPS or EPS structure from *L. lactis* G121.

The *in vitro* results obtained from transiently transfected HEK293 cells revealed that the EC TA was incapable of inducing activation via TLR2, TLR4, NOD1 or NOD2. These data confirmed previous observation, mentioned initially, showing that TA do not display a typical bacterial pattern which triggers mammalian innate immune responses. Additionally, these experiments proved the EC TA preparation to be free of lipoproteins, LPS or PGN (Gram-positive as well as Gram-negative) impurities.

Since the TA was extractable with watery solutions according to the CPS protocol it was denoted as EC TA indicating a rather loosely association to the cell wall. Such EC TA are deposits of the WTA [also cell wall teichoic acid (CW TA)] which is connected to the *O*-6 of NAM within the PGN. Hence, it is very likely that the structures are the same as it

has been presented for *S. epidermidis* RP62A and *S. aureus* MN8m (155,156). First experiments implied that the EC TA and WTA of *L. lactis* G121 are structurally very similar. The loss of the CPS structure can only be explained as an adaption of *L. lactis* G121 to laboratory conditions, indicating that the CPS was necessary for survival in the natural environment (dust, soil) but not in a pure lab culture.

5.4   MNC are activated by LTA from *L. lactis* G121 independently of TLR2

LTA can be subdivided into four different types according to the nature of the repeating unit. Type I is made up of GroP repeats (e.g., *S. aureus*), type II of Gal-Gal-GroP repeats (e.g., *L. garviae*) and type III of Gal-Gro-P repeats (e.g., *Clostridium innocuum*). Type IV LTA is so far unique to *S. pneumoniae* strains and consist of complex tetrasaccharide repeating units which are modified with phosphorylcholine and interlinked by RboP. However, type I is the most frequent one found (81,142,244).

The LTA of *L. lactis* G121 could be identified as type I LTA consisting of a poly(1,3-GroP) backbone which was substituted at *O*-2 of Gro by D-Ala and α-D-Gal. The average chain length was 14–16 units. ESI-MS experiments showed a vast heterogeneity within the preparation. This could be attributed, amongst other things, to the different FA combinations found for the diacyl-anchor. The single FA found were 14:0, 16:0, 16:1, 18:1 and Δ-19:0. These were already detected for the LTA of *L. lactis* Kiel 42172 which additionally contained 14:1 (245). Not only the diverse chain lengths but also the number of D-Ala decorations contributed to a further heterogeneous make-up of the LTA.

Several LTA compositions from different *L. lactis* strains have been elucidated. D-Ala and α-D-Gal*p* substitutions of the backbone have been reported earlier for the strains Kiel 48337 and NCDO 712 [termed *Streptococcus lactis* until 1985 (246)] and IL 1403 (247–249). Furthermore, *L. lactis* IL 1403 (16 repeats), Kiel 48337 and NCDO 712 (both 18 repeats) possessed short chain LTA just like *L. lactis* G121 (average 14–16 repeats). Opposed to that is the LTA of *S. aureus* a long chain molecule with an average of 45–50 GroP units (199). In general, alanylation and glycosylation of Gro are confessed substitutions of type I LTA (e.g., α-D-Glc in *L. brevis* and α-D-GlcNAc in *S. aureus*) as well as of Rbo in type IV LTA (Ala and α-D-GalNAc), whereas Type II and III LTA do not feature such modifications (81,142,200).

Although evident from chemical composition analysis and NMR spectroscopy, no mass peaks demonstrating the Hex substitution of Gro were identified from the ESI-MS spectra of the intact LTA. Fortunately, such prove was found from the deacLTA which was co-isolated with the EC TA. Experiments at 5 V and fragmentation at high orifice voltage clearly showed mass peaks and ions, respectively, which comprised Hex residues. The deacLTA was free of D-Ala. It remains unclear why D-Ala and α-D-Gal furnished LTA species could not be recorded by means of ESI-MS analysis. Furthermore, slight differences in average chain length and degree of Hex substitution were identified for intact LTA (14–16 GroP repeats, 3 α-D-Gal) compared to ESI-MS findings of deacLTA (max. 19 GroP repeats, 7 Hex substitutions). Most likely the reason for the difference was that the intact LTA preparation was extracted from 24 hours old bacteria and the deacLTA preparation from 12 hours old bacteria, clearly reflecting structural changes during growth.

To investigate the composition of the linker which connected the backbone with the lipid part the backbone was cleaved with 48% HF and the resulting lipid anchor was *O*-deacylated by N_2H_4 treatment. NMR spectra resolved the linker as α-D-Glc*p*(1→2)-α-D-Glc*p*-(1→3)-Gro and this finding was affirmed by methylation analysis. This kojibiose structure was found already for LTA of both *L. lactis* strains Kiel 48337 and NCDO 712, and other lactococci, streptococci as well as *E. faecalis* (143). A recent study identified the same linker for the LTA of bovine mastitis strains *S. uberis, S. agalactiae* and *S. dysgalactiae,* again confirming that this structure is conserved among Streptococcaceae (250). In comparison to that β-D-Glc*p*-(1→6)-β-D-Glc-(1→3)-Gro was found in the anchor of several bacilli, staphylococci, and other streptococci (142).

The immunomodulatory properties of LTA have been emphasized in a variety of studies. Cytokine and chemokine release upon LTA stimulation (IL-1β, CXCL-8, IL-10, IL-23, TNF-α and GM-CSF) as well as antibody production against LTA were reported (158–165). To find out whether the LTA of *L. lactis* G121 had similar properties and might mediate the allergy-protective effect it was tested *in vitro*.

The LTA isolate of *L. lactis* G121 did not activate TLR2 or TLR4 transfected HEK293 hepatocytes. Additionally, no signaling via the intracellular receptors NOD1 or NOD2 was observed. However, stimulation of hMNC with LTA led to an IL-6 induction. IL-6 has complex pro-inflammatory functions regulating survival, apoptosis or proliferation of

T$_H$ lymphocytes (251,252). Does this necessarily mean that the LTA of *L. lactis* G121 causes inflammation? This seems rather unlikely since only 10 µg/ml of LTA resulted in an IL-6 level representing three-fourths of the level which was obtained with 1 ng/ml of LPS. Apart from that, IL-6 has further functions. It is known as a key transistor between innate and acquired responses and can have even anti-inflammatory effects by suppressing TNF-α for instance (253,254). As already mentioned antibodies against *L. lactis* G121 were found in the sera of children from the farms. Whether the LTA structure displays a possible epitope could be investigated in future experiments. Moreover, the full spectrum of immune cells, chemokines and cytokines influenced by LTA need to be evaluated to get a clearer picture.

With regard to the receptor which could transmit the LTA signal TLR2 was unambiguously ruled out in case of *L. lactis* G121. However, reports about the LTA of mainly *S. aureus* attributed its activity to TLR2 (166–169). Even TLR4 was considered as receptor (170). Experiments with synthetic LTA analoga revealed that the immunostimulatory components were lipoproteins and not LTA (171–173). Due to the similar amphiphilic properties these are isolated together with the LTA by the widely used BuOH extraction method and HIC is probably incapable of complete separation. The ongoing re-evaluation was supported by studies which worked with LTA preparations which were H$_2$O$_2$ treated. This procedure oxidizes the typical *N*-terminal cysteine-thioether group to the sulfoxide-form which is TLR2-inactive (78,80). Last doubts were erased by crystallographic studies performed by Kang et al. They showed that the heterodimerization of TLR2 and TLR6, which is necessary for receptor signaling, can only be enabled by diacylated structures carrying a peptide head group. Since LTA lacks such head group it can indeed bind to TLR2 but not enable the heterodimer with TLR6 (255).

Currently, the signaling pathway of LTA isolated from *L. lactis* G121 remains unknown. Preliminary experiments showed that uptake of *L. lactis* G121 from DC as well as acidification is crucial for expression of the allergy protection (data from Dr. H. Heine and K. Stein). Therefore, cytoplasmic proteins belonging to the NLR family display potential receptors targeted by LTA (Wilmanski et al. 2008). Perhaps complement activation is a further possible route one should keep in mind for following studies. In fact, the lectin

pathway was found out to play a role for recognition of *S. aureus* and *S. pneumoniae* LTA (81).

5.5 The *lgt* sequence of *L. lactis* G121 and its knockout

To obtain a mutant of *L. lactis* G121 deficient in lipidation of prelipoproteins, the *lgt* gene coding for the prolipoprotein diacylglyceryl transferase had to be identified first in the genome of the bacterium. Using the GenomeWalker™ technology for amplification of unknown DNA sequences adjacent to a highly conserved DNA sequence within the *lgt* gene of different *L. lactis* subspecies, the DNA sequence of the *lgt* region of *L. lactis* G121 carrying the *ygaF', ptsK*, *lgt*, *ygaI* and *ygaJ'* genes could be successfully determined. While *ygaF* and *ygaJ* code for hypothetical proteins of unknown functions, the *ygaI* gene was predicted to code for a methyl-accepting chemotaxis-like protein. The gene product of *ptsK* is most likely a bifunctional HPr kinase/phosphorylase involved in regulation of carbon source utilization in Gram-positive bacteria (256). Alignment of the *L. lactis* G121 sequence of 2.687 kbp with the *lgt* regions of *L. lactis* KF147, IL1403, cremoris MG1363 and cremoris NZ9000 revealed that *lgt* and the genes up- and downstream of *lgt* are highly conserved across *L. lactis* subspecies. However, due to a frame shift by insertion of a single guanosine at position 784 of *lgt*, the open reading frame of *lgt* of the herein investigated strain G121 was 18 bp longer (806 bp) compared to the coding sequences of *lgt* of the other strains (786 bp). Thus, the deduced amino acid sequence of *lgt* of G121 consisted of 267 instead of 261 amino acids predicted for Lgt of *L. lactis* subspecies IL1403, cremoris MG1363 and cremoris NZ9000.

In order to functionally inactivate the *lgt* gene of *L. lactis* G121, the method of suicide plasmid directed mutagenesis based on plasmid pUC18 as a carrier of a Cm resistance cassette targeting the *lgt* gene was used. To allow genetic exchange by homologous recombination, the wild-type cells were transformed with the knockout plasmid by electroporation as described earlier for *S. aureus* SA113 (184,217). As Gram-positive bacteria have multiple PGN layers of 20–80 nm thickness, efficient uptake of DNA by the cells is likely the most critical issue (257). Three different transformation protocols were used, which involved the growth of the bacterial cells in media containing glycine. This should decrease the formation of interpeptide bridges by replacement of D-Ala in the stem peptide and increase the permeability of the cell wall (214,216,217). None of these methods

yielded Cm-resistant transformants, even with varying glycine (1, 2 or 10%) and DNA concentrations (1–4 µg). In another method, lysozyme was used to enzymatic digest the PGN sacculus as it was described for *L. lactis* and *cremoris* (215). However, this approach was ineffective as well and could be attributed to the *O*-acetylation identified for the PGN of *L. lactis* G121. To examine the transformation efficiency, the shuttle vector pORI23 was used as a positive control for electroporation according to Wells et al. (218,219,258).

The successful electroporation of *L. lactis* G121 with pORI23 indicated that the protocol of Wells et al. is a suitable method to efficiently transform *L. lactis* G121 cells. Nonetheless, no transformants were obtained using this method with the *lgt* knockout plasmid pUC18C1'*cat*D1'. Taken together, the data suggests that the function of the Lgt enzyme is essential for viability of *L. lactis* G121 as it was shown recently for the first time for Gram-positive bacterium *Streptomyces coelicolor* (179).

5.6   Perspectives

A steadily growing number of epidemiological observations showed that the farming environment exhibits factors which contribute to a non-allergic development of the human immunity (48,127). Besides the main hypothesis that the life on a farm primes the newborn immune system to the non-allergic T_H1 phenotype additional actors have entered the scenery. To date we know that the T_{Reg} lymphocytes have an important impact, that certain parasites can suppress the T_H2 response, that epigenetic mechanisms as well as genetic predisposition play a role and that defined structures such as arabinogalactan from grass or the LPS of *A. lwoffii* F78 prevent from allergies (45,47). This thesis was performed to identify cell wall structures of *L. lactis* G121 which are responsible for its antiallergic properties, while at the same time further elucidating basic mechanisms of bacterial transmitted allergy protection.

L. lactis G121, the most frequent Gram-positive dust isolate, has shown to enrich its biomass with CLA when supplemented with LA in a non-growing stage. CLA can diminish atopic hypersensitivities (193–195). If an enhanced CLA production of *L. lactis* G121 is a possible mode to contribute to prevent from asthma is currently tested *in vivo*. In these tests BALB/c mice are sensitized and challenge with OVA to evoke an asthmatic phenotype in their lungs. Very preliminary data (from Hani Harb/Marburg) indicated that a

treatment with CLA-enriched *L. lactis* G121 diminished eosinophil count in the BAL, to an even lower amount as it was shown for the non-enriched *L. lactis* G121. On the opposite a slight increase in neutrophils was observed. To verify these results further *in vivo* experiments will be performed.

Previous studies demonstrated that *L. lactis* G121 signals via NOD2 (46). This activation can now clearly be attributed to its Lys-type PGN fragments. The asthma-protective effect of *L. lactis* G121 seems to be based on shifting the T_H2 domination in newborns to a T_H1/T_H2 balance, for instance, by induction of IL-12p70. Whether this mechanism involves NOD2 activation could be investigated in future *in vivo* studies with *Nod2*$^{-/-}$ mice and defined PGN structures. Since the uptake of *L. lactis* G121 by DC was found out to be essential for the protection a participation of intracellular recognition molecules seems very likely. Furthermore, it is important to test the naturally occurring PGN fragments of *L. lactis* G121 rather than synthetic analoga to resolve the influence of *N*-deacetylation and *O*-acetylation on the biological activity.

LTA was often generally referred to as Gram-positive endotoxin (167,199). Experiments of this study illustrated that the LTA of *L. lactis* G121 possessed a TLR2-independent cytokine-inducing activity in hMNC. Thus, the role of LTA as a TLR2 ligand was invalidated once more (80,81). The identification of a putative LTA-recognition receptor, which is assumed to be located in the cytoplasm, is addressed at present *in vitro* studies. Additional mouse experiments, in which the mice are pretreated with the purified LTA, will be pivotal to evaluate its importance for allergy protection. The induction of IL-6 in hMNC needed much higher concentrations of LTA compared to LPS (approximately 1:10,000), thus the term "endotoxin" should not be used for LTA.

To address the role of lipoproteins in *L. lactis* G121, a molecular biological approach has been chosen. As it was achieved for *S. aureus* SA113, a Δ*lgt* mutant should provide insights into structure-function relations. A vast number of transformation experiments with a knockout plasmid failed to generate a mutant, leading to the conclusion of an indispensable role of *lgt* for *L. lactis* G121. Hence, it seems that information about the biological activity of lipoproteins could only be obtained with purified structures, for example, tested in HEK293 assays.

The EC TA identified from *L. lactis* G121 was inactive in tests with TLR2-, TLR4-, NOD1- or NOD2-transfected HEK293 cells. Additional stimulation of hMNC or DC

would be helpful to further corroborate no biological activity or prove the contrary how it was the case for the LTA. However, TA are known to be essential for physico-chemical properties of bacterial surfaces (147,150,153–156). The detection of TA structures in biofilms of *L. lactis* G121 could indicate that this structure is involved in the adherence of the bacterium. At least for allergy protection the EC TA seems to play no role.

This thesis offered improved methodology for the isolation of cell wall components of the asthma protective farm isolate *L. lactis* G121. With the help of *in vitro* tests it was found that PGN and LTA have biological relevance. The obtained substances will contribute to not only the discovery of the role of PGN or LTA for allergy protection but also to understand molecular basics of the hygiene hypothesis.

6   Summary

The hygiene hypothesis was founded by investigations of the British epidemiologist David P. Strachan in 1989. It is meant to explain why children from the farming milieu show a lower prevalence for asthma bronchiale or other atopic sensitizations compared to those who did not grow up on a farm. This observation was proven in epidemiological terms due to profound cohort studies. Just recently we began to understand the molecular basis of such processes. One main concept is that a permanent exposure to livestock, fodder and microorganisms or raw milk consumption offers proper immune stimuli which lead to a non-allergic balance of T_H1/T_H2 lymphocytes.

This thesis was performed to find out whether the allergy-protective effect mediated by *L. lactis* G121 could be related to one or more defined cell envelope structures. In general, literature about completely characterized structures isolated from *L. lactis* G121, although many strains are used as dairy starter cultures, is rare. Therefore, the cell envelope was studied. The major polymers LTA, EC TA and PGN were isolated, structurally characterized and subjected to immunological investigations. The biological relevance of lipoproteins should be investigated with the help of a Δlgt *L. lactis* G121 mutant. Moreover, the capability of *L. lactis* G121 to isomerize CLA from LA was examined.

Evidence for an involvement of CLA in allergy suppression was reported by different groups. Since it was shown for *L. acidophilus* La-5 that this LAB isomerized LA to CLA it was tested whether *L. lactis* G121 possessed the same abilities. The supplementation of PBS washed *L. lactis* G121 with LA led to enrichment of the biomass with CLA. The effect was observed from 24 to 72 hours whereas the concentrations measured after 24 hours did not significantly differ to that of 48 and 72 hours. From literature it is known that bacteria build CLA from other PUFA during nutrient-poor times to sustain membrane fluidity. Due to the fact that internalization of *L. lactis* G121 by DC is necessary for the protective effect, it seems possible that CLA are released inside of the DC and influence the immune response. Ongoing mouse *in vivo* studies are dedicated to find out whether the CLA enriched *L. lactis* G121 biomass offers an even stronger anti-allergic stimulus than the non-enriched already did.

Previous *in vitro* data clearly revealed that *L. lactis* G121 activates NOD2. Studies with synthetic analoga showed that the minimal structure needed for NOD2 activation in MDP, a fragment of DAP-type as well as Lys-type PGN. Therefore, the PGN of *L. lactis* G121 was extracted and solubilized with mutanolysin. Chemical and ESI-MS analysis defined it as Lys-type PGN with a primary structure of NAG-NAM-L-Ala-γ-D-Glu (or iGlu)-L-Lys-D-Ala-D-Ala, with D-Asn (or D-Asp) in the crossbridge connecting the D-Ala of the adjacent stem peptide. Some fragments had specific modifications in the form of *N*-deacetylations and *O*-acetylations. These kind of modifications were identified earlier in *L. lactis* MG1363. They display a bacterial regulation mechanism since *N*-deacetylations prevent from autolysin and *O*-acetylations from lysozyme degradation. It clearly indicated that *L. lactis* G121 could colonize the nasal epithelium without being cleared by the lysozyme from the nasal mucosa.

The PGN fragments of *L. lactis* G121 activated HEK293 cells which were transfected with NOD2 but not with NOD1. This finding related the NOD2 activity found for intact cells to PGN. Since the mutanolysin digest resulted in a myriad of different PGN structures RP HPLC separation was carried out but did not yield completely pure fragments. From a number of substances two were chosen to be further separated by re-chromatography to have pure mono- and dimeric PGN structures at hand. So far, no re-chromatography could be conducted because the amounts of the respective substance peaks were insufficient. Subsequent experiments are needed to give defined pure structures which are important to test the impact of PGN for allergy protection, for example, in a mouse model. On the other hand it can be investigated whether the *N*-deacetylated and *O*-acetylated fragments offer different magnitudes of activation or even different function.

Due to the detection of antibodies against WTA in human sera these envelope structures seem to be immunologically relevant. The structure of the EC TA of *L. lactis* G121 could be defined as a -6)-[β-D-Glc*p*-(1→3)-][α-D-Glc*p*NAc-(1→4)-]α-D-Gal*p*NAc-(1→3)-β-D-Glc*p*NAc-(1→2)-glycerol-(1-P-. Eight different species of the poly(glycosylglycerol phosphate) were detected with respect to the number of repeating units. Results obtained from TLR2-, TLR4-, NOD1- or NOD2-transfected HEK293 cells showed that the EC TA was not signaling via these innate receptors. Preliminary experiments found the EC TA and the WTA of *L. lactis* G121 to be structurally very similar. It is known from other bacteria that WTA are important envelope molecules mediating adherence to tissues and artificial surfaces. Hence, future studies could verify the role of the *L. lactis* G121 WTA for

adherence to nasal epithelium and possibly explain how the bacterium could stay in the nose and enter the sub mucosa.

The LTA preparation of *L. lactis* G121 had a poly(GroP) backbone and the average chain length was 14–16 units with random substitutions at *O*-2 of Gro by D-Ala and α-D-Gal. The lipid anchor was build up of α-D-Glc*p*(1→2)-α-D-Glc*p*-(1→3)-diacylglycerol with different combinations of 14:0, 16:0, 16:1, 18:1 and Δ-19:0. The LTA isolate of *L. lactis* G121 revealed no ligand function for TLR2. Nevertheless, the LTA induced IL-6 release in hMNC. Ongoing *in vitro* studies can elucidate the mechanism behind the activation and especially receptor(s) for LTA need to be figured out. Since the allergy-protective effect of the bacterium depends on the phagocytosis and acidification by DC the participation of intracellular receptors, maybe from the NLR family or from the complement system, seems very possible.

In order to investigate the function of lipoproteins for the *L. lactis* G121-mediated allergy protection, a molecular biological approach was used to generate a Δ*lgt* mutant defective in lipidation of prelipoproteins. The sequence of the *lgt* region obtained from the *L. lactis* G121 genome had a size of 2.687 kbp and was highly conserved across *L. lactis* strains such as KF147, IL1403, cremoris MG1363 and cremoris NZ9000. A knockout plasmid was constructed, which carried the Cm^R-encoding *cat* gene flanked by up- and down-stream sequences of *lgt* for homologous recombination. Different transformation protocols failed to obtain transformants, suggesting that Lgt was indispensable for viability of *L. lactis* G121. The *lgt* gene was demonstrated to be essential in many Gram-negative species and recently also in a Gram-positive bacterium. It appears that a biological evaluation of lipoproteins can only be performed in future with highly purified structures isolated from the bacterial biomass.

Taken together, NOD2 seems to be the most probable receptor which could trigger the *L. lactis* G121 provoked T_H1 promotion. The activation of NOD2 is caused by PGN fragments from the cell wall and for the future it could be considered to use such as possible prophylactic agents. The methods and structures resulting from this thesis will contribute to a deepened elucidation of the anti-allergic potential of cell wall components from *L. lactis* G121.

7   Zusammenfassung

Die Hygienehypothese wurde 1989 durch Untersuchungen des britischen Epidemiologen David P. Strachan begründet. Es ging dabei darum zu erklären, warum Kinder aus dem bäuerlichen Milieu geringere Inzidenzen für *Asthma bronchiale* oder andere atopische Sensibilisierungen aufweisen als Kinder, die nicht auf dem Bauernhof aufgewachsen sind. Durch profunde Kohortenstudien gelten diese Beobachtungen auf der epidemiologischen Ebene als bewiesen. Erst seit kurzem beginnt man zu verstehen, wie die molekularen Mechanismen dahinter aufgebaut sind. Eines der Hauptkonzepte besteht darin, dass ein permanenter Kontakt zu Nutztieren, Tierfutter und Mikroorganismen als auch Rohmilchkonsum die richtigen Immunstimulanzien für ein ausgeglichenes T_H1/T_H2 Lymphozyten Verhältnis liefert. In der Tat zeigt Arabinogalactan aus Gras oder *L. lactis* G121 und *A. lwoffii*, welche aus Stallstaub isoliert wurden, *in vitro* eine Induktion des T_H1-fördernden Zytokins IL-12p70 und schützten *in vivo* vor Allergie.

Diese Arbeit wurde durchgeführt, um herauszufinden ob der Allergie-protektive Effekt von *L. lactis* G121 einer oder mehreren definierten Zellhüll-Strukturen zugeordnet werden könnte. Im Allgemeinen gibt es kaum Literatur über komplett aufgeklärte Strukturen von *L. lactis*, obwohl viele Stämme Anwendung als Molkerei-Starterkultur finden. So wurde in dieser Arbeit die Zellhülle von *L. lactis* G121 studiert. LTA, EC TA und PGN, die größten Hüll-Polymere, wurden isoliert, strukturell charakterisiert und dienten weiteren immunologischen Untersuchungen. Die biologische Relevanz von Lipoproteinen sollte mithilfe einer Δ*lgt L. lactis* G121 Mutante beurteilt werden. Zudem wurde getestet ob *L. lactis* G121 in der Lage war CLA aus LA zu isomerisieren.

Hinweise auf eine Beteiligung von CLA an Allergie-unterdrückenden Prozessen wurden von mehreren Gruppen publiziert. Da für *L. acidophilus* La-5 bekannt war, dass dieses Milchsäurebakterium LA zu CLA isomerisieren kann, wurde untersucht, ob *L. lactis* G121 auch dazu fähig wäre. Die Ergänzung von PBS gewaschenen *L. lactis* G121 Kulturen mit LA führte zu einer Anreicherung von CLA in der Biomasse. Der Effekt wurde von 24 bis 72 Stunden beobachtet, wobei es keine signifikanten Unterschiede in den CLA Konzentrationen zwischen 24, 48 und 72 Stunden gab. Aus der Literatur weiß man, dass Bakterien unter nährstoffarmen Bedingungen aus anderen PUFA CLA bilden, um die

Fluidität der Membran zu gewährleisten. Angesichts der Tatsache, dass *L. lactis* G121 von DC aufgenommen und prozessiert werden muss, damit sich der protektive Effekt entwickeln kann (Daten von PD Dr. H. Heine und K. Stein), scheint es wahrscheinlich, dass CLA im Inneren der DC freigesetzt werden und so die Immunantwort beeinflussen können. Noch andauernde Maus *in vivo* Studien widmen sich der Frage, ob CLA angereicherte *L. lactis* G121 einen noch stärkeren anti-allergischen Stimulus darstellen, als es für die nicht angereicherten Zellen bereits gezeigt wurde.

Frühere *in vitro* Daten wiesen klar auf eine Aktivierung des intrazellulären Rezeptors NOD2 durch *L. lactis* G121. Studien mit synthetischen Analoga zeigten, dass MDP die Minimalstruktur für eine NOD2 Aktivierung ist, ein Fragment des DAP-Typ als auch des Lys-Typ PGN. Somit wurde der PGN Sacculus von *L. lactis* G121 extrahiert und mittels Mutanolysin solubilisiert. Die chemische Komponenten und ESI-MS Analyse definierten es als Lys-Typ PGN mit einer Primärstruktur von NAG-NAM-L-Ala-γ-D-Glu (oder iGlu)-L-Lys-D-Ala-D-Ala, mit D-Asn (oder D-Asp) in der Interpeptidbrücke als Verbindung zum D-Ala des angrenzenden Stammpeptids. Dabei wiesen mehrere Fragmente spezifische Modifikationen in Form von *N*-Desacetylierungen und *O*-Acetylierungen. Diese Modifikationen konnten schon vorher für *L. lactis* MG1363 gezeigt werden. Sie stellen einen bakteriellen Regulierungsmechanismus dar, bei dem *N*-Desacetylierungen vor Autolysin und *O*-Acetylierungen vor Lysozym Degradierung schützen. Damit gibt es einen Hinweis darauf, dass *L. lactis* G121 im Nasenepithelium persistieren könnte, ohne vom Lysozym der Nasenschleimhaut abgebaut zu werden.

Die PGN Fragmente von *L. lactis* G121 aktivierten HEK293 Zellen, die mit NOD2 transfiziert waren jedoch nicht diejenigen, die mit NOD1 transfiziert waren. Mit diesem Ergebnis konnte die NOD2 Aktivität, die für intakte Zellen gefunden wurde dem PGN zugeordnet werden. Da der Mutanolysin-Verdau eine Vielzahl unterschiedlicher PGN Strukturen ergab wurde RP HPLC Trennung durchgeführt. Jedoch führte dies nicht zu gänzlich reinen Fragmenten. Aus einer Reihe von Substanzen wurden zwei für die weitere Trennung mittels Re-Chromatographie ausgesucht. Damit sollten saubere mono- und dimerische PGN Strukturen erhalten werden. Bisher konnte keine Re-Chromatographie erfolgen, da die Substanzmengen der entsprechenden Signale unzulänglich waren. Daher sind Folgeexperimente nötig um reine PGN Strukturen zu erhalten, mit deren Hilfe der Einfluss von PGN für die Allergie Protektion im Maus Model getestet werden könnte. Desweiteren könnte mit definierten Strukturen untersucht werden, ob die *N*-

desacetylierten und *O*-acetylierten Fragmente möglicherweise eine andere Größenordnung der Aktivierung bieten oder gar andere Funktionen besitzen.

Aufgrund des Nachweises von Antikörpern gegen WTA in Humanseren scheinen diese Hüll-Strukturen immunologisch relevant zu sein. Die Struktur der EC TA von *L. lactis* G121 wurde als -6)-[β-D-Glc*p*-(1→3)-][α-D-Glc*p*NAc-(1→4)-]α-D-Gal*p*NAc-(1→3)-β-D-Glc*p*NAc-(1→2)-glycerol-(1-P- definiert. Acht verschiedene Spezies dieses poly(Glycosylglycerolphosphates) wurden im Bezug auf die Anzahl der Wiederholungseinheiten detektiert. Ergebnisse aus Untersuchungen mit TLR2-, TLR4-, NOD1- oder NOD2-transfizierten HEK293 Zellen zeigten, dass die EC TA über keinen dieser Rezeptoren Signale hervorrief. Erste Experimente ergaben, dass die EC TA und die WTA von *L. lactis* G121 strukturell sehr ähnlich sind. Es ist von anderen Bakterien bekannt, dass WTA wichtige Moleküle sind, die die Anheftung an Gewebe oder künstliche Oberflächen vermitteln. Zukünftige Studien könnten die Rolle der WTA für die Adhärenz am Nasenepithel beleuchten und damit eventuell klären, ob sie für das Bakterium von Nöten ist um in die Submucosa zu gelangen.

Das LTA Präparat aus *L. lactis* G121 bestand aus einem poly(Glycerolphosphat) Rückgrat mit einer durchschnittlichen Länge von 14–16 Einheiten welche unregelmäßig am *O*-2 des Gro mit D-Ala und α-D-Gal dekoriert waren. Der Lipidanker bestand aus α-D-Glc*p*(1→2)-α-D-Glc*p*-(1→3)-Diacylglycerol mit verschiedenen FA Kombinationen von 14:0, 16:0, 16:1, 18:1 und Δ-19:0. Somit wurde eine recht heterogene LTA Mischung identifiziert. Die einstige Rolle der LTA als TLR2 Ligand konnte in jüngsten Studien Verunreinigungen mit Lipoproteinen zugeschrieben werden. Diese Erkenntnis wurde durch HEK293 Tests für die LTA aus *L. lactis* G121 erweitert, in denen keine TLR2 Aktivierung festgestellt werden konnte. Nichtsdestotrotz war die LTA in der Lage eine IL-6 Freisetzung in hMNC zu induzieren. Zusätzliche *in vitro* Studien könnten zur Aufklärung des dahinter liegenden Mechanismus beitragen, insbesondere die involvierten Rezeptoren müssen identifiziert werden. Da das Bakterium durch DC aufgenommen und prozessiert wird scheint eine Partizipation von intrazellulären Rezeptoren, womöglich aus der NLR Familie oder des Komplementsystems, sehr wahrscheinlich.

Um die Funktion von Lipoproteinen für die *L. lactis* G121-vermittelte Allergie Protektion zu untersuchen, sollte ein molekularbiologischer Ansatz eine Δ*lgt* Mutante generieren, welche nicht zur Acylierung der Prelipoproteine befähigt ist. Die erhaltene Sequenz der

lgt Region aus *L. lactis* G121 hatte eine Größe von 2.687 kbp und war hoch konserviert im Vergleich zu derjenigen aus den Stämmen KF147, IL1403, cremoris MG1363 und cremoris NZ9000. Ein knockout Plasmid wurde konstruiert, in welchem eine *cat* Sequenz durch flankierenden Sequenzen des *lgt* Gens umschlossen war. Damit sollte über homologe Rekombination *lgt* gegen ein Cm^R-kodierendes Gen ausgetauscht werden. Verschiedene Transformationsprotokolle lieferten keine Transformanten. Daraus wurde geschlossen, dass Lgt für die Lebensfähigkeit von *L. lactis* G121 unerlässlich war. So wurde es bereits für viele Gram-negative Arten beobachtet und jüngst auch bei dem ersten Grampositive Bakterium beschrieben. Offensichtlich ist eine biologische Evaluierung der Lipoproteine in Zukunft nur mit aus Biomasse isolierten Strukturen machbar.

Zusammenfassend scheint NOD2 momentan der wahrscheinlichste Rezeptor, über den die durch *L. lactis* G121 ausgelöste T_H1 Promotion angeschaltet werden könnte. Verantwortlich für die NOD2 Aktivierung sind PGN Fragmente aus der Zellwand und es gilt für die Zukunft darüber nachzudenken, solche als prophylaktische Agenzien einzusetzen. Die Methoden und Strukturen aus dieser Arbeit können in Folgeexperimenten zu einer vertieften Erkenntnis über das anti-allergische Potenzial der Zellhüll Komponenten von *L. lactis* G121 beitragen.

8 Reference List

1. WHO. Key facts on asthma. Fact sheet N°307. 2011. 1–3.

   http://www.who.int/mediacentre/factsheets/fs307/en/index.html

2. WHO. Prevention of allergy and allergic asthma. 2002. 1–14.

   http://whqlibdoc.who.int/hq/2003/WHO_NMH_MNC_CRA_03.2.pdf

3. Murphy K, Travers P, Walport M. *Immunologie*. 7th ed. Heidelberg: Spektrum Akademischer Verlag 2009.

4. Hershey GKK, Friedrich MF, Esswein LA, Thomas ML, Chatila TA. The association of atopy with a gain-of-function mutation in the α subunit of the interleukin-4 receptor. *The New England Journal of Medicine* 1997; **337**:1720–1725.

5. Vercelli D. Discovering susceptibility genes for asthma and allergy. *Nature Reviews Immunology* 2008; **8**:169–182.

6. Weiss ST, Raby BA, Rogers A. Asthma genetics and genomics 2009. *Current Opinion in Genetics & Development* 2009; **19**:279–282.

7. Murdoch JR, Lloyd CM. Chronic inflammation and asthma. *Mutation Research* 2010; **690**:24–39.

8. Wan H, Winton HL, Soeller C, Tovey ER, Gruenert DC, Thompson PJ, et al. Der p 1 facilitates transepithelial allergen delivery by disruption of tight junctions. *The Journal of Clinical Investigation* 1999; **104**:123–133.

9. Grunstein MM, Veler H, Shan X, Larson J, Grunstein JS, Chuang S. Proasthmatic effects and mechanisms of action of the dust mite allergen, Der p 1, in airway smooth muscle. *The Journal of Allergy and Clinical Immunology* 2005; **116**:94–101.

10. Riffo-Vasquez Y, Spina D. Role of cytokines and chemokines in bronchial hyperresponsiveness and airway inflammation. *Pharmacology & Therapeutics* 2002; **94**:185–211.

11. Romagnani S. Cytokines and chemoattractants in allergic inflammation. *Molecular Immunology* 2002; **38**:881–885.

12. Kulczycki A, Metzger H. The interaction of IgE with rat basophilic leukemia cells. *The Journal of Experimental Medicine* 1974; **140**:1676–1695.

13. Maddox L, Schwartz DA. The pathophysiology of asthma. *Annual Reviews in Medicine* 2002; **53**:477–498.

14. Luster AD, Tager AM. T-cell trafficking in asthma: lipid mediators grease the way. *Nature Reviews Immunology* 2004; **4**:711–724.

15. Galli SJ, Nakae S, Tsai M. Mast cells in the development of adaptive immune responses. *Nature Immunology* 2005; **6**:135–142.

16. Taube C, Nick JA, Siegmund B, Duez C, Takeda K, Rha YH, et al. Inhibition of early airway neutrophilia does not affect development of airway hyperresponsiveness. *American Journal of Respiratory Cell and Molecular Biology* 2004; **30**:837–843.

17. Park SJ, Wiekowski MT, Lira SA, Mehrad B. Neutrophils regulate airway responses in a model of fungal allergic airway disease. *The Journal of Immunology* 2012; **176**:2538–2545.

18. Nakagome K, Matsushita S, Nagata M. Neutrophilic inflammation in severe asthma. *International Archives of Allergy and Immunology* 2012; **158**:96–102.

19. Galli SJ, Tsai M, Piliponsky AM. The development of allergic inflammation. *Nature* 2008; **454**:445–454.

20. Foster PS, Mould AW, Yang M, Mackenzie J, Mattes J, Hogan SP, et al. Elemental signals regulating eosinophil accumulation in the lung. *Immunological Reviews* 2001; **179**:173–181.

21. Parronchi P, De Carli M, Manetti R, Simonelli C, Sampognaro S, Piccinni MP, et al. IL-4 and IFN-(α and γ) exert opposite regulatory effects on the development of cytolytic potential by Th1 or Th2 human T-cell clones. *Journal of Immunology* 1992; **149**:2977–2983.

22. Maggi E, Parronchi P, Manetti R, Simonelli C, Piccinni MP, Rugiu FS, et al. Reciprocal regulatory effects of IFN-γ and IL-4 on the in vitro development of human Th1 and Th2 clones. *Journal of Immunology* 1992; **148**:2142–2147.

23. Louahed J, Toda M, Jen J, Hamid Q, Renauld JC, Levitt RC, et al. Interleukin-9 upregulates mucus expression in the airways. *American Journal of Respiratory Cell and Molecular Biology* 2000; **22**:649–656.

24. Kuperman DA, Huang X, Koth LL, Chang GH, Dolganov GM, Zhu Z, et al. Direct effects of interleukin-13 on epithelial cells cause airway hyperreactivity and mucus overproduction in asthma. *Nature Medicine* 2002; **8**:885–889.

25. Busse W, Elias J, Sheppard D, Banks-Schlegel S. Airway remodeling and repair. *American Journal of Respiratory and Critical Care Medicine* 1999; **160**:1035–1042.

26. D'Amato G. Role of anti-IgE monoclonal antibody (omalizumab) in the treatment of bronchial asthma and allergic respiratory diseases. *European Journal of Pharmacology* 2006; **533**:302–307.

27. Taylor A, Verhagen J, Akdis CA, Akdis M. T regulatory cells and allergy. *Microbes and Infection* 2005; **7**:1049–1055.

28. Xu W, Lan Q, Chen M, Chen H, Zhu N, Zhou X, et al. Adoptive transfer of induced-Treg cells effectively attenuates murine airway allergic inflammation. *PloS One* 2012; **7**:e40314.

29.   Akdis M, Blaser K, Akdis CA. T regulatory cells in allergy: novel concepts in the patho-genesis, prevention, and treatment of allergic diseases. *The Journal of Allergy and Clinical Immunology* 2005; **116**:961–968.

30.   Medzhitov R, Shevach EM, Trinchieri G, Mellor AL, Munn DH, Gordon S, et al. High-lights of 10 years of immunology in *Nature Reviews Immunology*. *Nature Reviews Immu-nology* 2011; **11**:693–702.

31.   Riedler J, Braun-Fahrländer C, Eder W, Schreuer M, Waser M, Maisch S, et al. Exposure to farming in early life and development of asthma and allergy: a cross-sectional survey. *Lancet* 2001; **358**:1129–1133.

32.   Braun-Fahrländer C, Gassner M, Grize L, Neu U, Sennhauser FH, Varonier HS, et al. Prevalence of hay fever and allergic sensitization in farmer's children and their peers liv-ing in the same rural community. *Clinical and Experimental Allergy* 1999; **29**:28–34.

33.   Adler A, Tager I, Quintero DR. Decreased prevalence of asthma among farm-reared chil-dren compared with those who are rural but not farm-reared. *The Journal of Allergy and Cinical Immunology* 2005; **115**:67–73.

34.   Downs SH, Marks GB, Mitakakis TZ, Lëuppi JD, Car NG, Peat JK. Having lived on a farm and protection against allergic diseases in Australia. *Clinical and Experimental Al-lergy* 2001; **31**:570–575.

35.   Douwes J, Travier N, Huang K, Cheng S, McKenzie J, Le Gros G, et al. Lifelong farm exposure may strongly reduce the risk of asthma in adults. *Allergy* 2007; **62**:1158–1165.

36.   Dimich-Ward H, Chow Y, Chung J, Trask C. Contact with livestock–a protective effect against allergies and asthma□? *Clinical and Experimental Allergy* 2006; **36**:1122–1129.

37.   Strachan DP. Hay fever, hygiene, and household size. *British Medicine Journal* 1989; **299**:1259–1260.

38.   Strachan DP. Family size, infection and atopy: the first decade of the "hygiene hypothe-sis". *Thorax* 2000; **55**:S2–S10.

39.   Holbreich M, Genuneit J, Weber J, Braun-Fahrlaender C, Waser M, von Mutius E. Amish children living in northern Indiana have a very low prevalence of allergic sensitization. *The Journal of Allergy and Cinical Immunology* 2012; **129**:1671–1673.

40.   Braun-Fahrländer C, Riedler J, Herz U, Eder W, Waser M, Grize L, et al. Environmental exposure to endotoxin and its relation to asthma in school-age children. *The New England Journal of Medicine* 2002; **347**:869–877.

41.   Liu AH. Endotoxin exposure in allergy and asthma: reconciling a paradox. *Journal of Al-lergy and Clinical Immunology* 2002; **109**:379–392.

42.   Tulić MK, Knight DA, Holt PG, Sly PD. Lipopolysaccharide inhibits the late-phase re-sponse to allergen by altering nitric oxide synthase activity and interleukin-10. *American Journal of Respiratory Cell and Molecular Biology* 2001; **24**:640–646.

43. Peters M, Kauth M, Schwarze J, Körner-Rettberg C, Riedler J, Nowak D, et al. Inhalation of stable dust extract prevents allergen induced airway inflammation and hyperresponsiveness. *Thorax* 2006; **61**:134–139.

44. Gorelik L, Kauth M, Gehlhar K, Bufe A, Holst O, Peters M. Modulation of dendritic cell function by cowshed dust extract. *Innate Immunity* 2008; **14**:345–355.

45. Peters M, Kauth M, Scherner O, Gehlhar K, Steffen I, Wentker P, et al. Arabinogalactan isolated from cowshed dust extract protects mice from allergic airway inflammation and sensitization. *The Journal of Allergy and Cinical Immunology* 2010; **126**:648–656.

46. Debarry J, Garn H, Hanuszkiewicz A, Dickgreber N, Blümer N, von Mutius E, et al. *Acinetobacter lwoffii* and *Lactococcus lactis* strains isolated from farm cowsheds possess strong allergy-protective properties. *The Journal of Allergy and Cinical Immunology* 2007; **119**:1514–1521.

47. Debarry J, Hanuszkiewicz A, Stein K, Holst O, Heine H. The allergy-protective properties of *Acinetobacter lwoffii* F78 are imparted by its lipopolysaccharide. *Allergy* 2010; **65**:690–697.

48. Von Ehrenstein OS, Von Mutius E, Illi S, Baumann L, Böhm O, von Kries R. Reduced risk of hay fever and asthma among children of farmers. *Clinical and Experimental Allergy* 2000; **30**:187–193.

49. Ege MJ, Frei R, Bieli C, Schram-Bijkerk D, Waser M, Benz MR, et al. Not all farming environments protect against the development of asthma and wheeze in children. *The Journal of Allergy and Cinical Immunology* 2007; **119**:1140–1147.

50. Karadag B, Ege MJ, Scheynius A, Waser M, Schram-Bijkerk D, van Hage M, et al. Environmental determinants of atopic eczema phenotypes in relation to asthma and atopic sensitization. *Allergy* 2007; **62**:1387–1393.

51. van Strien RT, Engel R, Holst O, Bufe A, Eder W, Waser M, et al. Microbial exposure of rural school children, as assessed by levels of *N*-acetyl-muramic acid in mattress dust, and its association with respiratory health. *The Journal of Allergy and Cinical Immunology* 2004; **113**:860–867.

52. Heederik D, von Mutius E. Does diversity of environmental microbial exposure matter for the occurrence of allergy and asthma? *The Journal of Allergy and Cinical Immunology* 2012; **130**:44–50.

53. Perkin MR, Strachan DP. Which aspects of the farming lifestyle explain the inverse association with childhood allergy? *The Journal of Allergy and Cinical Immunology* 2006; **117**:1374–1381.

54. Waser M, Michels KB, Bieli C, Flöistrup H, Pershagen G, von Mutius E, et al. Inverse association of farm milk consumption with asthma and allergy in rural and suburban populations across Europe. *Clinical and Experimental Allergy* 2007; **37**:661–670.

55. Macpherson AJ, Harris NL. Interactions between commensal intestinal bacteria and the immune system. *Nature Reviews Immunology* 2004; **4**:478–485.

56. Rastall RA. Bacteria in the gut: friends and foes and how to alter the balance. *The Journal of Nutrition* 2004; **134**:2022S–2026S.

57. Noverr MC, Noggle RM, Toews GB, Huffnagle GB. Role of antibiotics and fungal microbiota in driving pulmonary allergic responses. *Infection and Immunity* 2004; **72**:4996–5003.

58. Karadag B, Ege M, Bradley JE, Braun-Fahrländer C, Riedler J, Nowak D, et al. The role of parasitic infections in atopic diseases in rural schoolchildren. *Allergy* 2006; **61**:996–1001.

59. Yang J, Zhao J, Yang Y, Zhang L, Yang X, Zhu X, et al. *Schistosoma japonicum* egg antigens stimulate CD4+ CD25+ T cells and modulate airway inflammation in a murine model of asthma. *Immunology* 2007; **120**:8–18.

60. Pacifico LGG, Marinho FAV, Fonseca CT, Barsante MM, Pinho V, Sales-Junior PA, et al. *Schistosoma mansoni* antigens modulate experimental allergic asthma in a murine model: a major role for CD4+ CD25+ Foxp3+ T cells independent of interleukin-10. *Infection and Immunity* 2009; **77**:98–107.

61. Daniłowicz-Luebert E, O'Regan NL, Steinfelder S, Hartmann S. Modulation of specific and allergy-related immune responses by helminths. *Journal of Biomedicine & Biotechnology* 2011; **2011**:1–18.

62. Kraft M. Asthma. *Seminars in Respiratory and Critical Care Medicine*. 2002; **23**:315–316.

63. Park SJ, Lee YC, Rhee YK, Lee HB. Seroprevalence of *Mycoplasma pneumoniae* and *Chlamydia pneumoniae* in stable asthma and chronic obstructive pulmonary disease. *Journal of Korean Medical Science* 2005; **20**:225–228.

64. Yasuda H, Suzuki T, Zayasu K, Ishizuka S, Kubo H, Sasaki T, et al. Inflammatory and bronchospastic factors in asthma exacerbations caused by upper respiratory tract infections. *The Tohoku Journal of Experimental Medicine* 2005; **207**:109–118.

65. Fishbein AB, Fuleihan RL. The hygiene hypothesis: does exposure to infectious agents protect us from allergy? *Current Opinion in Pediatrics* 2012; **24**:98–102.

66. Shirakawa T, Enomoto T, Shimazu SI, Hopkin JM. The inverse association between tuberculin responses and atopic disorder. *Science* 1997; **275**:77–79.

67. Arnoldussen DL, Linehan M, Sheikh A. BCG vaccination and allergy: a systematic review and meta-analysis. *The Journal of Allergy and Cinical Immunology* 2011; **127**:246–253.

68. Silverberg JI, Norowitz KB, Kleiman E, Silverberg NB, Durkin HG, Joks R, et al. Association between varicella zoster virus infection and atopic dermatitis in early and late childhood: a case-control study. *The Journal of Allergy and Cinical Immunology* 2010; **126**:300–305.

69. Rook GAW. *The hygiene hypothesis and Darwinian medicine.* Basel, Boston, Berlin: Birkhäuser Verlag AG 2009.

70. Vogel K, Blümer N, Korthals M, Mittelstädt J, Garn H, Ege M, et al. Animal shed *Bacillus licheniformis* spores possess allergy-protective as well as inflammatory properties. *The Journal of Allergy and Cinical Immunology* 2008; **122**:307–312.

71. Conrad ML, Ferstl R, Teich R, Brand S, Blümer N, Yildirim AO, et al. Maternal TLR signaling is required for prenatal asthma protection by the nonpathogenic microbe *Acinetobacter lwoffii* F78. *The Journal of Experimental Medicine* 2009; **206**:2869–2877.

72. Medzhitov R, Janeway CA Jr. Innate immunity: impact on the adaptive immune response. *Current Opinion in Immunology* 1997; **9**:4–9.

73. Janeway CA Jr, Medzhitov R. Innate immune recognition. *Annual Review of Immunology* 2002; **20**:197–216.

74. Fraser IP, Koziel H, Ezekowitz RAB. The serum mannose-binding protein and the macrophage mannose receptor are pattern recognition molecules that link innate and adaptive immunity. *Seminars in Immunology* 1998; **10**:363–372.

75. Wiesner J, Vilcinskas A. Antimicrobial peptides. The ancient arm of the human immune system. *Virulence* 2010; **1**:440–464.

76. Lemaitre B, Nicolas E, Michaut L, Reichhart JM, Hoffmann JA. The dorsoventral regulatory gene cassette *spätzle/Toll/cactus* controls the potent antifungal response in *Drosophila* adults. *Cell* 1996; **86**:973–983.

77. Diacovich L, Gorvel JP. Bacterial manipulation of innate immunity to promote infection. *Nature Reviews Microbiology* 2010; **8**:117–128.

78. Morr M, Takeuchi O, Akira S, Simon MM, Mühlradt PF. Differential recognition of structural details of bacterial lipopeptides by Toll-like receptors. *European Journal of Immunology* 2002; **32**:3337–3347.

79. Takeuchi O, Kawai T, Mühlradt PF, Morr M, Radolf JD, Zychlinsky A, et al. Discrimination of bacterial lipoproteins by Toll-like receptor 6. *International Immunology* 2001; **13**:933–940.

80. Zähringer U, Lindner B, Inamura S, Heine H, Alexander C. TLR2–promiscuous or specific? A critical re-evaluation of a receptor expressing apparent broad specificity. *Immunobiology* 2008; **213**:205–224.

81. Schmidt RR, Pedersen CM, Qiao Y, Zähringer U. Chemical synthesis of bacterial lipoteichoic acids: an insight on its biological significance. *Organic & Biomolecular Chemistry* 2011; **9**:2040–2052.

82. Travassos LH, Girardin SE, Philpott DJ, Blanot D, Nahori MA, Werts C, et al. Toll-like receptor 2-dependent bacterial sensing does not occur via peptidoglycan recognition. *EMBO Reports* 2004; **5**:1000–1006.

83. Li H, Nooh MM, Kotb M, Re F. Commercial peptidoglycan preparations are contaminated with superantigen-like activity that stimulates IL-17 production. *Journal of Leukocyte Biology* 2008; **83**:409–418.

84. da Silva Correia J, Soldau K, Christen U, Tobias PS, Ulevitch RJ. Lipopolysaccharide is in close proximity to each of the proteins in its membrane receptor complex. *The Journal of Biological Chemistry* 2001; **276**:21129–21135.

85. Smith KD, Andersen-Nissen E, Hayashi F, Strobe K, Bergman MA, Barrett SLR, et al. Toll-like receptor 5 recognizes a conserved site on flagellin required for protofilament formation and bacterial motility. *Nature Immunology* 2003; **4**:1247–1253.

86. Medzhitov R, Janeway CA Jr. The Toll receptor family and microbial recognition. *Trends in Microbiology* 2000; **8**:452–456.

87. Medzhitov R. Toll-like receptors and innate immunity. *Nature Reviews Immunology* 2001; **1**:135–145.

88. Trinchieri G, Sher A. Cooperation of Toll-like receptor signals in innate immune defence. *Nature Reviews Immunology* 2007; **7**:179–190.

89. Blander JM, Medzhitov R. Toll-dependent selection of microbial antigens for presentation by dendritic cells. *Nature* 2006; **440**:808–812.

90. Martinon F, Tschopp J. NLRs join TLRs as innate sensors of pathogens. *Trends in Immunology* 2005; **26**:447–454.

91. Inohara N, Nuñez G. The NOD: a signaling module that regulates apoptosis and host defense against pathogens. *Oncogene* 2001; **20**:6473–6481.

92. Kanneganti TD, Lamkanfi M, Núñez G. Intracellular NOD-like receptors in host defense and disease. *Immunity* 2007; **27**:549–559.

93. Inohara, Chamaillard, McDonald C, Nuñez G. NOD-LRR proteins: role in host-microbial interactions and inflammatory disease. *Annual Review of Biochemistry* 2005; **74**:355–383.

94. Chamaillard M, Hashimoto M, Horie Y, Masumoto J, Qiu S, Saab L, et al. An essential role for NOD1 in host recognition of bacterial peptidoglycan containing diaminopimelic acid. *Nature Immunology* 2003; **4**:702–707.

95. Inohara N, Ogura Y, Fontalba A, Gutierrez O, Pons F, Crespo J, et al. Host recognition of bacterial muramyl dipeptide mediated through NOD2. Implications for Crohn's disease. *The Journal of Biological Chemistry* 2003; **278**:5509–5112.

96. Fritz JH, Girardin SE, Fitting C, Werts C, Mengin-Lecreulx D, Caroff M, et al. Synergistic stimulation of human monocytes and dendritic cells by Toll-like receptor 4 and NOD1- and NOD2-activating agonists. *European Journal of Immunology* 2005; **35**:2459–2470.

97. Correa RG, Milutinovic S, Reed JR. Roles of NOD1 (NLRC1) and NOD2 (NLRC2) in innate immunity and inflammatory diseases. *Bioscience Reports* 2012; **in press**. doi:10.1042/BSR20120055.

98. Janeway CA Jr, Bottomly K. Signals and signs for lymphocyte responses. *Cell* 1994; **76**:275–285.

99. Kapsenberg ML. Dendritic-cell control of pathogen-driven T-cell polarization. *Nature Reviews Immunology* 2003; **3**:984–993.

100. Killeen N, Irving BA, Pippig S, Zingier K. Signaling checkpoints during the development of T lymphocytes. *Current Opinion in Immunology* 1998; **10**:360–367.

101. Swain SL. Helper T cell differentiation. *Current Opinion in Immunology* 1999; **11**:180–185.

102. Hsieh C, Macatonia SE, Tripp CS, Wolf SF, Garra AO, Murphy KM. Development of TH1 CD4+ T cells through IL-12 produced by *Listeria*-induced macrophages. *Science* 1993; **260**:547–549.

103. Underhill DM, Bassetti M, Rudensky A, Aderem A. Dynamic interactions of macrophages with T cells during antigen presentation. *The Journal of Experimental Medicine* 1999; **190**:1909–1914.

104. Krug A, Veeraswamy R, Pekosz A, Kanagawa O, Unanue ER, Colonna M, et al. Interferon-producing cells fail to induce proliferation of naive T cells but can promote expansion and T helper 1 differentiation of antigen-experienced unpolarized T cells. *The Journal of Experimental Medicine* 2003; **197**:899–906.

105. Casbon AJ, Long ME, Dunn KW, Allen LAH, Dinauer MC. Effects of IFN-γ on intracellular trafficking and activity of macrophage NADPH oxidase flavocyto-chrome b558. *Journal of Leukocyte Biology* 2012; **92**:1–14.

106. Suda T, Suda J, Ogawa M, Ihle JN. Permissive role of interleukin 3 (IL-3) in proliferation and differentiation of multipotential hemopoietic progenitors in culture. *Journal of Cellular Physiology* 1985; **124**:182–190.

107. Bowen H, Kelly A, Lee T, Lavender P. Control of cytokine gene transcription in Th1 and Th2 cells. *Clinical and Experimental Allergy* 2008; **38**:1422–1431.

108. Schmitt E, Van Brandwijk R, Fischer HG, Rüde E. Establishment of different T cell sublines using either interleukin 2 or interleukin 4 as growth factors. *European Journal of Immunology* 1990; **20**:1709–1715.

109. Nakanishi K. Basophils as APC in Th2 response in allergic inflammation and parasite infection. *Current Opinion in Immunology* 2010; **22**:814–820.

110. Hymowitz SG, Filvaroff EH, Yin JP, Lee J, Cai L, Risser P, et al. IL-17s adopt a cystine knot fold: structure and activity of a novel cytokine, IL-17F, and implications for receptor binding. *The EMBO Journal* 2001; **20**:5332–5341.

111. Annunziato F, Cosmi L, Liotta F, Maggi E, Romagnani S. The phenotype of human Th17 cells and their precursors, the cytokines that mediate their differentiation and the role of Th17 cells in inflammation. *International Immunology* 2008; **20**:1361–1368.

112. Sakaguchi S. Naturally arising Foxp3-expressing CD25+CD4+ regulatory T cells in immunological tolerance to self and non-self. *Nature Immunology* 2005; **6**:345–352.

113. Sakaguchi S, Ono M, Setoguchi R, Yagi H, Hori S, Fehervari Z, et al. Foxp3+DC25+CD4+ natural regulatory T cells in dominant self-tolerance and autoimmune disease. *Immunological Reviews* 2006; **212**:8–27.

114. Sykes L, Macintyre DA, Yap XJ, Teoh TG, Bennett PR. The Th1:Th2 dichotomy of pregnancy and preterm labour. *Mediators of Inflammation* 2012; **2012**:1–12.

115. Bach JF. The effect of infections on susceptibility to autoimmune and allergic diseases. *New England Journal of Medicine* 2002; **347**:911–920.

116. Abrahamsson TR, Sandberg Abelius M, Forsberg A, Björkstén B, Jenmalm MC. A Th1/Th2-associated chemokine imbalance during infancy in children developing eczema, wheeze and sensitization. *Clinical and Experimental Allergy* 2011; **41**:1729–1739.

117. Holt P. Developmental factors associated with risk for atopic disease: implications for vaccine strategies in early childhood. *Vaccine* 2003; **21**:3432–3435.

118. Wills-Karp M, Santeliz J, Karp CL. The germless theory of allergic disease: revisiting the hygiene hypothesis. *Nature Reviews Immunology* 2001; **69**:69–75.

119. Pfefferle PI, Büchele G, Blümer N, Roponen M, Ege MJ, Krauss-Etschmann S, et al. Cord blood cytokines are modulated by maternal farming activities and consumption of farm dairy products during pregnancy: the PASTURE study. *The Journal of Allergy and Cinical Immunology* 2010; **125**:108–115.

120. von Mutius E, Schmid S. The PASTURE project: EU support for the improvement of knowledge about risk factors and preventive factors for atopy in Europe. *Allergy* 2006; **61**:407–413.

121. Brand S, Teich R, Dicke T, Harb H, Yildirim AÖ, Tost J, et al. Epigenetic regulation in murine offspring as a novel mechanism for transmaternal asthma protection induced by microbes. *The Journal of Allergy and Cinical Immunology* 2011; **128**:618–625.

122. Renz H, Autenrieth IB, Brandtzæg P, Cookson WO, Holgate S, von Mutius E, et al. Gene-environment interaction in chronic disease: a European science foundation forward look. *The Journal of Allergy and Cinical Immunology* 2011; **128**:S27–S49.

123. Ege MJ, Bieli C, Frei R, van Strien RT, Riedler J, Ublagger E, et al. Prenatal farm exposure is related to the expression of receptors of the innate immunity and to atopic sensitization in school-age children. *The Journal of Allergy and Cinical Immunology* 2006; **117**:817–823.

124. Eder W, Klimecki W, Yu L, von Mutius E, Riedler J, Braun-Fahrländer C, et al. Toll-like receptor 2 as a major gene for asthma in children of European farmers. *The Journal of Allergy and Cinical Immunology* 2004; **113**:482–488.

125. Schaub B, Liu J, Höppler S, Haug S, Sattler C, Lluis A, et al. Impairment of T-regulatory cells in cord blood of atopic mothers. *The Journal of Allergy and Cinical Immunology* 2008; **121**:1491–1499.

126. Schaub B, Liu J, Höppler S, Schleich I, Huehn J, Olek S, et al. Maternal farm exposure modulates neonatal immune mechanisms through regulatory T cells. *The Journal of Allergy and Cinical Immunology* 2009; **123**:774–782.

127. von Mutius E, Vercelli D. Farm living: effects on childhood asthma and allergy. *Nature Reviews Immunology* 2010; **10**:861–868.

128. Pfefferle PI, Sel S, Ege MJ, Büchele G, Blümer N, Krauss-Etschmann S, et al. Cord blood allergen-specific IgE is associated with reduced IFN-γ production by cord blood cells: the protection against allergy-study in rural environments (PASTURE) study. *The Journal of Allergy and Cinical Immunology* 2008; **122**:711–716.

129. Stern DA, Riedler J, Nowak D, Braun-Fahrländer C, Swoboda I, Balic N, et al. Exposure to a farming environment has allergen-specific protective effects on TH2-dependent isotype switching in response to common inhalants. *The Journal of Allergy and Cinical Immunology* 2007; **119**:351–358.

130. Holgate ST. Innate and adaptive immune responses in asthma. *Nature Medicine* 2012; **18**:673–683.

131. Seltmann G, Holst O. *The bacterial cell wall.* Berlin, Heidelberg, New York: Springer-Verlag 2002.

132. Delcour J, Ferain T, Deghorain M, Palumbo E, Hols P. The biosynthesis and functionality of the cell-wall of lactic acid bacteria. *Antonie van Leeuwenhoek* 1999; **76**:159–184.

133. Royet J, Dziarski R. Peptidoglycan recognition proteins: pleiotropic sensors and effectors of antimicrobial defences. *Nature Reviews Microbiology* 2007; **5**:264–277.

134. Girardin SE, Boneca IG, Carneiro LAM, Antignac A, Jéhanno M, Viala J, et al. Nod1 detects a unique muropeptide from gram-negative bacterial peptidoglycan. *Science* 2003; **300**:1584–1587.

135. Kusumoto S, Fukase K, Shiba T. Key structures of bacterial peptidoglycan and lipopoly-saccharide triggering the innate immune system of higher animals: chemical synthesis and functional studies. *Proceedings of the Japan Academy, Series B* 2010; **86**:322–337.

136. Fujimoto Y, Fukase K. Structures, synthesis, and human Nod1 stimulation of immunostimulatory bacterial peptidoglycan fragments in the environment. *Journal of Natural Products* 2011; **74**:518–525.

137. Pradipta AR, Fujimoto Y, Hasegawa M, Inohara N, Fukase K. Characterization of natural human nucleotide-binding oligomerization domain protein 1 (Nod1) ligands from bacterial culture supernatant for elucidation of immune modulators in the environment. *The Journal of Biological Chemistry* 2010; **285**:23607–23613.

138. Nadesalingam J, Dodds AW, Reid KBM, Palaniyar N. Mannose-binding lectin recognizes peptidoglycan via the *N*-acetyl glucosamine moiety, and inhibits ligand-induced proinflammatory effect and promotes chemokine production by macrophages. *The Journal of Immunology* 2005; **175**:1785–1794.

139. Coyette J, Ghuysen J. Structure of the walls of *Lactobacillus acidophilus* strain 63 AM Gasser. *Biochemistry* 1970; **9**:2935–2943.

140. Swoboda JG, Campbell J, Meredith TC, Walker S. Wall teichoic acid function, biosynthesis, and inhibition. *Chembiochem* 2010; **11**:35–45.

141. Armstrong JJ, Baddiley J, Buchanan JG, Carss B, Greenberg GR. Isolation and structure of ribitol phosphate derivatives (teichoic acids) from bacterial cell walls. *Journal of the Chemical Society* 1958; **1958**:4344–4354.

142.   Neuhaus FC, Baddiley J. A continuum of anionic charge: structures and functions of D-alanyl-teichoic acids in Gram-positive bacteria. *Microbiology and Molecular Biology Reviews* 2003; **67**:686–723.

143.   Fischer W, Mannsfeld T, Hagen G. On the basic structure of poly(glycero-phosphate) lipoteichoic acids. *Biochemistry and Cell Biology* 1990; **68**:33–43.

144.   Iwasaki H, Shimada A, Ito E. Comparative studies of lipoteichoic acids from several *Bacillus* strains. *Journal of Bacteriology* 1986; **167**:508–516.

145.   Oku Y, Kurokawa K, Matsuo M, Yamada S, Lee BL, Sekimizu K. Pleiotropic roles of polyglycerolphosphate synthase of lipoteichoic acid in growth of *Staphylococcus aureus* cells. *Journal of Bacteriology* 2009; **191**:141–151.

146.   Xia G, Maier L, Sànchez-Carballo P, Li M, Otto M, Holst O, et al. Glycosylation of wall teichoic acid in *Staphylococcus aureus* by tarM. *The Journal of Biological Chemistry* 2010; **285**:13405–13415.

147.   Kohler T, Weidenmaier C, Peschel A. Wall teichoic acid protects *Staphylococcus aureus* against antimicrobial fatty acids from human skin. *Journal of Bacteriology* 2009; **191**:4482–4484.

148.   Hughes AH, Hancock IC, Baddiley J. The function of teichoic acids in cation control in bacterial membranes. *The Biochemical Journal* 1973; **132**:83–93.

149.   van Wely KH, Swaving J, Freudl R, Driessen AJ. Translocation of proteins across the cell envelope of Gram-positive bacteria. *FEMS Microbiology Reviews* 2001; **25**:437–454.

150.   Bera A, Biswas R, Herbert S, Kulauzovic E, Weidenmaier C, Peschel A, et al. Influence of wall teichoic acid on lysozyme resistance in *Staphylococcus aureus*. *Journal of Bacteriology* 2007; **189**:280–283.

151.   Peschel A, Vuong C, Otto M, Götz F. The D-alanine residues of *Staphylococcus aureus* teichoic acids alter the susceptibility to vancomycin and the activity of autolytic enzymes. *Antimicrobial Agents and Chemotherapy* 2000; **44**:2845–2847.

152.   Weidenmaier C, Peschel A. Teichoic acids and related cell-wall glycopolymers in Gram-positive physiology and host interactions. *Nature Reviews Microbiology* 2008; **6**:276–287.

153.   Bychowska A, Theilacker C, Czerwicka M, Marszewska K, Huebner J, Holst O, et al. Chemical structure of wall teichoic acid isolated from *Enterococcus faecium* strain U0317. *Carbohydrate Research* 2011; **346**:2816–2819.

154.   Weidenmaier C, Kokai-Kun JF, Kristian SA, Chanturiya T, Kalbacher H, Gross M, et al. Role of teichoic acids in *Staphylococcus aureus* nasal colonization, a major risk factor in nosocomial infections. *Nature Medicine* 2004; **10**:243–245.

155.   Sadovskaya I, Vinogradov E, Li J, Jabbouri S. Structural elucidation of the extracellular and cell-wall teichoic acids of *Staphylococcus epidermidis* RP62A, a reference biofilm-positive strain. *Carbohydrate Research* 2004; **339**:1467–1473.

156. Vinogradov E, Sadovskaya I, Li J, Jabbouri S. Structural elucidation of the extracellular and cell-wall teichoic acids of *Staphylococcus aureus* MN8m, a biofilm forming strain. *Carbohydrate Research* 2006; **341**:738–743.

157. Markham JL, Knox KW, Schamschula RG. Antibodies to teichoic acids in man. *Archives of Oral Biology* 1973; **18**:313–319.

158. Wergeland HI, Haaheim LR, Wesenberg F. Antibodies to staphylococcal peptidoglycan and its peptide epitopes, teichoic acid, and lipoteichoic acid in sera from blood donors and patients with staphylococcal infections. *Journal of Clinical Microbiology* 1989; **27**:1286–1291.

159. Kim HG, Gim MG, Kim JY, Hwang HJ, Ham MS, Lee JM, et al. Lipoteichoic acid from *Lactobacillus plantarum* elicits both the production of interleukin-23p19 and suppression of pathogen-mediated interleukin-10 in THP-1 cells. *FEMS Immunology and Medical Microbiology* 2007; **49**:205–214.

160. Bucki R, Byfield FJ, Kulakowska A, McCormick ME, Drozdowski W, Namiot Z, et al. Extracellular gelsolin binds lipoteichoic acid and modulates cellular response to proinflammatory bacterial wall components. *Journal of Immunology* 2008; **181**:4936–4944.

161. Draing C, Pfitzenmaier M, Zummo S, Mancuso G, Geyer A, Hartung T, et al. Comparison of lipoteichoic acid from different serotypes of *Streptococcus pneumoniae*. *The Journal of Biological Chemistry* 2006; **281**:33849–33859.

162. Jones KJ, Perris AD, Vernallis AB, Worthington T, Lambert PA, Elliott TSJ. Induction of inflammatory cytokines and nitric oxide in J774.2 cells and murine macrophages by lipoteichoic acid and related cell wall antigens from *Staphylococcus epidermidis*. *Journal of Medical Microbiology* 2005; **54**:315–321.

163. Hirose Y, Murosaki S, Fujiki T, Yamamoto Y, Yoshikai Y, Yamashita M. Lipoteichoic acids on *Lactobacillus plantarum* cell surfaces correlate with induction of interleukin-12p40 production. *Microbiology and Immunology* 2010; **54**:143–151.

164. Theilacker C, Kaczynski Z, Kropec A, Fabretti F, Sange T, Holst O, et al. Opsonic antibodies to *Enterococcus faecalis* strain 12030 are directed against lipoteichoic acid. *Infection and Immunity* 2006; **74**:5703–5712.

165. Theilacker C, Kaczyński Z, Kropec A, Sava I, Ye L, Bychowska A, et al. Serodiversity of opsonic antibodies against *Enterococcus faecalis*–glycans of the cell wall revisited. *PloS One* 2011; **6**:e17839.

166. Schwandner R, Dziarski R, Wesche H, Rothe M, Kirschning CJ. Peptidoglycan- and lipoteichoic acid-induced cell activation is mediated by Toll-like receptor 2. *The Journal of Biological Chemistry* 1999; **274**:17406–17409.

167. Kimbrell MR, Warshakoon H, Cromer JR, Malladi S, Hood JD, Balakrishna R, et al. Comparison of the immunostimulatory activities of candidate Gram-positive endotoxins, lipoteichoic acid, peptidoglycan, and lipopeptides in murine and human cells. *Immunology Letters* 2008; **118**:132–141.

168. Morath S, von Aulock S, Hartung T. Structure/function relationships of lipoteichoic acids. *Journal of Endotoxin Research* 2005; **11**:348–356.

169. Gillrie MR, Zbytnuik L, McAvoy E, Kapadia R, Lee K, Waterhouse CCM, et al. Divergent roles of Toll-like receptor 2 in response to lipoteichoic acid and *Staphylococcus aureus in vivo*. *European Journal of Immunology* 2010; **40**:1639–1650.

170. Takeuchi O, Hoshino K, Kawai T, Sanjo H, Takada H, Ogawa T, et al. Differential roles of TLR2 and TLR4 in recognition of Gram-negative and Gram-positive bacterial cell wall components. *Immunity* 1999; **11**:443–451.

171. Pedersen CM, Figueroa-Perez I, Lindner B, Ulmer AJ, Zähringer U, Schmidt RR. Total synthesis of lipoteichoic acid of *Streptococcus pneumoniae*. *Angewandte Chemie* 2010; **49**:2585–2590.

172. Hashimoto M, Furuyashiki M, Kaseya R, Fukada Y, Akimaru M, Aoyama K, et al. Evidence of immunostimulating lipoprotein existing in the natural lipoteichoic acid fraction. *Infection and Immunity* 2007; **75**:1926–1932.

173. Hashimoto M, Yasuoka J, Suda Y, Takada H, Yoshida T, Kotani S, et al. Structural feature of the major but not cytokine-inducing molecular species of lipoteichoic acid. *Journal of Biochemistry* 1997; **121**:779–786.

174. Qi HY, Sankaran K, Gan K, Wu HC. Structure-function relationship of bacterial prolipoprotein diacylglyceryl transferase: functionally significant conserved regions. *Journal of Bacteriology* 1995; **177**:6820–6824.

175. Zhang YM, Rock CO. Membrane lipid homeostasis in bacteria. *Nature Reviews Microbiology* 2008; **6**:222–233.

176. Bertram R, Schlicht M, Mahr K, Nothaft H, Saier MH Jr, Titgemeyer F. In silico and transcriptional analysis of carbohydrate uptake systems of *Streptomyces coelicolor* A3(2). *Journal of Bacteriology* 2004; **186**:1362–1373.

177. Hutchings MI, Palmer T, Harrington DJ, and Sutcliffe IC. Lipoprotein biogenesis in Gram-positive bacteria: knowing when to hold 'em, knowing when to fold 'em. *Trends in Microbiology* 2009; **17**:13–21.

178. Nielsen JB, Lampen JO. Glyceride-cysteine lipoproteins and secretion by Gram-positive bacteria. *Journal of Bacteriology* 1982; **152**:315–322.

179. Thompson BJ, Widdick DA, Hicks MG, Chandra G, Sutcliffe IC, Palmer T, et al. Investigating lipoprotein biogenesis and function in the model Gram-positive bacterium *Streptomyces coelicolor*. *Molecular Microbiology* 2010; **77**:943–957.

180. Hantke K, Braun V. Covalent binding of lipid to protein. *European Journal of Biochemistry* 1973; **34**:284–296.

181. Mizushima S. Post-translational modification and processing of outer membrane prolipoproteins in *Escherichia coli*. *Molecular and Cellular Biochemistry* 1984; **60**:5–15.

182. Rahman O, Dover LG, Sutcliffe IC. Lipoteichoic acid biosynthesis: two steps forwards, one step sideways? *Trends in Microbiology* 2009; **17**:219–225.

183. Robichon C, Vidal-Ingigliardi D, Pugsley AP. Depletion of apolipoprotein *N*-acyltransferase causes mislocalization of outer membrane lipoproteins in *Escherichia coli*. *The Journal of biological chemistry* 2005; **280**:974–83.

184. Stoll H, Nerz C, Go F. *Staphylococcus aureus* deficient in lipidation of prelipoproteins is attenuated in growth and immune activation. *Infection and Immunity* 2005; **73**:2411–2423.

185. Leskelä S, Wahlström E, Kontinen VP, Sarvas M. Lipid modification of prelipoproteins is dispensable for growth but essential for efficient protein secretion in *Bacillus subtilis*: characterization of the *lgt* gene. *Molecular Microbiology* 1999; **31**:1075–1085.

186. Petit CM, Brown JR, Ingraham K, Bryant AP, Holmes DJ. Lipid modification of prelipoproteins is dispensable for growth in vitro but essential for virulence in *Streptococcus pneumoniae*. *FEMS Microbiology Letters* 2001; **200**:229–233.

187. Mühlradt BPF, Kieß M, Meyer H, Süßmuth R, Jung G. Isolation, structure elucidation, and synthesis of a macrophage stimulatory lipopeptide from *Mycoplasma fermentans* acting at picomolar concentration. *The Journal of Experimental Medicine* 1997; **185**:1951–1958.

188. Cronan JE, Gelmann EP. Physical properties of membrane lipids: biological relevance and regulation. *Microbiology and Molecular Biology Reviews* 1975; **39**:232–256.

189. Aguilar PS, Hernandez-Arriaga AM, Cybulski LE, Erazo AC, de Mendoza D. Molecular basis of thermosensing: a two-component signal transduction thermometer in *Bacillus subtilis*. *The EMBO journal* 2001; **20**:1681–1691.

190. Macouzet M, Lee BH, Robert N. Production of conjugated linoleic acid by probiotic *Lactobacillus acidophilus* La-5. *Journal of Applied Microbiology* 2009; **106**:1886–1891.

191. Wallace RJ, McKain N, Shingfield KJ, Devillard E. Isomers of conjugated linoleic acids are synthesized via different mechanisms in ruminal digesta and bacteria. *Journal of Lipid Research* 2007; **48**:2247–2254.

192. Lourenço M, Ramos-Morales E, Wallace RJ. The role of microbes in rumen lipolysis and biohydrogenation and their manipulation. *Animal* 2010; **4**:1008–1023.

193. Jaudszus A, Krokowski M, Möckel P, Darcan Y, Avagyan A, Matricardi P, et al. *Cis*-9,*trans*-11-conjugated linoleic acid inhibits allergic sensitization and airway inflammation via a PPARγ-related mechanism in mice. *The Journal of Nutrition* 2008; **138**:1336–1342.

194. Kanwar RK, Macgibbon AK, Black PN, Kanwar JR, Rowan A, Vale M, et al. Bovine milk fat enriched in conjugated linoleic and vaccenic acids attenuates allergic airway disease in mice. *Clinical and Experimental Allergy* 2008; **38**:208–218.

195. Nugent AP, Roche HM, Noone EJ, Long A, Kelleher DK, Gibney MJ. The effects of conjugated linoleic acid supplementation on immune function in healthy volunteers. *European Journal of Clinical Nutrition* 2005; **59**:742–750.

196. Hanuszkiewicz A. *Isolation and structural as well as immunological characterization of the cell wall components from cowshed bacteria.* 2008; 1–142.

http://www.students.informatik.uni-luebeck.de/zhb/ediss581.pdf

197. Birnboim HC, Doly J. A rapid alkaline extraction procedure for screening recombinant plasmid DNA. *Nucleic Acids Research* 1979; **7**:1513–1524.

198. de Jonge BL, Chang YS, Gage D, Tomasz A. Peptidoglycan composition of a highly methicillin-resistant *Staphylococcus aureus* strain. *The Journal of Biological Chemistry* 1992; **267**:11248–11254.

199. Morath S, Geyer A, Hartung T. Structure-function relationship of cytokine induction by lipoteichoic acid from *Staphylococcus aureus*. *The Journal of Experimental Medicine* 2001; **193**:393–397.

200. Sánchez-Carballo PM, Vilen H, Palva A, Holst O. Structural characterization of teichoic acids from *Lactobacillus brevis*. *Carbohydrate Research* 2010; **345**:538–542.

201. Rosenthal RS, Dziarski R. Isolation of peptidoglycan fragments and soluble peptidoglycan fragments. *Methods in Enzymology* 1994; **235**:253–285.

202. Dionisi F, Golay PA, Elli M, Fay LB. Stability of cyclopropane and conjugated linoleic acids during fatty acid quantification in lactic acid bacteria. *Lipids* 1999; **34**:1107–1115.

203. Sawardeker J, Sloneker J. Quantitative determination of monosaccharides as their alditol acetates by gas liquid chromatography. *Analytical Chemistry* 1965; **37**:1602–1603.

204. Gerwig GJ, Kamerling JP, Vliegenthart JF. Determination of the absolute configuration of monosaccharides in complex carbohydrates by capillary G.L.C. *Carbohydrate Research* 1979; **77**:10–17.

205. Ciucanu I, Kerek F. A simple and rapid method for the permethylation of carbohydrates. *Carbohydrate Research* 1984; **131**:209–217.

206. Chen PS, Toribara TY, Warner H. Microdetermination of phosphorus. *Analytical Chemistry* 1956; **28**:1756–1758.

207. Bidlingmeyer B, Cohen S, Tarvin T. Rapid analysis of amino acids using pre-column derivatization. *Journal of Chromatography* 1984; **336**:93–104.

208. Holst O. Deacylation of lipopolysaccharides and isolation of oligosaccharide phosphates. In: Holst O, ed. *Methods in Molecular Biology. Bacterial toxins: Methods and Protocols.* Totowa, USA: Humana Press Inc. 2000. 345–353.

209. Heine H, Gronow S, Zamyatina A, Kosma P, Brade H. Investigation on the agonistic and antagonistic biological activities of synthetic *Chlamydia* lipid A and its use in *in vitro* enzymatic assays. *Journal of Endotoxin Research* 2007; **13**:126–132.

210. Böyum A. Isolation of mononuclear cells and granulocytes from human blood. *Scandinavian Journal of Clinical and Laboratory Investigation* 1968; **21**:77–89.

211. Marmur J. A procedure for the isolation of deoxyribonucleic acid from micro-organisms. *Journal of Molecular Biology* 1961; **3**:208–218.

212. Dower WJ, Miller JF, Ragsdale CW. High efficiency transformation of *E. coli* by high voltage electroporation. *Nucleic Acids Research* 1988; **16**:6127–6145.

213. Sanger F, Nicklen S, Coulson AR. DNA sequencing with chain-terminating inhibitors. *Proceedings of the National Academy of Sciences USA* 1977; **74**:5463–5467.

214. Gerber SD, Solioz M. Efficient transformation of *Lactococcus lactis* IL1403 and generation of knock-out mutants by homologous recombination. *Journal of Basic Microbiology* 2007; **47**:281–286.

215. Powell IB, Achen MG, Hillier AJ, Davidson BE. A simple and rapid method for genetic transformation of lactic streptococci by electroporation. *Applied and Environmental Microbiology* 1988; **54**:655–660.

216. Group of Molecular Genetics (MolGen), Rijksuniversiteit Groningen (RUG). Technical manual 2000.

    www.molgenrug.nl/intranet/tm2000/tm2000.pdf.

217. Brückner R. Gene replacement in *Staphylococcus carnosus* and *Staphylococcus xylosus*. *FEMS Microbiology Letters* 1997; **151**:1–8.

218. Wells JM, Wilson PW, W LPRF. Improved cloning vectors and transformation procedure for *Lactococcus lactis*. *Journal of Applied Bacteriology* 1993; **74**:629–636.

219. Que Y, Haefliger J, Francioli P, Moreillon P. Expression of *Staphylococcus aureus* clumping factor A in *Lactococcus lactis* subsp. *cremoris* using a new shuttle vector. *Infection and Immunity* 2000; **68**:3516–3522.

220. Martin S, Rosenthal RS, Biemann K. Fast atom bombardment mass spectrometry and tandem mass spectrometry of biologically active peptidoglycan monomers from *Neisseria gonorrhoeae*. *The Journal of Biological Chemistry* 1987; **262**:7514–7522.

221. Courtin P, Miranda G, Guillot A, Wessner F, Mézange C, Domakova E, et al. Peptidoglycan structure analysis of *Lactococcus lactis* reveals the presence of an L,D-carboxypeptidase involved in peptidoglycan maturation. *Journal of Bacteriology* 2006; **188**:5293–5298.

222. Datsenko KA, Wanner BL. One-step inactivation of chromosomal genes in *Escherichia coli* K-12 using PCR products. *Proceedings of the National Academy of Sciences of the United States of America* 2000; **97**:6640–6645.

223. Dunder T, Kuikka L, Turtinen J, Räsänen L, Uhari M. Diet, serum fatty acids, and atopic diseases in childhood. *Allergy* 2001; **56**:425–428.

224. Wijga AH, Smit HA, Kerkhof M, de Jongste JC, Gerritsen J, Neijens HJ, et al. Association of consumption of products containing milk fat with reduced asthma risk in pre-school children: the PIAMA birth cohort study. *Thorax* 2003; **58**:567–572.

225. Kraft J, Collomb M, Mockel P, Sieber R, Jahreis G. Differences in CLA isomer distribution of cow's milk lipids. *Lipids* 2003; **38**:657–664.

226. Loffeld B, Keweloh H. *cis/trans* Isomerization of unsaturated fatty acids as possible control mechanism of membrane fluidity in *Pseudomonas putida* P8. *Lipids* 1996; **31**:811–815.

227. Kandler O, König H. Cell wall polymers in Archaea (Archaebacteria). *Cellular and Molecular Life Sciences* 1998; **54**:305–308.

228. Deghorain M, Fontaine L, David B, Mainardi JL, Courtin P, Daniel R, et al. Functional and morphological adaptation to peptidoglycan precursor alteration in *Lactococcus lactis*. *The Journal of Biological Chemistry* 2010; **285**:24003–24013.

229. Veiga P, Erkelenz M, Bernard E, Courtin P, Kulakauskas S, Chapot-Chartier MP. Identification of the asparagine synthase responsible for D-Asp amidation in the *Lactococcus lactis* peptidoglycan interpeptide crossbridge. *Journal of Bacteriology* 2009; **191**:3752–3757.

230. Schleifer KH, Kandler O. Peptidoglycan types of bacterial cell walls and their taxonomic implications. *Bacteriological Reviews* 1972; **36**:407–477.

231. Araki Y, Fukuoka S, Oba S, Ito E. Enzymatic deacetylation of *N*-acetylglucosamine residues in peptidoglycan from *Bacillus cereus* cell walls. *Biochemical and Biophysical Research Communications* 1971; **45**:751–758.

232. Logardt IM, Neujahr HY. Lysis of modified walls from *Lactobacillus fermentum*. *Journal of Bacteriology* 1975; **124**:73–77.

233. Meyrand M, Boughammoura A, Courtin P, Mézange C, Guillot A, Chapot-Chartier MP. Peptidoglycan *N*-acetylglucosamine deacetylation decreases autolysis in *Lactococcus lactis*. *Microbiology* 2007; **153**:3275–3285.

234. Pfeffer JM, Strating H, Weadge JT, Clarke AJ. Peptidoglycan *O*-acetylation and autolysin profile of *Enterococcus faecalis* in the viable but nonculturable state. *Journal of Bacteriology* 2006; **188**:902–908.

235. Hamada S, Torii M, Kotani S, Masuda N, Ooshima T, Yokogawa K, et al. Lysis of *Streptococcus mutans* cells with mutanolysin, a lytic enzyme prepared from a culture liquor of *Streptomyces globisporus* 1829. *Archives of Oral Biology* 1978; **23**:543–549.

236. Clarke AJ. Extent of peptidoglycan *O*-acetylation in the tribe Proteeae. *Journal of Bacteriology* 1993; **175**:4550–4553.

237. Clarke AJ, Dupont C. *O*-acetylated peptidoglycan: its occurrence, pathobiological significance, and biosynthesis. *Canadian Journal of Microbiology* 1992; **38**:85–91.

238. Majcherczyk PA, Rubli E, Heumann D, Glauser MP, Moreillon P. Teichoic acids are not required for *Streptococcus pneumoniae* and *Staphylococcus aureus* cell walls to trigger the release of tumor necrosis factor by peripheral blood monocytes. *Infection and Immunity* 2003; **71**:3707–3713.

239. Weidenmaier C, McLoughlin RM, Lee JC. The zwitterionic cell wall teichoic acid of *Staphylococcus aureus* provokes skin abscesses in mice by a novel CD4+ T-cell-dependent mechanism. *PloS One* 2010; **5**:e13227.

240. Meredith TC, Swoboda JG, Walker S. Late-stage polyribitol phosphate wall teichoic acid biosynthesis in *Staphylococcus aureus*. *Journal of Bacteriology* 2008; **190**:3046–3056.

241. Wicken AJ, Ayres A, Campbell LK, Knox KW. Effect of growth conditions on production of rhamnose-containing cell wall and capsular polysaccharides by strains of *Lactobacillus casei* subsp. *rhamnosus*. *Journal of Bacteriology* 1983; **153**:84–92.

242. Looijesteijn PJ, Boels IC, Kleerebezem M. Regulation of exopolysaccharide production by *Lactococcus lactis* subsp. *cremoris* by the sugar source. *Applied and Environmental Microbiology* 1999; **65**:5003–5008.

243. Gruter M, Leeflang BR, Kuiper J, Kamerling JP, Vliegenthart JF. Structure of the exopolysaccharide produced by *Lactococcus lactis* subspecies *cremoris* H414 grown in a defined medium or skimmed milk. *Carbohydrate Research* 1992; **231**:273–291.

244. Greenberg JW, Fischer W, Joiner KA. Influence of lipoteichoic acid structure on recognition by the macrophage scavenger receptor. *Infection and Immunity* 1996; **64**:3318–3325.

245. Koch HU, Fischer W. Acyldiglucosyldiacylglycerol-containing lipoteichoic acid with a poly(3-*O*-galabiosyl-2-*O*-galactosyl-*sn*-glycerol-1-phosphat) chain from *Streptococcus lactis* Kiel42172. *Biochemistry* 1978; **17**:5275–5281.

246. Schleifer KH, Kraus J, Dvorak C, Kilpper-Bälz R, Collins MD, Fischer W. Transfer of *Streptococcus lactis* and related streptococci to the genus *Lactococcus* gen. nov. *Systematic and Applied Microbiology* 1985; **6**:183–195.

247. Schurek J, Fischer W. Distribution analyses of chain substituents of lipoteichoic acids by chemical degradation. *European Journal of Biochemistry* 1989; **186**:649–655.

248. Fischer W, Koch HU, Rösel P, Fiedler F. Alanine ester-containing native lipoteichoic acids do not act as lipoteichoic acid carrier. Isolation, structural and functional characterization. *The Journal of Biological Chemistry* 1980; **255**:4557–4562.

249. Kramer NE, Hasper HE, van den Bogaard PTC, Morath S, de Kruijff B, Hartung T, et al. Increased D-alanylation of lipoteichoic acid and a thickened septum are main determinants in the nisin resistance mechanism of *Lactococcus lactis*. *Microbiology* 2008; **154**:1755–1762.

250. Czabanska A, Neiwert O, Lindner B, Leigh J, Holst O, Duda KA. Structural analysis of the lipoteichoic acids isolated from bovine mastitis *Streptococcus uberis* 233, *S. dysgalactiae* 2023 and *S. agalactiae* 0250. *Carbohydrate Research* 2012; **in press.** http://dx.doi.org/10.1016/j.carres.2012.09.007.

251. Larsson BM, Larsson K, Malmberg P, Palmberg L. Gram-positive bacteria induce IL-6 and IL-8 production in human alveolar macrophages and epithelial cells. *Inflammation* 1999; **23**:217–230.

252. Heinrich PC, Behrmann I, Haan S, Hermanns HM, Müller-Newen G, Schaper F. Principles of interleukin (IL)-6-type cytokine signaling and its regulation. *The Biochemical Journal* 2003; **374**:1–20.

253. Jones SA. Directing transition from innate to acquired immunity: defining a role for IL-6. *Journal of Immunology* 2005; **175**:3463–3468.

254. Petersen AMW, Pedersen BK. The anti-inflammatory effect of exercise. *Journal of Applied Physiology* 2005; **98**:1154–1162.

255. Kang JY, Nan X, Jin MS, Youn SJ, Ryu YH, Mah S, et al. Recognition of lipopeptide patterns by Toll-like receptor 2-Toll-like receptor 6 heterodimer. *Immunity* 2009; **31**:873–884.

256. Gao Y, Lu Y, Teng KL, Chen ML, Zheng HJ, Zhu YQ, et al. Complete genome sequence of *Lactococcus lactis* subsp. *lactis* CV56, a probiotic strain isolated from the vaginas of healthy women. *Journal of Bacteriology* 2011; **193**:2886–2887.

257. Reith J, Mayer C. Peptidoglycan turnover and recycling in Gram-positive bacteria. *Applied Microbiology and Biotechnology* 2011; **92**:1–11.

258. Asmat TM, Klingbeil K, Jensch I, Burchhardt G, Hammerschmidt S. Heterologous expression of pneumococcal virulence factor PspC on the surface of *Lactococcus lactis* confers adhesive properties. *Microbiology* 2012; **158**:771–780.

9   Appendix

TSK I
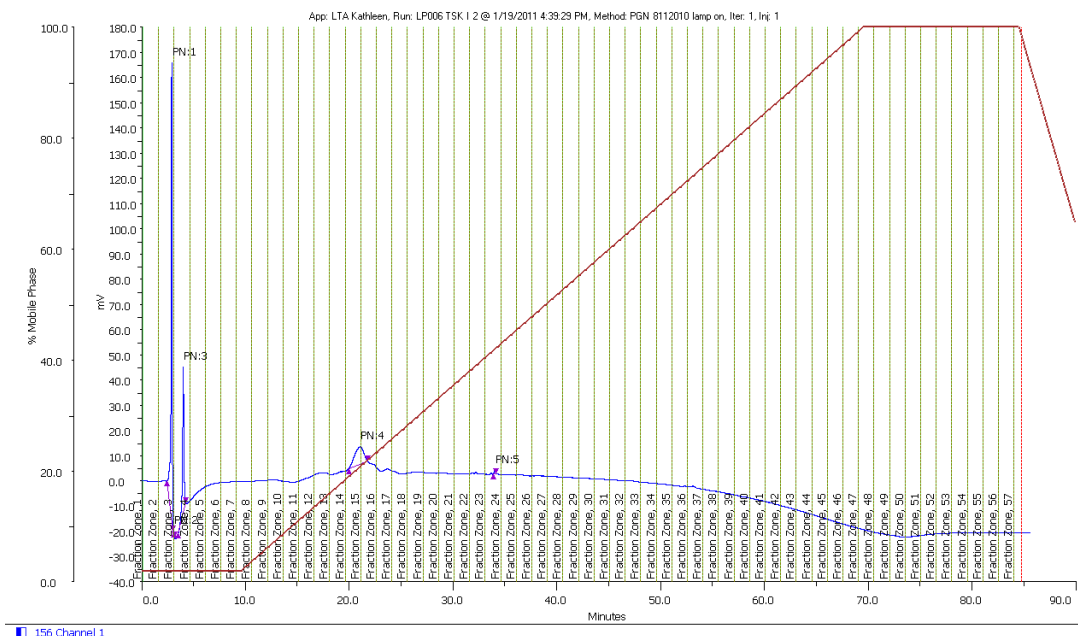
TSK II
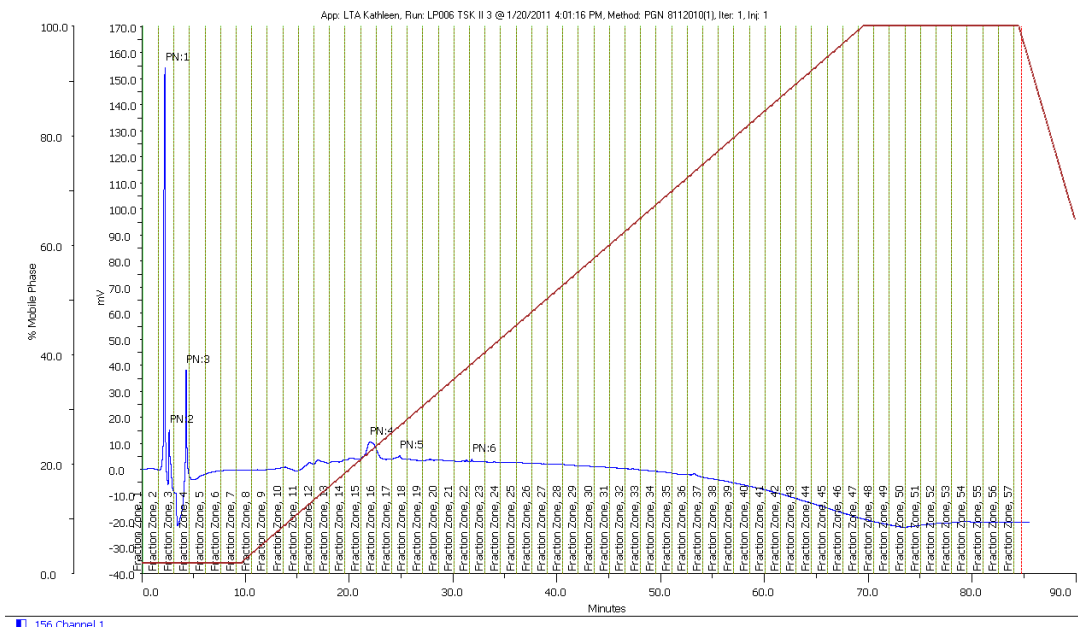
Figure 9.1 RP-12 HPLC chromatograms of PGN TSK I–VI. The gradient of 2–100% buffer B (aqueous CH$_3$CN in 0.1% TFA) was applied to obtain a first draft of the elution profile of 100 µg of each TSK fraction. TSK I–V yielded the main sample peaks in the void volume and a minor not well resolved pool from minute 17–23, which was only marginal present in the separation of TSK V. The chromatogram of TSK VI revealed mainly a similar sample cluster from minute 17–23 with improved but not complete resolution of the containing sample peaks.

TSK III
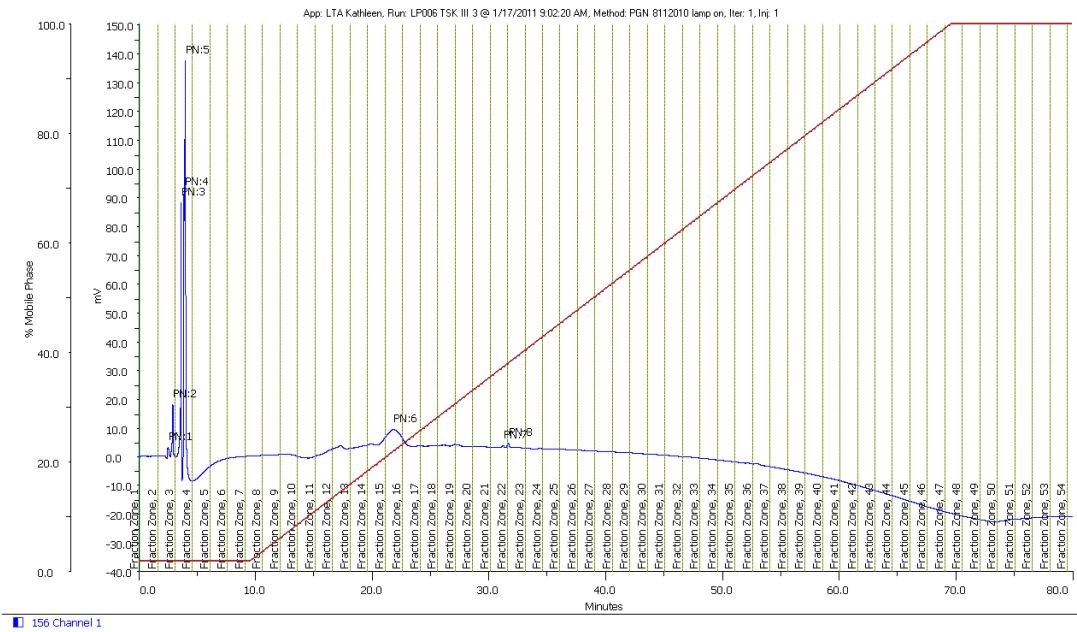
TSK IV
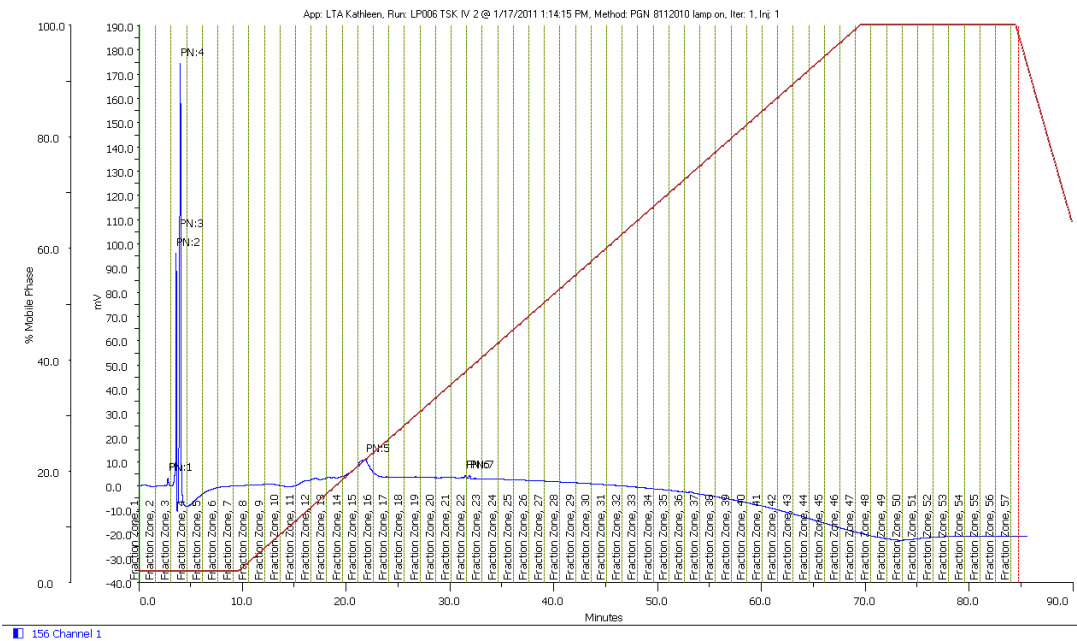
Figure 9.1 continued

TSK V
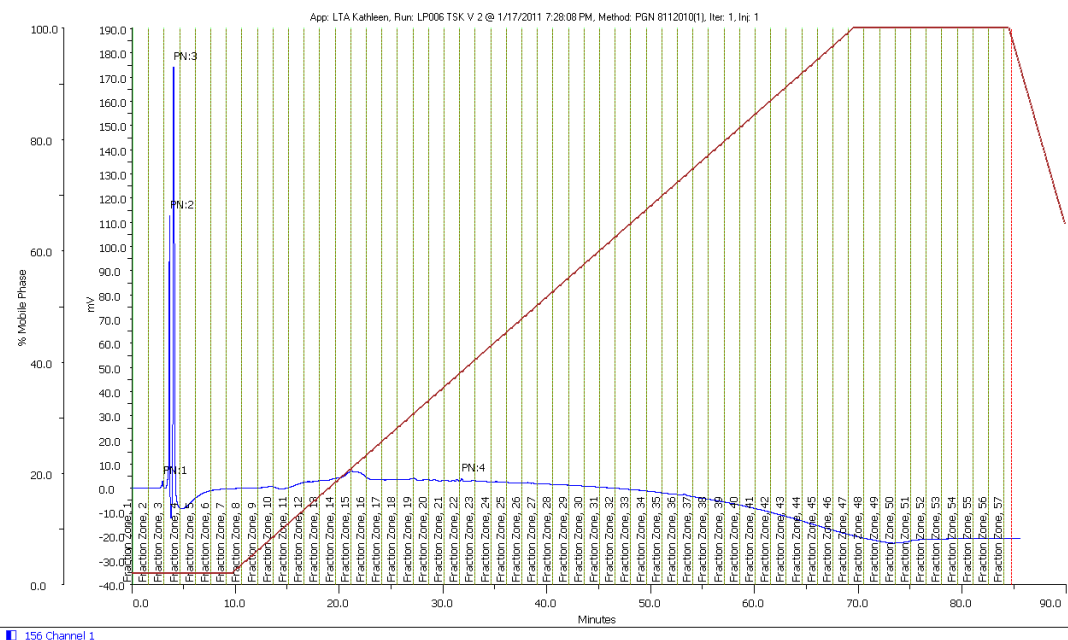
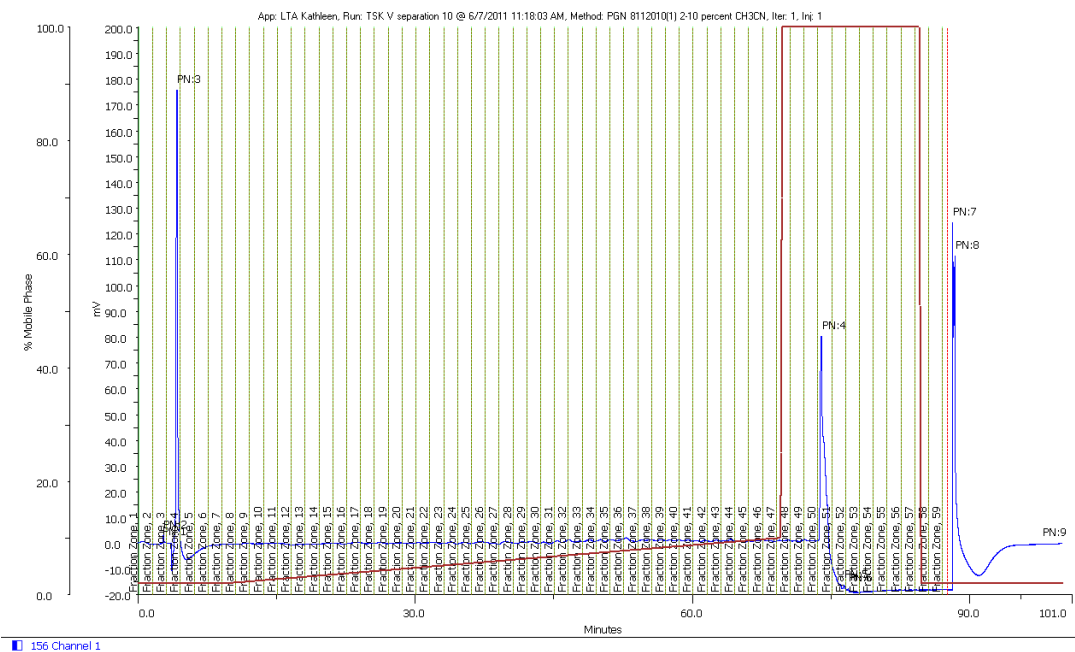# TSK VI
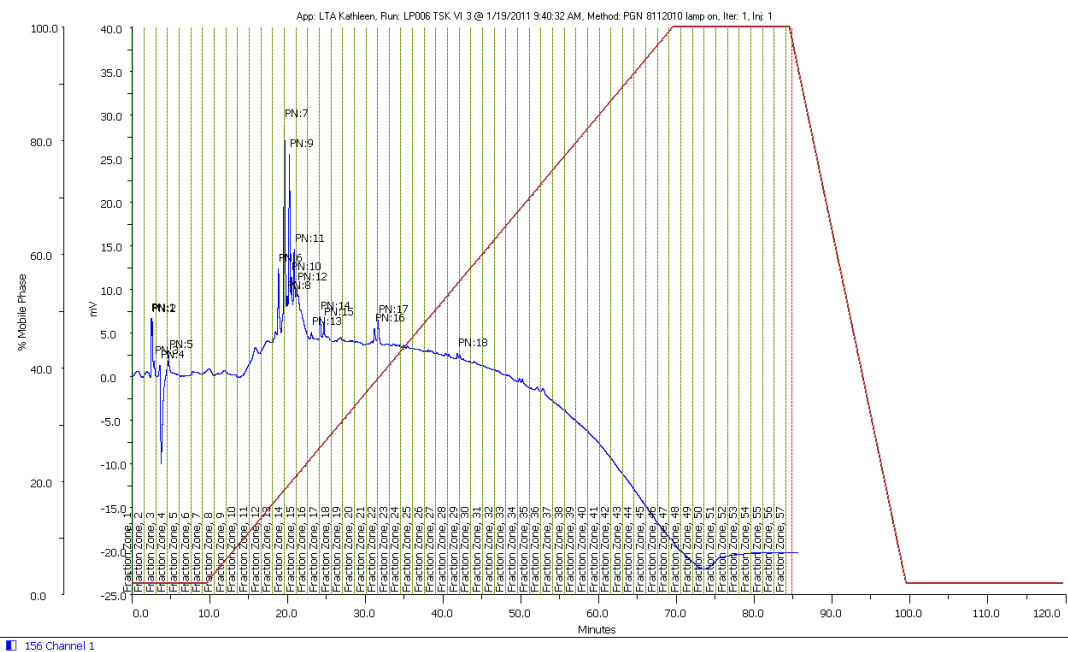
Figure 9.1 continued

Figure 9.2 RP-12 HPLC chromatogram of TSK V separation with 2–10% buffer B (aqueous CH₃CN in 0.1% TFA). The main substance peak (200 µg were injected) eluted in the void volume.
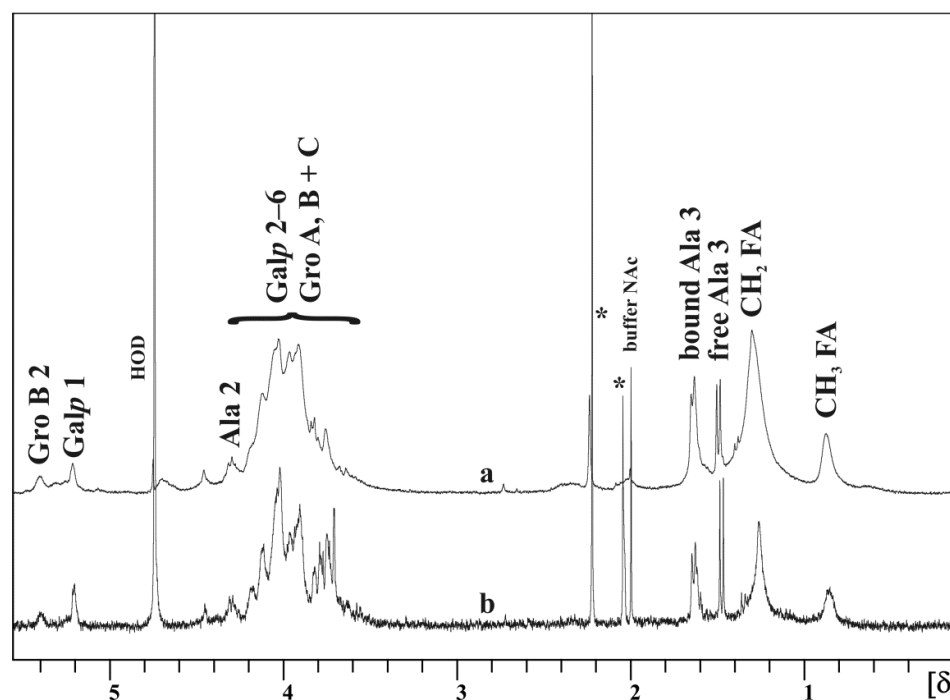

Figure 9.3 ¹H NMR spectra of a) untreated LTA and b) LTA which was incubated with 5% TCA for 24 hours at 4°C. The TCA treatment did not change the LTA structure. Spectra were recorded in D₂O at 360 MHz and 27°C. * no component of the LTA.
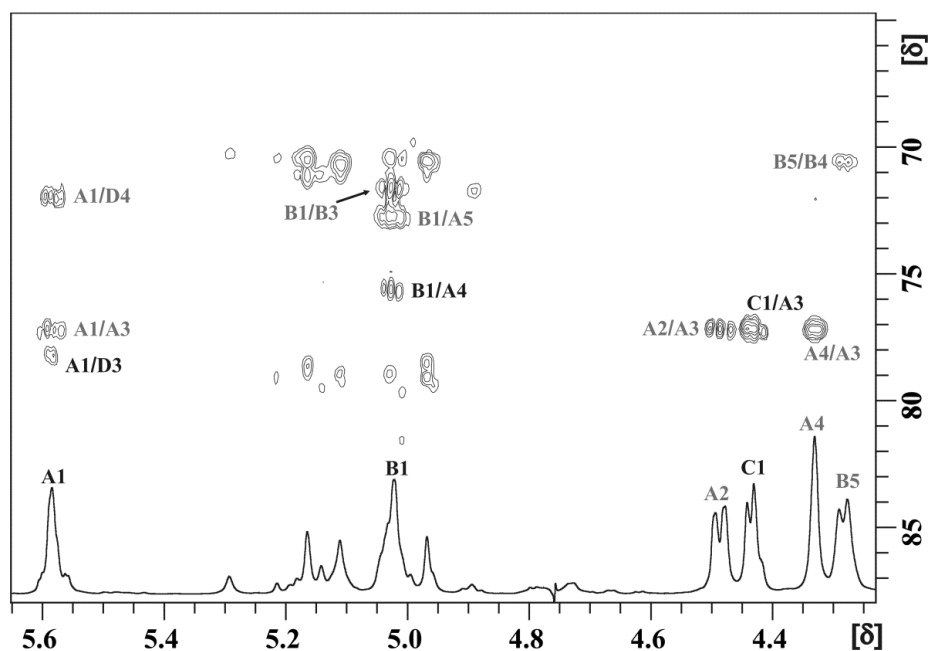
Figure 9.4 Section of the overlayed ^{1}H and ^{1}H,^{13}C HMBC NMR spectra of the EC TA. Arabic numerals indicate the respective protons/carbon atom and capital letters are explained in **Table 4.3** and **Figure 4.15**. Cross peak denotations in black highlight the linkages between the sugars A, B and C. Unlabeled cross peaks refer to the contaminating L-rhamnan. Measurements were carried out in D$_2$O at 700 MHz and 27°C.
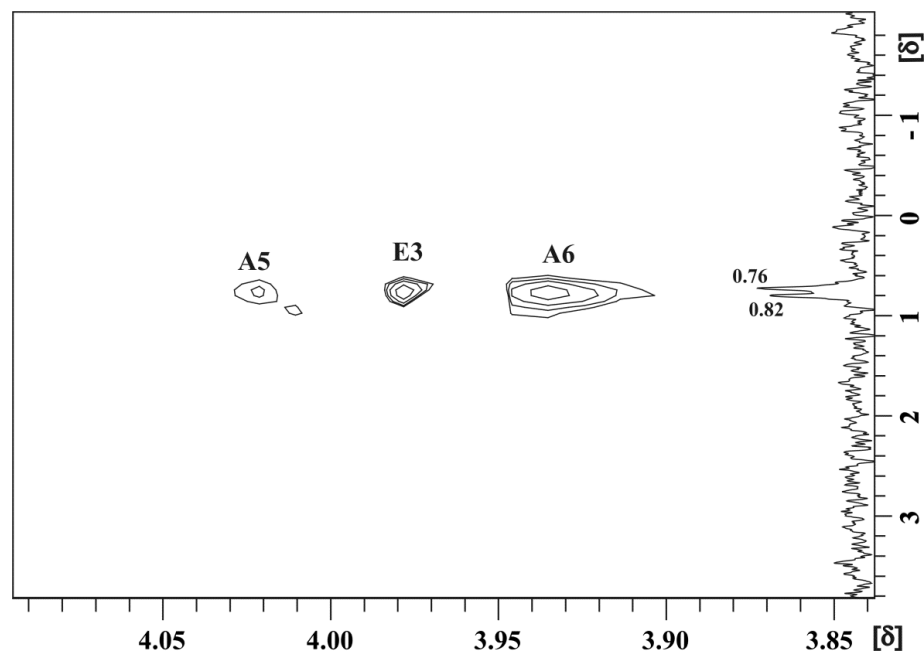

Figure 9.5 Overlay of the ^{31}P and ^{1}H,^{31}P HMQC spectra of the EC TA. Depicted is the first Bio-Gel P-2 fraction (390 µg) obtained after SEC of the HF treated sample. Detected phosphate resonances are indicated with their respective shifts (δ_P 0.76 and δ_P 0.82). Capital letters are explained in **Table 4.3** and **Figure 4.15**, whereas Arabic numerals refer to the respective protons. Spectra were recorded in D$_2$O at 700 MHz and 27°C.
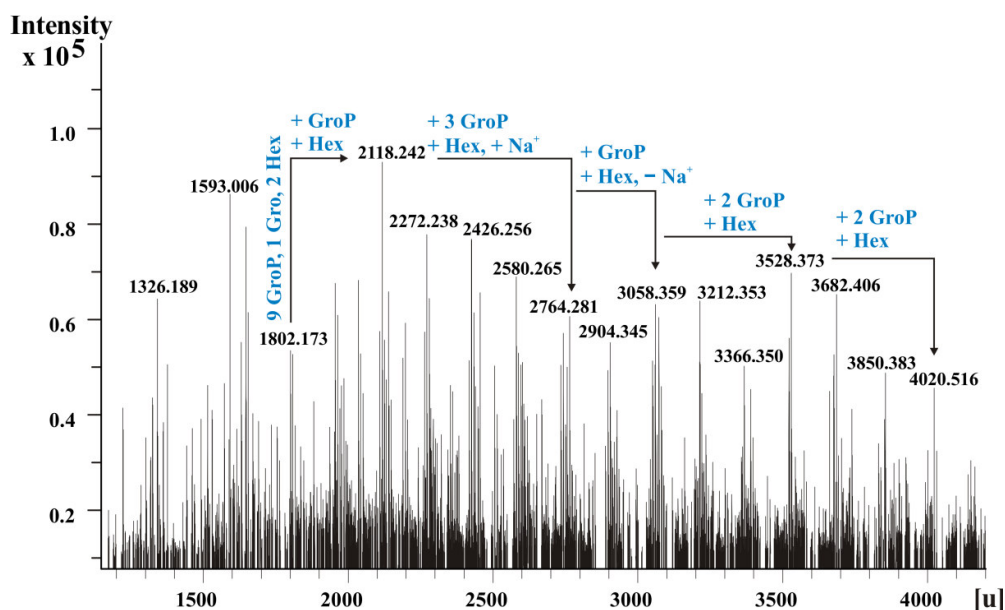
Figure 9.6 ESI-mass spectrum of deacLTA recorded at 5 V in the negative ion mode. Based on the species of 9 GroP, 1 Gro and 2 Hex (1802.173 u) GroP and Hex substitutions are depicted. **Table 9.1** summarizes all identified deacLTA species. The longest backbone was detected with 19 GroP repeats (3850.383 u). However, the mass peak of 4020.516 u revealed the highest degree of Hex decorations. Alanylated species were not found. Non-labeled peaks are attributed to Na^+ and/or K^+ adducts of the deacLTA.

Table 9.1 Summary of the identified deacLTA mass peaks from the 5 V spectrum. For calculations average mass units of 79.966 for P, 74.036 for Gro, 162.052 for Hex and 21.982 for Na^+ were used.

Detected u	Components	Calculated u
1326.189	4 GroP, 4 Hex, + 2 Na^+	1326.198
1802.173	10 Gro, 9 P, 2 Hex	1802.181
2118.242	11 Gro, 10 P, 3 Hex	2118.236
2272.238	12 Gro, 11 P, 3 Hex	2272.240
2426.256	13 Gro, 12 P, 3 Hex	2426.243
2580.265	14 Gro, 13 P, 3 Hex	2580.246
2764.281	14 Gro, 13 P, 4 Hex + Na^+	2764.281
2904.345	14 Gro, 13 P, 5 Hex	2904.351
3058.359	15 Gro, 14 P, 5 Hex	3058.355
3212.359	16 Gro, 15 P, 5 Hex	3212.358

Table 9.1 continued

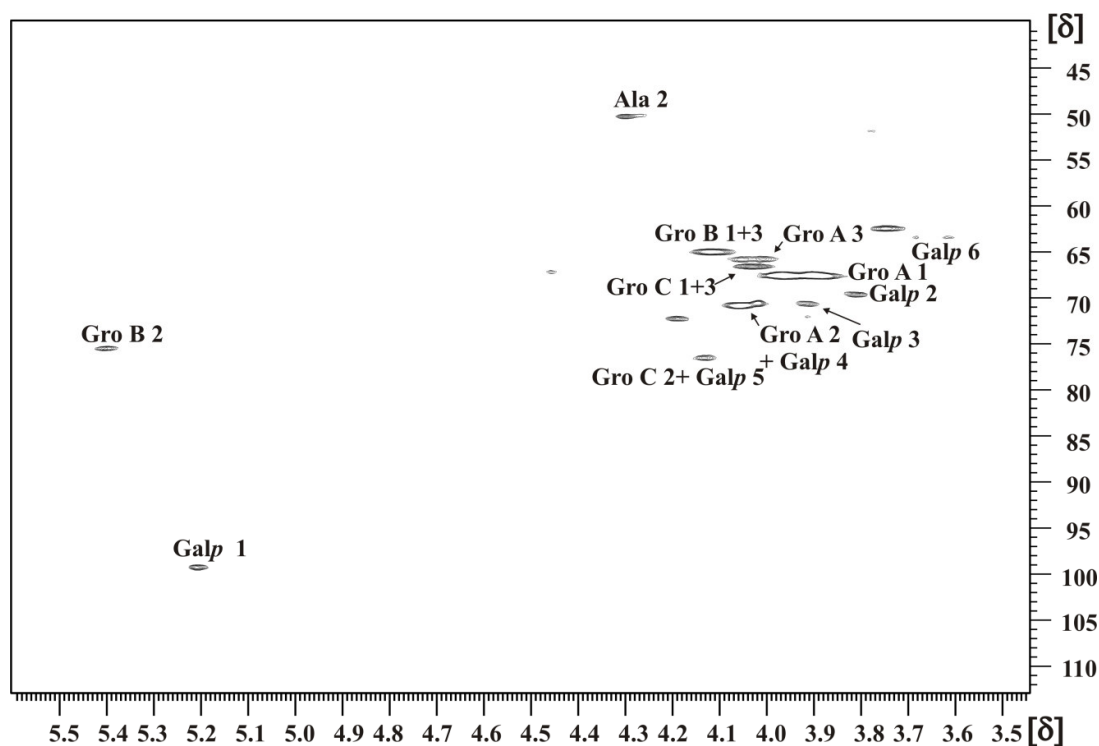|		
3366.350	17 Gro, 16 P, 5 Hex	3366.361
3528.373	17 Gro, 16 P, 6 Hex	3528.414
3682.406	18 Gro, 17 P, 6 Hex	3682.417
3850.383	20 Gro, 19 P, 5 Hex + Na$^+$	3850.352
4020.516	19 Gro, 18 P, 7 Hex + Na$^+$	4020.455

Figure 9.7 ^{1}H,^{13}C HSQC NMR spectrum of the LTA from *L. lactis* G121. Arabic numerals label the protons/carbon atoms of the respective residue indicated in **Figure 4.25**. The identified chemical shifts are listed it **Table 4.6**. Recordings were carried out in D$_2$O at 700 MHz and 27°C.

List of Own Publications Contributing to This Study

Printed publications

Fischer K, Stein K, Ulmer AJ, Lindner B, Heine H, Holst O. Cytokine-inducing lipoteichoic acids of the allergy-protective bacterium *Lactococcus lactis* G121 do not activate via Toll-like receptor 2. *Glycobiology* 2011; **21**:1588–1595.

Fischer K, Vinogradov E, Lindner B, Heine H, Holst O. The structure of the extracellular teichoic acids from the allergy-protective bacterium *Lactococcus lactis* G121. *Biological Chemistry* 2012; **393**:749–755.

Selected poster presentations

Fischer K, Kurdewan S, Duda KA, Holst O. Analyses of the structure of lipoteichoic acids from *Lactococcus lactis* G121, an allergy-protective farm isolate. Summer Course Glycosciences, *11*[th] *European Training Course on Carbohydrates*, May 17–20, 2010.Wageningen, The Netherlands.

Fischer K, Lindner B, Holst O. Structural elucidation of *Lactococcus lactis* G121 lipoteichoic acids. *16th European Carbohydrate Symposium*, July 3–8, 2011. Sorrento, Italy.

Fischer K, Lindner B, Holst O. The structure of the wall teichoic acid of *Lactococcus lactis* G121–simply lipoteichoic acid without fatty acids? *Frontiers in Glycostructure and Membrane Biology*. September 14–16, 2011. Borstel, Germany.

Fischer K, Lindner B, Mamat U, Holst O. Allergy-protective components from *Lactococcus lactis* G121: structure, function, signal transduction. *Annual Symposium SFB/TR22*, October 26–28, 2011. Lübeck, Germany.

Acknowledgements

First of all, I would like to thank Prof. Dr. Otto Holst for giving me the great opportunity to perform my Ph.D. thesis under his supervision. The past three years in the Division of Structural Biochemistry at the RCB were extremely educational as well as productive for me. Otto, I want to thank you for your strong support with very valuable discussions as well as guidance in preparation of publications and presentation of research data on congresses. I appreciate that you gave me the possibility to work in a highly intellectual environment with cutting-edge technology, always leaving enough room for many own ideas.

Secondly, I thank PD Dr. Holger Heine for co-supervising me during my work in line with the BBRS mentoring program. Furthermore, I want to express my gratitude for our fruitful collaboration in the SFB/TR22 project A02 together with Karina Stein. Ina Goroncy and Suhad Al-Badri are gratefully acknowledged for the performance of HEK293 and hMNC *in vitro* tests.

Special thanks go to my colleagues of the Structural Biochemistry, especially to Dr. Katarzyna A. Duda, Katharina Jakob, Regina Engel and Volker Grote for technical assistance and scientific discussions. The same is true for Prof. Dr. Ulrich Zähringer, Buko Lindner, Dr. Nicolas Gisch, Heiko Käßner, Hermann Moll, Birte Buske, Brigitte Kunz and Ursula Schombel from the former Division of Immunochemistry. The technical cooperation and exchange of knowledge between these two groups was exemplary and considerably contributed to the success of my research. Kasia and Nicolas, I want to thank you for teaching me 2D NMR spectroscopic analysis and always having time to answer my questions. Buko, I thank you for valuable ESI-MS discussions.

For the collaboration in order to generate a Δlgt mutant of *L. lactis* G121 Dr. Uwe Mamat and Kathleen Wilke are gratefully acknowledged. Uwe, I appreciate your tremendous molecularbiological know-how, and can only say "thank you" for teaching me modern techniques and planning the knockout experiments.

I thank Dr. Gerhard Burchhardt for providing me with a transformation protocol and pORI23. I thank Dr. Evgueny Vinogradov for NMR spectroscopy of the EC TA polymer.

Moreover, I wish to thank Prof. Dr. Tamas Laskay for the examination of this thesis as a second referee. In this context I also want to thank Prof. Dr. Thomas Peters for taking the chair of the doctoral examination.

The Deutsche Forschungsgemeinschaft (SFB/TR22) is gratefully acknowledged for financial support.

Finally, I want to express my warmest "thank you" to my unique family and friends for their unconditional support not only during my time as a Ph.D. student but also in all situations all times.

Lübeck, 28.9.2012

Erklärung

Die vorliegende Arbeit wurde von September 2009 bis September 2012 unter der Betreuung von Herrn Prof. Dr. Otto Holst am Forschungszentrum Borstel in der Forschergruppe Strukturbiochemie angefertigt.

Ich versichere, dass ich die Dissertation ohne fremde Hilfe angefertigt und keine anderen als die angegebenen Hilfsmittel verwendet habe. Weder vorher noch gleichzeitig habe ich andernorts einen Zulassungsantrag gestellt oder diese Dissertation vorgelegt. Ich habe mich bisher noch keinem Promotionsverfahren unterzogen.

K. Fischer

Kathleen Fischer